

The *Staphylococcus epidermidis* biofilm matrix: functional components, molecular interactions and targeted enzymatic disruption

Doctoral thesis

Dissertation with the aim of achieving a doctoral degree at the
faculty of Mathematics, Informatics and Natural Sciences

Department of Microbiology and Biotechnology

Universität Hamburg

Submitted by Hanaë Agathe Henke

Hamburg, 2015

The grant for this work has been financed by the Werner-Otto-Stiftung (Hamburg, Germany) and the graduation termination scholarship of the University of Hamburg (Germany).

Day of oral defense: 27.03.2015

First Assessor: Prof. Dr. Wolfgang Streit

Second Assessor: Prof. Dr. Holger Rohde

Bestätigung der Korrektheit der englischen Sprache

Hiermit bestätige ich die Korrektheit der englischen Sprache in der vorliegenden Dissertation „The *Staphylococcus epidermidis* biofilm matrix: functional components, molecular interactions and targeted enzymatic disruption“ von Hanaë Agathe Henke (2015).

Mit freundlichen Grüßen,



Jun.-Prof. Dr. Mirjam Perner

Hamburg, der 05.01.2015

Confirmation of language

Hereby I confirm the correctness of the English language used in the present dissertation “The *Staphylococcus epidermidis* biofilm matrix: functional components, molecular interactions and targeted enzymatic disruption“ by Hanaë Agathe Henke (2015).

Kind regards,



Jun.-Prof. Dr. Mirjam Perner

Hamburg, January 5th 2015

Table of content

I.	Introduction.....	1
I.1.	Biofilms, a survival strategy of bacteria	1
I.2.	Development of monospecies biofilms and their medical importance.....	1
I.2.1.	Steps of biofilm formation	3
I.3.	Proteins and polysaccharides involved in biofilm formation of Staphylococci.....	4
I.3.1.	Polysaccharide intercellular adhesin (PIA).....	4
I.3.2.	Extracellular matrix binding protein (Embp), accumulation associated protein (Aap) and small basic protein (Sbp)	6
I.4.	Difficulties to combat <i>S. epidermidis</i> biofilm infections.....	7
I.5.	Anti-Biofilm treatment	8
I.5.1.	Dispersin B (DspB)	9
I.6.	Intention of this work	10
II.	Material and Methods.....	11
II.1.	General materials for microbiological research	11
II.1.1.	Culture mediums and additive components.....	11
II.1.2.	Used bacterial strains, vectors and primers.....	14
II.1.3.	Antibodies and Wheat germ agglutinin (WGA).....	26
II.2.	Culture conditions and storage	28
II.2.1.	Culture Conditions of used bacterial strains	28
II.2.2.	Culture bedding of bacterial strains.....	28
II.3.	Strategies to screen metagenomic libraries.....	29
II.3.1.	Biofilm disintegration assay in microwell plates.....	29
II.3.2.	Large scale preparation of cell raw extract.....	30
II.3.3.	Gel filtration using Äkta System	31

II.3.4.	PIA-preparation and analysis	33
II.4.	Molecularbiological Techniques.....	33
II.4.1.	DNA Isolation and purification procedures.....	33
II.4.2.	Agarose-Gel electrophoresis	36
II.4.3.	Enzymatic modification of DNA	36
II.5.	Transformation of <i>Staphylococcus spec.</i> cells with Phages	45
II.5.1.	Phage Preparation.....	45
II.5.2.	Phage Titration	45
II.5.3.	Phage Transduction.....	46
II.5.4.	Phage Transduction after Ultracentrifugation.....	46
II.6.	Competent cells.....	47
II.6.1.	Chemically competent <i>E. coli</i> cells	47
II.6.2.	Chemically competent <i>P. antarctica</i> cells	47
II.6.3.	Electro competent <i>Staphylococcus epidermidis</i> RN4220 cells.....	48
II.6.4.	Electro competent <i>S. aureus</i> PS187 Δ hdsR Δ sau USI cells.....	48
II.6.5.	Electro competent <i>Pichia pastoris</i> cells	48
II.7.	Protein analysis.....	49
II.7.1.	Expression of recombinant proteins	49
II.7.2.	SDS-gel electrophoresis.....	49
II.7.3.	Treatment of Inclusion Bodies with stepwise pH adjustment.....	51
II.7.4.	Protein dialysis	52
II.7.5.	Western Blotting	52
II.7.6.	Dot Blot.....	52
II.7.7.	Tryptic digest of silver stained gels for mass spectrometry.....	53
II.8.	Immunologic methods.....	54
II.8.1.	Antibody staining of Western Blots and Dot Blots.....	54

II.8.2.	Antibody staining of static biofilms for microscopy.....	55
II.8.3.	Antibody staining of biofilms under flow conditions.....	55
II.8.4.	Antibody/protein labeling with fluorescence dye using a kit	56
II.9.	Microscopy	56
II.9.1.	Biofilm growth under static conditions and Live/Dead Staining	57
II.9.2.	Preparation of Live-Cell Imaging using Bioflux 200.....	57
II.10.	DNA-Sequence Analysis	58
II.11.	Used Software.....	58
III.	Results	60
III.1.	Protein factors and polysaccharides involved in biofilm formation.....	60
III.1.1.	Spatial PIA organization.....	61
III.1.2.	Spatial PIA and Sbp distribution	63
III.1.3.	Influence of sub-domains of Aap on <i>S. epidermidis</i> biofilm formation.....	66
III.1.4.	Co-localization of Embp and PIA and spatial distribution of Embp.....	74
III.2.	Effect of antibiotics on <i>S. epidermidis</i> 1585 biofilm formation.....	80
III.2.1.	Influence of Tigecycline, Chloramphenicol, Erythromycin, Linezolid and Oxacillin on the formation of <i>S. epidermidis</i> 1585 biofilms.....	80
III.2.2.	Influence of phagocytosis after Tigecycline induced biofilm formation on <i>S. epidermidis</i> 1585	85
III.3.	Influence of fosmid clone extracts 100 E3, 100 B3 and 64 F4 on <i>S. epidermidis</i> 1457 biofilms.....	88
III.3.1.	Microscopic analysis of <i>S. epidermidis</i> 1457 biofilms disrupted by cell raw extracts of fosmid clones 100 E3, 100 B3 and 64 F4.....	88
III.3.2.	Influence of heat-inactivated and gel filtered fosmid clone extracts on <i>S. epidermidis</i> 1457 biofilms	93
III.3.3.	Mass-spectrometry of fraction B2.....	96

III.3.4.	Fragment analysis of 100 E3 and over expression of putative biofilm disrupting enzymes	97
III.4.	Bioinformatic analysis of fosmid clones, specifically 100 E3	106
III.4.1.	Bioinformatic determination of putative biofilm disrupting enzymes	106
IV.	Discussion	114
IV.1.	Proteins and Polysaccharides involved in biofilm formation	114
IV.1.1.	Spatial PIA organization	114
IV.1.2.	Spatial PIA and Sbp distribution	115
IV.1.3.	Influence of sub-domains of Aap on <i>S. epidermidis</i> biofilm formation.....	115
IV.1.4.	Co-localization of Embp and PIA and spatial distribution of Embp.....	117
IV.2.	Antibiotic influence on <i>S. epidermidis</i> 1585 biofilm formation.....	119
IV.2.1.	Influence of Tigecycline and phagocytosis after Tigecycline induced biofilm formation on <i>S. epidermidis</i> 1585	120
IV.3.	Influence of fosmid clone extracts 100 E3, 100 B3 and 64 F4 on <i>S. epidermidis</i> 1457 biofilms	121
IV.3.1.	Heat-inactivation of fosmid clone extracts and identification of gel-filtered proteins encoded on fosmid clone 100 E3.....	122
IV.4.	Bioinformatic analysis of fosmid clones, specifically 100 E3	123
IV.4.1.	Protein motifs and possible functions of the most promising enzymes encoded on fosmid clone 100 E3	125
IV.5.	Final conclusion.....	127
V.	List of references	128
VI.	Appendix.....	140
VI.1.	Used Sizemarker	140
VI.1.1.	λ DNA <i>Hind</i> III/ Φ X- <i>Hae</i> III.....	140
VI.1.2.	SDS gel protein marker	141
VI.2.	Vector maps	141

VI.2.1.	Plasmid vector pBluescript II SK +	141
VI.2.2.	Fosmid vector pCC1FOS.....	142
VI.2.3.	Plasmid vector pUC19.....	142
VI.2.4.	Plasmid vector pET21 a.....	143
VI.2.5.	Plasmid vector pET19b	143
VI.2.6.	Entry vector, plasmid pENTR/D-TOPO.....	144
VI.2.7.	Expression vector pDEST15	144
VI.2.8.	Expression vector pDEST17	145
VI.2.9.	Plasmid vector pBBR-MCS5 for <i>Pseudomonas antarctica</i>	145
VI.2.10.	Expression vector pFLD1 for <i>Pichia pastoris</i>	146
VI.2.11.	Expression vector pMALc2x.....	146
VI.2.12.	Plasmid vector pTZ19R	147
VI.2.13.	Plasmid vector pDrive.....	147
VI.2.14.	Expression vector pBAD/Myc-His	148
VI.2.15.	Plasmid vector pCN57.....	148
VI.3.	GC Plots of fosmid clones 100 B3 & 64 F4 and putative biofilm disrupting ORFs of fosmid clone 100 E3	149
VI.3.1.	GC Plot of fosmid clone 100 B3	149
VI.3.2.	GC Plot of fosmid clone 64 F4.....	149
VI.3.3.	GC Plot of Glycosyltransferase 1 of fosmid clone 100 E3.....	150
VI.3.4.	GC Plot of Glycosyltransferase 2 of fosmid clone 100 E3.....	150
VI.3.5.	GC Plot of UDP-3-O-[3-hydroxymyristol]-N-acyltransferase of fosmid clone 100 E3	151
VI.3.6.	GC Plot of Polysaccharide export protein of fosmid clone 100 E3.....	151
VI.4.	Alignment file of putative biofilm disrupting enzymes and the closest relatives	152

VI.5.	Nucleotide and protein sequences of putative biofilm disrupting enzymes on fosmid clone 100 E3	155
VI.6.	Videos	163
VI.6.1.	Video <i>S. epidermidis</i> 1457 PIA formation	163
VI.6.2.	Video <i>S. epidermidis</i> 1457-M10	163
VI.6.3.	Video <i>S. epidermidis</i> 1457 flow conditions	164
VI.6.4.	Video <i>S. epidermidis</i> 1457-M10 flow conditions	164
VI.6.5.	Video <i>S. epidermidis</i> 1457 3D dSTORM Embp+PIA	165
VII.	Acknowledgment	166
VIII.	Declaration on oath	167

List of Figures

- Fig. I-1: Pictures of clean and infected hip joints. A. Hip joint model (private picture taken at the “Deutsches Museum” in Munich, 07.10.2014). B. Biofilm remnants surrounding an explanted acetabular cup of an infected hip prosthesis (arrow) (courtesy of Prof. C.L. Romanò, Galeazzi Orthopaedic Institute, Milan, Italy; http://ec.europa.eu/research/health/infectious-diseases/antimicrobial-drug-resistance/projects/087_en.html; 14.11.14). 2
- Fig. I-2: Schematic representation of the steps of staphylococcal biofilm formation. After the primary attachment induced through multiple factors, the accumulation and maturation of the biofilm starts under expression of proteins and polysaccharides. Some cells naturally detach from the matured biofilm into the planktonic state again to colonize new surfaces [1, modified]. 3
- Fig. I-3: Schematic representation of PIA. The homoglycan is responsible for intercellular adhesion of the cells and very difficult to destroy. It consists of β -1,6-linked 2-acetamide-2-deoxy-D-glucopyranosyl of which 80-85% are acetylated (GlcNAc). The structurally similar deacetylated 20 % of negatively charged residues (GlcNH₃) lead to the strong electrochemical property of PIA. Ester bound succinates at the negatively charged part of PIA are anionic (RO). PIA has a mass of approx. 30.000 kDa [52]. 5
- Fig. I-4: The *ica*ADBC operon is responsible for the synthesis of PIA. Upstream from the operon is the regulator *icaR* [52]. This operon is essential for the production of PIA and therefore the ability to form biofilms. Strains lacking this operon are usually biofilm negative such as *S. epidermidis* M10 [53]. 5
- Fig. I-5: Schematic structure of Embp in *S. epidermidis* 1585. A fibronectin binding protein composed of 59 “Found in various architectures” (FIVAR) and 38 “G-related albumin-binding” (GA) domains following the export signal. The transmembrane region is composed of a domain of unknown function 1542 (DUF1542 TM) region and the cell wall anchor [35, modified]. This large protein contains 10.204 amino acids. 6
- Fig. I-6: Schematic structure of Aap. The image shows domain A, the procession side of 212 amino acids and domain B. The cell wall anchor motif consists of a G rich region and a LPXTG motif at the C-terminus [28, modified]. The whole protein has a size of ~ 220 KDa [95]. 7

- Fig. III-1: Dynamic PIA production and biofilm assembly over a 13 hour period. Images show representative areas at seven independent time points of *S. epidermidis* 1457xpCM29 biofilm growth at 37 °C under static conditions. PIA was visualized with WGA Texas red. Improvise spinning disk microscope (Perkin Elmer, Waltham, USA). It can be seen, that PIA was expressed from the start and the cells grew around the PIA scaffold (Zoom: 400 %). Magnification 630 x. White bar: 21 µM. 61
- Fig. III-2: Growth experiment of the non-biofilm forming bacterium *S. epidermidis* 1457-M10. The images show time points of growth of *S. epidermidis* 1457-M10xpCM29 at 37 °C under static conditions showing that cell aggregates were formed while all cells were moving planktonic through the medium. Improvise spinning disk microscope (Perkin Elmer, Waltham, USA). Magnification 630x. White bar: 21 µM. 62
- Fig. III-3: PIA production and biofilm assembly under flow conditions. Images show the time points of *S. epidermidis* 1457xpCM29 biofilm growth at 37 °C under flow conditions in the Bioflux 200 (Fluxion, San Francisco, USA). PIA was visualized with WGA Texas red. Olympus microscope (Olympus, Tokyo, Japan). It is visible that PIA was expressed from the start and the cells grew around the scaffold without flowing off the surface. Magnification 400x, White bar (left side of each image): 31 µM. 63
- Fig. III-4: Growth of *S. epidermidis* 1457-M10 under flow conditions without biofilm assembly. Images show the time points of growth of *S. epidermidis* 1457-M10xpCM29 at 37 °C under flow conditions in the Bioflux 200 (Fluxion, San Francisco, USA) showing that no biofilm was formed and all cells were moving planktonic through the medium. Olympus microscope (Olympus, Tokyo, Japan). Magnification 400x. White bar: 31 µM. 63
- Fig. III-5: Sbp localization in *S. epidermidis* 1457 wild type and *sbp* deletion mutant. The *S. epidermidis* 1457 wild type (WT) expressing natural Sbp was stained with rabbit-rSbp anti-serum and rabbit-IgG AlexaFluor 568 antibody (image kindly provided by MSc Katharina Sass). Improvise spinning disk (Perkin Elmer, Waltham, USA). It is visible that Sbp was located at the bottom of the well. In comparison *S. epidermidis* 1457Δ*sbp* with additional rSbp-Dylight550 and WGA647 (visualisation of PIA) also showed that Sbp was mainly located on the surface of the microscope chamber while PIA spread through the biofilm. Leica SP2 confocal microscope (Leica, Solms, Germany). Sbp: yellow, PIA: red, cells: green, Magnification 630x, White bar (right side of each image): 11 µM. 64

- Fig. III-6: Sbp surface attachment is independent of sedimentation. Images of *S. epidermidis* 1457xpCM29 grown as a hanging biofilm, i.e. bottom up. Natural Sbp has been stained with rabbit-rSbp anti-serum and rabbit-IgG Cy5 antibody (blue). The striking surface localization of Sbp did not result from sedimentation but from directed events that retain the protein on the surface. Leica SP2 confocal microscope (Leica, Solms, Germany). Sbp: blue, cells: green, Magnification 630x, White bar (right side of each image): 13 μ M. 65
- Fig. III-7: Schematic representation of full length Aap and the sub-domains. This image shows the scheme of clones produced to express each sub-domain of Aap separately. Each plasmid containing one of the domains (A, B, or B+212) had a tetracycline inducible promotor. The strains *S. epidermidis* 1457 Δ aap, *S. epidermidis* 1457-M10 Δ aap and *S. epidermidis* 1457-M10 Δ aap Δ sbp have been complemented with each construct. 66
- Fig. III-8: Function of Aap sub-domains on biofilm formation in *S. epidermidis* 1457 Δ aap. The images show *S. epidermidis* 1457 Δ aap strains each complemented with one sub-domain of Aap. WGA 647 was added to the growing culture to visualize PIA. After 24 h incubation at 37 °C static the cultures have been immuno stained with the corresponding antibodies (table II-5) and a secondary fluorescent antibody (Cy5). The strain expressing domain A (DomA) showed non-structured cell layers, while domain B (DomB) and domain B+212 (DomB+212) showed mushroom-like structured biofilms. The structure was more distinct when DomB has been expressed, but the protein was less abundant in the biofilm. PIA has been expressed evenly in all strains. Leica SP2 confocal microscope (Leica, Solms, Germany). PIA: red, DomA, B, or B+212: white, cells: green. Magnification 630x, White bar (right side of each image): 13 μ M. 67
- Fig. III-9: Biofilm height of *S. epidermidis* 1457 Δ aap clones expressing each sub-domain of Aap. Graphic illustration of the biofilm height of *S. epidermidis* 1457 Δ aap complemented with each sub-domain of Aap separately showing that the unstructured cell layers that derive from domain A were \sim 12 μ M in height while the more structured biofilms due to domain B and domain B+212 were \sim 7, respectively \sim 6 μ M in height. 68
- Fig. III-10: Biofilm assay of *S. epidermidis* 1457-M10 Δ aap and 1457-M10 Δ aap Δ sbp complemented with each sub-domain of Aap. Strains were grown in the presence of 1,25 μ g/ml tetracycline in order to induce expression of the respective domains. It is obvious that *S. epidermidis* 1457-M10 Δ aap could not form a biofilm even when the domain A of Aap was

present. Only when domain B, or domain B+212 were expressed a biofilm could be produced. The same results showed for <i>S. epidermidis</i> 1457-M10 Δ aap Δ sbp.	69
Fig. III-11: Photometric evaluation of biofilm formation by <i>S. epidermidis</i> 1457-M10 aap and sbp deletion mutants complemented with sub-domains of Aap. Extinction of crystal violet used for staining of biofilm at 570 nm. <i>S. epidermidis</i> 1457-M10 Δ aap and <i>S. epidermidis</i> 1457-M10 Δ aap Δ sbp strains expressing each sub-domain of Aap have been tested for their biofilm forming ability showing that a biofilm was formed when domain B, or domain B+212 of Aap were expressed. Expression of domain A of Aap led to some attached cells, but not to structured biofilms. The extinction has been measured in the Infinite 200 pro plate reader (Tecan, Männedorf, Switzerland).....	70
Fig. III-12: Biofilm formation by <i>S. epidermidis</i> 1457-M10 Δ aap strains complemented with sub-domains A, or B+212 of Aap. The images show that domain A led to non structured cell layers, while domain B+212 led to distinct mushroom-like structures and multiple cell layers. The sub-domains were visualized by immuno staining with rabbit anti-rDomA anti-serum, or rabbit anti-rDomB anti-serum and rabbit-IgG Cy5 antibody. Leica SP2 confocal microscope (Leica, Solms, Germany). DomA, B+212: white, cells: green. Magnification 630x, White bar (right side of each image): 13 μ M.	71
Fig. III-13: Biofilm formation of <i>S. epidermidis</i> 1457-M10 Δ aap Δ sbp strains complemented with either sub-domain A, B or B+212 of Aap. The images show that domain A led to non structured cell layers, while domain B and B+212 led to distinct mushroom-like structures. The structure was more distinct when only domain B has been expressed. The domains were visualized by immuno staining with rabbit-DomA anti-serum, or rabbit-DomB anti-serum and rabbit-IgG Cy5 antibody. Recombinant Sbp has been added to the growing culture, showing that even in strains expressing only one domain of Aap, Sbp was located mainly on the ground of the microscope chamber. Leica SP2 confocal microscope (Leica, Solms, Germany). rSbp: yellow, DomA, B, B+212: white, cells: green. Magnification 630x, White bar (right side of each image): 13 μ M.	72
Fig. III-14: Evaluation of biofilm height and Aap/Sbp-specific fluorescence volume in clones expressing each sub-domain of Aap. The graphs of the biofilm height of 1457-M10 Δ aap and 1457-M10 Δ aap Δ sbp complemented with Aap domain A, domain B or domain B+212 show that the cell layers deriving from domain A were not higher than cell layers of control strains	

lacking Aap (a). While the biofilm formed due to domain B+212 only increased slightly in height compared to domain A, the biofilm formed due to domain B was twice the height of the other sub-domains (a). Regarding the protein-specific fluorescence volume of each sub-domain of Aap it could be seen that domain A was expressed in amounts around $130.000 \mu\text{M}^3$ in Aap deletion mutants. The mutant lacking Aap and Sbp expressed domain A only around $40.000 \mu\text{M}^3$. Domain B+212 was expressed less than $50.000 \mu\text{M}^3$ in both deletion mutants while domain B was expressed only around $25.000 \mu\text{M}^3$ none the less domain B led to the only distinctively structured biofilm. In control strains lacking Aap which have been immuno stained to verify that neither the DomA, nor the DomB antibodies bind unspecific, no signal could be detected (b)..... 73

Fig. III-15: Raster electron microscope images of *S. epidermidis* 1585 and *S. epidermidis* 1585 $P_{xyl/tet}::embp$. *S. epidermidis* 1585 (left) and *S. epidermidis* 1585 $P_{xyl/tet}::embp$ (right) induced with 0,2 $\mu\text{g}/\text{mL}$ Tetracycline for Embp expression. It can be seen that the clone expressing Embp was able to form cell aggregates and a web-like matrix. Image kindly provided by Dr. Rudolph Reimer..... 74

Fig. III-16: Transmission electron microscope images of *S. epidermidis* 1585 and *S. epidermidis* 1585 $P_{xyl/tet}::embp$. *S. epidermidis* 1585 (left) and *S. epidermidis* 1585 $P_{xyl/tet}::embp$ (right) induced with 0,2 $\mu\text{g}/\text{mL}$ Tetracycline for Embp expression. To visualize Embp in the matrix immuno gold labelling has been performed (right picture) showing that Embp was expressed in the clone (the black spots are immuno gold particles bound to Embp), while the control did not express Embp. Image kindly provided by Carola Schneider..... 75

Fig. III-17: Simultaneous expression of Embp and PIA in *S. epidermidis* 1585. The microscope images of *S. epidermidis* 1585 $P_{xyl/tet}::embpxpCM29xpTXica$ expressing *gfp*, PIA after 2 % Xylose induction and Embp due to 10 $\mu\text{g}/\text{mL}$ Tetracycline induction show that PIA and Embp were spread throughout the whole biofilm. A co-localization of PIA and Embp could be assumed due to the pink spots in the overlay picture of PIA and Embp. Leica SP2 confocal microscope (Leica, Solms, Germany). PIA: red, Embp: blue, cells: green. Magnification 630x, White bar (right side of each image): 13 μM 76

Fig. III-18: dSTORM images of *S. epidermidis* 1585 $P_{xyl/tet}::embpxpCM29xpTXica$ with co-localization spots of PIA and Embp. The strain has been induced with 2 % Xylose and 10

µg/mL Tetracycline. PIA was visualized with WGA 647 and Embp was visualized using rabbit-Emb7762 anti-serum and rabbit-IgG AlexaFluor568 antibody. PIA is displayed red and Embp blue. The bacterial cells express *gfp* and are displayed green. It is visible that PIA was mainly located in regions where Embp was less present while Embp was more closely related to the bacterial cells. The co-localization channel showed that Embp and PIA distinctively co-localize in elongated horizontal parts (Co-loc., yellow). This image is a 3D illustration, kindly provided by Dr. Dennis Eggert. Magnification 1.000x, Zoom 1000 %. PIA: red, Embp: blue, cells: green. 77

Fig. III-19: Graphic illustration of clones expressing Embp, PIA, or both in either *S. epidermidis* 1457, or *S. epidermidis* 1585. Graph (a) shows PIA-specific fluorescence volume and living cells in the biofilm. The wild type (WT) of *S. epidermidis* 1585 as anticipated did not express PIA, while the WT of *S. epidermidis* 1457 did. In *S. epidermidis* 1585xpTXica PIA expression could be obtained. *S. epidermidis* 1585 $P_{xyl/tet}::embp$ showed very high and 1457 $P_{xyl/tet}::embp$ showed quite low Embp expression. Graph (b) shows the Embp-specific fluorescence volume in all clones and the wild types, verifying that only the clones containing $P_{xyl/tet}::embp$ were able to express Embp. *S. epidermidis* 1585 WT did naturally express low amounts of Embp. Graph (c) shows the biofilm height of each clone and the wild types showing that the height increased with PIA expression and was highest when PIA and Embp were expressed at the same time. 78

Fig. III-20: dSTORM images of *S. epidermidis* 1457 expressing natural PIA and Embp. The strain has been induced with 75 pg/mL tigeicycline to promote natural Embp production. PIA was visualized with WGA 647 and Embp was visualized using rabbit-Emb7762 anti-serum and rabbit-IgG AlexaFluor568 antibody. It could be seen that Embp formed the same elongated structures as in Fig. III-18 and PIA formed a web-like structure. Furthermore the vertical arrangement of Embp can be seen in the 3D image indicated with the white box. The corresponding video can be found in the appendix (VI.6.5 Video *S. epidermidis* 1457 3D dSTORM Embp+PIA). Magnification 10.000x. Images kindly provided by Dr. Dennis Eggert. 79

Fig. III-21: Induction of Embp expression by different antibiotics in *S. epidermidis* 1585. Dot Blot analysis of *S. epidermidis* 1585 cell surface proteins obtained after growth in the presence of different antibiotics. The supernatant has been diluted up to 1:4096 in water and then 10 µL each have been spotted onto a PVDF membrane. It is visible that 0,625

$\mu\text{g}/\text{mL}$ Tigecycline and $1,25 \mu\text{g}/\text{mL}$ Chloramphenicol led to increased Embp production, while $1,25 \mu\text{g}/\text{mL}$ Oxacillin and $0,3 \mu\text{g}/\text{mL}$ Linezolid led to a low increase of Embp expression compared to the control. Erythromycin did not lead to Embp expression at all. The dot blot has been stained with rabbit-Embp7762 anti-serum and rabbit-IgG HPO and then exposed to X-ray films for 30 sec. 81

Fig. III-22: Induction of biofilm formation by tigecycline in *S. epidermidis* 1585 wild type. The microscope images of *S. epidermidis* 1585 wild type (WT) with and w/o $0,3 \mu\text{g}/\text{mL}$ Tigecycline. It is visible that the amount of Embp as well as the biofilm height increased due to antibiotic treatment. The cells formed closely attached cell layers without mushroom-like structures. Embp was spread through the biofilm. Embp was stained with rabbit anti-rEmbp anti-serum and anti-rabbit IgG AlexaFluor568 antibody. Leica SP2 confocal microscope (Leica, Solms, Germany). Embp: magenta, cells: green. Magnification 630x, White bar (right side of each image): $13 \mu\text{M}$ 82

Fig. III-23: Graphic illustration of Embp-specific fluorescence signal volume obtained by *S. epidermidis* 1585 wild type treated with Tigecycline concentrations of $0,3$, $0,45$ and $0,6 \text{ ng}/\mu\text{L}$. It is visible that the Embp-specific fluorescence signal increased up to approximately $18.000 \mu\text{M}^3$ in the presence of $0,45 \text{ ng}/\mu\text{L}$ Tigecycline, whereas the control (*S. epidermidis* 1585 w/o added tigecycline) only reached $1.500 \mu\text{M}^3$ Embp-specific fluorescence. When the concentration of Tigecycline reached $0,6 \text{ ng}/\mu\text{L}$ the Embp-specific fluorescence volume amount decreased down to the level of $0,3 \text{ ng}/\mu\text{L}$ 83

Fig. III-24: Induction of biofilm formation based on Embp by different antibiotics in *S. epidermidis* 1585. The microscopic images of *S. epidermidis* 1585 wild type grown in the presence of antibiotics as indicated show an increased Embp production after the treatment with $1,25 \mu\text{g}/\text{mL}$ Oxacillin, as well as with $1,25 \mu\text{g}/\text{mL}$ Chloramphenicol and $0,3 \mu\text{g}/\text{mL}$ Linezolid. The treatment of bacterial cells with $0,625 \mu\text{g}/\text{mL}$ Erythromycin showed no increase in Embp production and the cells did not grow as much as in the other cultures. For all tested antibiotics, but Erythromycin a thin biofilm could be obtained. Leica SP2 confocal microscope (Leica, Solms, Germany). Embp: magenta, cells: green. Magnification 630x, White bar (right side of each image): $13 \mu\text{M}$ 84

Fig. III-25: Evaluation of biofilm height and Embp-specific fluorescence signal volume after the treatment of *S. epidermidis* 1585 with different antibiotics. Graphic illustration showing

the evaluation of confocal microscopy images presented in Fig. III-24. (a) The comparison of the biofilm height of all cultures treated with different antibiotics to induce Embp production showed that Oxacillin, Chloramphenicol and Linezolid led to higher biofilms than the treatment with Erythromycin. (b) The volume of Embp-specific fluorescence of cultures treated with different antibiotics showed that Oxacillin and Chloramphenicol led to a strong increase in Embp production, while Linezolid led to a low increase in Embp production and Erythromycin even decreased the amount of Embp compared to a control.⁸⁵

Figure III-26: Bacterial cells organized in a biofilm are protected from phagocytotic killing. Images of *S. epidermidis* 1585xpCM29 and a biofilm induced with 0,3 µg/mL Tigecycline, each incubated with J774A.1 mouse macrophages (MP J774) for 6 h. The bacterial cells were stained using a rabbit anti-*S. epidermidis* antiserum and an anti-rabbit IgG AlexaFluor568 antibody. Since macrophages were not permeabilized, only bacteria outside the macrophages were stained. Yellow arrows indicate macrophages that internalized bacterial cells (green), while blue arrows indicate empty macrophages. It was visible that more macrophages were able to internalize bacterial cells, when these were not organized in a biofilm. The bacterial cells organized in a biofilm showed strong adherence among each other and the macrophages could not internalize as many bacterial cells as in the control. Improvisation confocal microscope (Perkin Elmer, Waltham, USA). Magnification 630x, White bar (right side of each image): 13 µM. 86

Figure III-27: Statistic evaluation of internalized bacteria by macrophages with and w/o tigecycline induced biofilm formation. *S. epidermidis* 1585 has been treated with and without 0,3 µg/mL Tigecycline to induce biofilm formation. It can be seen that less bacterial cells could be internalized by macrophages after a biofilm has been formed. An unpaired t-test performed with Graph Pad prism 5 proved the significancy of this different bacterial uptake counts ($p < 0,005$). 87

Figure III-28: Biofilm disintegration assay of *S. epidermidis* 1457 treated with fosmid clone extract 100 E3. Biofilms grew for 24 h at 37 °C static and have then been treated with different amounts of cell raw extract from fosmid clone 100 E3 for 24 h at 37 °C static. It could be visualized that the biofilm was disrupted intensively after the treatment with fosmid extract compared to the control. 88

Fig. III-29: Graphic illustration of the biofilm disruption after the treatment with cell raw extracts of fosmid clones 100 E3, 100 B3 and 64 F4. It shows that 100 E3 had the strongest biofilm disrupting properties with up to 80 % less biofilm, while 100 B3 and 64 F4 disrupted 40-60 % of the biofilm. 1 x PBS also disrupted the biofilm up to 30 % due to the lack of nutrients (a). Graphic illustration of the biofilm height after the treatment with cell raw extracts of the different fosmid clones 100 E3, 100 B3 and 64 F4 showing that *S. epidermidis* 1457 biofilms were only 4 μM in height compared to the control that showed a biofilm height of approx. 13 μM (b). 89

Fig. III-30: Mature *S. epidermidis* 1457 biofilms got disrupted after treatment with fosmid clone extracts. The control with 3 % BSA in 1xPBS showed an island like structure of the biofilm, while the biofilm treated with extracts of fosmid clone 100 B3 and 64 F4 showed a thin cell layer and an increased amount of dead cells/eDNA. The biofilm treated with extract of 100 E3 also showed an increase in dead cells/eDNA (red), as well as a decrease in height and living cell volume (green). The biofilms have been stained with Live/Dead[®] BacLight[™] Bacterial Viability Kit (Invitrogen, Oregon, USA). Improvisation spinning disk microscope (Perkin Elmer, Waltham, USA). Magnification 630x, White bar (left side of each image): 13 μM 90

Fig. III-31: Biofilm disruption after the treatment of mature *S. epidermidis* 1457 biofilms with mixtures of fosmid clone extracts. The control extract of *E. coli* Epi300 did not have any effect on the biofilm and the control protein 3 % FCS (fetal calf serum) even showed a biofilm strengthening effect. The mixture of extract 100 E3 + 100 B3 and 100 B3 + 64 F4 showed a biofilm disruption of ~20 %, and ~ 25 %, while the mixture of 100 E3 + 64 F4 disrupted the biofilm up to 50 %. A mixture of all three fosmid extracts disrupted the biofilm up to 60 %..... 91

Fig. III-32: Mature *S. epidermidis* 1457 biofilm disruption by mixtures of fosmid clone extracts. It is visible that the biofilm was disrupted strongly by mixtures containing extracts of 100 E3 + 64 F4 and when all three extracts were mixed. The biofilm disruption, as well as the amount of dead cells/eDNA (red) was also visible when fosmid extracts 100 E3 + 100 B3 and 100 B3 + 64 F4 were mixed, but not as strong as in the other treatments. The biofilms have been stained with Live/Dead[®] BacLight[™] Bacterial Viability Kit (Invitrogen, Oregon,

USA). Improvisation spinning disk microscope (Perkin Elmer, Waltham, USA). Magnification 630x, White bar (left side of each image): 13 μ M.....	92
Fig. III-33: Mature <i>S. epidermidis</i> 1457 biofilms disruption after heat inactivation of fosmid clone extracts. Graphic illustration of <i>S. epidermidis</i> 1457 biofilms treated with fosmid extracts before and after heat inactivation of the extract at 60-70 °C oN. It is visible that the extract of 100 E3 still disrupted the biofilm up to 60 % after heat inactivation. This showed a decrease of biofilm disrupting properties of only 10 % compared to unheated extract. The fosmid extracts of 100 B3 and 64 F4 lost approx. 30-50 % of their activity after heat inactivation, that meant the unheated extracts disrupted a biofilm between ~22 % for 100 B3 and 25 % for 64 F4, while the heat inactivated extracts disrupted the biofilm ~18 % for 100 B3 and 12 % for 64 F4.....	93
Fig. III-34: Fraction B2 after gel filtration disrupted a <i>S. epidermidis</i> 1457 biofilm effectively. Graphic illustrations of the average biofilm disruption of fosmid extract 100 E3 after gel filtration that excluded proteins by size. Fraction B2 shown here disrupted the biofilm up to 80 % compared to the unfiltered and with this not concentrated fosmid extract of 100 E3. The protein sizes in fraction B2 laid between 17-70 KDa.	94
Fig. III-35: Gel filtration fraction B2 degrades PIA. Dot Blot showing the reduction of PIA after treatment with fractions derived from the gel filtration of fosmid extract 100 E3 showing that fraction B2 reduced PIA more than the other fractions, indicating that the proteins responsible for PIA degradation were concentrated in this fraction. The membrane has been stained with rabbit-PIA anti-serum and rabbit-IgG HPO for visualization on X-ray films. This film has been exposed to the membrane for 30 sec.	95
Fig. III-36: SDS gel of fraction B2 after gel filtration used for mass-spectrometry. Silver stained 10 % SDS gel showing the fractions of the gel filtration. The eight bands of fraction B2 have been prepared for mass spectrometry to determine the proteins.	96
Fig. III-37: SDS gel of an over expression experiment of GT3 with MBP tag. The gel shows that the desired protein has only been expressed in the insoluble fraction. GT3 had neither been expressed in the soluble fraction at 37 °C nor if the expression temperature had been decreased down to 16 °C.	104
Fig. III-38: Steps of breaking inclusion bodies and refolding the protein. The wash steps I and II of the insoluble fractions showing that after the second wash almost no additional protein	

retained in the supernatant. After breaking the unfolded protein extracted from inclusion bodies it has been refolded. Lane 3 shows the proteins in Refold Buffer prior to concentration with 3 kDa Amicon filters, while lane 4 shows the Concentrate of the protein solution. Lane 5 showing the Flow through of the 3 kDa Amicon filter showing that no protein rushed through the filter. The concentrate has then been used for Dialysis on at 4 °C to exchange the refold buffer by 1 x PBS, or MBP-binding buffer. The protein solution in 1xPBS has been used for biofilm disintegration assays on *S. epidermidis* 1457 biofilms, but no activity could be achieved..... 105

Fig. III-39: Length and GC content of fosmid clones 100 E3, 100 B3 and 64 F4 as well as the GC Plot of fosmid clone 100 E3. This illustration shows 100 E3 has a very high GC content of 63,80 %, while 100 B3 and 64 F4 have a GC content less than 60 %. The graph on the right shows the GC Plot of fosmid clone 100 E3 indicating the high GC content in the middle of the fosmid around base ~16.000..... 106

Fig. III-40: Scheme of fosmid clone 100 E3 showing all encoded genes and the annotated ORFs. Most promising enzyme candidates responsible for the biofilm disrupting effect are indicated in green. The operon at the N-terminal side of the fosmid encoding an operon with 3 Glycosyltransferases (GT1-3) and a Polysaccharide export transporter (PET). In the middle of the sequence a Dehydrogenase (DH) and Amidohydrolase (AH), as well as the UDP-3-O-[hydroxymyristol]-glucosamine-N-acyltransferase (N-ace) could also be responsible for biofilm disruption and PIA degradation..... 107

Fig. III-41: GC-Plot of Glycosyltransferase 3. This illustration of the GC content of Glycosyltransferase 3 (GT3) shows that the GC content is very high at almost 65 %. Especially around base pairs 450 and 850 the GC-Plot showed the highest GC peaks..... 108

Fig. III-42: Phylogenetic tree of the most promising enzyme candidates encoded on fosmid clone 100 E3. The Glycosyltransferases 1 & 3 show similarities to *Chloroflexus sp.* and *Lyngbya sp.*, while Glycosyltransferase 2, as well as the N-Acyltransferase and Polysaccharide export transporter show similarities to *Rhizobium sp.* and *Candidatus solibacter usitatus*, or *Acidobacteria sp.* These bacterial species are common in soil, as well as marine habitats.. 110

Fig. III-43: Protein motifs encoded by fosmid clone 100 E3. Glycosyltransferase 1 (GT 1) encodes an S-adenosyl dependent Methyltransferase (SAM) and a UDP-Glycosyltransferase. GT 2 & 3 show similar motifs belonging to Glycosyltransferase family 1 while for GT 2 also

Glycosyltransferase family 4 could be annotated. The UDP-3-O-[hydroxymyristol]-glucosamine-N-acyltransferase (N-Ace, UDP-3-O-[...]) shows four hexapeptide repeats (HX) typical for bacterial transferases, as well as a LpxA and LpxD protein motif indicating lipid A biosynthesis. The Polysaccharide export protein (PET) shows the conserved domain for export proteins as well as a soluble ligand binding protein motif (SLBB).....	113
Figure VI-1: DNA Ladder λ DNA <i>Hind</i> III/ Φ X- <i>Hae</i> III (Finnzymes, Pittsburgh, USA), each fragment shows 1 band in the gel.....	140
Figure VI-2: Images are from a 4-20% Tris-glycine gel (SDS-PAGE) and subsequent transfer to membrane. http://www.thermoscientificbio.com/protein-electrophoresis/pageruler-prestained-protein-ladder/ (Thermo Scientific, Waltham, USA).....	141
Figure VI-3: The vectorcard of plasmid vector pBluescript II SK + (Manual of pBluescript II SK + from Agilent Technologies, La Jolla, USA)	141
Figure VI-5: The vectorcard of plasmid vector pUC19 (http://www1.qiagen.com/literature/vectors_pcr.aspx ; Access: 23.06.2011)	142
Figure VI-4: The vectorcard of fosmid vector pCC1FOS (http://www.epibio.com/images/catalog/i_CopyControl_VectorMap.gif ; Access: 07.06.2009)	142
Figure VI-6: Expression vector pET21a, C-terminal HIS taq (Novagen, Merck Millipore, Darmstadt, Germany).....	143
Figure VI-7: Expression vector pET19b, N-terminal HIS Taq (Novagen, Merck Millipore, Darmstadt, Germany).....	143
Figure VI-8: Plasmid vector pENTR/D-TOPO, entry vector for pDEST15 and pDEST17 (Invitrogen Life technologies, Carlsbad, USA).....	144
Figure VI-9: Expression vector pDEST15, N-terminal GST Taq (Invitrogen Life technologies, Carlsbad, USA).....	144
Figure VI-10: Expression vector pDEST17, N-terminal HIS Taq (Invitrogen Life technologies, Carlsbad, USA).....	145
Figure VI-11: Plasmid vector pBBR-MCS5 for <i>Pseudomonas antarctica</i>	145
Figure VI-12: Expression vector pFLD1 for yeast expression in <i>Pichia pastoris</i> (Invitrogen Life technologies, Carlsbad, USA).	146

Figure VI-13: Expression vector pMALc2x, N-terminal Maltose binding protein (New England Biolabs, Frankfurt am Main, Germany).....	146
Figure VI-14: Phagemid vector pTZ19r (Thermo Scientific, Waltham, USA).....	147
Figure VI-15: pDrive Cloning vector for PCR products (Qiagen, Hilden, Germany).	147
Figure VI-16: Expression vector pBAD/Myc-His, C-terminal His Tag (Invitrogen Life technologies, Carlsbad, USA).	148
Figure VI-17: Tetracycline inducible vector pCN57 (modified at AG Rohde, UKE, Hamburg, Germany).....	148
Figure VI-18: The GC content of fosmid clone 100 B3 shows the highest GC amount around base 8500 and has a total GC content of 59,15 %.	149
Figure VI-19: The GC content of fosmid clone 64 F4 shows the highest GC amount around base 30.000 and has a total GC content of 53,09 %.	149
Figure VI-20: GC content of glycosyltransferase 1 of fosmid clone 100 E3 showing the highest peaks around base 10, 580 and 1150. The total amount of GC is 65,59 %.	150
Figure VI-21: GC content of glycosyltransferase 2 of fosmid clone 100 E3 showing the highest peaks around base 50, 200, 600 and 850. The total amount of GC is 64,47 %.	150
Figure VI-22: GC content of UDP-3-O-[3-hydroxymyristol]-N-acyltransferase of fosmid clone 100 E3 showing the highest peak around base 1200. The total amount of GC is 64,00 %. ..	151
Figure VI-23: GC content of Polysaccharide export protein of fosmid clone 100 E3 showing the highest peaks around base 100 and 600. The total amount of GC is 66,87 %.	151
Figure VI-24: The Alignment file of the glycosyltransferases, the N-acyltransferase and polysaccharide export protein and their closest relatives. The scheme shows that conserved regions for glycosyltransferase family 1 are similar in the glycosyltransferases 1-3. In the case of the N-acyltransferase of fosmid clone 100 E3 distinct regions show that all UDP-3-O-glucosamine-N-acyltransferases of the closest relatives share the same protein motifs. The polysaccharide export transporter shows conserved domains indicating the export transporter function but only shows close relatives that are have been annotated as hypothetical proteins.	154

List of Tables

Table II-1: Used additives and antibiotics in their final concentration	13
Table II-2: Bacterial strains used in this study.....	14
Table II-3: Vectors used in this study	19
Table II-4: Oligonucleotides used in this study	21
Table II-5: Specific antibodies used for Western Blots, Dot Blots and microscopic samples ..	26
Table II-6: Culture conditions of bacterial strains	28
Table II-7: Purification columns for the Äkta System.....	32
Table II-8: Used Type II restriction enzymes and buffer from NEB (Frankfurt am Main, Germany) and their reaction- and inactivation temperature.....	37
Table II-9: Used reaction protocols for analytic and preparative DNA restriction reactions ..	38
Table II-10: Restriction enzymes for pFLD1 Linearization.....	38
Table II-11: PCR program depending on the polymerase used	40
Table II-12: Electro pulse adjustment	44
Table II-13: SDS-gel recipe.....	50
Table II-14: Used Software, databases and reference sources.....	58
Table III-1: Result of mass spectrometry of the fraction B2 encoding proteins on fosmid clone 100 E3	97
Table III-2: Restriction enzymes used to digest fosmid clone 100 E3. Further subcloning of the smaller fragments into different host vectors has been done. These enzymes have been chosen based on the sequence to gain fragments between 1000 and 5000 bp.....	98
Table III-3: Putative biofilm disrupting enzymes cloned into different vectors. All putative biofilm disrupting enzymes encoded on fosmid clone 100 E3 have been amplified via PCR and then subcloned into different plasmid, and expression vectors using variable host strains for over expression.....	98
Table III-4: GC content in ORFs of fosmid clone 100 E3 indicating that the GC content is very high in all ORFs	108
Table III-5: Assembly of the protein motifs encoded in the most promising biofilm disrupting ORFs, showing the length of the protein, the integrated protein motif and its position as well as the function.....	111
Table IV-1: Biofilm building matrix components and their functions.....	119

Table IV-2: Biofilm disruption characteristics of fosmid clones 64 F4, 100 B3 and 100 E3 ... 122

Table IV-3: Overview of putative biofilm disrupting enzyme candidates from fosmid clone 100 E3 124

List of Abbreviations

<i>ad.</i>	Adjust to		mM	Milli Molar
Aap	Accumulation protein	association	mm	Millimeter
			ng	Nanogramm
			nm	Nanometer
AG	Working group		OD	Optical Density
Amp	Ampicillin		oN	Overnight
AU	Absorbance Unit		pg	Picogramm
<i>Aq</i>	Solved in water		PIA	Polysaccharide intercellular adhesin
<i>bidest.</i>	Bidistilled		Pro	Promoter
bp	Basepair(s)		XYZ ^R	Resistance
°C	Degree Celsius		rpm	Rounds per minute
Chl	Chloramphenicol		RT	Roomtemperature (~20 °C)
CLSM	Confocal Laser Scanning Microscopy		Sbp	Small basic protein
DMF	Dimethylformamid		Sec	Second(s)
DMSO	Dimethylsulfoxid		Ter	Terminator
dSTORM	Direct stochastic optical reconstruction microscopy		Tet	Tetracycline
EC	Enzyme Class		THR	Hip joint replacement
eDNA	Extracellular DNA		Tig	Tigecycline
Embp	extracellular matrix binding protein		U/μL	Units per Microliter
e.g.	For example		UKE	University hospital Hamburg- Eppendorf
EtOH	Ethanol		Vol.	Volume
EMT	Eppendorf micro test tube		V	Volt
FBS	Fetal bovine serum		WGA	Wheat germ agglutinin
Fig.	Figure		X-Gal	5-Brom-4-chlor-3-indoxyl-β-D- galactopyranosid
g	Gramm			
GlcNac	N-acetylglucosamine			

List of Abbreviations

Gm	Gentamicin		
GSH	Reduced Gluthation		
GSSG	Oxidized Gluthation		
h	Hour(s)	Ze	Zeocin
H ₂ O	Water	µg	Microgramm
HPO	Horse radish peroxidase	µL	Microliter
IPTG	Isopropyl-beta-D-thiogalactopyranoside		
Kan	Kanamycin	α	Anti (for antibodies)
kB	Kilobase	%	Percent
kF	Kilofarad	Ω	Ohm (Electroresistance)
kV	Kilovolt	Δ	Delta (knock-out gene)
L	Liter		
LB-AIX-Plates	LB-Agarplates with Ampicillin, IPTG and X-Gal		Nucleobases
mg	Milli Gramm	A	Adenine
min	Minute(s)	C	Cytosine
mL	Milliliter	G	Guanine
M	Molar	T	Thymine

Abstract

This work focuses on *Staphylococcus epidermidis* biofilm formation. Interactions between relevant protein factors contributing to biofilm formation, as well as their spatial distribution inside a developing and a mature biofilm are important to understand their function. The main factor involved in *S. epidermidis* biofilm accumulation, polysaccharide intercellular adhesin (PIA), has been investigated in live cell imaging experiments, showing that some starter cells expressed PIA from the initiation of cell aggregation and biofilm formation. The biofilm started to enhance height before spreading over the whole colonization surface. The extracellular matrix binding protein Embp showed to be inducible by antibiotic treatment and led to biofilm formation with the same protective properties against macrophages as PIA-based biofilms. Co-localization of Embp and PIA has been investigated, showing an increase in biofilm strength when both components were expressed simultaneously. Identification of the function of each sub-domain of Accumulation association protein Aap (A, B and B+212) has been achieved by complementing Aap deletion mutants *S. epidermidis* 1457 Δ aap, *S. epidermidis* 1457-M10 Δ aap and *S. epidermidis* 1457-M10 Δ aap Δ sbp with each sub-domain. It could be shown that domain B was mainly responsible for the typical mushroom-like biofilm structure, while domain A led to a multi layered non structured biofilm. The expression of domain B+212 led to a semi-structured biofilm with some aggregates and non-structured cell layers. The analysis of Sbp and the sub-domains of Aap did not show significant co-localization.

The investigation of putative biofilm disrupting fosmid clones derived from a metagenomic library brought up 3 fosmid clones (100 E3, 100 B3 and 64 F4) with biofilm degrading properties. All fosmid clones have been analyzed for their biofilm disrupting properties using Live/Dead experiments, biochemical tests, bioinformatic tools, mass spectrometry and gel filtration. Glycosyltransferases encoded on fosmid clone 100 E3 seemed the most promising enzymes, but their over expression has not been successful in neither *E. coli*, *Pichia pastoris*, *Pseudomonas antarctica*, nor in vitro expression. The effect of the fosmid clones on *S. epidermidis* 1457 biofilms has been investigated using microscopy techniques showing a reproducible destruction of *S. epidermidis* 1457 biofilms. Fosmid clone 100 E3 even showed disrupting properties after heat treatment at 70 °C.

Zusammenfassung

Die vorliegende Arbeit beschäftigt sich mit der Bildung von *Staphylococcus epidermidis* Biofilmen. Vorrangig untersucht wurde die räumliche Anordnung der Proteine in Proteinbasierten Biofilmen. Hier bei konnte festgestellt werden, dass das small basic protein (Sbp) für die Oberflächenadhärenz verantwortlich ist. Des Weiteren wurde das aus 3 Subdomänen (A & B) bestehende Accumulation association protein (Aap) untersucht. Es wird angenommen, dass jede Domäne eine eigene Funktion besitzt, wobei eine 212 Aminosäuren große Region zwischen den Domänen proteolytisch gespalten werden muss, um die volle Strukturierung eines Biofilmes zu erreichen. Es wurden Deletionsmutanten mit je einer der Aap Domänen A und B, sowie der Domäne B + die 212 Region komplementiert. Es zeigte sich, dass Domäne A für die Oberflächenadhärenz und Domäne B für die typische Pilzähnliche Biofilmstruktur, sowie Zell-Zell Adhärenz verantwortlich ist. Darüber hinaus konnte festgestellt werden, dass Domäne B+212 zu einer Biofilm-Mischform führt, welche die Oberflächen Adhärenz von Domäne A mit der Zell-Zell Adhärenz von Domäne B zeigte. Der Biofilm war nicht so strukturiert wie durch den Einfluss von Domäne B. Dies unterstützt die These, dass die 212 Aminosäureregion proteolytisch gespalten werden muss, um die typische Biofilmstruktur zu erhalten. Ein weiteres untersuchtes Protein Embp (extracellular matrix binding protein) zeigte eine heterogene Verteilung innerhalb des Biofilmes, sowie direkte Kolo-kalisation zu dem Polysaccharide intercellular adhesin (PIA). Es konnte festgestellt werden, dass Embp direkt an den Bakterienzellen haftet und diese durch elongierte Strukturen miteinander verbindet. Darüber hinaus konnte festgestellt werden, dass Embp vermehrt produziert wird, wenn die Bakterienzellen antibiotischem Stress ausgesetzt werden. So bildete der Biofilm negative Stamm *S. epidermidis* 1585 unter antibiotischem Stress Biofilme auf Embp Basis, welche protektive Eigenschaften gegenüber Phagozytose zeigten.

Die Untersuchung putativ Biofilm zerstörender Fosmidklon Extrakte (100 E3, 100 B3 und 64 F4) aus einer Metagenombank zeigten reproduzierbare Degradation eines *S. epidermidis* 1457 Biofilmes. Weitere Charakterisierungsversuche durch Mikroskopie, Live/Dead Färbung, biochemischer Tests und bioinformatischer Untersuchungen, sowie Massenspektrometrie und Gelfiltration zeigten, dass vor allem Zucker modifizierende Enzyme die auf dem Fosmidklon 100 E3 kodiert sind die vielversprechendsten Kandidaten für die Disruption des Biofilmes sind. Sogar nach Hitzeinaktivierung zeigte der Extrakt des Fosmidklones 100 E3 noch Biofilm abbauende Wirkung. Daher wurde Fosmidklon 100 E3 genauer untersucht, indem die vielversprechenden Enzyme subkloniert und versuchsweise überexprimiert wurden. Eine Überexpression war nicht erfolgreich, weder in *Escherichia coli*, *Pichia pastoris*, *Pseudomonas antarctica*, noch in vitro.

I. Introduction

I.1. Biofilms, a survival strategy of bacteria

In nature bacteria often form multi cellular communities, called biofilms, on different biotic and abiotic surfaces. Bacteria not only live in biofilms in nature, but also have the ability to attach to household items like showerheads, plumbing material, shower curtains or drinking water systems [53, 54, 55]. *Pseudomonas aeruginosa* is a known biofilm forming organism that is very abundant in the household [53]. Bacterial communities can be composed of different bacterial species, or just one bacterial species [54, 56]. Each biofilm is arranged in multiple cell layers, while some biofilms form mushroom-like structures as for *Staphylococcus epidermidis* and different *Pseudomonas* species. *Bacillus subtilis* and *Vibrio cholerae* form colonies that seem dry, flat and wrinkled on agar plates [59, 60, 62], while *Myxococcus xanthus* forms biofilms that look like small yellow air balloons [25, 26]. *Anoxybacillus flavithermus* can form biofilms in silica and is a threat in food processing [24]. A general feature of all bacterial biofilms is a matrix that surrounds the bacteria, a slimy surrounding on the surface and around each bacterial cell that protects the cells and functions as a nutrient and water provider [59, 60]. This matrix consists of proteins, polysaccharides, phospholipides and extracellular DNA [35, 36, 37, 63, 96]. Sometimes the matrix seems colored (pink, brown, or blackish) to avoid DNA damage through sun light [55]. Nutrients and other compounds can be shared between the cells by passive diffusion through the porous matrix, and act as cell communication components, this phenomenon is called quorum sensing [57]. The most important effect of the matrix is the protection against external influences and mechanical destruction. The matrix also protects the cells from chemical influences such as antibiotics, antimicrobials and disinfectants. Furthermore, the biofilm protects bacterial cells against physical and chemical stresses, shearing forces, and limited nutrient availability [56, 57]. The cells inside the matrix benefit from each other and support each other's growth and survival [55, 59].

I.2. Development of monospecies biofilms and their medical importance

Most bacteria are able to form a biofilm and in a clinical environment this may lead to biofilm-associated diseases, in animals as well as humans [23]. These are often observed in an oral surrounding such as caries and periodontitis, or in respiratory tract infections in cystic fibrosis patients [22, 41] but also on other surfaces such as implanted medical devices. Within this framework threatening are coagulase-negative, gram-positive staphylococci (e.g. *S. epidermidis*) and coagulase-positive *S. aureus* that form biofilms on abiotic surfaces [1, 2, 3, 4, 9]. This ability enhances their pathogenicity and often results in infections on artificial medical devices such as hip joints (Fig. I-1), or surgical pins [44]. Cardiac pacemakers with a following endocarditis, as well as intravenous catheters can get infected as a result of human extracellular matrix and serum coating the implant which is a nutrient rich environment for

the bacteria [41, 44]. Approximately 240.000 infections occur in the USA per year that lead to treatment costs of approx. \$ 1.8 billion [1, 42]. But morbidity and mortality of hospital acquired, nosocomial infections increase every year [1, 4]. Almost 80 % of the cells involved in material-associated infections are *S. epidermidis* cells, because as a skin habitant they get easy access to wounds and implants [6]. Another main problem is biofilm formation on abiotic surfaces during food production and food processing. Milk and meat can be contaminated through multi-resistant staphylococcal species after contact with the biofilm coated surface [3, 5].



Fig. I-1: Pictures of clean and infected hip joints. A. Hip joint model (private picture taken at the “Deutsches Museum” in Munich, 07.10.2014). B. Biofilm remnants surrounding an explanted acetabular cup of an infected hip prosthesis (arrow) (courtesy of Prof. C.L. Romanò, Galeazzi Orthopaedic Institute, Milan, Italy; http://ec.europa.eu/research/health/infectious-diseases/antimicrobial-drug-resistance/projects/087_en.html; 14.11.14).

Procedures to prevent or remove these biofilms are very limited, not only due to the growing antibiotic resistance of staphylococcal species, but also due to the enhanced resistance of biofilm-organized staphylococci against antimicrobials and disinfectants [2, 6, 7]. The main component of the biofilm that is protecting the bacteria against external influences is the matrix composed of extracellular polymeric substances, such as proteins, nucleic acids, humic acids, lipids and polysaccharides. These matrix compounds also lead to the typical mushroom-like biofilm structure [47]. Understanding the complex regulatory network leading to biofilm formation and organization of the matrix in detail as well as innovative approaches are necessary to disrupt established staphylococcal biofilms and prevent those on abiotic surfaces to improve clinical patient management and food safety. So far new targets for antibiotic screening, vaccines and prevention of staphylococcal

biofilms are promising, but they are based on molecular methods, e.g. Peptidoglycan, teichoic acid-, or PIA biosynthesis [8].

I.2.1. Steps of biofilm formation

Biofilm formation occurs in mainly four steps in every bacterial species and is regulated by different proteins (Fig. I-2). This work is focused on biofilms produced by *S. epidermidis*, so the given examples in this chapter refer to this organism. The proteins specific for the biofilm formation of staphylococci are described more precisely in I.3. Biofilm formation is depending on the surrounding medium, the nutrient availability, as well as pH, temperature and oxygen [43]. The surface also plays a major role for attachment because each attachment protein has the ability to bind to a different surface, e.g. extracellular matrix binding protein (Embp) from *S. epidermidis* 1585 binds to fibronectin, while the small basic protein (Sbp) expressed by *S. epidermidis* 1457 attaches to polystyrene surfaces and glass [35]. The first primary cells are not sessile and start attaching to the surface due to the expression of host depending proteins. Another protein expressed by *S. epidermidis* is the 148 kDa surface protein AtIE (AutolysinE) that attaches to polystyrene and vitronectin [96]. It is supposed that cell wall metabolic activities lead to an up regulation and with this to the attachment [31]. *S. epidermidis* strains lacking AtIE show a reduced virulence. A primary attachment polysaccharide of *S. aureus* is PS/A, which is an *N*-succinylated β -1,6-linked Polyglucosamine similar to Polysaccharide intercellular adhesin (PIA) from *S. epidermidis* [31]. Both polysaccharides are encoded by the *icaADBC* locus and responsible for primary adhesion especially to catheters, as well as intercellular adhesion and bacterial aggregation during maturation process of the biofilm [31]. These proteins and polysaccharides are involved in the first steps of biofilm formation from single cells attaching to the surface to a multilayered structure [31].

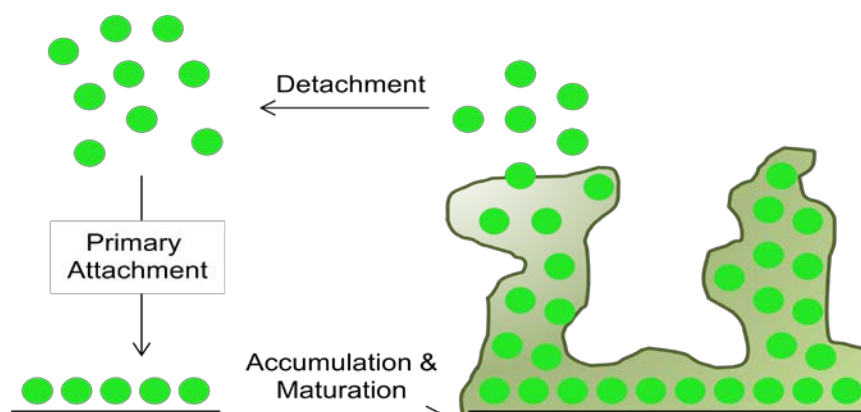


Fig. I-2: Schematic representation of the steps of staphylococcal biofilm formation. After the primary attachment induced through multiple factors, the accumulation and maturation of the biofilm starts under expression of proteins and polysaccharides. Some cells naturally detach from the matured biofilm into the planktonic state again to colonize new surfaces [1, modified].

In the second phase, the accumulation phase of the biofilm, accumulation association protein (Aap) expression levels increase additionally to PIA expression [31]. In PIA and Aap lacking strains, Embp can take the role of the intercellular adhesin. However, given the broad distribution of Embp, *icaADBC* and Aap in clinical *S. epidermidis* populations, it is reasonable to speculate that under certain conditions, independent intercellular adhesins could also function cooperatively during biofilm accumulation [35]. The third step of biofilm formation is the maturation of the biofilm that includes differentiation of the cell layers and channel building. The biofilm then shows a highly organized structure with mushroom-like biofilm compartments containing river-like channels for the transport of fresh medium, blood, etc. The mushroom-like structures of living cells are built around the intercellular adhesins and dead cells like a frame. The last step includes preliminary cells that detach the bacterial consortium to colonize new surface spots [1]. It is supposed that increased activity of the quorum sensing *agr* system which can additionally to the production and recognition of peptide-based pheromones, lead to a surfactant-like δ -hemolysin that promotes biofilm detachment. This process is supported by the down regulation of the former accumulation proteins due to stationary phase [31]. Also AtlE seems to be regulated by the *agr* system and is also up regulated during cell detachment showing that AtlE has two main functions during biofilm formation [31]. The molecular mechanisms leading to staphylococcal biofilm formation have been studied intensively during the past years.

I.3. Proteins and polysaccharides involved in biofilm formation of Staphylococci

Staphylococcus species biofilms are either polysaccharide, or protein based, depending on the genetic background. eDNA is also a part of the extracellular matrix and supposed to be involved in the early accumulative phase of biofilm formation [103]. Either way, mechanisms involved biofilm assemblies are very complex. A balanced expression of proteins is necessary to form a matured biofilm. An accumulation associated protein (Aap), the small basic protein (Sbp), the extracellular matrix binding protein (Embp) and especially polysaccharide intercellular adhesin (PIA) play significant roles in biofilm formation [6, 29, 30, 31, 32]. The most important and interesting factor in polysaccharide based *S. epidermidis* 1457 biofilms is PIA, which is referred to in point I.3.1. Factors that lead to biofilm formation are often stress induced like high levels of Glucose, Glucosamine, zinc, high osmolarity, high temperatures, pH and the presence of ethanol. Therefore biofilm formation appears to be a survival strategy of the cells [9, 6, 28, 34].

I.3.1. Polysaccharide intercellular adhesin (PIA)

The matrix in biofilm formation in *Staphylococcus epidermidis* is composed of PIA. The high molecular weight (M_r of 30,000 Da) homoglycan PIA consists of approximately 130 β -1,6-

linked-2-acetamido-2-deoxy-D-glucopyranosyl residues (Fig. I-3). An amount of 15 % of the residues are deacetylated which leads to positive charges important for the adhesive properties of the molecule. The rest of the molecule is *N*-acetylated [27]. In addition, PIA carries ester-linked succinates which introduce negative charges into the molecule. The parallel presence of positive and negative charges contributes to the intercellular adhesive properties of PIA. Poly-*N*-acetyl glucosamine found in *S. aureus*, *Escherichia coli* and *Aggregatibacter actinomycetemcomitans* are structurally related if not identical [10].

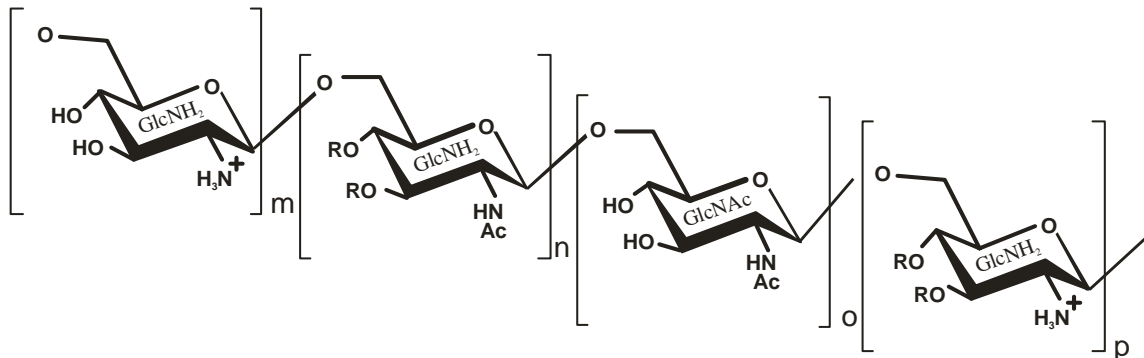


Fig. I-3: Schematic representation of PIA. The homoglycan is responsible for intercellular adhesion of the cells and very difficult to destroy. It consists of β -1,6-linked 2-acetamido-2-deoxy-D-glucopyranosyl of which 80-85% are acetylated (GlcNAc). The structurally similar deacetylated 20 % of negatively charged residues (GlcNH₃) lead to the strong electrochemical property of PIA. Ester bound succinates at the negatively charged part of PIA are anionic (RO). PIA has a mass of approx. 30.000 kDa [52].

PIA is synthesized by the *icaADBC* operon (Fig. I-4) [10, 31]. Most of the clinical and food processing samples of *S. epidermidis* carry this operon, suggesting that in vivo PIA-dependent biofilm formation is a widespread characteristic trait of virulent *S. epidermidis* populations [3, 11, 12]. PIA has been proven as an important virulence factor through animal models using defined *S. epidermidis* strains as well as PIA-negative mutants [2].



Fig. I-4: The *icaADBC* operon is responsible for the synthesis of PIA. Upstream from the operon is the regulator *icaR* [52]. This operon is essential for the production of PIA and therefore the ability to form biofilms. Strains lacking this operon are usually biofilm negative such as *S. epidermidis* M10 [53].

PIA and structural relatives such as the polysaccharide PNAG from *S. aureus* are of general importance not only in staphylococcal but also in other bacterial organisms. Structures similar to PIA are all encoded by orthologous *icaADBC* operons, even in Gram negative bacteria such as *E. coli*, *A. actinomycetemcomitans* and *Yersinia pestis* [13, 14]. Every gene in the operon has a certain function. *icaA* encodes an *N*-acetyl glucosamine transferase that

has been identified as a transmembrane protein using UDP-N-acetyl glucosamine as a substrate. The chaperone protein that is responsible for the correct folding and membrane insertion of the N-acetyl glucosamine is the product encoded by *icaD*. *icaC* encodes a transmembrane protein responsible for the externalization and elongation of PIA. This protein also functions as a possible anchor for PIA as well as the membrane protein adjuvant for the translocation of PS/A to the cell surface. The gene product of *icaB* is a cell surface protein consisting of 259 amino acids. It is responsible for deacetylation of the N-acetyl glucosamine and shows homologies to chitin deacetylases [31, 52]. This step leads to the electrochemical properties mentioned above [27].

I.3.2. Extracellular matrix binding protein (Embp), accumulation associated protein (Aap) and small basic protein (Sbp)

The extracellular matrix binding protein Embp is expressed in slight variations by different bacterial species, e.g. Ebh in *S. aureus* and Emb in *Streptococcus defectivus* [36, 38, 39]. In *S. epidermidis* Embp is 1.1 MDa in size and encoded by the *embp* gene (Fig. I-5). It is composed of 59 found in various architectures (FIVAR) and 38 protein G-related albumin-binding domains [35]. Linnes et al recently showed that Embp regulation is correlated to neither *icaA* Expression which is responsible for PIA nor *agr* expression. But Embp expression of the gene and protein seems to be highly up regulated during high osmotic stress which leads to protein-mediated resistance against plasmolysis [37]. For *S. epidermidis* strain 1585 it was shown, that Embp is associated to fibronectin (Fn) and polystyrene adhesion [30, 35, 37]. For fibronectin adhesion it could be shown that Embp binds to Fn domain type III12 [35].



Fig. I-5: Schematic structure of Embp in *S. epidermidis* 1585. A fibronectin binding protein composed of 59 “Found in various architectures” (FIVAR) and 38 “G-related albumin-binding” (GA) domains following the export signal. The transmembrane region is composed of a domain of unknown function 1542 (DUF1542 TM) region and the cell wall anchor [35, modified]. This large protein contains 10.204 amino acids.

Fig. I-6 shows the accumulation associated protein Aap that is expressed in polysaccharide, as well as protein based biofilms [28]. Aap is involved in the first attachment to surfaces as well as the second accumulation step of biofilm formation [32, 95, 96]. It is encoded by the *aap* gene and has a molecular weight of about 140-220 KDa, depending on the number of repeats in domain B [29, 31, 95]. Aap extends 120 nm away from the cell wall in local tufts and is a thin fibrillar, cell wall anchored protein. It is composed of three domains. N-Terminal domain A has 556 amino acids in total which are composed of 10-11 degenerated 16-aa

repeats, it is mostly responsible for primary attachment [95, 96]. Domain B contains a variable number of 5 to 17 nearly identical 128-aa repeats (each repeat called G5 domain), terminating in a “half-repeat” and a “collagen-like” repeat [28, 30]. The G5 domains are functional related to the property of self-association in this protein while the spacer “E” regions prevent misfolding of the protein and realizes the elongated structure of Aap [95]. A C-terminal LPXTG motif behind domain B is relevant to the covalent attachment of Aap to the bacterial cell surface. A 212 amino acid L-type lectin domain lies between domain A and B and is the cleavage site for proteolytic procession. The remaining domain B leads to the typical mushroom-like structure of protein-based biofilms [28, 95, 96].

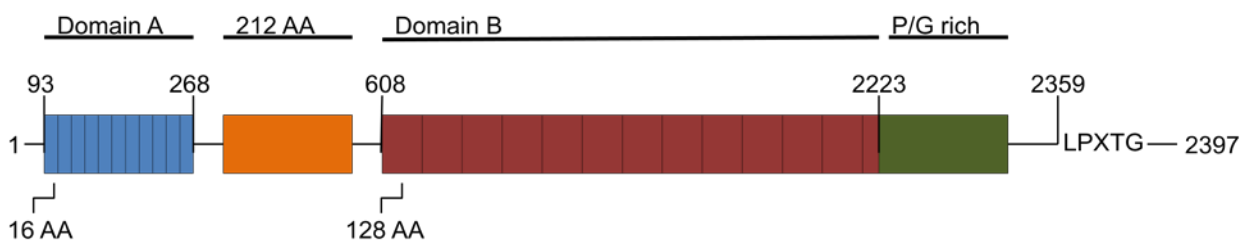


Fig. I-6: Schematic structure of Aap. The image shows domain A, the procession side of 212 amino acids and domain B. The cell wall anchor motif consists of a G rich region and a LPXTG motif at the C-terminus [28, modified]. The whole protein has a size of ~ 220 KDa [95].

I.4. Difficulties to combat *S. epidermidis* biofilm infections

The disruption of a once matured biofilm on a medical device is challenging and in the majority of cases only the removal of the implant can palliate infection. But this usually implies a second surgery, new risks for the patient and a following infection [1]. The protection of *S. epidermidis* biofilms from disruption through phagocytosis, antimicrobial agents, or antibiotics is given by different mechanisms. Usually the human immune system disrupts planktonic bacterial cells by phagocytosis through macrophages and neutrophils [45]. Also defensins, cathelicidins, lysozymes and reactive oxygen species define the antimicrobial activity of neutrophils, while macrophages produce proinflammatory cytokines, as well as reactive oxygen and nitrogen species [45, 100]. Dying phagocytes release lytic enzymes that are capable of killing planktonic bacterial cells [45]. These strategies are decreased once the bacterial cells are organized in a biofilm. Furthermore, extracellular binding proteins such as Embp in *S. epidermidis*, Ebh in *S. aureus* and Emb in *Streptococcus defectivus* lead to a strong attachment to serum proteins such as fibronectin, fibrinogen, vitronectin, collagen, thrombospondin, bone sialoprotein, von Willebrand factor and elastin [35, 37, 38, 39]. In the case of *S. aureus* the fibronectin binding protein can act invasive due to its property to form a bridge between the bacterium and the integrin on the surface of nonprofessional phagocytes [39]. Not only the mechanical obstacles and insufficient contact between macrophages and bacterial cells due to biofilm matrix prevent

uptake [100]. Alternate activation of macrophages by bacterial compounds lead to increased urea and ornithine production and activates collagen formation and tissue remodeling instead of phagocytosis [45]. As already mentioned collagen is a biofilm attachment supporting substance [46]. The weak proinflammatory activation results from insufficient NF- κ B-mediated macrophage response and less IL-1 β production [100]. Biofilm positive strains such as 1457, 5179 and M135 show less effective NF- κ B activation, indicating that this mechanism is not linked to a specific extracellular matrix compound, but more to biofilm formation itself [100]. Bacterial cells organized in biofilms are less susceptible to effector mechanisms of the host immune system or being killed by antimicrobial peptides [15, 16]. Furthermore the production of biofilm matrix components such as PIA, Aap and Embp increase resistance against antimicrobials, antibiotics and disinfectants [7, 17]. Therefore it is important to disrupt the biofilm matrix in order to make them vulnerable for phagocytotic killing, antimicrobials and disinfectants [7, 57, 95]. Another idea to combat staphylococcal infection is to interfere with the quorum sensing system of Staphylococci, specifically the *agr* system that is involved in the natural detachment process [101]. But experiments with *agr* mutants showed the opposite effect and led to increased virulence, biofilm formation, primary attachment and higher AtlE production [99, 101]. Even biofilm negative strains developed the ability to form biofilms after *agr* deletion and controlled PIA expression [99]. The addition of cross inhibiting peptides unfortunately mimicks an *agr* mutation and lead to higher virulence too [99]. Additionally the immune system responds to staphylococcal infections with an increasing Zn²⁺ level up to 12-16 μ M in plasma indicating cytokine release and a boost of the immune system [28]. This increased Zn²⁺ level leads to extensive adhesive contact between the G5 domains of Aap molecules, forming a “zinc-zipper”, which means that intercellular adhesion inside the biofilm becomes stronger and acts as a defense mechanism against immune cell action [28, 96].

The disintegration of the biofilm must be a sensitizing process that offers new strategies to attack and remove persisting biofilms. One way to achieve this could be the interference with the regulators of the *icaADBC*-expression and PIA-synthesis [18]. Due to the complexity of this system this way is not very promising. Another way to perish an infection could be the enzymatic disruption of the extracellular matrix.

I.5. Anti-Biofilm treatment

The most important and common treatment of bacterial infections are antibiotics. Depending on the drug it is given oral, or as infusion. But antibiotic treatment seems not to be effective against microorganisms organized in biofilms [56]. Due to reduced growth rates of bacterial cells in biofilms they are less susceptible for antibacterial treatment especially with β -lactames that require fast growth rates for proper function [104]. Amino glycoside antibiotics bind to the biofilm matrix which leads to limited antibiotic access [104]. Other physiological changes, as well as the protective matrix and especially the development of

subpopulations called persister cells play major roles in antibiotic resistance [1, 97, 104]. These persister cells are resistant against antimicrobials and grow independently from the rest of the biofilm, while they can stand antibiotic concentrations that usually eradicate planktonic cells [1, 105]. Persister cells develop during stationary phase of biofilm growth and are able to form new colonies after antibiotic treatment and death of all other cells [104]. Another problem is the increasing count of menacing resistances in Staphylococci, e.g. against methicillin. This resistance causes the well known MRSA and MRSE (methicillin resistant *S. aureus* and *S. epidermidis*) that are responsible for the majority of nosocomial infections [1]. Additionally to that Staphylococci develop increasing resistances and further more dispose of efflux transporter, that are capable of exporting tetracycline-like antibiotics [1, 96]. Some biofilm forming bacteria such as *P. aeruginosa* also developed multidrug pumps to avoid antibiotic killing [104]. Some antibiotics, such as linezolid and vancomycin also show biofilm supporting properties by up regulation of genes responsible for major biofilm proteins like *icaA*, *atlE* and *aap* in *S. epidermidis* RP62A [29]. Furthermore some strains have developed a linezolid resistance [96]. So far research concentrated on preventing biofilm formation via coating of implants and biofilm associated materials. Some agents such as EDTA seem to be promising substances to prevent biofilm formation of *S. epidermidis* on polychloride vinyl biomaterials but not usable for the treatment of mature biofilms [40]. Ideas of treating *S. aureus* and *P. aeruginosa* biofilms with honey showed effects, due to antimicrobial effects of honey [61]. And sodium salicylate has been reported to inhibit staphylococcal biofilm formation [106]. Novel natural components, small molecules and peptides as well as ionized gases are currently tested for their antimicrobial activity [97]. Mechanical ways to detach a biofilm could be ultrasonication, or the use of a direct electric field to make the bacterial cells vulnerable to antibiotics [1, 107].

I.5.1. Dispersin B (DspB)

The most promising agent to disrupt mature *S. epidermidis* biofilms so far is Dispersin B, a glycoside hydrolase [19]. This PIA-degrading hexosaminidase has been identified in *A. actinomycetemcomitans* [19, 58, 102]. DspB specifically hydrolysis β -1,6-glycosidic bonds and interferes with *S. epidermidis* biofilms by cleaving PIA [21, 102]. The complex structure of PIA gets degraded into glycosaminoglycans, total hexosamines and low-sulfated polysaccharides leading to detachment of the bacterial cells [102]. This means it destroys the extracellular matrix of the biofilms effectively, but without killing the bacteria. After heat-inactivation, DspB does not show any effect and is so far the only identified enzyme to disrupt PIA [102]. Catheters coated with triclosan and DspB showed an antimicrobial effect and prevent infection [58].

This proves that bacterial derived enzymes can serve as tools to specifically disrupt staphylococcal exopolysaccharide matrix structures. It is very likely that more of those enzymes can be identified by screening metagenomic libraries from environmental samples.

Metagenomics is one of the key technologies to identify new enzymes and antimicrobials [48, 49]. There is high potential to also discover substances degrading not only *S. epidermidis* biofilms, but other biofilm matrix structures e.g. Gram negative bacterial biofilms. Several polysaccharide modifying enzymes have already been discovered in metagenomic libraries [20, 50].

I.6. Intention of this work

Understanding the spatial distribution of proteins and polysaccharides inside *S. epidermidis* biofilms is a major point in perishing infections. The knowledge of protein functions in detail is necessary for the comprehension of each step during biofilm formation. Determining Sbp as the surface attachment protein, as well as clarifying the functions of each sub-domain of Aap during accumulation have been important tasks in this work. Furthermore, the role of Embp expressed in combination with PIA could show interesting facts in the co-localization of biofilm forming factors, not least because Embp is known to form very weak biofilms. Experiments with different antibiotics should purge the role of stress induced biofilm formation and show the difficulties in biofilm treatment. In addition the role of macrophages should be settled.

The second part of this work was focused on the characterization of 3 fosmid clones encoding genes capable of disrupting mature *S. epidermidis* 1457 biofilms. The clones have been sequenced and analyzed with different bioinformatic tools to predict putative biofilm disrupting enzymes. Over expression experiments should enable a distinct biochemical analysis. The characterization of the fosmid clone extracts using microscopy and Live/dead staining should reveal their destroying abilities. To determine highly potential candidates gel filtration and mass spectrometry have been performed.

II. Material and Methods

II.1. General materials for microbiological research

II.1.1. Culture mediums and additive components

All following mediums have been autoclaved for 20 min at 121 °C. All heat instable components and antibiotics have been filter sterilized and added to the medium (cooled down to 56 °C).

II.1.1.1. TSB-Medium by BD (BD, Madison, USA)

TSB-Medium by BBL	30 g
H ₂ O _{bidest.}	ad 1.000 mL

II.1.1.2. Luria-Bertani (LB)-Medium and Agar

Peptone	10 g	For Agar-plates add	15 g Agar
Yeast extract	5 g		
NaCl	5 g	H ₂ O _{bidest.}	ad 1000 mL

II.1.1.3. SOC Medium

Tryptone	20 g	MgSO ₄ *7 H ₂ O	10 mM
NaCl	0,6 g	Glucose	20 mM
Yeast extract	5 g		
KCl	0,2 g	H ₂ O _{bidest.}	ad 1000 mL
MgCl ₂ *6 H ₂ O	10 mM	Final pH 6.8 - 7.0	

The medium was autoclaved for 20 min at 121 °C without the Magnesium solution. 10 mL/L magnesium solution composed of 1 M MgCl₂*6 H₂O and 1M MgSO₄*7 H₂O were added after autoclaving.

II.1.1.4. BM Broth and Agar

Tryptone	10 g	For Agar-plates add	15 g Agar
NaCl	5 g		
Yeast extract	5 g		
K ₂ HPO ₄	1 g		
Glucose	1 g	H ₂ O _{bidest.}	ad 1000 mL

II.1.1.5. BHI Broth and Agar

Brain-Heart Infusion Medium (OXOID)	30 g	For Agar-plates add	15 g Agar
		For Soft agar-plates add	7 g Agar
		H ₂ O _{bidest.}	ad 1000 mL

II.1.1.6. BHI+ Broth

Brain-Heart Infusion Medium (OXOID)	3 g		
NaCitrat	1,76 g	H ₂ O _{bidest.}	ad 100 mL

II.1.1.7. STA Agar and Soft agar

Nutrient Broth No.2 (OXOID)	20 g	For Agar-plates add	15 g Agar
		For Soft agar-plates add	7 g Agar
NaCl	5 g		
CaCl ₂	0,4 g	H ₂ O _{bidest.}	ad 1000 mL

II.1.1.8. NB2+ Broth

Nutrient Broth No.2 (OXOID)	20 g		
CaCl ₂	0,4 g	H ₂ O _{bidest.}	ad 1000 mL

II.1.1.9. YPD Medium and Agar

Yeast Extract	10 g	For Agar-plates add	15 g Agar
Peptone	20 g		
Glucose	2 %	H ₂ O _{bidest.}	ad 1000 mL

The medium was autoclaved for 20 min at 121 °C then 100 mL of sterile 20 % Glucose solution have been added after cooling down.

II.1.1.10. B2

Caseinhydrolysate	10 g	Glucose	5 g
Yeast extract	25 g	NaCl	25 g
K ₂ HPO ₄	1 g	H ₂ O _{bidest.}	ad 1000 mL

II.1.1.11. Additive components

All used additives and antibiotics are enlisted in table II-1 in their finally used concentration.

Table II-1: Used additives and antibiotics in their final concentration

Additive/Antibiotic	Final Concentration	Solvent liquid
Chloramphenicol	10-12,5 µg/mL	96 % EtOH
Ampicillin	100 µg/mL	H ₂ O _{bidest.}
Kanamycin	50 µg/mL	H ₂ O _{bidest.}
Gentamicin	<i>E. coli</i> : 15 µg/mL <i>P. antarctica</i> : 50 µg/mL	H ₂ O _{bidest.}
Zeocin	100 µg/mL	H ₂ O _{bidest.}
Tetracycline	10 µg/mL	Methanol
Erythromycin	10 µg/mL	Methanol
Tigecycline	36 µg-0,3 ng/mL	H ₂ O _{bidest.}
Anhydrotetracycline	0,2 µg/mL	Methanol
Linezolid	2,1 – 125 µg/mL	H ₂ O _{bidest.}
IPTG	100 µg/mL	H ₂ O _{bidest.}
X-Gal	50 µg/mL	DMF
Xylose	2 %	H ₂ O _{bidest.}

II.1.2. Used bacterial strains, vectors and primers

All in this thesis used bacterial strains, vectors and primers can be found in table II-2, II-3 and II-4.

Table II-2: Bacterial strains used in this study

Strain	Properties	Supplier
<i>E. coli</i> Top10 DH10B	<i>recA, endA1, lacZΔM15, mcrA, mcrB, mcrC, mrr</i>	Invitrogen (Karlsruhe, Germany)
<i>E. coli</i> DH5α	<i>recA, endA1, lacZΔM15, hsdR17(r_K-m_K+), supE44, thi-1, gyrA96, relA1</i>	Invitrogen (Karlsruhe, Germany)
<i>E. coli</i> XL 1- Blue	<i>recA, endA1, gyrA96, thi-1, hsdR17, supE44, relA1, F'[pro AB lacIq lacZΔM15, Tn10 (Tet_r)]</i>	Invitrogen (Karlsruhe, Germany)
<i>E. coli</i> BL 21 Star™	<i>F⁻, ompT, hsdS_B (r_B⁻, m_B⁻), dcm, gal, λ(DE3), pLysS, Cm^R</i>	Invitrogen (Karlsruhe, Germany)
<i>E. coli</i> BL 21 AI	<i>F⁻ ompT hsdS_B (r_B⁻ m_B⁻) gal dcm araB::T7RNAP-tetA</i>	Lifetechnologies (Darmstadt, Germany)
<i>E. coli</i> BL 21 DE3	<i>fhuA2 [lon] ompT gal (λ DE3) [dcm] ΔhsdS λ DE3 = λ sBamHI ΔEcoRI-B int::(lacI::PlacUV5::T7 gene1) i21 Δnin5</i>	Lifetechnologies (Darmstadt, Germany)
<i>E. coli</i> Stellar	<i>F⁻, ara, Δ(lac-proAB) [Φ80d lacZΔM15], rpsL(str), thi, Δ(mrr-hsdRMS-mcrBC), ΔmcrA, dam, dcm</i>	Clontech (Mountain View, California, USA)
<i>Pseudomonas antarctica</i>	Wildtype	AG Streit, University of Hamburg
<i>Pichia pastoris</i> X-33	Wildtype	Lifetechnologies (Darmstadt, Germany)
<i>Pichia pastoris</i> SMD1168H	<i>His4, pep4</i>	Lifetechnologies (Darmstadt, Germany)

Strain	Properties	Supplier
<i>Staphylococcus epidermidis</i> 1457	Wildtype, <i>icaADBC</i> -positive, biofilm positive, Embp-negative	Isolated from medical devices (UKE, Hamburg)
<i>Staphylococcus aureus</i> RN 4220	<i>hsdR</i> ⁻ , Wildtype, Strain for electroporation	AG Rohde, UKE, Hamburg
<i>Staphylococcus aureus</i> M12	Strain for electroporation and phage transduction into <i>S. epidermidis</i> 1457	AG Rohde, UKE, Hamburg
<i>Staphylococcus epidermidis</i> 1457xpCN57 <i>tetM::rfp</i>	<i>icaADBC</i> -positive, biofilm positive, Embp-positive, Tet ^R , <i>rfp</i>	AG Rohde, UKE, Hamburg
<i>Staphylococcus epidermidis</i> 1457xpCM29	<i>icaADBC</i> -positive, biofilm positive, Embp-positive, Chl ^R , <i>gfp</i>	AG Rohde, UKE, Hamburg Incl. [98]
<i>Staphylococcus epidermidis</i> 1457Δ <i>aap::tetM</i>	<i>icaADBC</i> -positive, biofilm negative, Sbp- positive, Embp-positive, Tet ^R	AG Rohde, UKE, Hamburg
<i>Staphylococcus epidermidis</i> 1457Δ <i>aap::tetM</i> xpCN57::DomAeCX	<i>icaADBC</i> -positive, biofilm negative, Sbp- positive, Embp-positive, only Domain A of Aap, Chl ^R	This work
<i>Staphylococcus epidermidis</i> 1457Δ <i>aap::tetM</i> xpCN57::DomB	<i>icaADBC</i> -positive, biofilm negative, Sbp- positive, Embp-positive, only Domain B of Aap, Chl ^R	This work
<i>Staphylococcus epidermidis</i> 1457Δ <i>aap::tetM</i> xpCN57::DomB+212	<i>icaADBC</i> -positive, biofilm negative, Sbp- positive, Embp-positive, only Domain B+212 of Aap, Chl ^R	This work
<i>Staphylococcus epidermidis</i> 1457Δ <i>aap</i> Δ <i>sbp</i> xpCM29	<i>icaADBC</i> -positive, biofilm negative, Aap-, Sbp- negative, Embp-positive, Chl ^R , <i>gfp</i>	AG Rohde, UKE, Hamburg incl. [98]

Strain	Properties	Supplier
<i>Staphylococcus epidermidis</i> 1457Δ <i>aap</i> :: <i>tetM</i> xpCM29	<i>icaADBC</i> -positive, biofilm negative, Sbp-, Embp-positive, Chl ^R , <i>gfp</i>	AG Rohde, UKE, Hamburg incl. [98]
<i>Staphylococcus epidermidis</i> 1457Δ <i>aap</i> Δ <i>sbp</i>	<i>icaADBC</i> -positive, biofilm negative, Aap-, Sbp- negative, Embp-positive, Tet ^R	AG Rohde, UKE, Hamburg
<i>Staphylococcus epidermidis</i> 1457Δ <i>sbp</i> xpCM29	<i>icaADBC</i> -positive, biofilm positive, Aap-positive, Sbp-negative, Embp-positive, Chl ^R , <i>gfp</i>	AG Rohde, UKE, Hamburg incl. [98]
<i>Staphylococcus epidermidis</i> 1457Δ <i>sbp</i> xpRBSbpFLAG ₃	<i>icaADBC</i> -positive, biofilm positive, Aap-, Embp-positive, Sbp 3-FLAG tag, Chl ^R , Tet ^R	AG Rohde, UKE, Hamburg
<i>Staphylococcus epidermidis</i> 1457Δ <i>sbp</i> pRBSbpFLAG3xpCM29	<i>icaADBC</i> -positive, biofilm positive, Aap-, Embp-positive, Sbp 3-FLAG tag, Chl ^R , Tet ^R , <i>gfp</i>	AG Rohde, UKE, Hamburg incl. [98]
<i>Staphylococcus epidermidis</i> 1457Δ <i>aap</i> :: <i>tetM</i> Δ <i>sbp</i> xpRBSbpFLAG	<i>icaADBC</i> -positive, biofilm positive, Aap-negative, Sbp FLAG Tag, Embp-positive, Chl ^R , <i>gfp</i>	AG Rohde, UKE, Hamburg
<i>Staphylococcus epidermidis</i> 1457-M10	biofilm negative, Aap-, Sbp-, Embp-positive, Ery ^R	AG Rohde, UKE, Hamburg
<i>Staphylococcus epidermidis</i> 1457-M10xpCM29	biofilm negative, <i>icaA</i> ::Tn917 insertion, Aap-, Sbp-, Embp-positive, Chl ^R	AG Rohde, UKE, Hamburg incl. [98]
<i>Staphylococcus epidermidis</i> 1457-M10Δ <i>aap</i> Δ <i>sbp</i> xpCM29	biofilm negative, <i>icaA</i> ::Tn917 insertion, Aap-, Sbp-negative, Embp-positive, Chl ^R , <i>gfp</i>	AG Rohde, UKE, Hamburg incl. [98]
<i>Staphylococcus epidermidis</i> 1457-M10Δ <i>aap</i> xpCM29	biofilm negative, <i>icaA</i> ::Tn917 insertion, Aap- & Embp-positive, Sbp- negative, Chl ^R , <i>gfp</i>	AG Rohde, UKE, Hamburg incl. [98]

Strain	Properties	Supplier
<i>Staphylococcus epidermidis</i> 1457-M10Δ <i>aap</i> Δ <i>sbp</i>	biofilm negative, <i>icaA</i> ::Tn917 insertion, Aap-, Sbp-negative, Embp-positive, Tet ^R , Ery ^R	AG Rohde, UKE, Hamburg
<i>Staphylococcus epidermidis</i> 1457-M10Δ <i>aap</i> :: <i>tetM</i> xpCN57::DomAeCX	<i>icaADBC</i> -positive, <i>icaA</i> ::Tn917 insertion, biofilm negative, Aap-, Sbp- positive, Embp-positive, Chl ^R	This work
<i>Staphylococcus epidermidis</i> 1457-M10Δ <i>aap</i> :: <i>tetM</i> xpCN57::DomB+212	<i>icaADBC</i> -positive, biofilm negative, Aap-, Sbp- positive, Embp-positive, Chl ^R	This work
<i>Staphylococcus epidermidis</i> 1457-M10Δ <i>aap</i> Δ <i>sbp</i> xpCN57Dom::AeCX	<i>icaADBC</i> -positive, biofilm negative, Aap-, Sbp- positive, Embp-positive, Chl ^R	This work
<i>Staphylococcus epidermidis</i> 1457-M10Δ <i>aap</i> Δ <i>sbp</i> xpCN57::DomB	<i>icaADBC</i> -positive, biofilm negative, Aap-, Sbp- positive, Embp-positive, Chl ^R	This work
<i>Staphylococcus epidermidis</i> 1457-M10Δ <i>aap</i> Δ <i>sbp</i> xpCN57::DomB+212	<i>icaADBC</i> -positive, biofilm negative, Aap-, Sbp- positive, Embp-positive, Chl ^R	This work
<i>Staphylococcus epidermidis</i> 1457-M10Δ <i>sbp</i> xpCM29	biofilm positive, Aap-positive, Sbp- negative, Embp-positive, Chl ^R , <i>gfp</i>	AG Rohde, UKE, Hamburg incl. [98]
<i>Staphylococcus epidermidis</i> 1457-M10Δ <i>aap</i> Δ <i>sbp</i> xpRB::DomB	biofilm negative, Aap-, Sbp-negative, Embp-positive, expressing Domain B of Aap, Chl ^R , <i>gfp</i>	AG Rohde, UKE, Hamburg
<i>Staphylococcus epidermidis</i> 1457-M10Δ <i>aap</i> xpRB::DomB	biofilm negative, Aap-negative, Sbp-, Embp-positive, expressing Domain B of Aap, Chl ^R , <i>gfp</i>	AG Rohde, UKE, Hamburg
<i>Staphylococcus epidermidis</i> 1585 Ra	<i>icaADBC</i> -negative, biofilm & Embp-positive	UKE, Hamburg

Strain	Properties	Supplier
<i>Staphylococcus epidermidis</i> 1585 <i>p_{xyI/tet}::embp</i>	biofilm negative, Aap-, Sbp-, Embp-positive, Embp inducible with 0,125 µg/mL Tet, Ery ^R	AG Rohde, UKE, Hamburg
<i>Staphylococcus epidermidis</i> 1585 <i>p_{xyI/tet}::embpxpTXica xpCM29</i>	biofilm negative, Aap-, Sbp-, Embp-positive, Embp inducible with 5 µg/mL Tet, PIA inducible with 2 % Xylose, Ery ^R , <i>gfp</i> , Tet ^R , Chl ^R	This work incl. [98]
<i>Staphylococcus epidermidis</i> 1585 <i>pTXicaxpCM29</i>	biofilm negative, Aap-, Sbp-, Embp-positive, PIA inducible with 2 % Xylose, <i>gfp</i> , Chl ^R	This work incl. [98]
<i>Staphylococcus epidermidis</i> 1585 <i>p_{xyI/tet}::embpxpCM29</i>	biofilm negative, Aap-, Sbp-, Embp-positive, Embp inducible with 0,125 µg/mL Tet, Ery ^R , <i>gfp</i> , Chl ^R	This work incl. [98]
<i>Staphylococcus aureus</i> PS187Δ <i>hsdR</i> Δ <i>sau</i> USI	<i>hsdR, sau</i> Strain for electroporation and further phage transduction in <i>S. epidermidis</i> 1457	AG Peschel, University of Tübingen

Table II-3: Vectors used in this study

Vector	Properties	Size [kb]	Supplier	Vector map (Appendix)
pUC19	Cloning vector pUC, Amp ^R , <i>lacZ</i> α , pMB1 ori	2,6	Fermentas (St. Leon Rot, Germany)	2.3
pBluescript II SK+	Cloning vector pUC, Plac, <i>lacZ</i> , T7 Promotor, T3 Promotor, Amp ^R	3,0	Agilent Technologies (La Jolla, USA)	2.1
pDrive	Cloning vector pUC, <i>lacZ</i> , T7 Promotor, SP6 Promotor, Kan ^R , Amp ^R	3,85	Qiagen (Hilden, Germany)	2.13
pTZ19r	Cloning vector pUC, <i>lacZ</i> , f1 packaging site, Amp ^R , <i>Chl</i> ^R	3,1	Thermo Scientific (Waltham, USA) modified at AG Streit (Hamburg, Germany)	2.12
pCC1FOS	fosmid vector <i>Chl</i> ^R , <i>lacZ</i> , <i>cos</i> site, <i>loxP</i> , T7 Promotor	8,1	Epicentre (Madison, USA)	2.2
pBBR-MCS 5	broad-host-range-Vector pBluescript II KS- <i>lacZ</i> α -Polylinker, P _{<i>lacZ</i>} , Gm ^R	4,7	AG Streit (University of Hamburg, Germany)	2.9
pET 19b	Expression vector pBR322, <i>lacO</i> , <i>lacI</i> , T7 Promotor, T7 transl_en_RBS, T7 Terminator, Amp ^R , His Tag	5,7	Merck Millipore (Darmstadt, Germany)	2.5

Vector	Properties	Size [kb]	Supplier	Vector map (Appendix)
pET 21a	Expression vector pBR322, T7 pro, T7 trans, T7 tag, MCS, His Tag, T7 term, <i>lacI</i> , <i>bla</i> , Amp ^R , f1 ori	5,4	Merck Millipore (Darmstadt, Germany)	2.4
pBad/Myc His A	Expression vector pBR322, <i>araBad</i> pro, MCS, <i>myc</i> epitope, Polyhis tag, <i>rrnB</i> transfer reg, AraC ORF, Amp ^R	4,1	Invitrogen (Darmstadt, Germany)	2.14
pMALc2x	Expression vector MBP tag, MCS, <i>malE</i> , P _{tag} pro, Amp ^R	6,6	NEB (Frankfurt am Main, Germany)	2.11
pENTR	Entry vector pUC, <i>rrnB</i> T1 & T2, <i>attL</i> 1 & 2. TOPO cloning site, T7 pro, M13 rev, Kan ^R	2,5	Invitrogen (Darmstadt, Germany)	2.6
pDEST17	Expression vector pBR322, T7 pro, RBS, 6x His Tag, <i>attR</i> 1 & 2, Cm ^R , <i>ccdB</i> , T7 term, <i>bla</i> pro, Amp ^R , <i>ROP</i> ORF	6,3	Invitrogen (Darmstadt, Germany)	2.8
pDEST15	Expression vector pBR322, T7 pro, RBS, GST Tag, <i>attR</i> 1 & 2, Cm ^R , <i>ccdB</i> , T7 term, <i>bla</i> pro, Amp ^R , <i>ROP</i> ORF	7,0	Invitrogen (Darmstadt, Germany)	2.7

Vector	Properties	Size [kb]	Supplier	Vector map (Appendix)
pFLD1	Yeast Expression vector pUC, <i>FLD1</i> pro, MCS, V5 epitope, 6x His Tag, <i>AOX1</i> trans, 3' <i>AOX1</i> prim, <i>bla</i> pro, Amp ^R , <i>TEF1</i> pro, T7 pro, Ze ^R , <i>CYC1</i> trans	4,4	Life Technologies (Waltham, USA)	2.10
pTXica	PIA coding with 2 % Xylose inducible vector		AG Rohde (UKE, Hamburg, Germany)	
pCN:: p _{xyI/tet}	ChI ^R , Tet inducible promotor		AG Rohde (UKE, Hamburg, Germany)	2.15
Promotor to induce Embp production				
p _{xyI/tet} :: <i>embp</i>	Embp promotor, inducible with 0,125 µg/mL Tet		[35]	

Table II-4: Oligonucleotides used in this study

Primer	Sequence (5' - 3')	GC [mol %]	Tm [°C]	Amplified region	Supplier/ Reference
M13-20 for	GTAAAACGACGGC CAGT	52,9	60,4	Inserts in pUC plasmids and M13 vectors	Eurofins MWG Operon (Köln, Germany)
M13 rev	CAGGAAACAGCTAT GACC	50,0	58,4		Eurofins MWG Operon (Köln, Germany)
T 7 Pro Primer	TAATACGACTCACT ATAGGG	40	56,3	Universal sequencing primer for T7 promotor vectors	Eurofins MWG Operon (Ebersberg, Germany)

II. Material and Methods

Primer	Sequence (5' - 3')	GC [mol %]	Tm [°C]	Amplified region	Supplier/ Reference
pCC1Fos/ EpiFos-5 rev	CTCGTATGTTGTGT GGAATTGTGAGC	46	65	Inserts in pCC1FOS vector (reverse), combined with T7 Pro	Epicentre Biotechnologies (Madison, USA)
N-Ace_for_EcoRI	GGAATTCGCCTTAT TCCCG	52,6	56,3	N-acyl-transferase with EcoRI restriction site, combine with IF_N-Ac_rev_XhoI	Eurofins MWG Operon (Ebersberg, Germany)
AH_for_NdeI_pET	GGAGCGCCATATG ATGCGGATTTTG	52	55,3	Amido hydrolase restriction sites for pET vector	Eurofins MWG Operon (Ebersberg, Germany)
AH_rev_NdeI_pET	TTCGCTCGAGGCTA CTTG	55,6	55,3		Eurofins MWG Operon (Ebersberg, Germany)
DH_rev_XhoI_pET	TTCGCTCGAGAAGG CTAATGC	52,4	60,5	Dehydrogenase with XhoI (reverse) and NdeI (forward) restriction site for pET vector	Eurofins MWG Operon (Ebersberg, Germany)
DH_for_NdeI_pET	CGGAGCTCCATATG ATGCTTGACCTTTC	50	60,5		Eurofins MWG Operon (Ebersberg, Germany)
PO_rev_BamHI_pET	CGCGGATCCAAAG GTCAAG	57,9	59,4	Peroxidase with BamHI (reverse) and NdeI (forward) restriction sites for pET vector	Eurofins MWG Operon (Ebersberg, Germany)
PO_for_NdeI_pET	GGAGCGCCATATG ATGAATCGAATTAA AG	41,4	59,4		Eurofins MWG Operon (Ebersberg, Germany)

Primer	Sequence (5' - 3')	GC [mol %]	Tm [°C]	Amplified region	Supplier/ Reference
GT3 for PstI (pMALc2x)	CTGCAGAAGATTCT ACTC	44,4	51,4	Glycosyltransferase 3 with HindIII (reverse) and PstI (forward) restriction sites for pMalc2x vector	Eurofins MWG Operon (Ebersberg, Germany)
GT3 rev HindIII (pMALc2x)	AAGCTTTCATCGGG TTG	47,1	50,4		Eurofins MWG Operon (Ebersberg, Germany)
GT3_for_KpnI_pFL (<i>Pichia pastoris</i>)	GGTACCGAAATGA AGATTCTACTCTC	42,3	51,6	Glycosyltransferase 3 with ApaI (reverse) and KpnI (forward) restriction sites for pFLD vector	Eurofins MWG Operon (Ebersberg, Germany)
GT3_rev_ApaI_pFL (<i>Pichia pastoris</i>)	GGGCCCTCGGGTT GGGATC	73,7	51,6		Eurofins MWG Operon (Ebersberg, Germany)
N-A_rev_EcoRI_pFL (<i>Pichia pastoris</i>)	GAATTCTTCCCGCC GGCTG	63,2	56,8	N-acyltransferase with EcoRI restriction sites for pFLD vector	Eurofins MWG Operon (Ebersberg, Germany)
N-A_for_EcoRI_pFL (<i>Pichia pastoris</i>)	GAATTCGAAATGAT CGGTTGGGATTTCC	42,9	56,8		Eurofins MWG Operon (Ebersberg, Germany)
PET_for_KpnI_pFLD (<i>Pichia pastoris</i>)	GGTACCGAAATGC GTTTCAGCAGC	54,2	64,4	Polysaccharid export protein with XhoI (reverse) and KpnI (forward) restriction sites for pFLD vector	Eurofins MWG Operon (Ebersberg, Germany)
PET_rev_XhoI_pFL (<i>Pichia pastoris</i>)	CTCGAGCCTGCGCC AAACGAG	66,7	65,7		Eurofins MWG Operon (Ebersberg, Germany)
IF_GT3_for_KpnI (<i>Pichia pastoris</i> , Infusion Cloning)	TCTCGGATCGGTAC CGAAATGTCTTCCG TTTACCG	51,4	57,0	Glycosyltransferase 3 KpnI (forward) restriction site	Eurofins MWG Operon (Ebersberg, Germany)

II. Material and Methods

Primer	Sequence (5' - 3')	GC [mol %]	Tm [°C]	Amplified region	Supplier/ Reference
IF_GT3_rev_Apal (<i>Pichia pastoris</i> , Infusion Cloning)	ACCCCAATTGGGCC CTCGGGTTGGGATC C	66,7	57,0	Glycosyltrans ferase 3 with Apal (reverse) restriction site	Eurofins MWG Operon (Ebersberg, Germany)
IF_N-Ac_for_KpnI (<i>Pichia pastoris</i> , Infusion Cloning)	TCTCGGATCGGTAC CGAAATGATCGGTT GGGATTTCC	51,4	57,9	N-acyl- transferase with XhoI (reverse) and KpnI (forward) restriction sites	Eurofins MWG Operon (Ebersberg, Germany)
IF_N- Ac_rev_XhoI (<i>Pichia pastoris</i> , Infusion Cloning)	CCGCCGCGGCTCGA GTTCCCGCCGGCTG	82,1	57,9		Eurofins MWG Operon (Ebersberg, Germany)
IF_GT3_for_1278 (<i>Pichia pastoris</i> , Infusion Cloning)	TCTCGGATCGGTAC CGAAATGAAGATTC TACTCTCGGCG	51,3	57,0	Glycosyltrans ferase 3 forward (no restriction, only 1278 bp, small version), combine with any GT3 reverse primer	Eurofins MWG Operon (Ebersberg, Germany)
Aap_inv_for2	GGTACCGAGCTCG AATTCTTAAATACA TGGGAGGTATAAT	40	58,3	Aap full length for pCN::tetM	Eurofins MWG Operon (Ebersberg, Germany)
Aap_inv_for1	TACCGAGCTCGAAT TCTTAAATACATGG GAGGTATAAT	37	59	Aap full length for pCN::ChI	Eurofins MWG Operon (Ebersberg, Germany)
Aap_inv_rev	TTTAGAATAGGCGC GCCAGTTTTTATAT GAAATTATTTTCA TTACCT	29	60,2	Aap full length for pCN57::ChI	Eurofins MWG Operon (Ebersberg, Germany)

II. Material and Methods

Primer	Sequence (5' - 3')	GC [mol %]	Tm [°C]	Amplified region	Supplier/ Reference
Embp125Asc_for	TTATGCTGGCGCGC CGTACCCATACGAT GTTCCAGATTACGC TCCAGGTGATCAAA AATTACAAAAAGCA	45,7	>75	Embp125 region with Ascl restriction site (forward)	Eurofins MWG Operon (Ebersberg, Germany)
Embp_Asc_rev	TATGGGTAGGCGC GCCAGCATAATCAG GAACATCATAAGG ATAACCAGCATAAT CAGGAACATCATAA GGATATGGATGTA AATCGTTTTAGTT AAATGAATG	37,5	>75	Embp125 region with Ascl restriction site (reverse)	Eurofins MWG Operon (Ebersberg, Germany)
Embp125_att_rev	GGGGACCACTTTGT ACAAGAAAGCTGG GTAAGCAAGTTTTT GATCACCATG	45,1	>75	Embp125 region with att recognition site for BP-clonase (reverse)	Eurofins MWG Operon (Ebersberg, Germany)
Embp125_att_for ₂	GGGGACAAGTTTG TACAAAAAAGCAG GCTTATAAGGATAA CATCAACCATGTGA C	40	73,9	Embp125 region with att recognition site for BP-clonase (forward)	Eurofins MWG Operon (Ebersberg, Germany)
Uni_HIS_pFLD – rev	CTCGAGTCAATGAT GATGATGATGATG ATGGTCGACAC	45,7	69,5	Universal primer to add a HIS tag from pFLD into pBBR-MCS5 vector	Eurofins MWG Operon (Ebersberg, Germany)
N-Ace_His_rev	ACTATGATGATGAT GATGATGTTCCCGC CGGCTGCCCTC	53,8	63,6	N-acyl-transferase primer to add a HIS tag from pFLD into pBBR-MCS5 vector	Eurofins MWG Operon (Ebersberg, Germany)

II.1.3. Antibodies and Wheat germ agglutinin (WGA)

Table II-5 shows the antibodies and preconjugated wheat germ agglutinin compounds used in this study.

Table II-5: Specific antibodies used for Western Blots, Dot Blots and microscopic samples

Antibody / Dye	Monoclonal/Polyclonal	Visualization of	Dilution	Supplier
anti-PIA rabbit serum (DM-385-1-4)	Polyclonal	PIA	1:600	AG Rohde, UKE, Hamburg
Rabbit anti-rDomA serum	Polyclonal	Domain A of Aap	1:500 for Biofilmstaining	AG Rohde, UKE, Hamburg
Rabbit anti-rDomB serum	Polyclonal	Domain B and Domain B+212 of Aap	1:500 for Biofilmstaining	AG Rohde, UKE, Hamburg
Rabbit anti-rSbp serum (91435)	Polyclonal	Sbp	1:10.000 for Western-Blotting/Dot Blot	AG Rohde, UKE, Hamburg
Rabbit anti-rEmbp6559 serum	Polyclonal	Embp	1:500 for Biofilmstaining 1:10.000 for Western-Blotting/Dot Blot	AG Rohde, UKE, Hamburg
Rabbit anti-rEmbp7762 serum	Polyclonal, purified IgG fraction	Embp	1:500 for Biofilmstaining 1:10.000 for Western-Blotting/Dot Blot	AG Rohde, UKE, Hamburg
Anti-FLAG-Cy5	polyclonal, preconjugated with Cy5	FLAG-Tag	1:500 for Biofilmstaining	BIOSS
Anti-FLAG [®] M2 mouse labeled with Dylight 550	monoclonal, labeled with Dylight 550 kit	FLAG-Tag	1:250 for Biofilmstaining	Sigma-Aldrich (St. Louis, USA)

II. Material and Methods

Antibody	Monoclonal/Polyclonal	Visualization of	Dilution	Supplier
Dylight550	/	/	Used for conjugation to proteins/ antibodies	Dylight550 (Thermo Scientific, Waltham, USA)
Monoclonal Anti-polyhistidine-Alkaline Phosphatase, mouse	Monoclonal	HIS-Tag	1:10.000 for Western-Blotting/Dot Blot	Sigma-Aldrich (St. Louis, USA)
Anti-rabbit IgG Alexa Fluor 405	Monoclonal	Rabbit IgG (Blue Fluorescence)	1:500 for Biofilmstaining	Life technologies (Eugene, USA)
Anti-rabbit IgG Alexa Fluor 568	Monoclonal	Rabbit IgG (Far Red/Blue Fluorescence)	1:500 for Biofilmstaining	Life technologies (Eugene, USA)
Anti-rabbit IgG Cy5	Monoclonal	Rabbit IgG (Blue Fluorescence)	1:500 for Biofilmstaining	Life technologies (Eugene, USA)
WGA Alexa Fluor 647 conjugate		PIA (red fluorescence)	1:100 in a growing biofilm	Life technologies (Eugene, USA)
WGA Texas red-X conjugate		PIA (red fluorescence)	1:100 in a growing biofilm	Invitrogen (Eugene, USA)
Anti-rabbit IgG gold conjugated Protein A 10nm	Monoclonal	Gold Labeling	1:20 for electron microscopy	Aurion (Wageningen, Netherlands)

II.2. Culture conditions and storage

II.2.1. Culture Conditions of used bacterial strains

The culture conditions of all used bacterial strains can be found in table II-6.

Table II-6: Culture conditions of bacterial strains

Bacterial strain	Temperature [°C]	Shaker [rpm]	Incubation time
All <i>Staphylococcus</i> and <i>E. coli</i> strains on agar plates	37	0	1 to 3 days
All <i>Staphylococcus</i> and <i>E. coli</i> strains in liquid media	37	180 - 200	oN, maximum 24 hours
<i>Pseudomonas antarctica</i> on agar plates	22	0	1 to 3 days
<i>Pseudomonas antarctica</i> in liquid medium	22	180-200	1 to 3 days
<i>Pichia pastoris</i> strains on agar plates	30	0	2-4 days
<i>Pichia pastoris</i> strains in liquid medium	30	200	oN, for expression up to 5 days

All *Staphylococcus epidermidis* strains have been grown oN in 5 mL TSB-Medium. The next day the strains have been inoculated 1 % into 100 mL fresh TSB-Medium in a 300 mL Erlenmeyer flask. The flasks were incubated at 37 °C, shaking at 180 rpm until OD₆₀₀ reached 0,5 for further use in the Biofilm disintegration assay in Microtiterplates (II.3.1).

II.2.2. Culture bedding of bacterial strains

For further use of liquid bacterial cultures up to several days the cultures were placed in the fridge at 4 °C. Bacterial strains grown on agar plates were placed in the fridge at 4 °C up to 4 weeks, the agar plates were closed with Parafilm. For long term purpose aliquots of bacterial cultures were mixed with 86 % (m/V) sterile Glycerol_{aq} (ratio 3:2) and stored as cryo culture at -75 °C.

II.3. Strategies to screen metagenomic libraries

II.3.1. Biofilm disintegration assay in microwell plates

For biofilm formation of all used *S. epidermidis* strains microwell plates from Thermo Scientific (Nunclon™Δ Surface F, 96 wells) have been used.

200 µL of a *S. epidermidis* culture grown in TSB-Medium at 37 °C shaking at 180 rpm until $OD_{578} = 0,5$ have been pipetted into each well of the microwell plate using a multipipette (Eppendorf, Hamburg, Germany). To test for inhibition of biofilm formation the supernatant as well as the cell raw extracts of the fosmid clones have been tested. The fosmid clones gained in the overlay assay have been tested directly. Furthermore metagenomic plates that have not been tested in the overlay assay were tested by pooling 48 fosmid clones at a time. Those pools have been treated to gain cell supernatant as well as cell raw extract (II.3.2). Positive pools of fosmid clones have then been tested again in a pool of only 8 clones, then as single clones to determine the one fosmid clone inhibiting *S. epidermidis* cell growth. Single fosmid clones have then been investigated more thoroughly to identify the active gene.

The gained cell supernatant as well as cell raw extract have been added to the fresh *S. epidermidis* culture and incubated for 48 h at 37 °C, non-shaking.

To test Biofilm disintegration 200 µL of a *S. epidermidis* culture grown in TSB-Medium at 37 °C shaking at 180 rpm until $OD_{578} = 0,5$ have been pipetted into each well of the microwell plate using a multipipette (Eppendorf, Hamburg, Germany) and let grown for 24 h at 37 °C, non-shaking. After a biofilm has been formed cells supernatant as well as cell raw extract have been pipetted on the biofilm. The plates were incubated for 24 h at 37 °C, non-shaking.

After incubation all plates have been emptied by dumping the liquid out of the microwell plates. Then the plates were dried for approximately 1 h at 55 °C. Afterwards all microwell plates were stained with gentian violet. Therefore 50 µL of 100 % gentian violet have been pipetted on the dried biofilm and incubated for 1 min at RT. The color was then washed of carefully under a continuous waterflow in the sink. The plates dried at RT before they have been interpreted optically on a light table.

II.3.1.1. Preparation of cell supernatant and cell raw extract of fosmid clones

The metagenomic library build out of DNA of the sediment of the Elbe River (Teufelsbrück) has been stamped into 96well deep well plates, filled with 1 mL LB-medium per well and let grown oN at 37 °C shaking at 180 rpm. The next day 48 clones at a time were pooled into 50 mL Greinertubes and centrifuged (4 °C, 15 min, 4000 g). The supernatant has been stored for further use in 15 mL Falcon tubes at 4 °C. The cell pellet was then re suspended in 10 mL

PB-Buffer by pipetting or shaking. The cell suspension has then been treated with ultrasonic sound (UP 200 S/H, Hielscher, Germany) at a cycle of 0,5 and an amplitude of 50 – 65 % for 10 min. After sonification the cells have been centrifuged (4 °C, 15 min, 4000 g) and the supernatant (cell raw extract) has been stored for further use in 15 mL Falcon tubes at 4 °C. Pools of 8 fosmid clones have been treated equally, but were re suspended in only 1,6 mL PB-Buffer.

Single clones have been grown oN at 37 °C shaking at 180 rpm in 5 mL LB-medium and then treated as described above but the cells have been re suspended in only 500 µL PB-Buffer.

PB-Buffer (Phosphate Buffer) for 100 mL

Potassiumdihydrogenphosphate (KH ₂ PO ₄)	0,2 M	61 mL
Dipotassiumhydrogenphosphate (K ₂ HPO ₄)	0,2 M	39 mL

II.3.2. Large scale preparation of cell raw extract

To prepare a lot of the desired cell raw extract single clones have been grown in LB-medium containing Chloramphenicol (12,5 µg/mL) oN at 37 °C shaking at 180 – 200 rpm. Then the culture has been centrifuged at 5000 rpm at 4 °C for 15 min. The pellet has been re suspended in a quarter of the starting volume in 0,1 x PBS-buffer (e.g. starting volume of 60 mL, resuspension volume 15 mL). The cells have then been treated with ultrasonic for 5 cycles each (Cycle: 4 x 15 sec pulse on at 70 %, 4 x 5 sec pulse off for recovering). After each cycle one minute on ice to prevent overheating of the solution was given. The lysate has been centrifuged for 15 min at 5000 rpm and 4 °C. Afterwards the clear supernatant has been sterile filtered using a 0,22 µM filter. The sterile lysate could be stored at 4 °C for up to 7 days and has been used for further filtration (II.3.3), biofilm assay (II.3.1), microscopy (II.9) and PIA-preparation (II.3.4).

II.3.2.1. Filtration of cell raw extracts

Cell raw extracts have first been prepared as in II.3.3 and then been filtered through Amicon Ultra Filters (Millipore) to split the extract into fractions. Filters with pore sizes of 3, 10, 30, 50 and 100 KDa have been used. The extract was filled into the filter and then centrifuged at 4 °C and a maximum speed of 3500 rpm. The centrifugation time ranged from 1 to 50 min depending on the pore size and amount of extract.

Filtrates have been used either for biofilm assay (II.3.1), microscopy (II.7), or PIA-preparation (II.3.7).

To gain an extract sample for gel filtration only the flowthrough of the 100 KDa Amicon Ultra Filter has been used. 10 mL of this pre filtered extract has been concentrated to a final

volume of 1,5 – 2 mL using a 3 KDa Amicon Ultra Filter. The centrifugation time ranged from 40 - 60 min using 3500 rpm at 4 °C. The concentrated sample has then been used for gel filtration (II.3.5) and SDS-gel electrophoresis (II.6.4).

II.3.3. Gel filtration using Äkta System

To fraction the flow through of the 100 KDa Amicon Ultra Filter (II.3.2.1) gel filtration has been performed using a Super Dex 200 gel column (GE Healthcare, Chalfont St Giles, Great Britain) and the Äkta System. Using this method the extract could be separated by size in fractions of 1 mL each. These fractions have been used for biofilm assay (II.3.1) and SDS-gel electrophoresis (II.6.4).

Before loading the sample on the gel-column PBS-buffer had to be added to the sample to receive a final concentration of 0,5 x PBS-buffer.

Äkta program

- a) Washing and preparing the column with the appropriate buffer

To clean the gel column that was stored in 70 % Ethanol for long term storage the whole column was washed using ultrapure, sterile filtered water. It was flushed with a flow of 0,2 mL/min until 24 mL ran through the column. Then the column has been prepared with 0,5 x PBS-buffer (filter sterilized) at a flow of 0,4 mL/min until 24 mL of the buffer ran through the column.

- b) Loading the sample and collecting fractions

The prepared column was loaded with 2 mL of the sample at once. The sample ran through the column with 0,5 x PBS-buffer at a flow of 0,2 mL/min and fractions of 1 mL each have been collected. The UV measurement inside the Äkta system showed the appearance of proteins so that the system could be stopped after the last protein has been detected.

- c) Cleaning the column

After the whole sample ran through the gel column of the Äkta system, the whole system has been flushed with ultrapure, filter sterilized water over night at a flow of 0,1 mL/min for further usage. For long-term storage the column has been flushed with 70 % Ethanol after the water step.

II.3.3.1. Protein purification using the Äkta System

To purify a tagged protein the Äkta System has been used with the appropriate column, binding and elution buffer. Table II-7 shows the used columns and buffers specific for the tag of the over expressed protein.

Table II-7: Purification columns for the Äkta System

Tag	Column	Binding buffer	Elution buffer	Trap specifications
HIS	HisTrap FF (GE Healthcare, Uppsala, Sweden)	20 mM NaPO ₄ 250 mM Imidazol 500 mM NaCl pH 7,4	20 mM NaPO ₄ 40 mM Imidazol 500 mM NaCl	Max. Flow: 5 mL/min Max. Pressure: 0,7 MPa
GST	GSTTrap FF (GE Healthcare, Uppsala, Sweden)	140 mM NaCl 2,7 mM KCl 10 mM K ₂ HPO ₄ 1,8 mM KH ₂ PO ₄ pH 6,8	50 mM Tris 15 mM reduced Glutathione pH 8,5 (adj. with NaOH)	Max. Flow: 1 mL/min Max. Pressure: 0,3 MPa
MBP	MBPTrap HP (GE Healthcare, Uppsala, Sweden)	20 mM Tris-HCl 200 mM NaCl 1 mM EDTA pH 7,4	Binding buffer + 10 mM Maltose	Max. Flow: 20 mL/min Max. Pressure: 0,3 MPa

The Äkta System has been used with one program designed for the purification of tagged proteins. An overview of the program is given below (BB = binding buffer; EB = elution buffer; CV = column volume).

	HIS	GST	MBP
Equilibration	5 mL BB, 5 mL EB, 5 mL BB		
Binding of tagged protein	sample (5 mL) + 5 CV Binding buffer (25 mL)		Sample (1 mL) + 5 CV EB (5 mL)
Elution of tagged protein	5 CV EB (25 mL)	5 CV EB (25 mL)	5 CV EB (5 mL)

II.3.4. PIA-preparation and analysis

To determine whether the amount of the Polysaccharide intercellular adhesin (PIA) has been reduced, or fully diminished by the extracts of fosmid clones, PIA has been prepared and analyzed by Dot Blot.

An oN culture of the desired biofilm forming bacterium has been diluted 1:100 in TSB-medium with or without antibiotics, depending on the strain. The culture grew until OD₆₀₀ reached 0,5 and was then diluted again 1:100 in TSB-medium with or without antibiotics, depending on the strain. 5 mL of this dilution have been used to inoculate TC 60x15 cell culture dishes (Nunclon Δ Surface, Nunc, Roskilde, Denmark). The biofilm grew oN standing at 37 °C. The next day the medium was removed and replaced by 4 mL fosmid cell raw extract. The dishes have been incubated for 24-48 h standing at 37 °C.

Then the biofilm has been scratched from the plate using a cell scraper. The medium and the cells have been filled into a 15 mL Falcon tube and centrifuged at 5000 rpm and 4 °C for 15 min. The supernatant has been removed and the pellet was re suspended in 5 mL 0,1 x PBS-buffer. OD₆₀₀ has been measured and all suspensions have been diluted until they reached the smallest measured OD. The cells have been treated 3 times with ultra sonification (digital sonifier 250-D, Branson, Danbury, USA) at 70 % for 30 sec, each with a 30 sec break in between to detach PIA from the cells. The lysate has then been centrifuged again at 5000 rpm and 4 °C for 15 min. The supernatant has been decanted into a fresh tube and was then used for Dot-Blot (II.3.5.2), or TLC-preparation (II.3.6).

II.4. Molecularbiological Techniques

II.4.1. DNA Isolation and purification procedures

II.4.1.1. Isolation of plasmid and fosmid DNA with kit

Plasmid and fosmid DNA has been isolated using the Qiagen Plasmid Mini Kit (Qiagen, Hilden, Germany) out of 5 mL oN culture that grew at 37 °C shaking at 180 rpm. Fosmid clones had to be induced before fosmid isolation (II.4.1.2).

The protocol was then accomplished precisely and every solution and bin included in the kit has been used. The DNA has been checked by agarose gel electrophoresis (II.4.2).

II.4.1.2. Induction of fosmid clones

Fosmid clones grown oN in LB+Chl (12,5 µg/mL) -medium had to be induced before fosmid isolation by using the Copy Control™ Fosmid Library Production Kit Protocol (Epicentre, Madison, USA) to gain a higher fosmid copy count. Therefore 500 µL of the oN culture were inoculated into 4,5 mL LB+Chl (12,5 µg/mL) -medium with 5 µL Copy Control Induction solution added.

The tubes were incubated for 5 h at 37 °C shaking at 180 rpm. The tubes had to lay angular to gain a larger surface for oxygen provision of the cells. After induction the fosmids were isolated as described in II.4.1.1.

II.4.1.3. Plasmid- and fosmid-Isolation via alkaline Lysis (Quick and Dirty Prep)

1,5 mL of a 5 mL oN culture in LB+ adequate antibiotic, grown at 37 °C, shaking at 200 rpm, was transferred into an EMT and centrifuged in a cooling centrifuge (5415R, Eppendorf, Hamburg, Germany) for 30 sec at RT. The pellet was re suspended in 100 µL P1 buffer through vortexing or pipetting. The suspension was inverted with 200 µL P2 buffer and incubated for 1 min at RT until the lysate became clear. Then 200 µL Chloroform were added, the tube was inverted and incubated 1 min at RT. Afterwards 150 µL P3 buffer were added, the tube was inverted and centrifuged in a cooling centrifuge (5415R, Eppendorf, Hamburg, Germany) for 2 min at RT and 13.000 rpm. The supernatant has been transferred into a fresh sterile EMT on ice and mixed with 2,5 Vol. EtOH (96 %). Then the EMT has been centrifuged 13.000 rpm and 4 °C for 20 min in a cooling centrifuge (5415R, Eppendorf, Hamburg, Germany). Following the pellet has been washed two times with 70 % EtOH. After every washing step the EMT was centrifuged at 13.000 rpm and 4 °C for 2 min in a cooling centrifuge (5415R, Eppendorf, Hamburg, Germany). The liquid supernatant was then removed totally for that the pellet could dry at 65 °C for approximately 2 - 5 min. The pellet was then re suspended in 20 – 50 µL H₂O_{bidest.}. Before working with the plasmid/fosmid was possible the suspension had to incubate at RT for at least 30 min. The product and yield of DNA was checked through agarose gel electrophoresis (II.4.2).

P1 – buffer (per liter)	P2 – buffer (per liter)	P3 – buffer (per liter)
store at 4 °C	store at RT	store at RT
Tris 6.1 g	8.0 g NaOH in 900 ml H ₂ O	294 g KAcetate in 500 ml H ₂ O
EDTA-2*H ₂ O 3.7 g	100 ml of 10 % SDS	Adjust pH to 5.5 with Acetic Acid (~110 ml), ad. 1000 ml
Adjust to pH 8.0 with HCl.		
Add 100 µg/ml RNase A as needed, usually 10 mg RNase A in 100 ml batches.		

II.4.1.4. Gel Extraction

Purification of DNA-fragments from enzymatic digestions has been accomplished via gel extraction. Therefore the Nucleospin Extract II Kit (Macherey-Nagel, Düren, Germany) has been used. After a 0,8 % agarose gel with the samples ran for 1 h at 80 V the fragment has been cut out of the gel under UV light by using a scalpel. Afterwards the in the kit included protocol was followed precisely. Every solutions, bins and columns included in the kit have been used. All centrifugation steps have been accomplished in a micro centrifuge (minispin Plus, Eppendorf, Hamburg, Germany) at 13.000 rpm and RT, or in a cooling centrifuge (5415R, Eppendorf, Hamburg, Germany) at 11.000 rpm at 4 °C. The product was checked by agarose gel electrophoresis (II.4.2). The purified product was then used for ligation (II.4.3.3) into different plasmid vectors (table 3) and further for transformation (II.4.4.1) in different *E. coli* strains (table 2).

II.4.1.5. Purification of PCR products and enzymatic digestion products with kit

Purification of DNA-fragments from restriction reactions was accomplished by using Nucleospin Extract II Kit (Macherey-Nagel, Düren, Germany). The in the kit included protocol was followed precisely. Every solutions, bins and columns included in the kit have been used. All centrifugation steps have been accomplished in a micro centrifuge (minispin Plus, Eppendorf, Hamburg, Germany) at 13.000 rpm and RT. The product was checked by agarose gel electrophoresis (II.4.2).

II.4.1.6. Purification of enzymatic digestion products without kit

All enzymes used in restriction reactions have been inactivated at 65 °C for 5 min prior to purification.

Then 1/10 Vol. 3 M NaAc_{aq}, as well as 250 µL Chloroform were added. The solution was then centrifuged in a micro centrifuge (minispin Plus, Eppendorf, Hamburg, Germany) at 13.000 rpm for 5 min at RT. The upper phase has been transferred into a fresh sterile 1,5 mL EMT and inverted with 2,5 vol. EtOH (96 %). The EMT has then been centrifuged in a cooling centrifuge (5415R, Eppendorf, Hamburg, Germany) at 13.000 rpm for 20 min at 4 °C. The supernatant has been discarded and the pellet was washed two times with EtOH (70 %). After every washing step the EMT has been centrifuged in a micro centrifuge (minispin Plus, Eppendorf, Hamburg, Germany) at 13.000 rpm for 5 min at RT. Afterwards, the liquid has been removed completely and the pellet has been dried at 65 °C for 2 – 5 min. The pellet was then re suspended in 20-50 µL H₂O_{bidest.} The product was checked by agarose gel electrophoresis (II.4.2).

II.4.2. Agarose-Gel electrophoresis

For preparation, fragment size and concentration determination all DNA fragments have been checked on a 1 % (m/V) agarose gel containing Red Safe Nucleic Acid staining solution (iNtRON biotechnology, Korea). The electrophoresis was accomplished with 130 V over 60 min in a gel electrophoresis chamber filled with 0,5 x TBE-buffer. The power supply unit EPS 3002 (Life technologies, USA) has been used. All samples have been mixed with 1/6 Vol. 6x loading dye prior to loading the gel. The analysis and documentation was accomplished with UV-light in the documentation facility GelDoc1000 (BIO-RAD, Milano, Italy) and the Software Quantity One 4.5.1.

To compare the fragment size the gene marker mix λ DNA *Hind* III/ Φ X-*Hae* III (Finnzymes, Pittsburgh, USA) (VI.1.1) was used. The marker was used in every electrophoretic separation.

Loading dye

Bromphenole blue	250 mg
Xylencyanole	250 mg

Both components were diluted in 33 mL 150 mM Tris (pH 7,6), then 60 mL Glycerol and 7 mL H₂O_{bidest.} have been added. The loading dye was stored at 4 °C.

TBE-Buffer (5x)

Tris	250 mM
Boric acid	250 mM
EDTA	10 mM

The pH was adjusted to 8,2 with glacial acetic acid. The buffer was stored at RT.

II.4.3. Enzymatic modification of DNA

II.4.3.1. *Enzymatic digestion of plasmid and fosmid DNA*

The digestion of plasmid- and fosmid DNA was accomplished with Type II restriction endonucleases from NEB (Frankfurt Main, Germany) and the corresponding buffers. Those

are shown in table II-8 with their reaction- and inactivation temperature. For double digestion the CutSmart Buffer has been used. The reaction volume of analytic digestions was 20 μ L, the volume of preparative digestions was 100 μ L. Analytic as well as preparative digestions were inactivated by adding 1/10 Vol. loading dye (II.4.2). The product has been checked via agarose gel electrophoresis (II.4.2).

Table II-8: Used Type II restriction enzymes and buffer from NEB (Frankfurt am Main, Germany) and their reaction- and inactivation temperature

Restriction enzyme	NEB-Buffer (10x)	Incubation temperature [°C] for 2-24 h	Inactivation temperature [°C] for 20 min
<i>Bam</i> HI (5'-GGATCC-3')	4	37	65
<i>Hind</i> III (5'-AAGCTT-3')	4	37	80
<i>Pst</i> I (5'-CTGCAG-3')	4	37	65
<i>Eco</i> RI (5'-GAATCC-3')	EcoR I Buffer	37	65
<i>Xho</i> I (5'-CTCGAG-3')	4	37	65
<i>Asc</i> I (5'-GGCGCGCC-3')	CutSmart	37	80
<i>Kpn</i> I (5'-GGTACC-3')	1	37	/
<i>Sma</i> I (5'-CCCGGG-3')	CutSmart	25	65
<i>Nde</i> I (5'-CATATG-3')	CutSmart	37	65
<i>Xba</i> I (5'-TCTAGA-3')	CutSmart	37	65

Restriction enzyme	NEB-Buffer (10x)	Incubation temperature [°C] for 2-24 h	Inactivation temperature [°C] for 20 min
<i>NotI</i> (5'-GCGGCCGC-3')	CutSmart	37	65
<i>EcoRV</i> (5'-GATATC-3')	CutSmart	37	80
<i>Sall</i> (5'-GTCGAC-3')	CutSmart	37	65

Table II-9: Used reaction protocols for analytic and preparative DNA restriction reactions

Components	Analytic Digestion	Preparative Digestion
DNA-Solution	3 µL	30 µL
Reaction buffer (10x)	2 µL	10 µL
Restrictionenzyme (10 U/µL)	0,5 µL	2,5 µL
Sterile H ₂ O _{bidest.}	ad 20 µL	ad 100 µL
Incubation time	2 h	oN

II.4.3.2. Preparation of linearized pFLD1 plasmids

For electroporation into Yeast cells 5-10 µg pFLD1 construct had to be linearized using specified restriction enzymes (table II-10) and reaction set up (table II-9). The enzymes cut at unique sites the insert should not contain.

Table II-10: Restriction enzymes for pFLD1 Linearization

Restriction enzyme	Restriction site (bp)	NEB-Buffer (10x)	Incubation temperature [°C] for 2 h	Inactivation temperature [°C] for 20 min
<i>Nsi I</i> (5'-ATGCAT-3')	285	3	37	65
<i>Nde I</i> (5'-CATATG-3')	406	CutSmart	37	65
<i>Cla I</i> (5'-ATCGAT-3')	493	CutSmart	37	65

The full linearization of the construct has been checked on a 1 % Agarose-gel (II.4.2). After heat inactivation of the enzyme 1 Vol Phenol/Chloroform has been added and then spinned for 1 min at RT at 14.000 rpm in a table-top centrifuge (Eppendorf, Hamburg, Germany). The linearized construct has then been ethanol precipitated using 1/10 Vol 3 M sodium acetate and 2,5 Vol 100 % ethanol. After centrifugation at 14.000 rpm at 4 °C for 20 min, the pellet has been washed with 1 mL 80 % ethanol. The pellet has been air-dried and re suspended in 10 µL deionized water and stored at -20 °C for further usage.

II.4.3.3. Enzymatic digestion of PCR products

After running a PCR (II.4.3.5) the product has been purified using Nucleo Spin Extract II Kit with all its components according to the included manual. The purified product has been digested with the according restriction enzymes to the following scheme and then purified again.

Components	Preparative Digestion
PCR-product	10 µL
Reaction buffer (10x)	5 µL
Restrictionenzyme (10 U/µL)	2 µL
Sterile H ₂ O _{bidest.}	<i>ad</i> 50 µL
Incubation time	oN

II.4.3.4. Dephosphorylation

To avoid religation of the linearized vector-DNA, the DNA has been dephosphorylized right after the digestion. Therefore 1 µL Fast AP (Fermentas, St. Leon-Rot., Germany) for every 20 µL reaction was used. The reaction was accomplished over 10 min at 37 °C and was stopped through incubation at 75 °C for 5 min. For further use of the dephosphorylated DNA it has been purified (II.4.1.5).

II.4.3.5. Polymerase chain reaction

Polymerase chain reactions (PCR) have been performed to amplify genes from plasmid, or fosmid DNA. For each gene specific primers had to be designed and used in the PCR.

Purified DNA	1 μ L (100 ng)	
Reaction buffer (5x, or 10x)	5 μ L (5x)	2,5 μ L (10x)
DNA Polymerase (10 U/ μ L)	0,5 μ L	
Primer (10 pM)	1 μ L each	
dNTP (10 μ M)	1 μ L	
Sterile H ₂ O _{bidest.}	ad 25 μ L	

Table II-11: PCR program depending on the polymerase used

PCR program	Phusion Polymerase		Tag Polymerase		Pfu Polymerase		Dynazyme Polymerase	
	Temp (°C)	Time (sec)	Temp (°C)	Time (sec)	Temp (°C)	Time (sec)	Temp (°C)	Time (sec)
1 First Denaturation	98	120	98	120	98	120	94	120
2 Denaturation	98	20	98	20	98	20	94	20
3 Annealing	Spec.	30	Spec.	30	Spec.	30	Spec.	30
4 Elongation	72	25 sec/ 1 kb	72	50 sec/ 1 kb	72	90 sec/ 1 kb	72	40 sec/ 1 kb
5	Repeat steps 2-4 30x							
6 Final Elongation	3-6 min							
7	Hold at 4 °C forever							

After running the PCR program the PCR products have been analyzed via agarose-gel electrophoresis (II.4.2) and purified using a kit (II.4.1.5). The purified PCR products have been used for further ligation (II.4.3.4) and transformation (II.4.3.5) into host cells.

II.4.3.6. Ligation

DNA-fragments and plasmid vectors had to be ligated to insert the fragment into the plasmid. All reactions were accomplished for either 2 h at 22 °C or oN at 16 °C.

Ligation of PCR products and enzymatic digestion products

Purified PCR products as well as enzymatic digestion products (II.4.1.5) have been ligated using T4-DNA-Ligase (Promega, Mannheim, Germany) after following protocol into either pBluescript II SK+, pUC19, pBBR-MCS5, pFLD1 or pET19b (table 3). All vectors needed to be linearized (II.4.3.1) with the corresponding digestion enzyme and dephosphorylated (II.4.3.2) before usage. The concentration ratio between insert-DNA to vector-DNA should be about 1:5.

Insert-DNA	6 µL
Vector	6 µL
T4-DNA-Ligase	1 µL
T4-DNA-Ligasebuffer	2 µL
H ₂ O _{bidest.}	<i>ad</i> 20 µL

Ligation of PCR products in pENTR vector system

Purified PCR products for pENTR/D/TOPO cloning system have been ligated into pENTR entry vector (table 3). Therefore the pENTR directional TOPO cloning kit has been used with all its components (Invitrogen, Darmstadt, Germany).

PCR product	0,5-4 µL (300 ng)
pENTR vector	0,5 µL
Salt Solution	1 µL
H ₂ O _{bidest.}	<i>ad</i> 6 µL

The reaction was accomplished over 10 min at room temperature and could be stored over night at -20 °C. After ligation of the PCR products the vector was transformed into *E. coli* Top10 host cells (table 2; II.4.4.1).

II.4.3.7. LR-Clonase reaction

PCR products ligated into entry vector pENTR have been transferred to the expression vector pDEST17 via LR-Clonase Gateway cloning reaction kit (Invitrogen, Darmstadt, Germany). This reaction gives the possibility to directly clone from one vector to another without digestion, or purification steps in-between.

pENTR entry clone with insert	1-7 μL (50-150 ng)
pDEST17 destination vector	1 μL (150 ng)
LR clonase II enzyme mix	2 μL
TE Buffer (pH 8,0)	<i>ad</i> 8 μL

The reaction was incubated for 1 h at 25 °C. Then 1 μL Proteinase K have been added for 10 min at 37 °C to stop the reaction. The reaction could be stored at -20 °C oN, or directly transformed into *E. coli* host cells (table 2; II.4.4.1) via heat shock transformation (II.4.4.2).

II.4.3.8. BP-Clonase reaction

The BP Clonase™ II enzyme mix (Invitrogen, Darmstadt, Germany) is used for the direct ligation and following transformation of *attB*-PCR products into expression vectors and the appropriate host (table 2; II.4.4.1). The reaction has been performed according to the manual and all components included in the kit have been used.

<i>attB</i> -PCR product	1-7 μL (15-150 ng)
Destination vector	1 μL (150 ng/ μL)
TE Buffer (pH 8,0)	<i>ad</i> 8 μL
BP clonase II enzyme mix	2 μL

The thawed enzyme mix has been vortexed two times for 2 sec each and then added to the reaction. After vortexing of the sample the reaction incubated at 25 °C for 1 h. 1 μL Proteinase K has been added to stop the reaction at 37 °C for 10 min. Then the sample has been cloned into host cells via heat shock transformation (II.4.4.2).

II.4.3.9. Transposon mutagenesis

A transposon mutagenesis has the effect of destroying the responsible gene by integrating unspecific in the target DNA. The transposon carries a Kanamycin resistance gene, so selection can be made via LB agar plates containing Kanamycin (50 µg/mL). A positively integrated transposon leads to a loss of function in the treated DNA when it is tested in the performed assay. The transposon mutagenesis has been accomplished by using the EZ Tn5 <Kan-2> Insertion Kit (Epicentre, Madison, USA). The protocol has been followed precisely and every solution included in the kit has been used.

II.4.4. Cloning of DNA-fragments

Amplification of DNA fragments was accomplished by transforming those into *E. coli*, or *P. antarctica* host cells (table 2). This is described in ligation (II.4.3.6) and heat shock transformation (II.4.4.1 & II.4.4.2).

II.4.4.1. Heat shock-transformation for *E. coli* chemically competent cells

To amplify DNA-fragments in plasmids (II.4.3.3) they have been transformed into *E. coli* host cells (table 2) by heat shock. Therefore chemically competent cells (II.6.1) had to be defrosted on ice for about 5 min. Then 10 – 20 µL of the ligation product have been added and the mix incubated on ice for 30 min. The cells were then heat shocked for 90 sec at 42 °C in a Thermostat Plus (Eppendorf, Hamburg, Germany) and immediately put back on ice for 2–5 min afterwards. The transformed cells were then preincubated with 800 µL SOC-medium at 37 °C shaking at 180 rpm for 45 – 60 min. Then 100 µL, 200 µL and the rest of the suspension has been plated out on LB-AIX agar plates (table 1). After incubation oN at 37 °C white colonies have been transferred to the same medium and were incubated at 37 °C oN. Those white colonies could be used for further investigation such as gene sequencing.

II.4.4.2. Heat shock transformation for *P. antarctica* chemically competent cells

To amplify DNA-fragments in plasmids (II.4.3.3) they have been transformed into *P. antarctica* host cells (table 2) by heat shock. Therefore 100 µL of the chemically competent cells (II.5.2) had to be transformed immediately after preparing them. 5 µL of the ligation product have been added to the cells and the mix has been incubated on ice for 60 min. A heat shock was done for 2 min at 42 °C in a Thermostat Plus Thermocycler (Eppendorf, Hamburg, Germany) and the cells had to be put back on ice immediately for 10 min afterwards. The transformed cells were then preincubated with 900 µL LB-medium at 22 °C shaking at 180 rpm for 2 h. Then the cells have been centrifuged at 5000 g for 1 min. The supernatant has been discarded and the cells have been re suspended in the flow back.

It has been plated out on LB-Gm agar plates (table II-1). After incubation up to two days at 22 °C white colonies have been transferred to liquid LB-medium with Gm and were incubated at 22 °C oN. These cultures have been used for further analysis of the insert as well as over expression (II.6) of the protein.

II.4.4.3. Electroporation transformation of Staphylococcus cells

Plasmids for Staphylococci have been transformed via electroporation into electro competent Staphylococcus cells (II.6.3). Therefore 100 µL of freshly prepared Staphylococcus cells have been incubated with 3-7 µL plasmid-DNA on ice for 30 min. The cells have then been placed into an electroporation cuvette (width 1mm) and pulsed using a BioRad electroshock instrument (table II-12).

Table II-12: Electro pulse adjustment

Strain	Voltage (kV)	Resistance (Ω)	Capacity (kf)	Recovery Medium
<i>S. epidermidis</i> RN4220	1	100	25	B2
<i>S. aureus</i> PS187 ΔsauUSIΔhsdRI	1	200	25	BM

390 µL recovery medium have been added immediately to the cells and everything has been transferred into a fresh 15 mL falcon-tube. The tube has been incubated for 1-2 h shaking at 180 rpm at 37 °C in a shaking incubator. Then different amounts of the suspension have been plated out on the corresponding agar plates and incubated at the corresponding temperature for 24-72 h.

II.4.4.4. Electro transformation of Yeast cells

pFLD1 plasmids for *Pichia pastoris* have been transformed via electroporation into electro competent cells (II.6.5). Therefore 80 µL freshly prepared *P. pastoris* X-33, or SM1168H cells have been incubated with 5-10 µg linearized plasmid on ice for 5 min. The cells have then been placed into an electroporation cuvette (width 2mm) and pulsed using a BioRad electroshock instrument.

Volt (kV)	2
Resistance (Ω)	200
Capacity (kf)	25

1 mL ice-cold 1 M Sorbitol has been added to the cells and transferred into a 15 mL falcon-tube. The tube has been incubated for 2-24 h at 30 °C without shaking. Then different amounts of the suspension have been plated out on YPD-Ze agar plates and incubated at 30 °C 24-72 h.

For a larger amount of transformed colonies, the recovery of the pulsed cells has been changed. After one hour of recovery at 30 °C in 1 M Sorbitol, 1 mL YPD-medium has been added and the suspension has been incubated for 1 h at 30 °C shaking at 200 rpm. Then different amounts of the suspension have been plated out on YPD-Ze agar plates and incubated at 30 °C 24-72 h.

II.5. Transformation of *Staphylococcus spec.* cells with Phages

II.5.1. Phage Preparation

The phage has been prepared with the desired plasmid. For *S. epidermidis* 1457 phage Φ 187 has been used. Therefore the desired plasmid first had to be transferred into *S. aureus* PS187 Δ hsdRI Δ sau USI.

For *S. epidermidis* 1585 phage Φ A6C has been used.

An oN culture of the bacterial strain containing the desired plasmid has been diluted to OD₆₀₀ 0,1-0,2 and 3x500 μ L of this dilution have been mixed with 3x500 μ L of the appropriate phage. 3 mL STA Soft agar have been added to each suspension and layered on three STA Agar plates. Incubation oN at 30 °C followed.

The Soft agar layer has been scratched of with a sterile glass-scraper and 5 mL NB2+ Broth. The suspension has been transferred into a 50 mL Falcon-tube and treated with ultrasonification at 70 % for 10 sec, or shaken for 5 min by hand. Centrifugation for 30-45 min at 5000 rpm and 4 °C followed. The supernatant has been transferred into a fresh 15 mL Falcon-tube and centrifuged again as mentioned, but only 15 min. The supernatant has then been filter sterilized using a 0,2 μ M filter.

II.5.2. Phage Titration

To determine the amount of phage a preculture of the target bacterial strain has been diluted to OD₆₀₀ 0,1. The phage (II.5.1) has been diluted in several steps down to 10⁻¹⁰ and 500 μ L of the dilution have been mixed with 500 μ L of the diluted preculture. 3 mL STA Soft agar have been added to each dilution step and layered on STA agar plate. Incubation at 30 °C oN followed.

The next day clear spots on the agar plate (Plaques) have been counted to determine the phage titer.

II.5.3. Phage Transduction

Cells of the target bacterial strain from agar plates (1 ½ plates) have been re suspended in NB2+ broth to an OD₆₀₀ 11. 1 mL of this suspension have been mixed with 1 mL prepared phage (II.5.1) and incubated at 37 °C for 30 min. 40 µL 1 M NaCitrat have been added to stop phage absorption. After centrifugation at 5000 rpm for 15 min at 4 °C the pellet has been washed two times with BHI+ broth. Then the pellet was re suspended in 3 mL BHI+ broth and has been incubated at 180 rpm at 37 °C for 1-2 h. 3 mL BHI Soft agar have been added to the suspension and layered on a BHI agar plate with the appropriate antibiotic. After 24-60 h at 37 °C colonies should have formed.

II.5.4. Phage Transduction after Ultracentrifugation

To gain a higher phage titer with constructs inside phage Φ187 ultracentrifugation has been performed. Therefore the phage solution (II.5.1) has been transferred into Ultra-Clear Centrifuge tubes (Beckman Coulter, Brea, USA). After carefully taring the weight the centrifuge tubes have been placed into SW 40 Ti Rotor (Swinging bucket, Beckman Coulter, Brea, USA) and centrifugation has been performed in an Optima L-100 XP ultracentrifuge (Beckman Coulter, Brea, USA) at 25100 rpm, 4 °C for 2 h. The supernatant has been discarded and the pellet has been re suspended in 500 µL TMN buffer.

The target bacterial strain has been diluted to OD₆₀₀ 0,5 and 200 µL of this dilution have been pelleted via centrifugation at highest speed for 5-10 min. The pellet has been dissolved in Phage buffer containing gelatin and 100 µL phage solution in TMN buffer have been added. After 15-45 min incubation at 37 °C and 350 rpm the whole mix has been spread out on BM agar plates with the appropriate antibiotic. Incubation at 37 °C for 24-48 h followed.

<u>TMN Buffer</u>		<u>Phage Buffer with gelatin</u>	
Tris HCl, pH 7,5	10 mM	Tris, pH 7,8	50 mM
MgSO ₄	10 mM	MgSO ₄	1 mM
NaCl	500 mM	NaCl	0,1 M
		CaCl ₂	4 mM
		Gelatine	0,1 %
		Ad H ₂ O _{bidest.}	200 mL

II.6. Competent cells

II.6.1. Chemically competent *E. coli* cells

2,5 mL of an *E. coli* culture grown in 5 mL LB-medium oN at 37 °C, shaking at 180 rpm was transferred into 250 mL fresh LB-medium, preheated to 37 °C, inside a 1 L Erlenmeyer flask. The flask needed to shake at 37 °C and 180 rpm for 90 – 120 min until OD₆₀₀ reached 0,5. The culture was then cooled on ice for 5 min and transferred into two sterile 250 mL centrifuge bins. Centrifugation at 4 °C and 4000 g for 5 min followed in a SLA-1500 rotor (Sorvall RC5C Plus, Sorvall, Langenselbold, Germany). The supernatant was carefully discarded. From now on the cells needed to constantly be held on ice. Each pellet was then re suspended in 37,5 mL of 4 °C cold TFB1-buffer. The cells incubated for 90 min on ice and were then centrifuged for 5 min at 4 °C and 4000 g in a SLA-1500 rotor (Sorvall RC5C Plus, Sorvall, Langenselbold, Germany). The supernatant was carefully discarded and each pellet was re suspended in 5 mL of 4 °C cold TFB2-buffer. 100 µL of the suspension were then pipetted into each EMT (about 100 EMTs) and stored at -70 °C.

TFB1-buffer (for 75 mL)

RbCl	0,91 g
MnCl ₂ *4*H ₂ O	0,74 g
Kaliumacetate	0,22 g
CaCl ₂ *2*H ₂ O	0,11 g
Glycerin (15 %)	11,25 mL
H ₂ O	64 mL

Adjust to pH 5,8 with 1 % acetic acid. Filter sterilize after every component is diluted properly.

TFB2-buffer (for 20 mL)

MOPS	0,042 g
RbCl	0,0242 g
CaCl ₂ *2*H ₂ O	0,221 g
Glycerin (15 %)	3 mL
H ₂ O	17 mL
Adjust to pH 6,8.	

Filter sterilize after every component is diluted properly.

II.6.2. Chemically competent *P. antarctica* cells

1 mL of a *P. antarctica* culture grown oN, or max. 48 h in 5 mL LB-medium shaking at 200 rpm at 22 °C has been transferred to 50 mL of fresh LB-medium. It was grown shaking at 22 °C and 200 rpm until OD₆₀₀ reached 0,5 (approx. 4 h) and was then cooled down on ice for 10 min. It has then been transferred to a sterile 50 mL falcon tube and was centrifuged at 4 °C for 10 min at 4000 g. The supernatant has been discarded and the cells were re suspended in 25 mL ice-cold sterile 10 mM NaCl. Then centrifugation at 4 °C for 10 min at 4000 g was performed. The supernatant has been discarded and the cells were re suspended in 25 mL ice-cold sterile 100 mM CaCl₂. The suspension has been incubated on ice for

20 min. Then centrifugation at 4 °C for 10 min at 4000 g was performed. The supernatant has been discarded and the cells were re suspended in 500 µL ice-cold sterile 100 mM CaCl₂. Heat shock transformation (II 4.4.2) had to be performed right after preparing the competent cells, they could not be stored.

II.6.3. Electro competent *Staphylococcus epidermidis* RN4220 cells

2 mL of an oN culture of *S. epidermidis* RN4220 grown in B2-Broth has been inoculated in 50 mL fresh B2- broth in an 500 mL Erlenmeyer flask and grew for 2-3 h until OD₆₀₀ 0,6-0,8 shaking at 180 rpm at 37 °C. In a fresh 50 mL Falcon-tube the cells have been centrifuged at 4.332xg for 10 min at 4 °C and then washed once with 5 mL 10 % sterile Glycerin. After a centrifugation step at 4.332 g for 15 min at 4 °C the cells have been washed in 2,5 mL 10 % sterile Glycerin and centrifuged again as mentioned. Depending on the cell density at the beginning the cell pellet has been re suspended in 600-800 µL 10 % sterile Glycerin and immediately used for electroporation (II.4.4.3).

II.6.4. Electro competent *S. aureus* PS187Δ*hsdR*Δ*sau* USI cells

A fresh oN culture has been inoculated in BM-broth at an OD_{578nm} 0,1 and grew until 1-2 h OD_{578nm} 0,45-0,5 shaking at 180 rpm at 37 °C. The culture has been transferred to two fresh 50 mL Falcon-tubes and centrifuged at 5000 rpm for 10 min at 4 °C. The cells have then been washed three times cold, sterile 10 % Glycerin. In between each step centrifugation has been done as mentioned. The final cell pellet has been re suspended in 200 µL 10 % Glycerin through vortexing. Aliquots of 50 µL have been used for immediate electroporation (II.4.4.4). It is possible to keep the competent cells at -80 °C for up to one week.

II.6.5. Electro competent *Pichia pastoris* cells

A colony of the desired *P. pastoris* strain has been transferred in 5 mL YPD medium in a 50 mL Falcon-tube and grew oN at 30 °C shaking at 200 rpm. 500 mL of fresh medium in a 2 L Erlenmeyer flask have been inoculated with 0,1-0,5 mL oN culture and grew at 30 °C shaking at 200 rpm until OD_{600nm} 1,3-1,5. The culture has been centrifuged carefully at 1500xg for 5 min at 4 °C. The pellet has been re suspended in 500 mL ice-cold, sterile deionized water and centrifuged again as mentioned. The pellet has then been re suspended in 250 mL ice-cold, sterile deionized water and centrifuged again as mentioned. Afterwards the pellet has been re suspended in 20 mL 1 M ice-cold, sterile Sorbitol and centrifuged again as mentioned. Finally the pellet has been re suspended in 1 mL ice-cold, sterile Sorbitol for a final volume of approx. 1,5 mL. The cells had to be used for electroporation (II.4.4.5) that day and could not be stored.

II.7. Protein analysis

II.7.1. Expression of recombinant proteins

Expressing proteins to analyze their molecular mass and to control the proper expression of the protein in the *E. coli* BL21 AI host cells has been performed in a small volume pilot expression. Therefore 20 mL of LB+Amp have been inoculated with 1 mL of an oN culture grown at 37 °C shaking at 180 rpm of the host cells contain the expression vector with the proper insert. The cells were grown shaking at 180 rpm at 37 °C until OD₆₀₀ reached 0,6. Then Arabinose has been added to a final concentration of 0,2 % to induct the expression for Arabinose inducible vectors. Concentrations between 0,01-1 M IPTG have been used for the induction of IPTG inducible vectors. The expression ran for up to 4 h. 500 µL samples have been taken at the starting point and every hour for 4 hours. The samples have then been prepared (II.7.1.1) for SDS-gel electrophoresis (II.7.3). Some samples produced Inclusion bodies during expression. To avoid this reaction the expression temperature has been decreased to 4-16 °C and the expression time has been elongated to 24 h before further analysis. Inclusion bodies that could not be avoided have then been further treated for break up and refolding of the locked-in protein (II.7.2.3).

II.7.1.1. Preparation of expression samples for SDS-gel electrophoresis

The expression samples have been centrifuged for 1 min at 13.000 rpm at RT. The supernatant has been either discarded, or stored in a fresh Eppendorf reaction tube for further analysis as well as SDS-gel electrophoresis (II.6.3). The cell pellet has been re suspended in 250 µL 1x PBS Buffer and the cell wall had to be destroyed to gain the expressed protein. This was done either by sonification (pulse on 5 sec, pulse off 3 sec, amplitude 40 %) for 5 min, or frosting (-80 °C) and defrosting (42 °C) the cells for 4-5 times. 20 µL of each sample have then been mixed with 5 µL 4x Nu-Page buffer (Invitrogen, Darmstadt, Germany) and heated up to 99 °C for 5 min. Then SDS-gel electrophoresis (II.6.3) has been performed.

II.7.2. SDS-gel electrophoresis

SDS-gel electrophoresis has been done to analyze the proper expression and the molecular mass of proteins. Therefore gels composed of a 10 % running gel and a 4 % stacking gel (table II-13). The electrophoresis was performed in a Miniprotean Tetra Cell chamber (BioRad) for 1,5 h at 150 V. 3 µL PageRuler™ protein ladder (Thermo Scientific, Waltham, USA) have been added to each gel run (VI.1.2).

Table II-13: SDS-gel recipe

	H ₂ O (mL)	30 % Acrylamid (mL)	Spec. Buffer (mL)	10 % SDS (mL)	TEMED (μ L)	APS (μ L)
10 % running gel	4,1	3,3	2,5	0,1	5	50
4 % stacking gel	6,1	1,3	2,5	0,1	10	50

Running gel buffer

1,5 M Tris-HCl, pH 8,8

Stacking gel buffer

0,5 M Tris-HCl, pH 6,8

10x Running Buffer for electrophoresis chamber

Glycin	288 g	ad. H ₂ O	2000 mL
Tris-Base	20 g		
SDS	20 g		

II.7.2.1. Staining of SDS-gels with Coomassie Blue

SDS-gels were placed in a plastic box after electrophoresis and stained with Coomassie Blue for 15 min shaking at RT. Then the gels have been destained with Destaining solution until clear bands were visible (approx. 2 h).

Coomassie Blue Solution

H ₂ O	500 mL
Methanol	400 mL
Acetic Acid	100 mL
Coomassie Blue R-250	1 g

Destaining solution

H ₂ O	500 mL
Methanol	400 mL
Acetic acid	100 mL

Filter the solution before usage.

The gels have then been placed in tap water over night and fixed on a filter membrane by vacuum drying at 72 °C for 1 h.

II.7.2.2. Silver staining of SDS-gels

SDS-gels have been additionally stained with silver stain to visualize proteins that were invisible using Coomassie Blue staining. Therefore the Pierce® Silver Stain for mass spectrometry kit (Thermo Scientific, Rockford, USA) has been used. All included components have been used as described in the manual. Only the last step has been improved and ultrapure water has been used instead of acetic acid. The lanes on the SDS gel have been prepared for mass spectrometry (II.7.6), or the gel has been dried as described in II.7.3.1.

II.7.3. Treatment of Inclusion Bodies with stepwise pH adjustment

Different protocols for breaking up inclusion bodies and refolding the locked in protein have been tried. The german Patent DE60034707T2 describes a method that destroys the inclusion bodies with 8 M Urea, 0,1 M Tris, 1 mM Glycin, 1 mM EDTA, 10 mM β -Mercaptoethanol, 10 mM DTT, 1 mM GSH, 0,1 mM GSSG, all pH 10. This step is used to solubilise the inclusion bodies followed by a stepwise decrease of the pH to 8,0 using Tris Base. Each step decreases the pH about 0,2 points for 24 h before the next decreasing step is performed. All pH adjusting steps are performed at 4 °C. After 24 h at pH 8,0 the solution can be ultra centrifuged and then purified via gel filtration.

II.7.3.1. Preparation and Extraction of insoluble (Inclusion-Body) proteins from *Escherichia coli* [Palmer & Wingfield, 2004, 51]

The protocol describes precisely the treatment of inclusion bodies derived from *E. coli* expressions. For the treatment of inclusion bodies in this work Basic protocol 1 has been used according to all descriptions with the following changes.

1. Step 2: The cell grinder precellys24 (Bertin technologies, France) has been used with the strongest shaking for 30 sec on, 30 sec off for 5 min in total.
2. Step 3: Instead of a french press ultra sonification for 5 minutes (10 sec on, 10 sec off) at 70 % has been performed using the digital sonifier Model 250-D (Branson Ultrasonics, Danbury, USA).
3. all centrifugation steps with 500 mL bottles: The centrifuge Sorvall RC 26 Plus (DuPont, Wilmington, USA) has been used with the rotor SuperLite GS-3 SLA-3000 (DuPont, Wilmington, USA); all centrifugation steps in 15-50 mL tubes: Multifuge 1 S-R with rotor Sorvall 75002005 F (both: Heraeus Systems, Hanau, Germany).
4. Step 6-10: Instead of a tissue homogenizer, the pellet has been re suspended using a large pipette and a vortex.

After the extraction of the protein with guanidine HCl the buffer has been exchanged via dialysis. A binding buffer for gel filtration has been used according to the binding tag and the column (II.7.3).

II.7.4. Protein dialysis

The Protein dialysis after over expression or extraction from inclusion bodies has been done to change the buffer. The sample could then be used for gel filtration, or purification on a binding tag specific column. Table II-7 shows tag specific binding buffers used for the purification of proteins with the Äkta system.

The dialysis has been done in Slide-A-Lyzer[®] Dialysis cassettes (Pierce, Rockford, USA) swimming in at least 1 L of new buffer for 24 h at 4 °C. The liquid has been slowly mixed during dialysis using magnetic stirrer.

II.7.5. Western Blotting

To visualize tagged proteins with antibodies specifically binding to the target protein, the SDS gel (II.7.3) has been blotted. Therefore 4 sponge filters have been soaked with 1 x transfer buffer and placed into a blotting chamber (XCell II Blot Module, Invitrogen, Carlsbad, USA). On top of the filters came one layer of filter paper, the SDS gel, one activated blotting membrane (15 sec in 100 % MeOH for activation, 15 sec washing in 1 x Transfer buffer), another layer of filter paper and 4 soaked sponge filters. This set up was packed firmly inside the blotting chamber which has been filled with 1 x transfer buffer. The blotting has been performed over 1 h at 150 V. Then only the blotting membrane has been blocked in 3 % BSA in 1 x PBS-buffer on shaking slowly at 4 °C. Afterwards antibody staining was possible (II.8.1).

20 x Transfer buffer

Bicine	10,2 g
Bis-Tris	13,1 g
EDTA	0,75 g
Chlorobutanol	0,025 g
<i>ad</i> H ₂ O _{<i>bidest.</i>}	125 mL
pH	7,2

1 x Transfer buffer

H ₂ O _{<i>bidest.</i>}	425 mL
Methanol	50 mL
20 x Transfer buffer	25 mL

II.7.6. Dot Blot

The samples used for a Dot-Blot have been diluted up to 1:128 in steps to get clear spots on the membrane. Samples gained from II.3.4.1 have been diluted in 0,1 x PBS-buffer and then vortexed. Other samples have been diluted in 1 x PBS.

A membrane of the desired size has been activated in 100 % Methanol for 15 sec and was then washed in 1 x PBS-buffer for 15 sec. The membrane was then placed on a wet filter

paper. It was important that the membrane never dried completely. 10 μ L of each dilution have been dropped on the membrane as spots in a lane. The spots had to sink into the membrane. Then the membrane was placed into a dish filled with 3 % BSA in 1 x PBS-buffer for blocking oN, or for 2 h at 4 °C shaking.

II.7.7. Tryptic digest of silver stained gels for mass spectrometry

The desired bands have been cut from the silver stained SDS gel and into small pieces (1x1 mm). Centrifuged gel pieces, with 500 μ L 100 % ACN added have been incubated for 10 min on a mixer at RT. The ACN had been removed and the gel pieces have been covered with enough DTT solution that the gels were still covered after swelling. The gel pieces have been incubated for 30 min at 56 °C. After removing the supernatant 500 μ L 100 % CAN have been added and the pieces were incubated for 10 min on a mixer at RT. The ACN had been removed and the gel pieces have been covered with IAA solution and incubated for 20 min at RT in the dark. After removing the supernatant 500 μ L 100 % CAN have been added and the pieces were incubated for 10 min on a mixer at RT. The ACN had been removed and the gel pieces have been washed with 500 μ L wash solution for 45 min at RT on a mixer. After removing the supernatant 500 μ L 100 % CAN have been added and the pieces were incubated for 10 min on a mixer at RT. The ACN had been removed and the gel pieces have been covered with enough Digest solution that the gels were still covered after digestion. The gel pieces have been incubated for 120 min on ice. The supernatant had been removed and the gel pieces have been covered with enough Digest buffer (without trypsin) to cover the gel pieces. They have been incubated at 37 °C oN.

The supernatant has been transferred to a fresh tube (use the same tube to collect the extracted solution of all following steps). Extraction solution has been added (2:1) and all has been incubated at 37 °C for 30 min on a mixer. The supernatant has been transferred to the collection tube, then 100 % ACN has been added to the gel (enough to cover it) and incubated at 37 °C for 15 min on a mixer. The supernatant has been transferred to the collection tube and then MS-H₂O has been added to the gel (enough to cover it) and incubated at 37 °C for 15 min on a mixer. The supernatant has been transferred to the collection tube and then extraction solution has been added to the gel (2:1) and incubated at 37 °C for 30 min on a mixer. The extracted digests were spinned and evaporated to complete dryness.

The experiments were performed on an Agilent 1100 LC-ESI-MS/MS system. The electrospray ionization system was the HPLC-Chip Cube system (Agilent Technologies, Waldbronn, Germany) containing two channels both filled with a reverse phase material (Zorbax 5 μ m 300SB-C18; 160 nL volume filled with chromatographic material for trapping; a channel with 150 mm x 75 μ m filled with chromatographic material for separation). The chip was loaded automatically and positioned into MS nanospray chamber. 5 μ L sample was loaded onto enrichment column with a flow rate of 4 μ L/min with a mixture of 98 % solvent

A (0.2 % formic acid in HPLC-grade water) and 2 % solvent B (acetonitrile). The separation of the peptides was performed with a flow rate of 0.2 $\mu\text{L}/\text{min}$ using a linear gradient elution of 2 - 40 % solvent B in 25 min, 40 - 70 % solvent B in 2 min, maintaining 70 % solvent B for 3,5 min. The MS/MS experiments were carried out in auto MS/MS mode by selecting the three most intense ions from each precursor MS scan for MS/MS analysis. Data Analysis Software for 6300 Series Ion Trap LC/MS version 3.4 Data interpretation was used to generate a peak list from LC-MS/MS. A protein data base search was performed by the online search engine MASCOT (version 2.4.01) and Swissprot protein sequence database. The variable modification for the search parameters carbamidomethylation on cysteine residues and oxidation on methionine residues were included. The precursor ion mass tolerance was set to 1.2 Da and the fragment ion mass tolerance to ± 0.6 Da.

Ammonium bicarbonate stock solution (AmBiCa) 1 M NH_4CO_3 (1,186 g/15 mL MS- H_2O)	Digest buffer 50 mM AmBiCa in 10 % ACN/ H_2O (750 μL AmBiCa + 12,75 mL MS- H_2O + 1,5 mL ACN)	Digest solution 1,5 mL Digest Buffer + 20 μg trypsin
Wash solution 50 mM AmBiCa in 50 % ACN (750 μL AmBiCa + 7,5 mL ACN + 6,75 mL MS- H_2O)	Swelling solution 100 mM AmBiCa (1,5 mL AmBiCa + 13,5 mL MS- H_2O)	Shrinking solution 100 % ACN
Peptide extraction solution 65 % ACN + 5 % formic acid (6,5 mL ACN + 500 μL formic acid + 3 mL MS- H_2O)	Dithiothreitol (DTT MW 154,2) 10 mM in swelling solution (1,542 mg/mL)	Iodacetamide (IAA MW 184,9) 55 mM in 100 mM AmBiCa (10,16 mg/mL)

II.8. Immunologic methods

II.8.1. Antibody staining of Western Blots and Dot Blots

The membrane (II.7.4 and II.7.5) has been washed three times for 15 min each in 1 x PBS-T Buffer (1 x PBS-buffer containing 0,05 % Tween 20).

The first antibody has been diluted 1:10.000 in 1 x PBS-T Buffer and the membrane has been incubated shaking at RT in this dilution for 1 h. Three times washing has been repeated and the secondary anti-rabbit peroxidase antibody has been diluted 1:10.000 in 1 x PBS-T Buffer.

The membrane has been placed in this dilution and was incubated shaking for 1 h at RT. The three times washing steps have been repeated.

The membrane has then been placed on barrier food wrap and 1 mL of Amersham™ ECL™ Western Blotting Detection Reagents (GE Healthcare, Buckinghamshire, UK) has been added. The barrier food wrap has been carefully clapped around the membrane without touching it to spread the detection reagent evenly.

The signal has then been detected using Super RX medical X-ray films (Fujifilm, Tokyo, Japan). Illumination varied from 20 sec to 1 min.

II.8.2. Antibody staining of static biofilms for microscopy

The biofilm grown on, or for 6 h at 37 °C in ibidi ibitreat microscope slides has been washed once with 1 x PBS buffer. Then the cells have been fixed using 3,7 % Formaldehyde with 0,05 % Glutaraldehyde for 10 min at 37 °C. After washing the cells again with 1 x PBS buffer, the cells have been blocked for 20 min at 4 °C with 20 % FBS. The cells have been washed again. Then the first antibody has been diluted 1:500 in 1,5 % FBS and pipetted on the biofilm for an incubation at 4 °C for at least 1 h. After washing the biofilm again, the secondary antibody conjugated to a fluorescent dye has been diluted 1:500 in 1,5 % FBS and pipetted on the biofilm. Incubation on at 4 °C assured competent binding of the antibody. The biofilm has been washed one last time using 1 x PBS buffer. A thin layer of 1 x PBS buffer stayed on the biofilm to avoid drying and for better microscopy pictures.

II.8.3. Antibody staining of biofilms under flow conditions

For antibody staining of biofilms after a flow experiment the Bioflux 200 system (Fluxion, South San Francisco, USA) has been used again. The biofilm grown inside the flow channel has been fixed, washed, blocked and stained after the following protocol. The solutions used have been inserted through the Inlet well always.

Step	Solution used	Pressure (DYN/cm ²)	Flow time (min)	incubation/ adherence time (h)	Incubation temperature (°C)
Fixing of the biofilm	3,7 % Formaldehyde + 0,05 % Glutaraldehyde	0,15	20	10	37
Washing	1 x PBS	0,4	30	/	RT
Blocking	20 % FBS	0,4	10	20	4
Washing	1 x PBS	0,4	30	/	RT
1 st Antibody	Antibody in 1,5 % FBS	0,4	10	60	4
Washing	1 x PBS	0,4	30	/	RT
2 nd Antibody	Antibody in 1,5 % FBS	0,4	10	60	4
Washing	1 x PBS	0,4	30	/	RT

After the last washing step the liquid stayed in the chamber for microscopy (II.9.1) at the Olympus cell[^]tool TIRFM microscope.

II.8.4. Antibody/protein labeling with fluorescence dye using a kit

Antibodies such as anti-FLAG, anti-Embp, or recombinant Sbp have been pre-labeled with a fluorescence dye for further usage. Therefore the kit “Dylight[®] 550 Microscale Antibody labeling kit” (Thermo Scientific, USA) has been used. All chemicals and included tubes have been used accordingly to the manual. The concentration of antibody/protein to be stained has been adjusted to 1 mg/mL.

II.9. Microscopy

The visualization of biofilms has been performed using either the Improvion Spinning Disk, or Leica TCS SP2 confocal microscope and the corresponding software (see table 10). For live cell Imaging using the Bioflux System (Fluxion) the Olympus cell[^]tool TIRFM microscope has been used. Analysis of all pictures has been performed using Volocity 6.0 Software (Perkin Elmer, Waltham, USA). The used microscopes and software were provided by the core facility UMIF (UKE, Hamburg, Germany).

All dSTORM pictures have been generated at the Heinrich-Pette Institute (Hamburg, Germany) with great help of Dr. Dennis Eggert.

II.9.1. Biofilm growth under static conditions and Live/Dead Staining

Biofilms were grown in sterile ibitreat μ -Slide 8 well chambers (ibidi, Martinsried, Germany) and then stained using Live/Dead[®] BacLight[™] Bacterial Viability Kit (Invitrogen, Oregon, USA). The growing medium has been removed and the biofilm has been washed once using 0,1 x PBS-buffer. The staining reagents have then been diluted as described in the protocol in 0,1 x PBS-buffer and 300 μ L of this dilution have been filled into each well of the ibitreat slide. The slide has then been incubated at RT in the dark.

The slide has then been placed on the microscope stage and the biofilm was visualized using the 63 x oil objective. The green and red lasers have been used to visualize living and dead bacteria. Z-Stack pictures have been performed with the corresponding software to determine the height of biofilms and to visualize the biofilm as a 3D picture. The biofilm structure was then analyzed using Volocity 6.0 (table 10).

II.9.2. Preparation of Live-Cell Imaging using Bioflux 200

The Bioflux 200 flow chamber system (Fluxion Biosciences, South San Francisco, USA) has been used to perform biofilm building experiments under flow conditions. The set up of the system contained the Bioflux 200, the vapor barrier, a laptop with the corresponding software "Bioflux" (table 13), a 48-well interface and Bioflux 48 well-microwell plates. Each Bioflux 48 well-microwell plate has a capacity of 24 flow experiments each with an Inlet and Outlet well. Loading of the chambers was performed after the following scheme.

Step	Insertion well	Pressure (DYN/cm ²)	Flow time (min)	incubation/ adherence time (h)	temperature (°C)
Priming with medium	Inlet	1	5	/	RT
Coating	Inlet	1	5	1	RT
Inoculation of cells	Outlet	1	0,5	1	37
Medium flow	Inlet	0,15	∞	24-60	37

The medium flow step has been started when the plate was installed at the Olympus microscope and the microscope chamber reached 37 °C. The microscope software Xellence rt has been started and programmed to take pictures of each flow channel every 30 min for minimum 24 h. brightfield, red and green fluorescence channels have been visualized.

II.10. DNA-Sequence Analysis

Sequencing of the DNA has been accomplished either via SeqLab (Bernhardt-Nocht Institute, Hamburg, Germany), or Eurofins MWG (Hamburg, Germany) based on the Sanger method. The samples have been purified as described in II.4.1.1 and II.4.1.5. The samples had to be eluted in H₂O_{bidest.} to avoid complications during sequencing process. 15 µL of the DNA have been sent in a 1,5 mL Eppendorf tube and either standard primer (already at Eurofins MWG), or 15 µL of the adequate primer have been sent (table 3). The chromatogram and sequence data has been aligned via Sequence Scanner and then blasted against a DNA-sequence database (<http://blast.ncbi.nlm.nih.gov/Blast.cgi>).

II.11. Used Software

In table II-14 all the used Software, databases and their reference sources can be found.

Table II-14: Used Software, databases and reference sources

Used Software / database	Reference Source
Finch TV	http://www.geospiza.com/Products/finchtv.shtml
Sequence Scanner	http://en.bio-soft.net/dna/ss.html
BLAST	http://blast.ncbi.nlm.nih.gov/Blast.cgi
Clone Manager Suite 7.0 and 9.0	Sci-Ed Software, Morrisville, USA
Volocity 6.0	Perkin-Elmer, Waltham, USA
Leica	Leica, Solms, Germany
Xellence rt	Olympus, Hamburg, Germany
Bioflux	Fluxion Biosciences, South San Francisco, USA
Clustal X 2	http://www.clustal.org/clustal2/ , UCD, Dublin, Ireland
Dendroscope	http://ab.inf.uni-tuebingen.de/software/dendroscope/ , Tübingen, Germany

Used Software / database	Reference Source
GC Plotter	http://tubic.tju.edu.cn/GC-Profile/ , Tianjin University, Tianjin, China [108]
Mascot	Matrix Science, online tool (http://www.matrixscience.com/cgi/search_form.pl?FORMVER=2&SEARCH=MIS)
InterProScan	Protein motif prediction (http://129.175.105.74/genomics/lbmgeiprscan.html)
Carbohydrate active enzymes	http://www.cazy.org/GlycosylTransferases.html

III. Results

Knowledge of organization and structure of proteins and polysaccharides involved in *S. epidermidis* biofilm assembly is the key for our understanding of biofilm formation, maturation and disruption. In this work the spatial arrangement of Embp, Aap, Sbp and PIA have been investigated in static and live cell experiments (III.1). The heterogeneity and arrangement of Embp inside a mature *S. epidermidis* 1585 biofilm, as well as possible co-localizations of Embp and PIA have been analyzed via dSTORM microscopy and subsequent bioinformatic analysis of images (III.1.2). Furthermore, the influence of different antibiotics, especially Tigecycline, on biofilm formation of *S. epidermidis* 1585 has been investigated via microscopy and immunological experiments (III.2.1). Phagocytosis of mature *S. epidermidis* 1585 biofilms after antibiotic induction has been investigated as well (III.2.2). Novel ways of disrupting a mature *S. epidermidis* 1457 biofilm have been further investigated building upon the previous work “Disruption of *Staphylococcus epidermidis* biofilms through novel metagenomic enzymes” [Henke H A, 2011, master thesis]. Putative biofilm disrupting enzymes from this work have been further analyzed by microscopy, heat-inactivation, filtration and mass-spectrometry. Over expression experiments of the putative enzymes were performed (III.3). Furthermore, bioinformatic analysis of the most promising candidates to be responsible of biofilm disruption has been performed (III.4).

III.1. Protein factors and polysaccharides involved in biofilm formation

Major biofilm inducing and supporting proteins have been detected in the recent years: Accumulation associated protein (Aap), Small basic protein (Sbp), which is predicted to be a surface attachment protein, and extracellular matrix binding protein (Embp). In addition, polysaccharide PIA is an important factor stabilizing biofilm formation. In III.1 the spatial organization, i.e. scattering and layers of distinct intercellular adhesins within a living biofilm have been elucidated by different microscopic techniques. To clarify how the biofilm is formed depending on PIA over time live cell imaging has been performed using static as well as flow assays (III.1.1). The distribution of Sbp and possible co-localization has been investigated (III.1.2) as well as the influence of each sub-domain of the protein Aap (III.1.3). Furthermore described in III.1.4 the direct co-localization of Embp and PIA has been identified. dSTORM microscopy showed the arrangement of Embp and its heterogeneity.

III.1.1. Spatial PIA organization

The determination of biofilm organizing proteins inside a mature *S. epidermidis* biofilm was addressed via confocal microscopy using either the Improvision confocal spinning disk microscope (Perkin Elmer, Waltham, USA), or the Leica SP2 confocal microscope (Leica, Solms, Germany). Strains used for microscopy are listed in table II-2. The determination of the major biofilm component PIA in *S. epidermidis* 1457 has been investigated using the strain *S. epidermidis* 1457xpCM29 allowing for constitutive *gfp* expression [98]. Texas red labelled wheat germ agglutinin (WGA) added to the growing bacterial culture was used to visualize PIA. WGA binds directly to PIA, thus its production inside the biofilm can be followed directly. Seven representative images taken during an experiment in which PIA-dependent biofilm formation was followed over a 13 hour period are presented in Fig. III-1, starting with time point T1 (also see the video starting at T2 in the appendix (VI.6.1 Video *S. epidermidis* 1457 PIA formation)). The experiment showed that some *S. epidermidis* cells already produced PIA from the very beginning, even before final cell sedimentation and stable adherence. This behaviour was observed only by microscopic analysis immediately after inoculation of growth medium (picture not shown). Some single cells stayed in the planktonic phase and did not express PIA. The PIA expressing starter cells then formed micro colonies, first growing in height and then spreading sideways over the bottom of cell culture dish to finally colonize the whole surface, forming a strong biofilm. The height of the biofilm increased steadily, but some planktonic cells still floated through the medium.

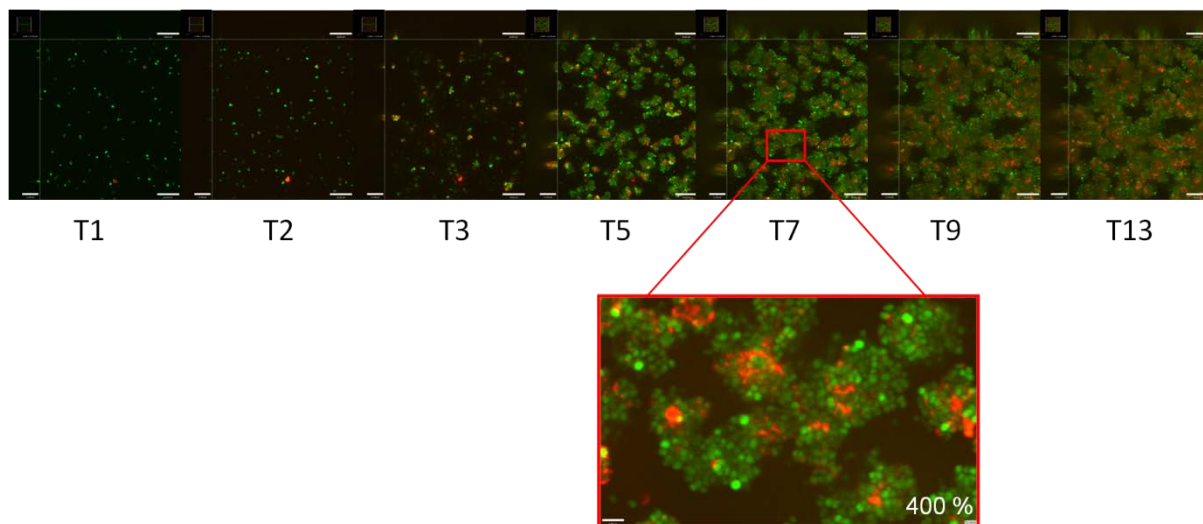


Fig. III-1: Dynamic PIA production and biofilm assembly over a 13 hour period. Images show representative areas at seven independent time points of *S. epidermidis* 1457xpCM29 biofilm growth at 37 °C under static conditions. PIA was visualized with WGA Texas red. Improvision spinning disk microscope (Perkin Elmer, Waltham, USA). It can be seen, that PIA was expressed from the start and the cells grew around the PIA scaffold (Zoom: 400 %). Magnification 630 x. White bar: 21 μ M.

The negative control of *S. epidermidis* 1457-M10 is not able to express PIA and thus, is not capable of forming a biofilm. Fig. III-2 shows dynamic growth of 1457-M10xpCM29 under static conditions identical as described above for *S. epidermidis* 1457. Apparently, the strain did not produce PIA and therefore did not show any red fluorescence. On the video in the appendix (VI.6.2 Video *S. epidermidis* 1457-M10) it is visible, that, despite cells appeared to accumulate over time, bacteria were not tightly linked to each other and moved slightly through the medium at each time point. Thus, it can be anticipated these cells represent sedimented rather than true attached, i.e. biofilm forming bacteria.

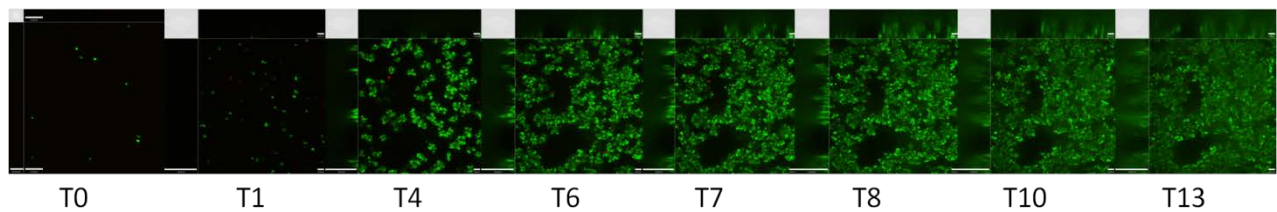


Fig. III-2: Growth experiment of the non-biofilm forming bacterium *S. epidermidis* 1457-M10. The images show time points of growth of *S. epidermidis* 1457-M10xpCM29 at 37 °C under static conditions showing that cell aggregates were formed while all cells were moving planktonic through the medium. Improvisation spinning disk microscope (Perkin Elmer, Waltham, USA). Magnification 630x. White bar: 21 μ M.

To more precisely determine PIA-dependent biofilm formation dynamic biofilm assembly was followed under flow conditions using the Bioflux 200 system (Fluxion, San Francisco, California, USA). Every 30 minutes an image of the bottom's surface of the Bioflux chamber was taken during the whole experiment (Olympus TIRFM confocal microscope Olympus, Tokyo, Japan). Fig. III-3 shows representative images of the growing biofilm of *S. epidermidis* 1457xpCM29 under flow conditions acquired at 7 time points (see appendix VI.6.3 Video *S. epidermidis* 1457 flow conditions). PIA was visible immediately after cell sedimentation and at the beginning of biofilm growth. The cells attached to the bottom as well as the margins of the Bioflux chamber. In some areas, this biofilm was stable and did not change over time, while planktonic cells were washed through the chamber without attaching to the surface. After 24 h of growth, the inlet well for the medium was overgrown and clogged, so that only small amounts of medium could flow through the chamber and the planktonic cells basically just floated around within biofilm compartments.

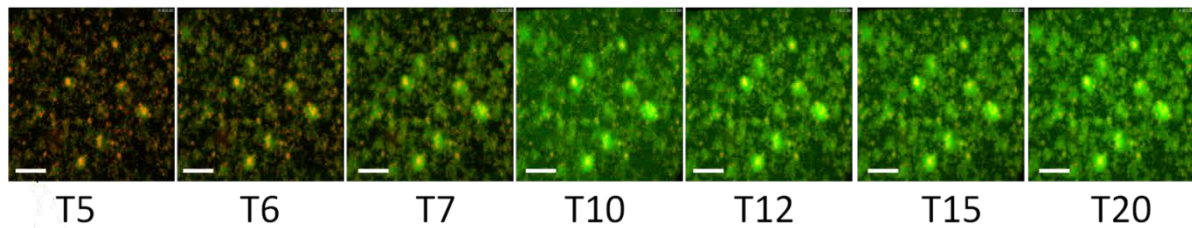


Fig. III-3: PIA production and biofilm assembly under flow conditions. Images show the time points of *S. epidermidis* 1457xpCM29 biofilm growth at 37 °C under flow conditions in the Bioflux 200 (Fluxion, San Francisco, USA). PIA was visualized with WGA Texas red. Olympus microscope (Olympus, Tokyo, Japan). It is visible that PIA was expressed from the start and the cells grew around the scaffold without flowing off the surface. Magnification 400x, White bar (left side of each image): 31 μ M.

In contrast to results obtained with 1457xpCM29, PIA-negative *icaA*-transposon insertion mutant *S. epidermidis* 1457-M10xpCM29 did not form a biofilm under flow conditions, but overgrew the chamber, possibly due to the low medium pressure. Fig. III-4 shows 8 time points of the bacteria where it is visible that there has been a raise in cell count but no surface attachment (see appendix VI.6.4 Video *S. epidermidis* 1457-M10 flow conditions). During 60 h of recording no biofilm has been build and the inlet well has not been clogged by cells. Planktonic cells were floating through the whole channel.

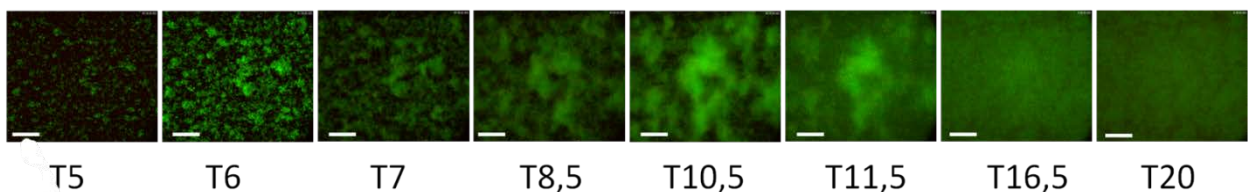


Fig. III-4: Growth of *S. epidermidis* 1457-M10 under flow conditions without biofilm assembly. Images show the time points of growth of *S. epidermidis* 1457-M10xpCM29 at 37 °C under flow conditions in the Bioflux 200 (Fluxion, San Francisco, USA) showing that no biofilm was formed and all cells were moving planktonic through the medium. Olympus microscope (Olympus, Tokyo, Japan). Magnification 400x. White bar: 31 μ M.

III.1.2. Spatial PIA and Sbp distribution

Previous studies have demonstrated that PIA is spread through all layers of the biofilm even from the beginning of biofilm formation, while other biofilm forming proteins have a distinct position inside the biofilm [100 & Decker, Rohde, unpublished results]. The small basic protein (Sbp) is supposed to have surface attachment properties. This hypothesis was validated by comparing the growth of *S. epidermidis* 1457xpCM29 and immuno staining of naturally expressed Sbp and *sbp*-knock out mutant 1457 Δ *sbp*xpCM29 grown in the presence

of DyLight550 labelled recombinant rSbp. Naturally expressed Sbp was detected using rabbit-rSbp anti-serum and rabbit-IgG Alexa568 antibody.

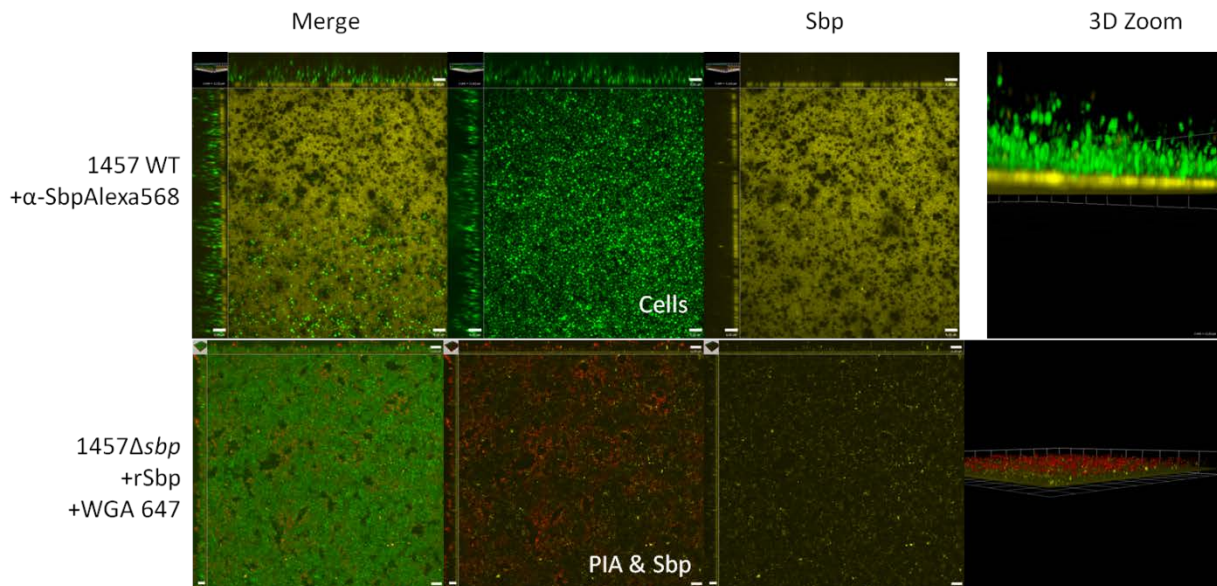


Fig. III-5: Sbp localization in *S. epidermidis* 1457 wild type and *sbp* deletion mutant. The *S. epidermidis* 1457 wild type (WT) expressing natural Sbp was stained with rabbit-rSbp anti-serum and rabbit-IgG AlexaFluor 568 antibody (image kindly provided by MSc Katharina Sass). Improvion spinning disk (Perkin Elmer, Waltham, USA). It is visible that Sbp was located at the bottom of the well. In comparison *S. epidermidis* 1457 Δ *sbp* with additional rSbp-Dylight550 and WGA647 (visualisation of PIA) also showed that Sbp was mainly located on the surface of the microscope chamber while PIA spread through the biofilm. Leica SP2 confocal microscope (Leica, Solms, Germany). Sbp: yellow, PIA: red, cells: green, Magnification 630x, White bar (right side of each image): 11 μ M.

In both cases Sbp was mainly located at the interface between the biofilm and bottom of the microscope chamber (Fig. III-5). To distinguish if Sbp is a true surface attachment protein, or sedimenting to the bottom of the culture dish due to gravity, an overhead experiment has been performed. Here, an oN culture of *S. epidermidis* 1457xpCM29 has been transferred into 35 mm cell culture dishes (ibidi, Martinsried, Germany). The culture dish was closed airtight and incubated for 2 h at 37 °C static. Then the culture dish was turned 180 degrees, allowing a hanging biofilm to be assembled. Fig. III-6 shows that even under these growth conditions, Sbp still mainly attached to the surface and partially between cell aggregates, resembling the organization structure also observed during conventional growth conditions. Thus, gravity does not induce the intriguing surface organization of Sbp, which is apparently, result of directed events.

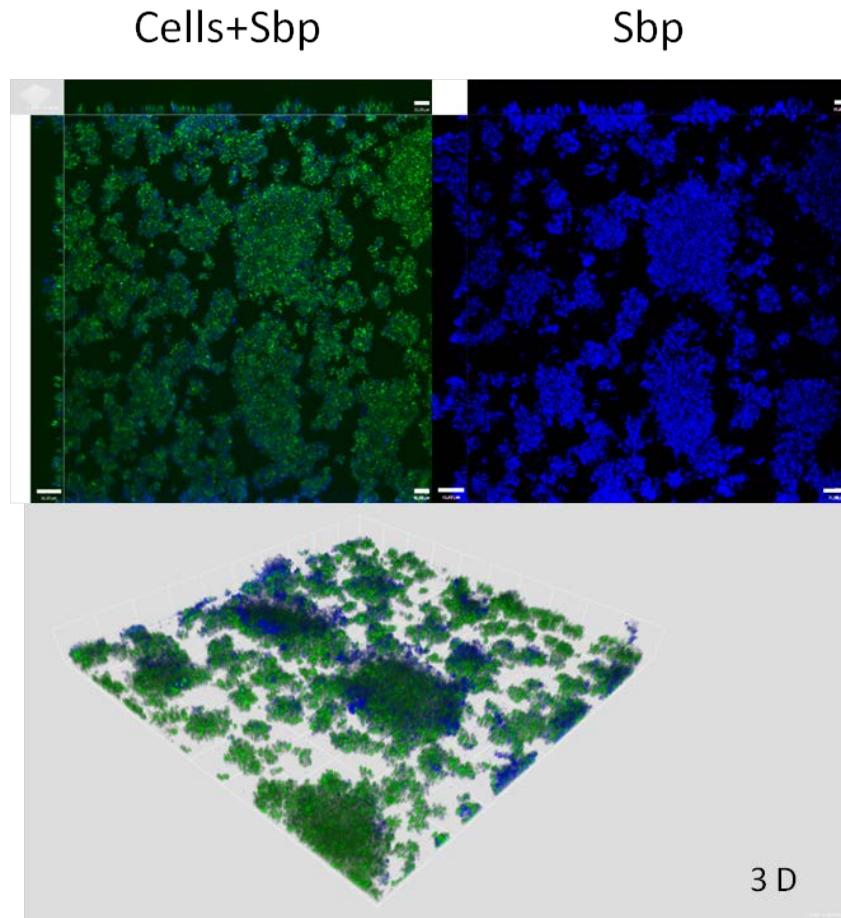


Fig. III-6: Sbp surface attachment is independent of sedimentation. Images of *S. epidermidis* 1457xpCM29 grown as a hanging biofilm, i.e. bottom up. Natural Sbp has been stained with rabbit-rSbp anti-serum and rabbit-IgG Cy5 antibody (blue). The striking surface localization of Sbp did not result from sedimentation but from directed events that retain the protein on the surface. Leica SP2 confocal microscope (Leica, Solms, Germany). Sbp: blue, cells: green, Magnification 630x, White bar (right side of each image): 13 μ M.

To determine the putative co-localization of Sbp and PIA microscope images have been investigated using the co-localization tool of the Volocity 6.1.1 software package. This tool counts the pixels acquired with independent wave lengths and estimates the number of those pixels in which signals from both wave lengths are evident. It is then possible to calculate the Manders coefficient, expressing the co-localization as a percentage of the total pixels from a given wave length. With this method the co-localization between Sbp and PIA has been calculated to less than approx $\sim 4,7\%$ and it, thus, is not significant.

III.1.3. Influence of sub-domains of Aap on *S. epidermidis* biofilm formation

The formation of biofilms is also dependent on the Accumulation associated protein Aap [109], a protein that contains defined domains (see Fig. III-7). Still, it is not clear how these different sub-domains contribute to biofilm formation and if, in living biofilms, Aap interacts with other biofilm matrix components (i.e. PIA or Sbp). To identify the exact position of Aap and Sbp inside the biofilm architecture, microscopy experiments using natural as well as recombinant Sbp were performed. To further clarify the position of Aap *S. epidermidis* 1457 Δ aap, 1457-M10 Δ aap and 1457-M10 Δ aap Δ sbp have been complemented with either pCN57::DomA, pCN57::DomB, or pCN57::DomB+212. Strains containing only one part of Aap could be used to detect the sub-domain responsible for biofilm attachment, as well as possible co-localization to other biofilm forming proteins. Fig. III-7 shows the scheme of clones containing the different sub-domains of Aap.

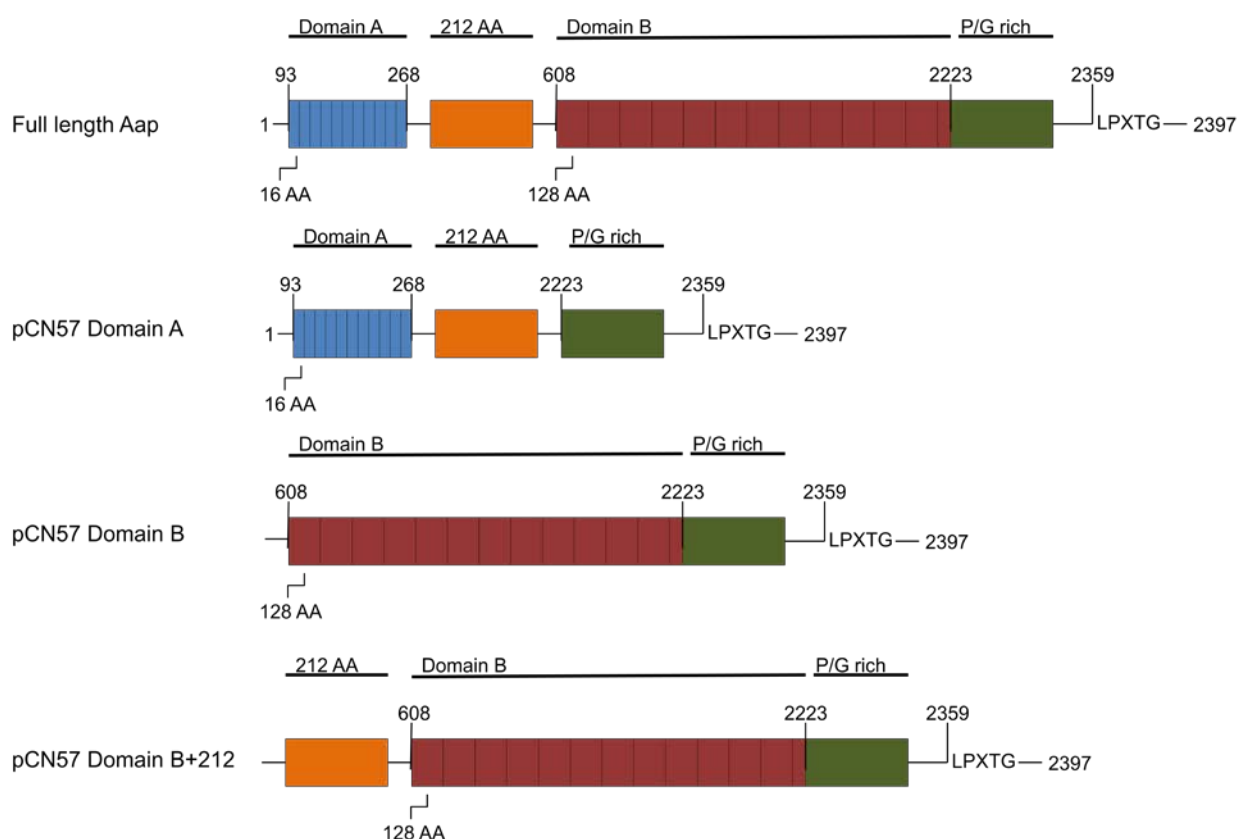


Fig. III-7: Schematic representation of full length Aap and the sub-domains. This image shows the scheme of clones produced to express each sub-domain of Aap separately. Each plasmid containing one of the domains (A, B, or B+212) had a tetracycline inducible promoter. The strains *S. epidermidis* 1457 Δ aap, *S. epidermidis* 1457-M10 Δ aap and *S. epidermidis* 1457-M10 Δ aap Δ sbp have been complemented with each construct.

Each clone containing only one of the Aap sub-domains has been investigated using confocal microscopy. 1,25 µg/mL Tetracycline have been used to induce the expression of the desired sub-domain of Aap. After fixing the cells, immuno staining with the corresponding primary anti-serum and a secondary antibody has been performed to finally visualize each sub-domain (see table II-5 for specific antibodies). Fig. III-8 shows strains *S. epidermidis* 1457Δ*aap* expressing each sub-domain of Aap separately. It is evident that the clones expressing either domain B, or domain B+212 formed biofilms with typical mushroom-like structures, while only domain A led to non structured cell layers. Fig. III-9 shows the analysis of biofilm height of the clones expressing each sub-domain of Aap separately. The unstructured cell layers of domain A were higher than the structured biofilms that derived from domain B and domain B+212. By co-localization analysis of the domains A, B and B+212 with PIA no evidence for significant co-localization molecular interactions was detected.

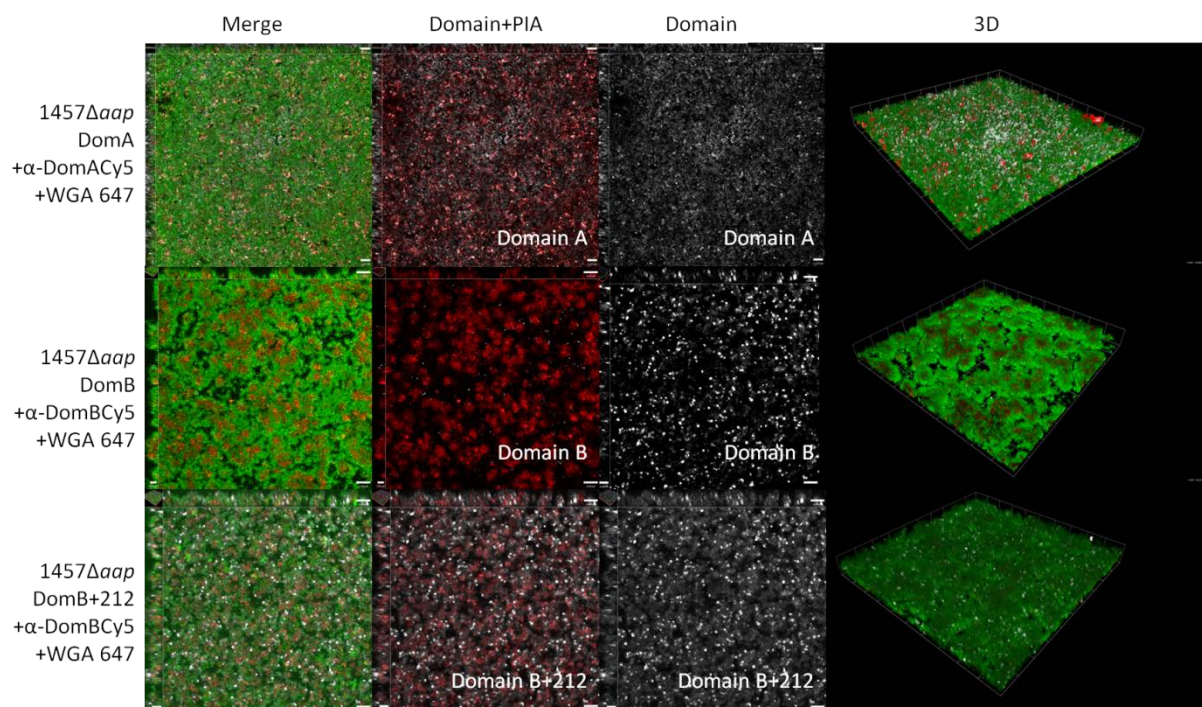


Fig. III-8: Function of Aap sub-domains on biofilm formation in *S. epidermidis* 1457Δ*aap*. The images show *S. epidermidis* 1457Δ*aap* strains each complemented with one sub-domain of Aap. WGA 647 was added to the growing culture to visualize PIA. After 24 h incubation at 37 °C static the cultures have been immuno stained with the corresponding antibodies (table II-5) and a secondary fluorescent antibody (Cy5). The strain expressing domain A (DomA) showed non-structured cell layers, while domain B (DomB) and domain B+212 (DomB+212) showed mushroom-like structured biofilms. The structure was more distinct when DomB has been expressed, but the protein was less abundant in the biofilm. PIA has been expressed evenly in all strains. Leica SP2 confocal microscope (Leica, Solms, Germany). PIA: red, DomA, B, or B+212: white, cells: green. Magnification 630x, White bar (right side of each image): 13 µM.

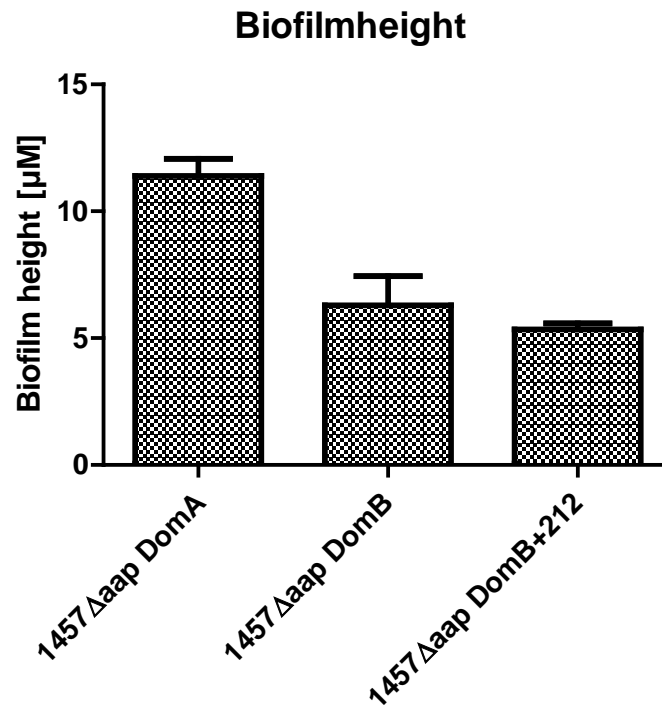


Fig. III-9: Biofilm height of *S. epidermidis* 1457 Δ aap clones expressing each sub-domain of Aap. Graphic illustration of the biofilm height of *S. epidermidis* 1457 Δ aap complemented with each sub-domain of Aap separately showing that the unstructured cell layers that derive from domain A were $\sim 12 \mu\text{M}$ in height while the more structured biofilms due to domain B and domain B+212 were ~ 7 , respectively $\sim 6 \mu\text{M}$ in height.

To test the effect of in trans expression of Aap domains A, B, or B+212 on biofilm formation in a PIA- and biofilm negative background, the respective plasmids were introduced into 1457-M10 Δ aap. First the phenotype of the respective strains was tested by using the conventional crystal violet staining based biofilm assay. Fig. III-10 shows representative results of this assay. It is evident that, while 1457-M10 Δ aap is unable to form a biofilm, in trans expression of each single Aap sub-domain quantitatively augments biofilm formation, with the most obvious biofilm increase being identified by expression of Aap domain B. Strikingly, inactivation of *sbp* did not alter the biofilm phenotype, suggesting that the Aap dependent biofilm does not functionally rely on Sbp. The strain *S. epidermidis* 1457-M10 Δ aapxpCN57::DomB expressing only domain B of Aap could not be established and is therefore lacking in this analysis.

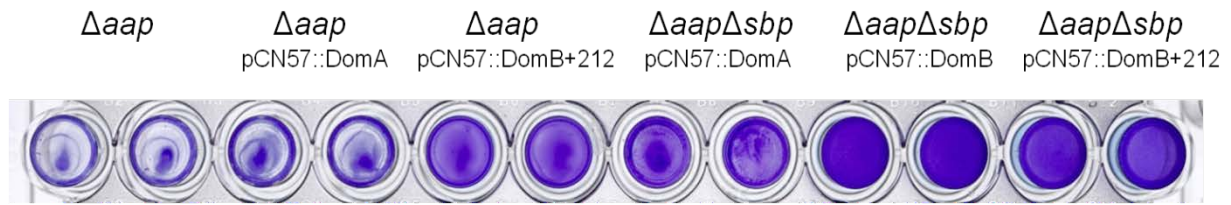


Fig. III-10: Biofilm assay of *S. epidermidis* 1457-M10 Δaap and 1457-M10 $\Delta aap\Delta sbp$ complemented with each sub-domain of Aap. Strains were grown in the presence of 1,25 $\mu\text{g/ml}$ tetracycline in order to induce expression of the respective domains. It is obvious that *S. epidermidis* 1457-M10 Δaap could not form a biofilm even when the domain A of Aap was present. Only when domain B, or domain B+212 were expressed a biofilm could be produced. The same results showed for *S. epidermidis* 1457-M10 $\Delta aap\Delta sbp$.

In Fig. III-11, the quantitative analysis of static biofilm assays is being shown, supporting the hypothesis that clones containing domain B, or domain B+212 could form a biofilm while domain A did not significantly augment biofilm formation as compared to the wild type. For strain *S. epidermidis* 1457-M10 $\Delta aap\Delta sbp$ the extinction of crystal violet when domain A of Aap is present indicated biofilm formation.

Extinktion of Crystal violet at 570 nm

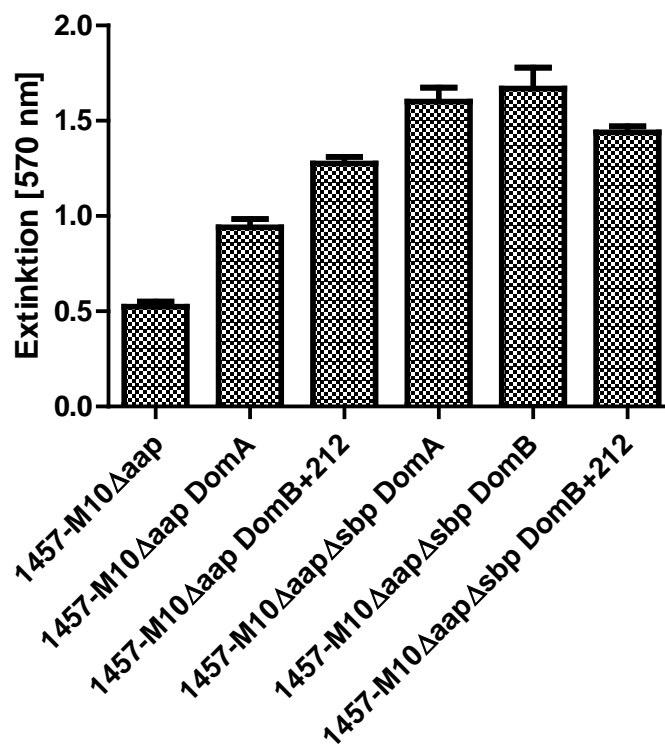


Fig. III-11: Photometric evaluation of biofilm formation by *S. epidermidis* 1457-M10 *aap* and *sbp* deletion mutants complemented with sub-domains of Aap. Extinction of crystal violet used for staining of biofilm at 570 nm. *S. epidermidis* 1457-M10Δ*aap* and *S. epidermidis* 1457-M10Δ*aap*Δ*sbp* strains expressing each sub-domain of Aap have been tested for their biofilm forming ability showing that a biofilm was formed when domain B, or domain B+212 of Aap were expressed. Expression of domain A of Aap led to some attached cells, but not to structured biofilms. The extinction has been measured in the Infinite 200 pro plate reader (Tecan, Männedorf, Switzerland).

To verify these results microscopy of all clones has been performed in order to test expression and localization of Aap sub-domains in living biofilms. Fig. III-12 shows images of *S. epidermidis* 1457-M10Δ*aap* complemented with DomA, or DomB+212. The strain containing DomB+212 assembled structured, mushroom-like biofilms, while 1457-M10Δ*aap* containing DomA was unable to form biofilms. The presence of only domain A of Aap has not been sufficient for biofilm formation but led to surface attached cell layers.

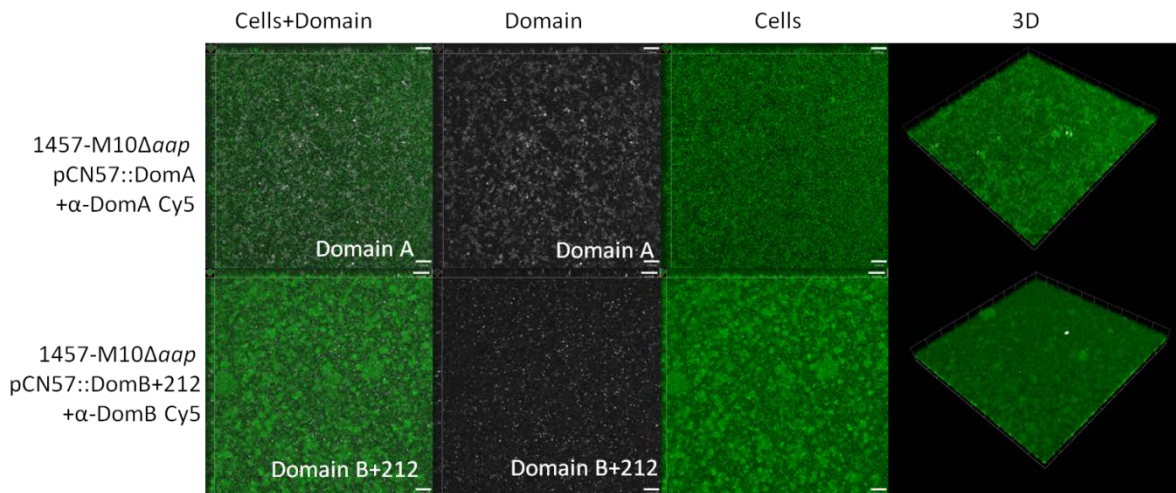


Fig. III-12: Biofilm formation by *S. epidermidis* 1457-M10Δaap strains complemented with sub-domains A, or B+212 of Aap. The images show that domain A led to non structured cell layers, while domain B+212 led to distinct mushroom-like structures and multiple cell layers. The sub-domains were visualized by immuno staining with rabbit anti-rDomA anti-serum, or rabbit anti-rDomB anti-serum and rabbit-IgG Cy5 antibody. Leica SP2 confocal microscope (Leica, Solms, Germany). DomA, B+212: white, cells: green. Magnification 630x, White bar (right side of each image): 13 μM.

Fig. III-13 shows the microscope images of strain *S. epidermidis* 1457-M10ΔaapΔsbp clones complemented with each domain of Aap. The same results as in the biofilm assay and the microscope study of *S. epidermidis* 1457-M10Δaap were obtained. Also for a strain lacking Aap and Sbp a mushroom-like biofilm structure could be achieved by expressing domain B, or domain B+212 of Aap. Domain A expression alone did not lead to a structured biofilm formation, but to a loose organization of cells in cell layers attached to the microscope chamber. Fig. III-14 shows the analysis of *S. epidermidis* 1457-M10Δaap and 1457-M10ΔaapΔsbp expressing each sub-domain of Aap separately, showing that the biofilm height increased when domain B was expressed compared to domain A, or domain B+212. The biofilm derived from domain B-expressing 1457-M10Δaap was almost about twice in height (~ 11 μM) compared to the cell layers produced by 1457-M10Δaap expressing domain A, or 1457-M10Δaap producing domain B+212.

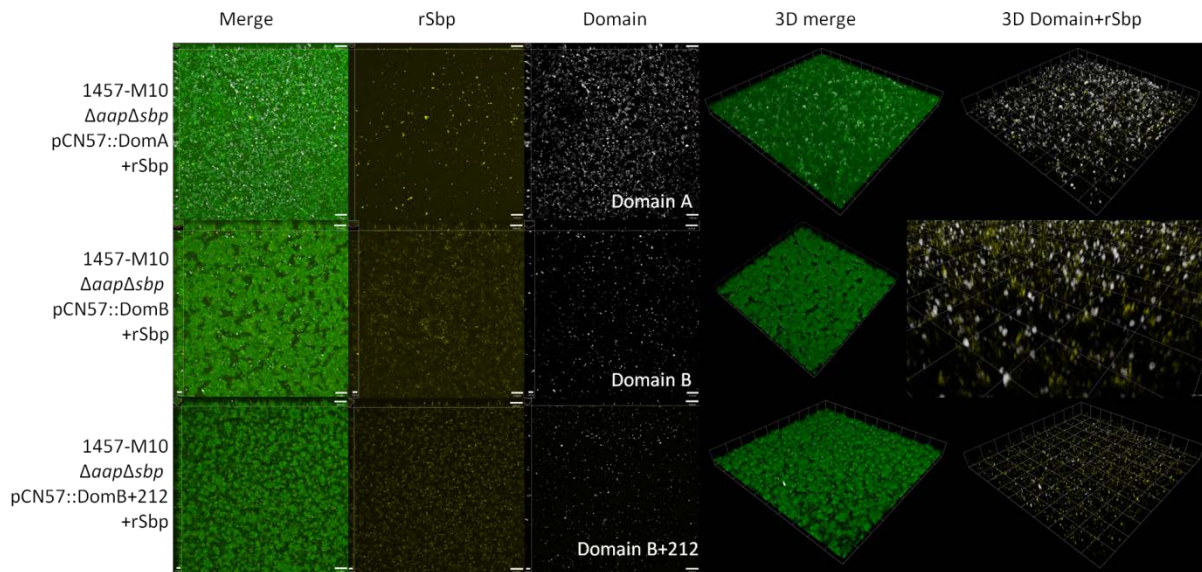


Fig. III-13: Biofilm formation of *S. epidermidis* 1457-M10 Δ aap Δ sbp strains complemented with either sub-domain A, B or B+212 of Aap. The images show that domain A led to non structured cell layers, while domain B and B+212 led to distinct mushroom-like structures. The structure was more distinct when only domain B has been expressed. The domains were visualized by immuno staining with rabbit-DomA anti-serum, or rabbit-DomB anti-serum and rabbit-IgG Cy5 antibody. Recombinant Sbp has been added to the growing culture, showing that even in strains expressing only one domain of Aap, Sbp was located mainly on the ground of the microscope chamber. Leica SP2 confocal microscope (Leica, Solms, Germany). rSbp: yellow, DomA, B, B+212: white, cells: green. Magnification 630x, White bar (right side of each image): 13 μ M.

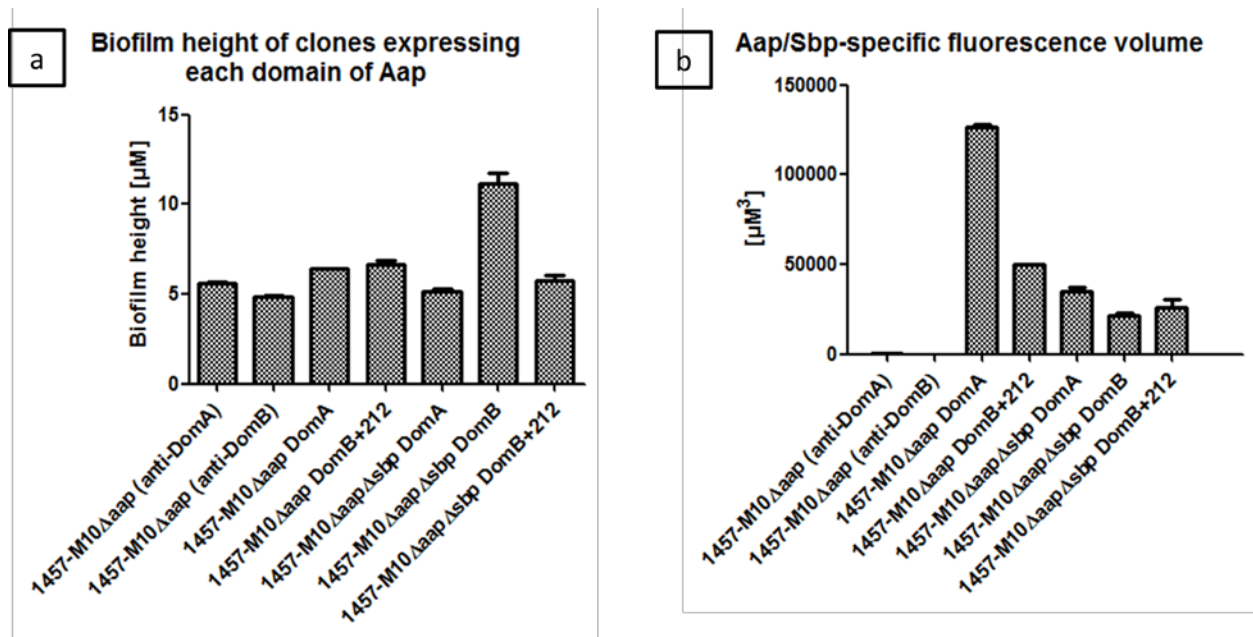


Fig. III-14: Evaluation of biofilm height and Aap/Sbp-specific fluorescence volume in clones expressing each sub-domain of Aap. The graphs of the biofilm height of 1457-M10 Δ aap and 1457-M10 Δ aap Δ sbp complemented with Aap domain A, domain B or domain B+212 show that the cell layers deriving from domain A were not higher than cell layers of control strains lacking Aap (**a**). While the biofilm formed due to domain B+212 only increased slightly in height compared to domain A, the biofilm formed due to domain B was twice the height of the other sub-domains (**a**). Regarding the protein-specific fluorescence volume of each sub-domain of Aap it could be seen that domain A was expressed in amounts around 130.000 μM^3 in Aap deletion mutants. The mutant lacking Aap and Sbp expressed domain A only around 40.000 μM^3 . Domain B+212 was expressed less than 50.000 μM^3 in both deletion mutants while domain B was expressed only around 25.000 μM^3 none the less domain B led to the only distinctively structured biofilm. In control strains lacking Aap which have been immuno stained to verify that neither the DomA, nor the DomB antibodies bind unspecific, no signal could be detected (**b**).

III.1.4. Co-localization of Embp and PIA and spatial distribution of Embp

While the biofilm associated proteins Aap and Sbp did not show co-localization with polysaccharide PIA, given the presence of putative N-acetylglucosamine binding modules it is reasonable to that the extracellular matrix binding protein Embp shows distinct co-localization with PIA. To test this hypothesis *S. epidermidis* 1585 $P_{xyl/tet}::embp$, allowing for inducible expression of 1 MDa giant protein Embp was complemented with pTXica for inducible PIA production. For visualization purposes, all strains used here were complemented with *gfp*-encoding plasmid pCM29. The biofilm forming properties, as well as the presence of Embp within the extracellular space of strain 1585 $P_{xyl/tet}::embp$ xpTXica was first visualized by raster electron microscopy (REM) and transmission electron microscopy (TEM). In these experiments *S. epidermidis* 1585 $P_{xyl/tet}::embp$ xpCM29 was induced to produce Embp by adding 0,2 μ g/mL tetracycline. Fig. III-15 shows the REM images that proved the formation of a biofilm by *S. epidermidis* 1585 $P_{xyl/tet}::embp$ xpCM29, while the wild type strain *S. epidermidis* 1585 did not show biofilm-like structures but only single cells, or small aggregates / tetrads spread over the microscope dish.

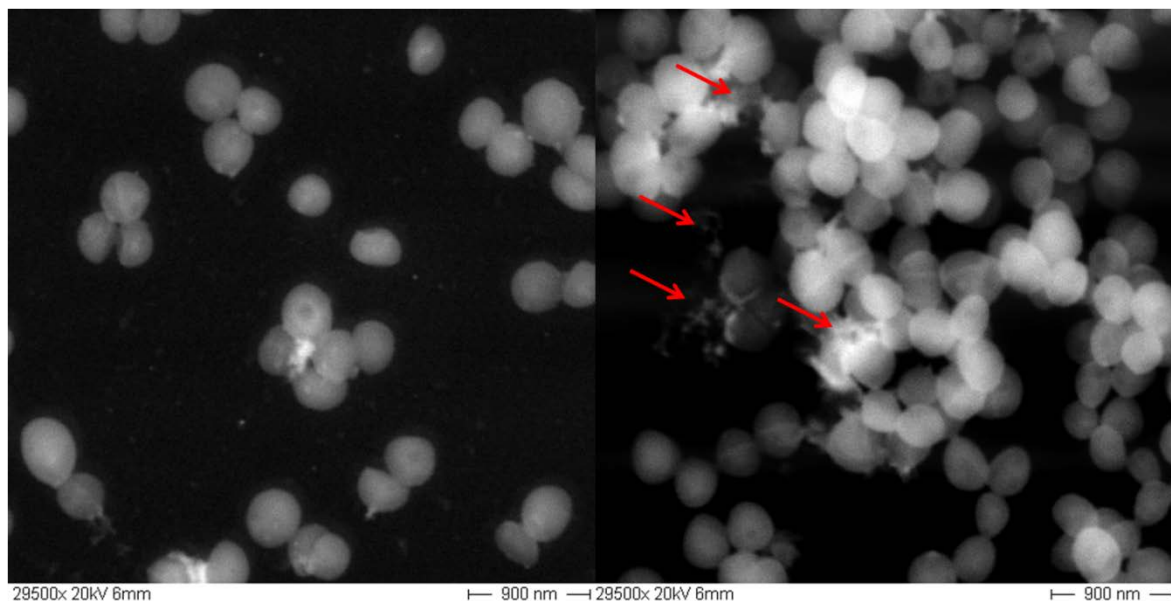


Fig. III-15: Raster electron microscope images of *S. epidermidis* 1585 and *S. epidermidis* 1585 $P_{xyl/tet}::embp$. *S. epidermidis* 1585 (left) and *S. epidermidis* 1585 $P_{xyl/tet}::embp$ (right) induced with 0,2 μ g/mL Tetracycline for Embp expression. It can be seen that the clone expressing Embp was able to form cell aggregates and a web-like matrix. Image kindly provided by Dr. Rudolph Reimer.

Fig. III-16 then shows the TEM images. All gold particles were associated with web-like structures localized between the bacterial cells. While this finding demonstrates the extracellular localization of Embp, due to harsh fixation procedures preceding TEM image

acquisition, the natural structure of Embp most likely was destroyed and the web-like structure crinkled in small aggregates in between the cells.

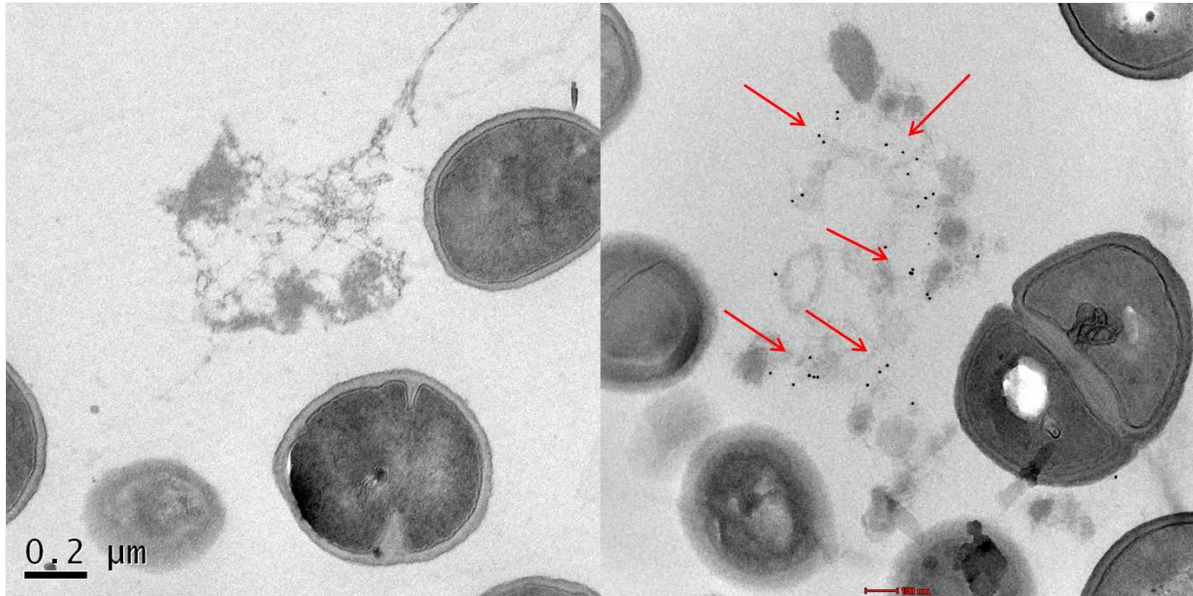


Fig. III-16: Transmission electron microscope images of *S. epidermidis* 1585 and *S. epidermidis* 1585 $P_{xyl/tet}::embp$. *S. epidermidis* 1585 (left) and *S. epidermidis* 1585 $P_{xyl/tet}::embp$ (right) induced with 0,2 $\mu\text{g}/\text{mL}$ Tetracycline for Embp expression. To visualize Embp in the matrix immuno gold labelling has been performed (right picture) showing that Embp was expressed in the clone (the black spots are immuno gold particles bound to Embp), while the control did not express Embp. Image kindly provided by Carola Schneider.

To demonstrate and estimate Embp and PIA co-localization interactions in living biofilm samples confocal microscopy as well as dSTORM microscopy was performed using *S. epidermidis* 1585 $P_{xyl/tet}::embpxp\text{CM29xpTXica}$ and the negative control *S. epidermidis* 1585. It could be visualized that Embp and PIA are closely associated and form stretched elongated fibres pervading the biofilm. PIA formed a honey comb-like structure within the biofilm architecture, thereby surrounding the bacterial cells. Embp was associated next to PIA and stretched horizontal and vertical indicating the heterogeneity of Embp. Vertical stretched Embp in *S. epidermidis* 1457 $P_{xyl/tet}::embpxp\text{CM29}$ can be seen in Fig. III-20 and the 3D video in the appendix (VI.6.5 Video *S. epidermidis* 1457 3D dSTORM Embp+PIA). The same vertically stretched pattern could be obtained for *S. epidermidis* 1585 $P_{xyl/tet}::embpxp\text{CM29pTXica}$ (data not shown). Moreover, Embp appeared to be closer associated with the bacterial cells than PIA. Overall, a huge variety of Embp positions was detected, demonstrating the morphological heterogeneity of Embp aggregates. Fig. III-17 shows an overview of *S. epidermidis* 1585 $P_{xyl/tet}::embpxp\text{CM29pTXica}$ where Embp was induced with 10 $\mu\text{g}/\text{mL}$ Tetracycline and PIA was induced with 2 % Xylose.

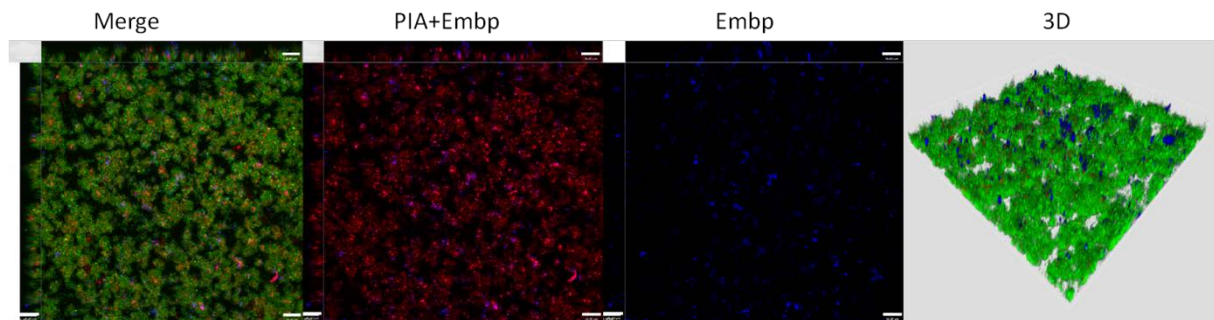


Fig. III-17: Simultaneous expression of Embp and PIA in *S. epidermidis* 1585. The microscope images of *S. epidermidis* 1585 $P_{xyl/tet}::embpxpCM29xpTXica$ expressing *gfp*, PIA after 2 % Xylose induction and Embp due to 10 μ g/mL Tetracycline induction show that PIA and Embp were spread throughout the whole biofilm. A co-localization of PIA and Embp could be assumed due to the pink spots in the overlay picture of PIA and Embp. Leica SP2 confocal microscope (Leica, Solms, Germany). PIA: red, Embp: blue, cells: green. Magnification 630x, White bar (right side of each image): 13 μ M.

To more precisely visualize Embp inside the biofilm and to clarify the co-localization with PIA, dSTORM microscopy has been performed. Fig. III-18 shows in 3D high resolution images the organization of a biofilm built of Embp and PIA after induction of *S. epidermidis* 1585 $P_{xyl/tet}::embpxpCM29xpTXica$. Clearly, *S. epidermidis* 1585 $P_{xyl/tet}::embpxpCM29xpTXica$ was able to form a strong biofilm due to the presence of Embp and PIA. Embp located directly to the bacterial cells and showed an elongated structure connecting the cells. It was visible that PIA formed a web-like structure mainly in sections where Embp was less represented. It is also visible, that Embp and PIA co-localized at certain sections of the biofilm. They lied next to each other and seemed to be interwoven. A co-localization analysis using the Manders coefficient showed that approximately 41,38 % of PIA co-localized with Embp and 42,38 % of Embp co-localized with PIA. A co-localization analysis of the matrix components PIA and Embp correlating to the bacterial cells showed that 24,36 % of the bacterial cells were in contact to Embp, while 10,36 % of Embp has been directly located at the cells. Regarding PIA only 7,74 % was located directly at the bacterial cells and 19,72 % of the bacterial cells directly touched PIA.

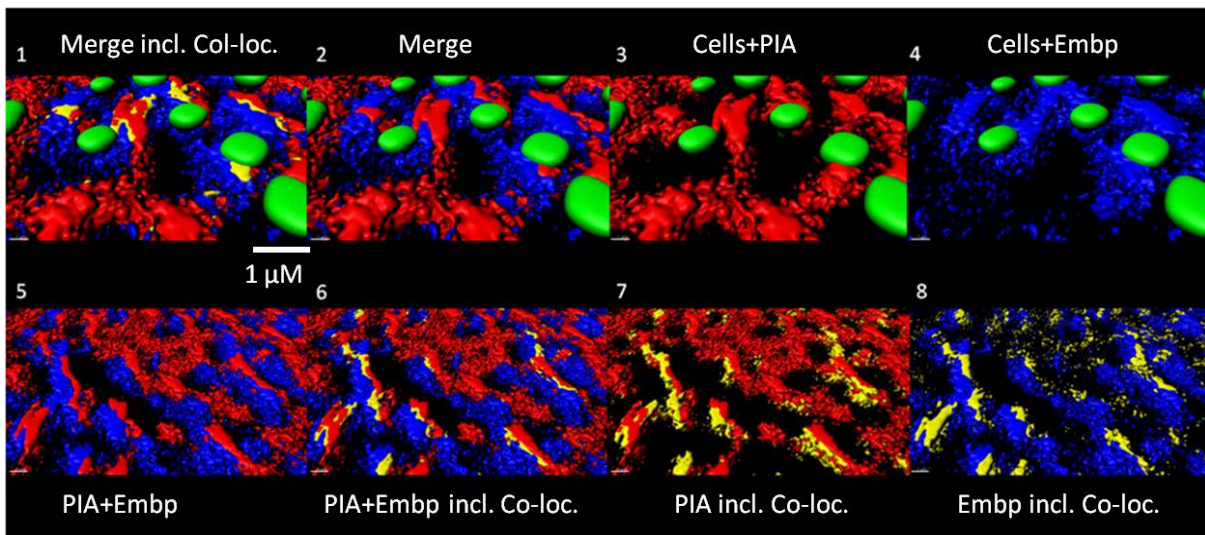


Fig. III-18: dSTORM images of *S. epidermidis* 1585 $P_{xyl/tet}::embpxpCM29xpTXica$ with co-localization spots of PIA and Embp. The strain has been induced with 2 % Xylose and 10 $\mu\text{g}/\text{mL}$ Tetracycline. PIA was visualized with WGA 647 and Embp was visualized using rabbit-Embp7762 anti-serum and rabbit-IgG AlexaFluor568 antibody. PIA is displayed red and Embp blue. The bacterial cells express *gfp* and are displayed green. It is visible that PIA was mainly located in regions where Embp was less present while Embp was more closely related to the bacterial cells. The co-localization channel showed that Embp and PIA distinctively co-localize in elongated horizontal parts (Co-loc., yellow). This image is a 3D illustration, kindly provided by Dr. Dennis Eggert. Magnification 1.000x, Zoom 1000 %. PIA: red, Embp: blue, cells: green.

To test if the co-localization of Embp and PIA potentially supports biofilm formation, all strains expressing only Embp or PIA or co-express both components were tested for their biofilm forming ability by CLSM. All images have been analyzed for their amount of cells, PIA and Embp by determining the fluorescence of the channels. Compared to *S. epidermidis* 1585 $P_{xyl/tet}::embp$ or 1585xpTXica, strain *S. epidermidis* 1585 $P_{xyl/tet}::embpxpCM29xpTXica$ formed higher biofilms with a larger amount of PIA even compared to the wild type strain *S. epidermidis* 1457 that expressed great amounts of PIA naturally. The amount of Embp expressed in *S. epidermidis* 1585 $P_{xyl/tet}::embp$ was 4-6 times higher, when there was no PIA present as in strain *S. epidermidis* 1585 $P_{xyl/tet}::embpxpCM29xpTXica$. *S. epidermidis* 1457 $P_{xyl/tet}::embp$ showed a very low amount of Embp if it was grown in full TSB medium. *S. epidermidis* 1457 strains form large amounts of PIA in full TSB medium. To avoid this massive PIA production that might suppress the Embp production glucose free TSB-medium has been used. Fig. III-19 shows the biofilm height, as well as the Embp- and PIA-specific fluorescence volume when *S. epidermidis* 1457 $P_{xyl/tet}::embp$ grew in glucose free medium. The *embp* expression did not increase much due to glucose free medium.

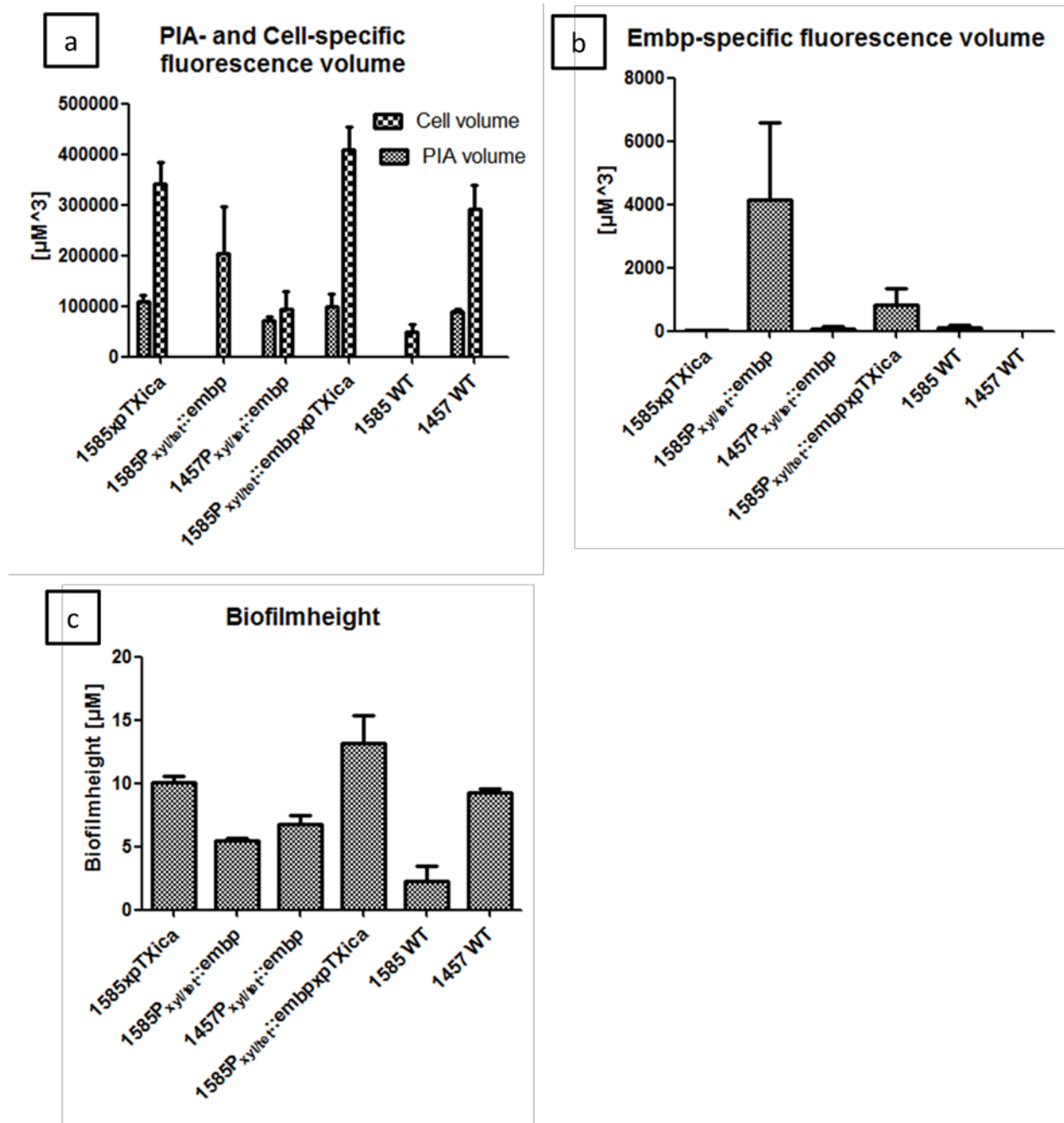


Fig. III-19: Graphic illustration of clones expressing Embp, PIA, or both in either *S. epidermidis* 1457, or *S. epidermidis* 1585. Graph (a) shows PIA-specific fluorescence volume and living cells in the biofilm. The wild type (WT) of *S. epidermidis* 1585 as anticipated did not express PIA, while the WT of *S. epidermidis* 1457 did. In *S. epidermidis* 1585xpTXica PIA expression could be obtained. *S. epidermidis* 1585P_{xyl/tet::embp} showed very high and 1457P_{xyl/tet::embp} showed quite low Embp expression. Graph (b) shows the Embp-specific fluorescence volume in all clones and the wild types, verifying that only the clones containing P_{xyl/tet::embp} were able to express Embp. *S. epidermidis* 1585 WT did naturally express low amounts of Embp. Graph (c) shows the biofilm height of each clone and the wild types showing that the height increased with PIA expression and was highest when PIA and Embp were expressed at the same time.

To compare whether the Embp distribution between the strain *S. epidermidis* 1585 $P_{xyl/tet}::embpxpCM29xpTXica$ which expressed Embp and PIA only under induced conditions was the same as in wild type *S. epidermidis* 1457 a naturally PIA expressing strain that also expressed Embp under slight antibiotic stress, dSTORM microscopy has been performed. To this end wild type strain *S. epidermidis* 1457 has been induced for 24 h with 75 pg/mL tigecycline to stimulate natural Embp production. Fig. III-20 shows that the distribution of PIA in a web-like structure as well as the Embp distribution throughout the whole biofilm looked similar to the arrangement in *S. epidermidis* 1585 $P_{xyl/tet}::embpxpCM29xpTXica$. The heterogeneity of Embp in its horizontal and vertical stretched form can be seen in Fig. III-20 and the 3D video in the appendix (VI.6.5 Video *S. epidermidis* 1457 3D dSTORM Embp+PIA). The findings support the hypothesis of a co-localization of Embp and PIA also in natural environment. Co-localization analysis showed also for strain *S. epidermidis* 1457 40,81 % of co localized Embp to PIA, while 32,08 % of PIA directly co-localize to Embp.

2D dSTORM image of Embp, PIA and bacterial cells

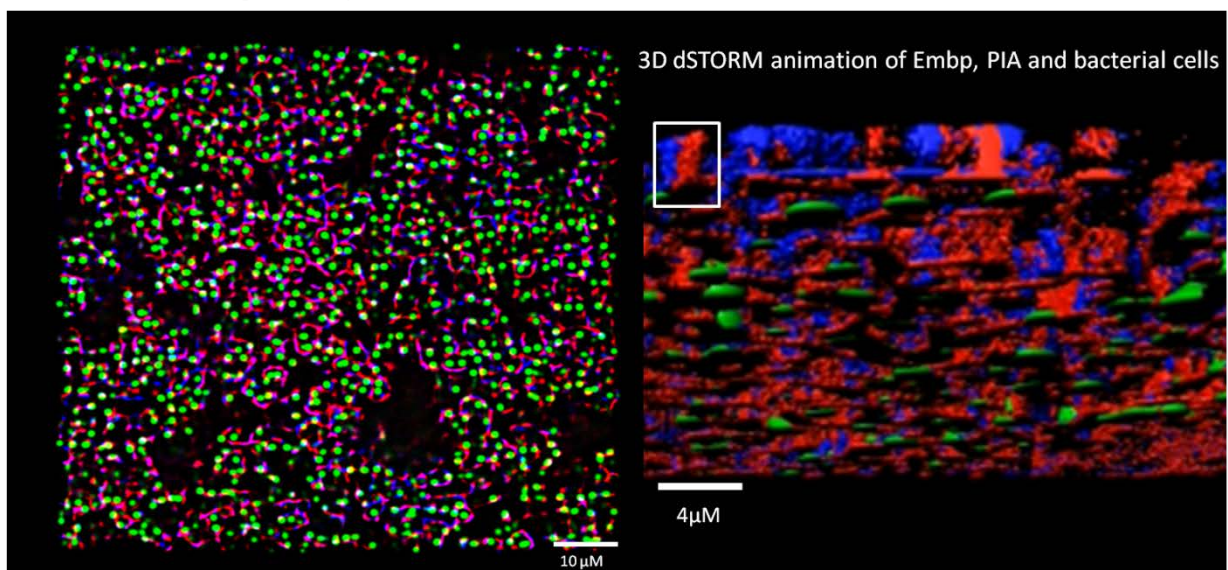


Fig. III-20: dSTORM images of *S. epidermidis* 1457 expressing natural PIA and Embp. The strain has been induced with 75 pg/mL tigecycline to promote natural Embp production. PIA was visualized with WGA 647 and Embp was visualized using rabbit-Embp7762 anti-serum and rabbit-IgG AlexaFluor568 antibody. It could be seen that Embp formed the same elongated structures as in Fig. III-18 and PIA formed a web-like structure. Furthermore the vertical arrangement of Embp can be seen in the 3D image indicated with the white box. The corresponding video can be found in the appendix (VI.6.5 Video *S. epidermidis* 1457 3D dSTORM Embp+PIA). Magnification 10.000x. Images kindly provided by Dr. Dennis Eggert.

III.2. Effect of antibiotics on *S. epidermidis* 1585 biofilm formation

Failure of antibiotic therapies is a common event in treatment courses of biofilm related infections. It has been demonstrated that indeed, antibiotics itself promote biofilm formation and thus could propel a phenotype that render bacteria even more unsusceptible to the effect of antibiotic substances. Here the idea was followed that antibiotics not only induce biofilm formation, but that this effect is related to the over expression of Embp.

III.2.1. Influence of Tigecycline, Chloramphenicol, Erythromycin, Linezolid and Oxacillin on the formation of *S. epidermidis* 1585 biofilms

Based on preliminary evidence that tigecycline most potently augments *S. epidermidis* biofilm formation through up-regulation of *embp* expression (Weiser, Henke, Rohde, unpublished). Therefore, here primarily the effect of tigecycline was studied in more detail. *S. epidermidis* 1585 was used as a model strain, given its clinical relevance, but biofilm negative phenotype under standard growth conditions in TSB [35, 100]. The finding that tigecycline induces Embp production was validated using a semi-quantitative immune dot blot approach in which preparations of cell surface associated proteins were analysed for the presence of Embp. Indeed, compared to the control grown in TSB, supplementation of the growth medium with sub-inhibitory concentrations of tigecycline induced over expression of Embp. This effect was also evident for other inhibitors of the protein biosynthesis (linezolid, chloramphenicol), but not a general phenomenon for this group of substances. Namely, presence of macrolid antibiotic erythromycin had no Embp inducing properties. Interestingly, also inhibitors of the cell wall biosynthesis, i.e. oxacillin, lead to an over expression of Embp (Fig. III-21).

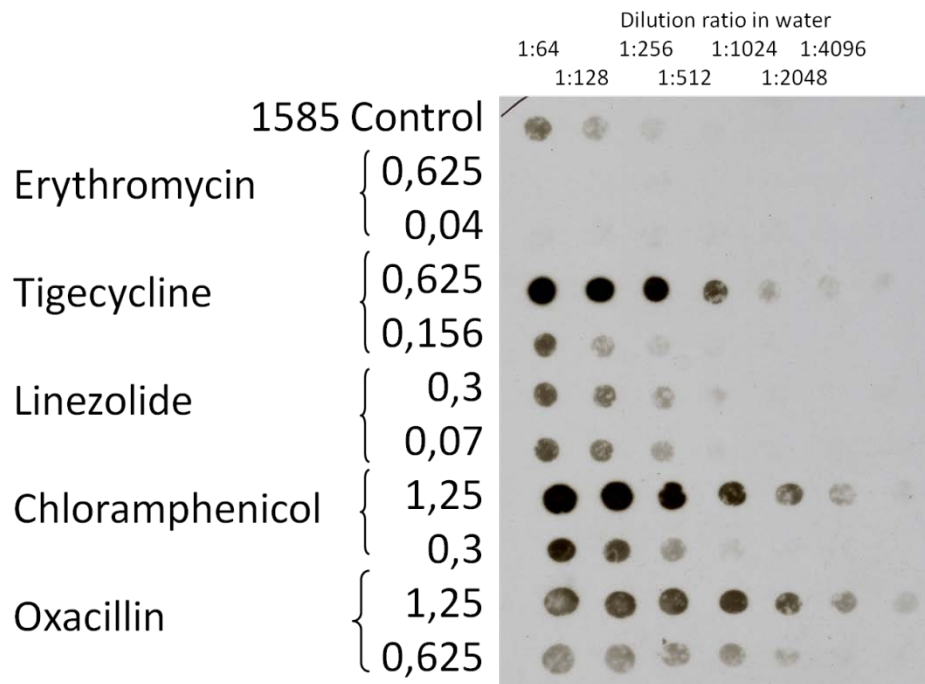


Fig. III-21: Induction of Embp expression by different antibiotics in *S. epidermidis* 1585. Dot Blot analysis of *S. epidermidis* 1585 cell surface proteins obtained after growth in the presence of different antibiotics. The supernatant has been diluted up to 1:4096 in water and then 10 μ L each have been spotted onto a PVDF membrane. It is visible that 0,625 μ g/mL Tigecycline and 1,25 μ g/mL Chloramphenicol led to increased Embp production, while 1,25 μ g/mL Oxacillin and 0,3 μ g/mL Linezolid led to a low increase of Embp expression compared to the control. Erythromycin did not lead to Embp expression at all. The dot blot has been stained with rabbit-Embp7762 anti-serum and rabbit-IgG HPO and then exposed to X-ray films for 30 sec.

Next, the question was addressed if the observed induction of Embp also resulted in a biofilm positive phenotype. To this end, confocal microscopy was used to monitor biofilm formation of *S. epidermidis* 1585 in the presence of antibiotics at concentrations that were shown to result in Embp over production. Fig. III-22 shows the immuno staining of Embp of the wild type strain *S. epidermidis* 1585 with and without 0,3 μ g/mL Tigecycline, showing that the amount of Embp increased dramatically after antibiotic induction. Embp was spread through the whole biofilm and the biofilm height was three times higher than in the control.

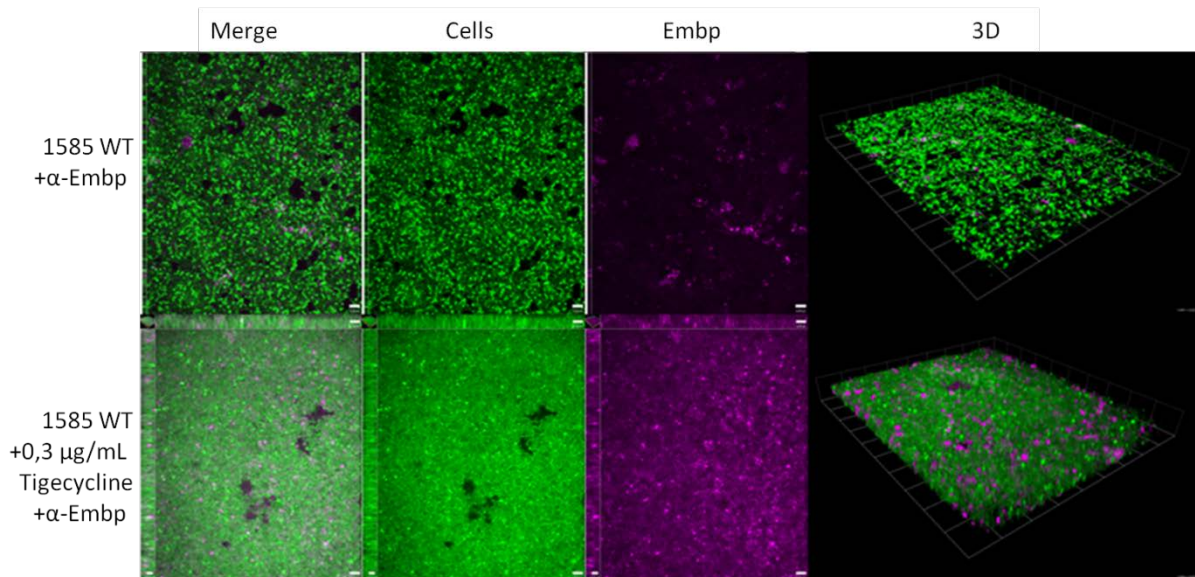


Fig. III-22: Induction of biofilm formation by tigecycline in *S. epidermidis* 1585 wild type. The microscope images of *S. epidermidis* 1585 wild type (WT) with and w/o 0,3 µg/mL Tigecycline. It is visible that the amount of Embp as well as the biofilm height increased due to antibiotic treatment. The cells formed closely attached cell layers without mushroom-like structures. Embp was spread through the biofilm. Embp was stained with rabbit anti-rEmbp anti-serum and anti-rabbit IgG AlexaFluor568 antibody. Leica SP2 confocal microscope (Leica, Solms, Germany). Embp: magenta, cells: green. Magnification 630x, White bar (right side of each image): 13 µM.

Indeed, the results obtained by dot blot immune assay were supported by the microscopic analysis, showing a striking increase in Embp-specific fluorescence signal (Fig. III-23). While under control conditions almost no Embp was detectable, in the presence of 0,3 and 0,6 µg/mL Tigecycline the volume of Embp-specific fluorescence signal increased up to 13.000 µM³. 0,45 µg/mL Tigecycline promoted the highest Embp production. Concentrations higher than 0,6 µg/mL led to a decreased Embp production again (data not shown).

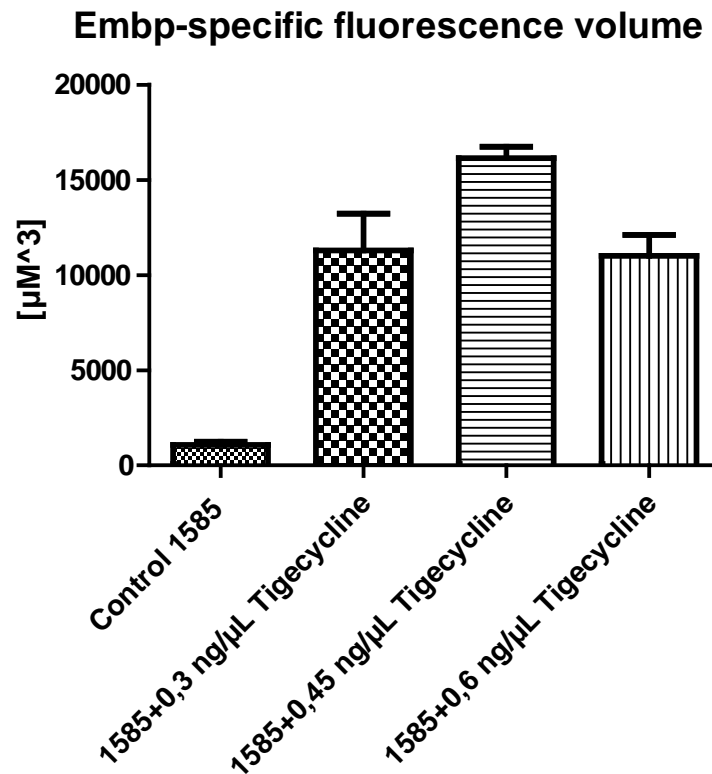


Fig. III-23: Graphic illustration of Embp-specific fluorescence signal volume obtained by *S. epidermidis* 1585 wild type treated with Tigecycline concentrations of 0,3 , 0,45 and 0,6 ng/ μL . It is visible that the Embp-specific fluorescence signal increased up to approximately 18.000 μM^3 in the presence of 0,45 ng/ μL Tigecycline, whereas the control (*S. epidermidis* 1585 w/o added tigecycline) only reached 1.500 μM^3 Embp-specific fluorescence. When the concentration of Tigecycline reached 0,6 ng/ μL the Embp-specific fluorescence volume amount decreased down to the level of 0,3 ng/ μL .

Similar results were obtained with *S. epidermidis* 1585 using additional antibiotics (i.e. Linezolid, Chloramphenicol and Oxacillin). At sub-inhibitory concentrations an increase of Embp production as well as biofilm formation was observed by CLSM. Fig. III-24 shows the comparison of biofilms after antibiotic induction in confocal microscopy. As expected from dot blot immune assays, Erythromycin did not induce biofilm formation in *S. epidermidis* 1585 wild type strain. There is only a thin layer of cells, not even as strong as in the control without any antibiotic induction (see Control in Fig. III-22).

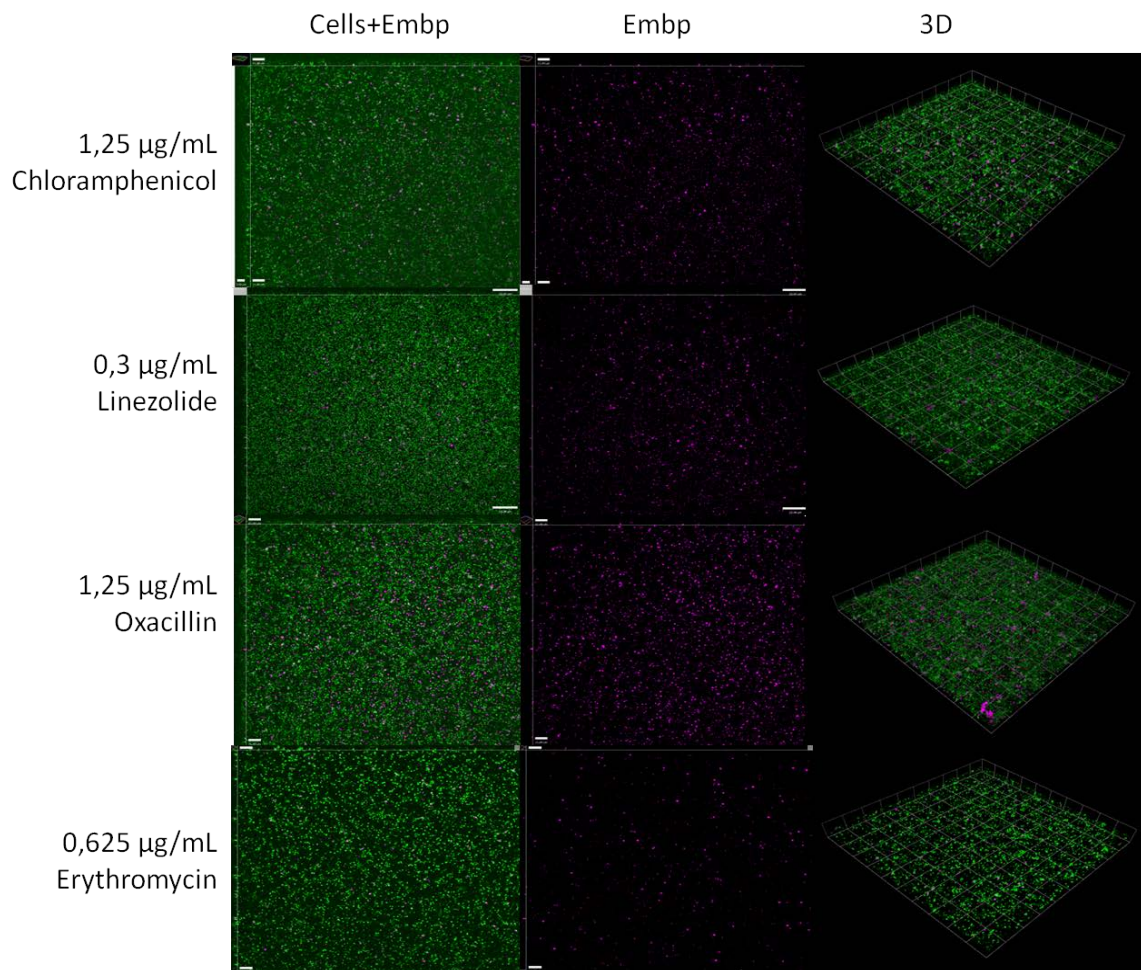


Fig. III-24: Induction of biofilm formation based on Embp by different antibiotics in *S. epidermidis* 1585. The microscopic images of *S. epidermidis* 1585 wild type grown in the presence of antibiotics as indicated show an increased Embp production after the treatment with 1,25 µg/mL Oxacillin, as well as with 1,25 µg/mL Chloramphenicol and 0,3 µg/mL Linezolid. The treatment of bacterial cells with 0,625 µg/mL Erythromycin showed no increase in Embp production and the cells did not grow as much as in the other cultures. For all tested antibiotics, but Erythromycin a thin biofilm could be obtained. Leica SP2 confocal microscope (Leica, Solms, Germany). Embp: magenta, cells: green. Magnification 630x, White bar (right side of each image): 13 µM.

Fig. III-25 shows the biofilm height of *S. epidermidis* 1585 biofilms after induction with the tested antibiotics. It was visible that the height of the biofilm formed by *S. epidermidis* 1585 after the treatment with Erythromycin was lower than of the cultures treated with Oxacillin, Chloramphenicol, or Linezolid. The Embp-specific fluorescence volume after treatment with Erythromycin has been even lower than in the control. The biofilm height of approx. 4 µM for Oxacillin and 4-4,5 µM for Chloramphenicol showed a correlation to the high amount of Embp, while the Embp amount after treatment with Linezolid was surprisingly low, even if the biofilm height was up to 4 µM.

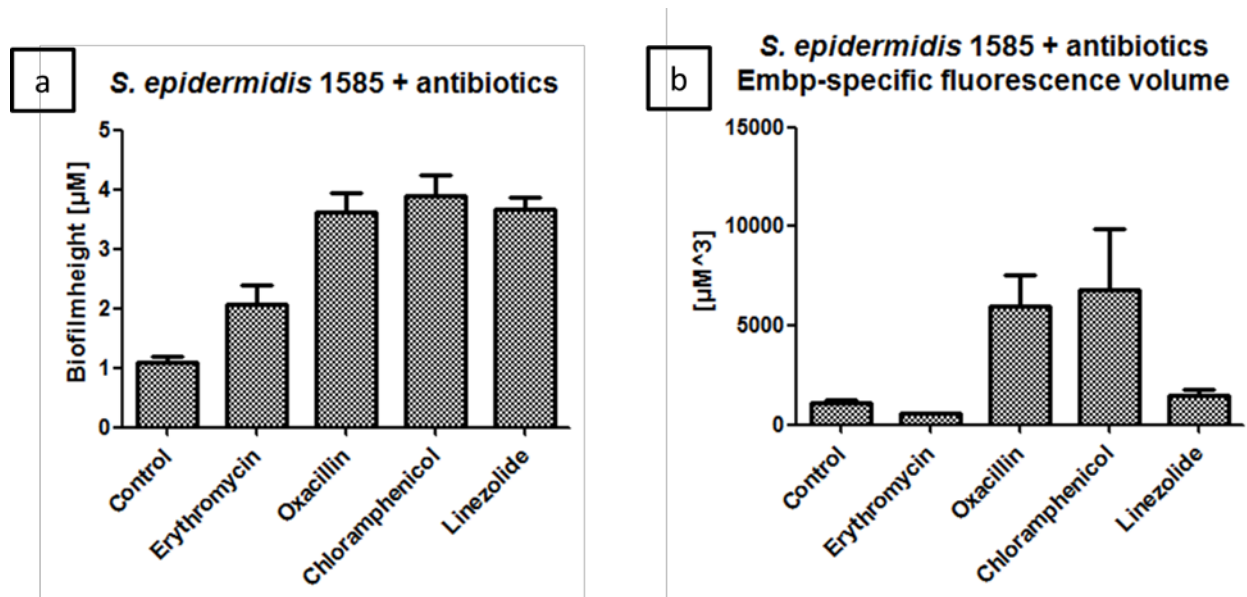


Fig. III-25: Evaluation of biofilm height and Embp-specific fluorescence signal volume after the treatment of *S. epidermidis* 1585 with different antibiotics. Graphic illustration showing the evaluation of confocal microscopy images presented in Fig. III-24. **(a)** The comparison of the biofilm height of all cultures treated with different antibiotics to induce Embp production showed that Oxacillin, Chloramphenicol and Linezolid led to higher biofilms than the treatment with Erythromycin. **(b)** The volume of Embp-specific fluorescence of cultures treated with different antibiotics showed that Oxacillin and Chloramphenicol led to a strong increase in Embp production, while Linezolid led to a low increase in Embp production and Erythromycin even decreased the amount of Embp compared to a control.

III.2.2. Influence of phagocytosis after Tigecycline induced biofilm formation on *S. epidermidis* 1585

To clarify if a Tigecycline induced biofilm has the same cell protecting properties as a natural biofilm, susceptibility of *S. epidermidis* 1585 grown in TSB and TSB supplemented with sub-inhibitory tigecycline concentrations against phagocytosis was tested. To this end, mouse macrophages J774A.1 have been added to a 24 h old culture of *S. epidermidis* 1585xpCM29, as well as to a mature Tigecycline (0,3 µg/mL) induced biofilm of *S. epidermidis* 1585xpCM29. A differential inside/outside staining approach was then used to specifically discriminate and quantify bacterial cells that were taken up by macrophages. Fig. III-26 shows the microscope images of macrophages inside the biofilms, while Fig. III-27 shows the graph of bacterial cells counted inside the macrophages.

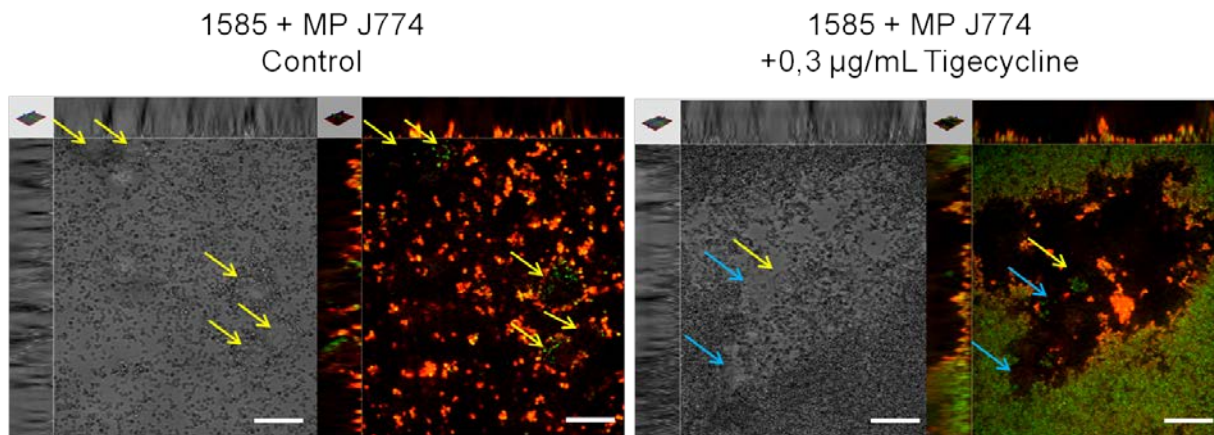


Figure III-26: Bacterial cells organized in a biofilm are protected from phagocytotic killing. Images of *S. epidermidis* 1585xpCM29 and a biofilm induced with 0,3 µg/mL Tigecycline, each incubated with J774A.1 mouse macrophages (MP J774) for 6 h. The bacterial cells were stained using a rabbit anti-*S. epidermidis* antiserum and an anti-rabbit IgG AlexaFluor568 antibody. Since macrophages were not permeabilized, only bacteria outside the macrophages were stained. Yellow arrows indicate macrophages that internalized bacterial cells (green), while blue arrows indicate empty macrophages. It was visible that more macrophages were able to internalize bacterial cells, when these were not organized in a biofilm. The bacterial cells organized in a biofilm showed strong adherence among each other and the macrophages could not internalize as many bacterial cells as in the control. Improvisation confocal microscope (Perkin Elmer, Waltham, USA). Magnification 630x, White bar (right side of each image): 13 µM.

The microscopic images showed that macrophages incubated with *S. epidermidis* 1585xpCM29 grown without antibiotics were able to internalize bacterial cells. Each macrophage contained approximately 20 bacterial cells. In contrast, significantly lower numbers were taken up when *S. epidermidis* 1585xpCM29 was grown in the presence of tigecycline. Here, each macrophage contained approximately 7 bacterial cells (Fig. III-27). In conclusion, the induction of biofilm formation by tigecycline leads to impaired bacterial uptake by mouse macrophages J774A.1.

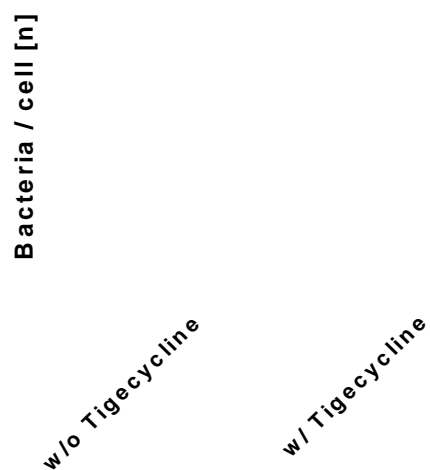


Figure III-27: Statistic evaluation of internalized bacteria by macrophages with and w/o tigecycline induced biofilm formation. *S. epidermidis* 1585 has been treated with and without 0,3 $\mu\text{g}/\text{mL}$ Tigecycline to induce biofilm formation. It can be seen that less bacterial cells could be internalized by macrophages after a biofilm has been formed. An unpaired t-test performed with Graph Pad prism 5 proved the significance of this different bacterial up-take counts ($p < 0,005$).

III.3. Influence of fosmid clone extracts 100 E3, 100 B3 and 64 F4 on *S. epidermidis* 1457 biofilms

In the former master thesis “Disruption of *Staphylococcus epidermidis* biofilms through novel metagenomic enzymes” [Henke H A, 2011, master thesis] biofilm disrupting fosmid clones encoding DNA derived from a metagenomic library from the Elbe River could be detected. These fosmid clones have been sequenced by Illumina sequencing to detect encoded genes. 3 fosmid clones, 100 E3, 100 B3 and 64 F4, have been further investigated in this work due to their high capability of disrupting a mature *S. epidermidis* 1457 biofilm. To further investigate the effect of the fosmid clone extracts (supernatant of oN cultures) microscopy (III.3.1) as well as heat inactivation, PIA degradation assays (III.3.2) and gel filtration has been done (III.3.3). Furthermore genes encoding for putative biofilm disrupting enzymes have been subcloned for over expression and activity experiments (III.3.4). Fosmid clone 100 E3 has been investigated carefully for its properties in bioinformatic analysis (III.4).

III.3.1. Microscopic analysis of *S. epidermidis* 1457 biofilms disrupted by cell raw extracts of fosmid clones 100 E3, 100 B3 and 64 F4

The biofilm disrupting effect of cell raw extracts has been visualized using the biofilm disintegration assay (II.3.1). Three fosmid clones (100 E3, 100 B3 and 64 F4) derived from a metagenomic library of the Elbe River showed reproducible biofilm disrupting properties. The fosmid clone showing the highest potential of disruption was 100 E3. Fig. III-28 shows 4 wells of a 96-microwell plate in which a mature *S. epidermidis* 1457 biofilm has been treated with cell raw extract of fosmid clone 100 E3. It was clear to see that the biofilm got destroyed even if only 50 μ L of the extract were added to the biofilm. The effect increased with the amount of extract used.

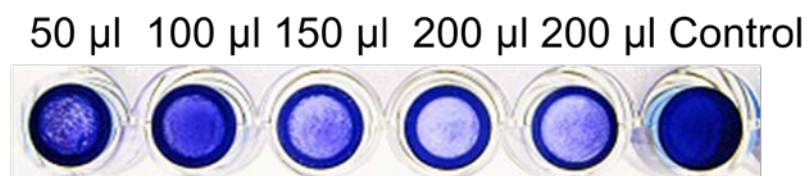


Figure III-28: Biofilm disintegration assay of *S. epidermidis* 1457 treated with fosmid clone extract 100 E3. Biofilms grew for 24 h at 37 °C static and have then been treated with different amounts of cell raw extract from fosmid clone 100 E3 for 24 h at 37 °C static. It could be visualized that the biofilm was disrupted intensively after the treatment with fosmid extract compared to the control.

The investigation of fosmid clone extract effects on *S. epidermidis* 1457 biofilms has been done via CLSM. The biofilm has been treated with cell raw extract of fosmid clone 100 E3, 100 B3 and 64 F4 for 24 h at 37 °C under static conditions. The biofilm height, as well as the fluorescence signal of living and dead cells has been measured using Volocity 6.1.1 software (II.11). Fig. III-29 displays the percentage of biofilm disruption showing that the extract of fosmid clone 100 E3 decreased the bacterial volume up to 80 %, while the extract of 100 B3 and 64 F4 decreased the bacterial volume for approx. 40 %. The control of 1 x PBS buffer on a mature biofilm also showed a little effect of approx 30 % less bacterial volume, due to the lack of nutrients. A decrease in height of about 2/3 compared to the untreated control *S. epidermidis* 1457 biofilm could be seen after treatment with each fosmid extract.

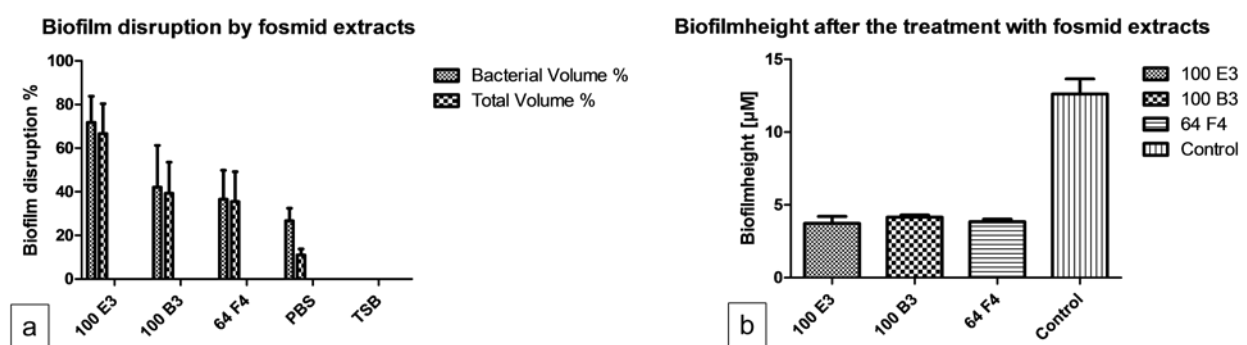


Fig. III-29: Graphic illustration of the biofilm disruption after the treatment with cell raw extracts of fosmid clones 100 E3, 100 B3 and 64 F4. It shows that 100 E3 had the strongest biofilm disrupting properties with up to 80 % less biofilm, while 100 B3 and 64 F4 disrupted 40-60 % of the biofilm. 1 x PBS also disrupted the biofilm up to 30 % due to the lack of nutrients **(a)**. Graphic illustration of the biofilm height after the treatment with cell raw extracts of the different fosmid clones 100 E3, 100 B3 and 64 F4 showing that *S. epidermidis* 1457 biofilms were only 4 μM in height compared to the control that showed a biofilm height of approx. 13 μM **(b)**.

Fig. III-30 shows the effect of fosmid extracts on the mature biofilm after Live/Dead Staining of the sample. It could be detected that the fluorescence signal of dead cells, respectively eDNA due to cell lysis was much higher than in the control biofilm treated with 3 % BSA. Fosmid extract of 100 B3 showed a disruption of the biofilm that was not as strong as for 100 E3, or 64 F4, but the dead cells, or eDNA were mainly located in between the mushroom-like biofilm structures. For the extract of 64 F4 it was visible that the dead cells or eDNA were located on top of the biofilm. The lower cell layers seemed to be intact. The extract of fosmid clone 100 E3 showed the strongest decrease of the biofilm and mainly the lower cell layers seemed to be disrupted. The propidium iodide of the dead Stain bound mainly to the cell layers directly attached to the surface.

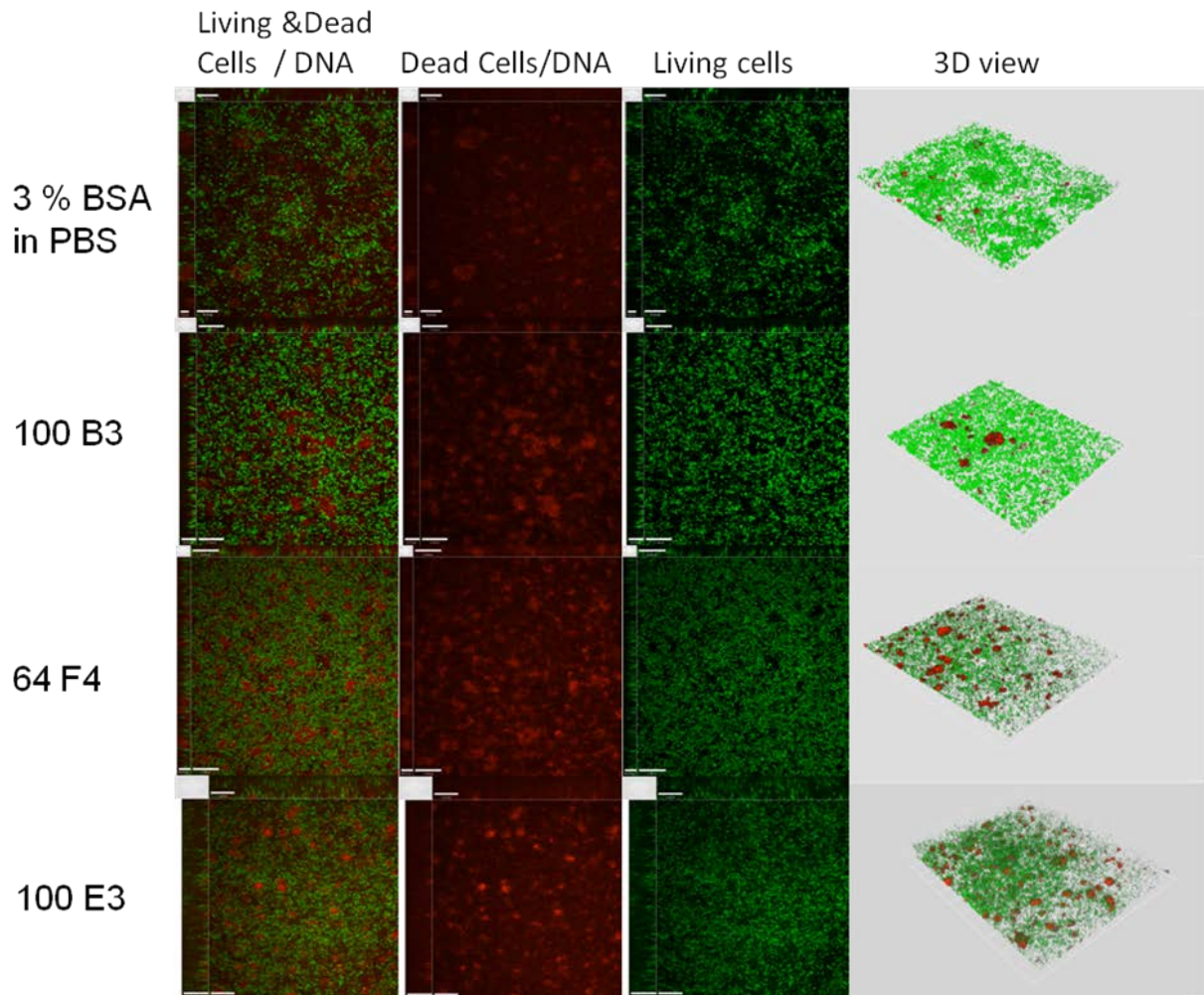


Fig. III-30: Mature *S. epidermidis* 1457 biofilms got disrupted after treatment with fosmid clone extracts. The control with 3 % BSA in 1xPBS showed an island like structure of the biofilm, while the biofilm treated with extracts of fosmid clone 100 B3 and 64 F4 showed a thin cell layer and an increased amount of dead cells/eDNA. The biofilm treated with extract of 100 E3 also showed an increase in dead cells/eDNA (red), as well as a decrease in height and living cell volume (green). The biofilms have been stained with Live/Dead® BacLight™ Bacterial Viability Kit (Invitrogen, Oregon, USA). Improvision spinning disk microscope (Perkin Elmer, Waltham, USA). Magnification 630x, White bar (left side of each image): 13 μ M.

To determine whether the extracts of the fosmid clones showed a stronger biofilm disruption when they were used in combination, all possible combinations have been tested. The effect of a biofilm disruption around 45 % of the fosmid clones 100 E3 and 64 F4 was almost 35 % less than the single effect of 100 E3 and not higher than the single effect of 64 F4. In comparison fosmid extract of 100 E3 together with 100 B3 showed a low biofilm disrupting effect of approx. 10 %. And when extracts of fosmid clone 100 B3 and 64 F4 were used together the biofilm disruption decreased to 25 %, while each extract itself had a biofilm disrupting effect of 40-60 %. When all three fosmid extracts at once were used for treatment the effect of biofilm disruption increased up to 60 %, but was not as high as the single effect of 100 E3 that has been around 80 %. Fig. III-31 shows the amount of biofilm

disruption in percentage. It has been shown, that the control extract of the pure *E. coli* Epi300 culture (which is the host for the fosmids used) did not have any effect on the biofilm, as well as 3 % FCS that has been used as a control.

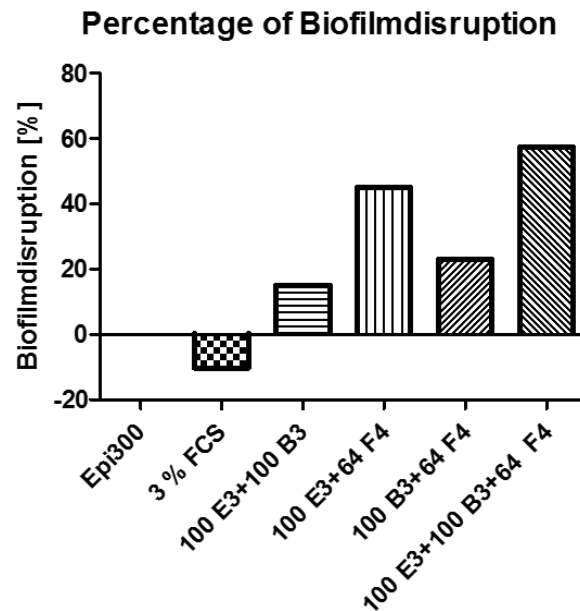


Fig. III-31: Biofilm disruption after the treatment of mature *S. epidermidis* 1457 biofilms with mixtures of fosmid clone extracts. The control extract of *E. coli* Epi300 did not have any effect on the biofilm and the control protein 3 % FCS (fetal calf serum) even showed a biofilm strengthening effect. The mixture of extract 100 E3 + 100 B3 and 100 B3 + 64 F4 showed a biofilm disruption of ~20 %, and ~ 25 %, while the mixture of 100 E3 + 64 F4 disrupted the biofilm up to 50 %. A mixture of all three fosmid extracts disrupted the biofilm up to 60 %.

To prove the biofilm disrupting effect with visual methods confocal microscopy has been performed. The bacterial cells have been stained with Live/Dead® *BacLight*TM Bacterial Viability Kit (Invitrogen, Oregon, USA) after a growth phase of 24 h and a biofilm disrupting phase with the added fosmid extracts of another 24 h. It was clear to see that the biofilm disruption when extract 100 B3 was included in the mixture was not as high as when the other two extracts 100 E3 and 64 F4 were included. There seemed to be an inhibiting effect of 100 B3 against the biofilm disrupting effects of 100 E3 and 64 F4. When all three fosmid extracts were mixed prior to biofilm treatment the effect was strong again. But still the single effect of 100 E3 was higher than in any mixture. Fig. III-32 shows the CLSM images of mixed fosmid clone extracts.

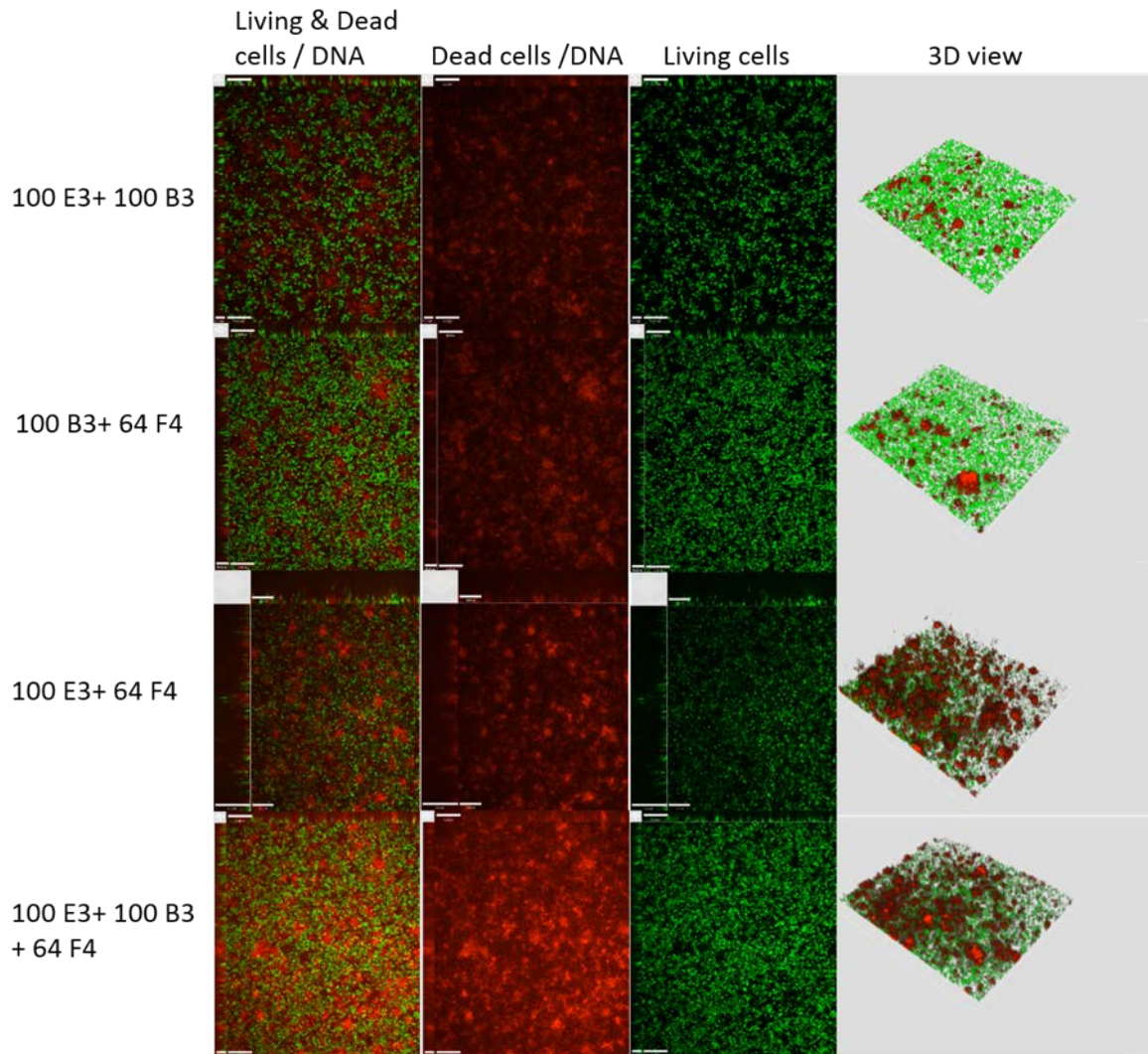


Fig. III-32: Mature *S. epidermidis* 1457 biofilm disruption by mixtures of fosmid clone extracts. It is visible that the biofilm was disrupted strongly by mixtures containing extracts of 100 E3 + 64 F4 and when all three extracts were mixed. The biofilm disruption, as well as the amount of dead cells/eDNA (red) was also visible when fosmid extracts 100 E3 + 100 B3 and 100 B3 + 64 F4 were mixed, but not as strong as in the other treatments. The biofilms have been stained with Live/Dead® BacLight™ Bacterial Viability Kit (Invitrogen, Oregon, USA). Improvisation spinning disk microscope (Perkin Elmer, Waltham, USA). Magnification 630x, White bar (left side of each image): 13 μ M.

III.3.2. Influence of heat-inactivated and gel filtered fosmid clone extracts on *S. epidermidis* 1457 biofilms

To further characterize the biofilm disrupting effects of fosmid clones 100 E3, 100 B3 and 64 F4 heat inactivation at 60-70 °C over night has been done. With this experiment all heat sensitive enzymes should have been inactivated. The fosmid extracts have then been used as already described for the biofilm disintegration assay (II.3.1). Fig. III-33 shows the amount of biofilm disruption of fresh fosmid extracts compared to heat inactivated fosmid extracts. It was visible that the effect of heat inactivated fosmid clone extract 100 E3 still disrupted the biofilm up to 60 %. Compared to the fresh extract this is only a difference of 10 % including meanderings. While the fresh extracts of 100 B3 and 64 F4 showed a quite similar biofilm disruption of approx. 25 % in the biofilm disintegration assay, the percentage of biofilm disruption decreased down to 17 % for heat inactivated extract of 100 B3 and down to 10 % for heat inactivated extract of 64 F4.

Biofilm disruption after heat inactivation

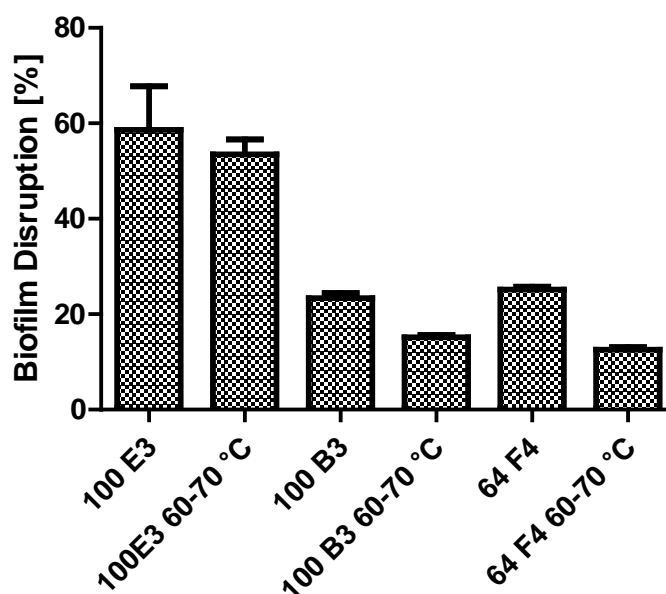


Fig. III-33: Mature *S. epidermidis* 1457 biofilms disruption after heat inactivation of fosmid clone extracts. Graphic illustration of *S. epidermidis* 1457 biofilms treated with fosmid extracts before and after heat inactivation of the extract at 60-70 °C oN. It is visible that the extract of 100 E3 still disrupted the biofilm up to 60 % after heat inactivation. This showed a decrease of biofilm disrupting properties of only 10 % compared to unheated extract. The fosmid extracts of 100 B3 and 64 F4 lost approx. 30-50 % of their activity after heat inactivation, that meant the unheated extracts disrupted a biofilm between ~22 % for 100 B3 and 25 % for 64 F4, while the heat inactivated extracts disrupted the biofilm ~18 % for 100 B3 and 12 % for 64 F4.

In this experiment 100 E3 showed the highest ability to disrupt a mature *S. epidermidis* 1457 biofilm even after heat inactivation. For the ongoing experiments only fosmid clone 100 E3 has been tested to determine which encoded gene on the fosmid clone was responsible for the disruption of a biofilm. Therefore gel filtration using the Äkta System (II.3.3.1) has been performed to gain fractions of the fosmid clone extract of 100 E3. Gel filtration is a method to separate extracts composed of many proteins of different sizes into smaller fractions with distinct molecular weights. These fractions of the fosmid clone extract of 100 E3 have been tested in the biofilm disintegration assay to determine in which fraction the active components were located. Fig. III-34 shows the average biofilm disruption of fraction B2, the only fraction that showed distinct biofilm disruption after gel filtration. The fraction showed a very high biofilm disruption of 78,18 % compared to the fresh extract of 100 E3 that showed a biofilm disruption of 12,53 %. The enzymes capable of disrupting a biofilm seemed to be concentrated in this fraction which led to the huge difference of the not concentrated extract compared to the fraction. Fraction B2 included proteins in sizes from 17-70 KDa. Mass spectrometry of fraction B2 has been performed (III.3.3) to identify the proteins.

Average of biofilm disruption after gel filtration

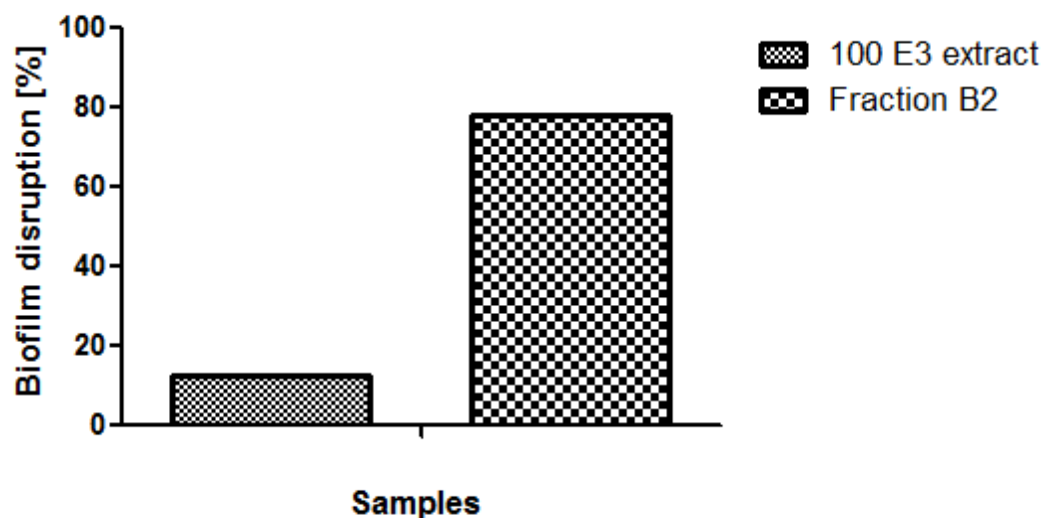


Fig. III-34: Fraction B2 after gel filtration disrupted a *S. epidermidis* 1457 biofilm effectively. Graphic illustrations of the average biofilm disruption of fosmid extract 100 E3 after gel filtration that excluded proteins by size. Fraction B2 shown here disrupted the biofilm up to 80 % compared to the unfiltered and with this not concentrated fosmid extract of 100 E3. The protein sizes in fraction B2 laid between 17-70 KDa.

All fractions derived from gel filtration have been tested for their capability to degrade PIA. Therefore PIA has been prepared (II.3.4) and 500 μL of PIA have been incubated with 500 μL of each fraction after gel filtration. A dot blot immune assay has been done (II.7.5) and stained with rabbit-PIA anti-serum and rabbit-IgG HPO (Fig. III-35). It was visible that fraction B2 removed PIA more than the other fractions. Fraction B1 and B3 showed a degrading effect as well, but as visible in Fig. III-36 some proteins of fraction B2 could be found in the other fractions too. That supported the idea of fraction B2 being the concentrate of biofilm disrupting components of fosmid clone 100 E3.

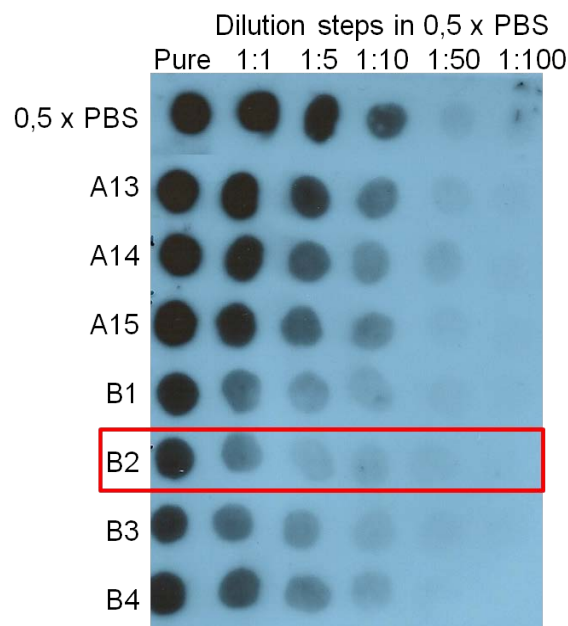


Fig. III-35: Gel filtration fraction B2 degrades PIA. Dot Blot showing the reduction of PIA after treatment with fractions derived from the gel filtration of fosmid extract 100 E3 showing that fraction B2 reduced PIA more than the other fractions, indicating that the proteins responsible for PIA degradation were concentrated in this fraction. The membrane has been stained with rabbit-PIA anti-serum and rabbit-IgG HPO for visualization on X-ray films. This film has been exposed to the membrane for 30 sec.

III.3.3. Mass-spectrometry of fraction B2

Based on the result of the gel filtration and the following biofilm disintegration assay mass spectrometry of fraction B2 has been performed. This method helped to further isolate the proteins responsible for biofilm disruption. Fig. III-36 shows the SDS gel stained with silver for further usage in mass spectrometry. Fraction B2, that showed biofilm disrupting as well as PIA degrading properties, is framed in red. The eight bands have been prepared for mass spectrometry and then analyzed using the Agilent 1100 LC-ESI-MS/MS system (Agilent technologies, Waldbronn, Germany).

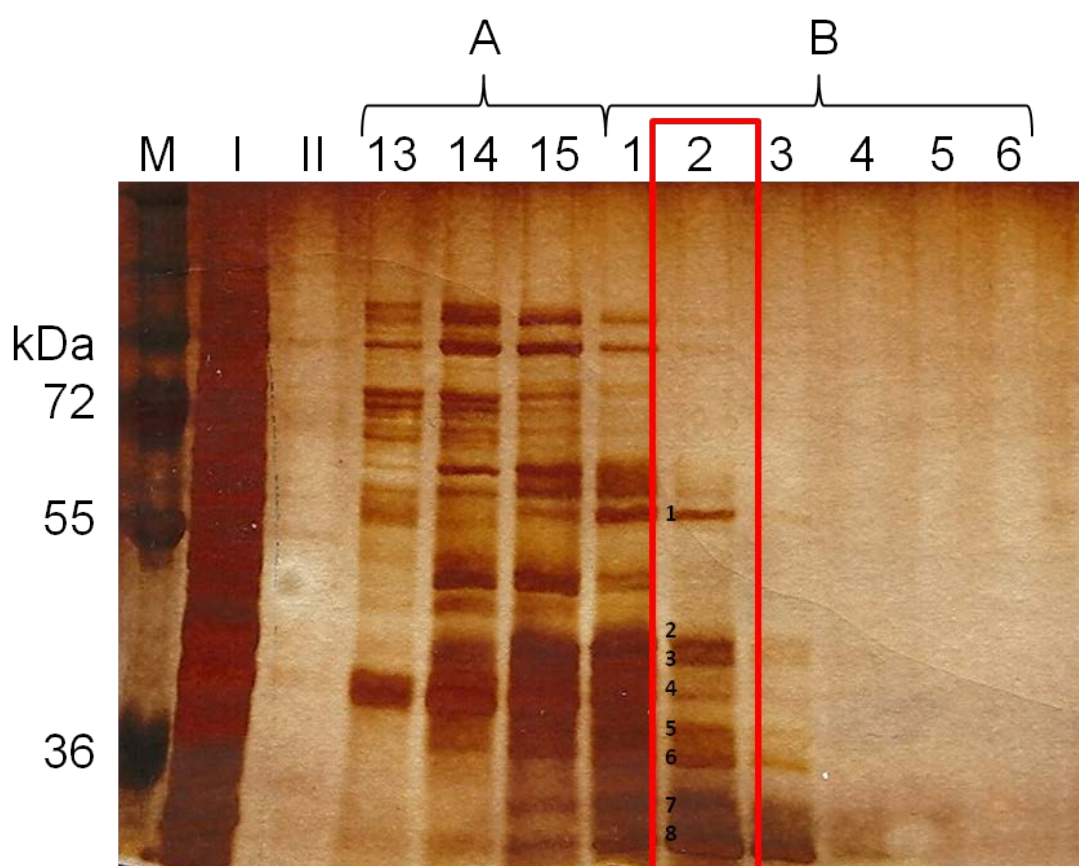


Fig. III-36: SDS gel of fraction B2 after gel filtration used for mass-spectrometry. Silver stained 10 % SDS gel showing the fractions of the gel filtration. The eight bands of fraction B2 have been prepared for mass spectrometry to determine the proteins.

The results of mass spectrometry have been analyzed using Mascot (table II.11) and the protein sequences have been aligned to the sequence of fosmid clone 100 E3. In part III.4 the bioinformatic analysis of the fosmid clones, specifically 100 E3 is described. Five bands out of eight mapped directly to proteins in the protein sequence of fosmid clone 100 E3. Table III-1 shows the ORFs as well as the amino acid and nucleotide number where the sample band fitted the sequence.

Table III-1: Result of mass spectrometry of the fraction B2 encoding proteins on fosmid clone 100 E3

Sample band	ORF	Amino acid number	Nucleotide number
2	Dehydrogenase (DH)	6144-6162	18432-18486
5	Peroxidase	7052-7067	21156-21201
6	Oligopeptide transporter	8137-8148	24411-24444
4	Amidohydrolase (AH)	9986-10007	29958-30021
4	Glycosyltransferase (GT3)	1767-1824	5301-5472
1, 3, 8, 7	No result		

These ORFs were supposed to be most promising for the disruption of *S. epidermidis* 1457 biofilms. Some promising proteins such as the Dehydrogenase (DH), the Amidohydrolase (AH) and the Glycosyltransferase (GT 3) have been analyzed carefully with different bioinformatic tools (III.4) and additionally subcloned to determine the function of the proteins (III.3.4).

III.3.4. Fragment analysis of 100 E3 and over expression of putative biofilm disrupting enzymes

In fosmid clone 100 E3 several genes have been determined as the most promising candidates for biofilm disruption. To narrow the sequence down to smaller fragments of the fosmid for determining the active genes on fosmid clone 100 E3, the fosmid has been cut with different restriction enzymes. In the master thesis "Molekularbiologische Untersuchung des Fosmidklons 100 E3 zur Desintegration von staphylokokkalen Biofilmen" (Aylin Bertram, 2012, data not published) all enzymes used are listed. Table III-2 shows the enzymes used for fosmid clone 100 E3.

Table III-2: Restriction enzymes used to digest fosmid clone 100 E3. Further subcloning of the smaller fragments into different host vectors has been done. These enzymes have been chosen based on the sequence to gain fragments between 1000 and 5000 bp.

Fosmid	Enzymes used to digest the fosmid	Vector	Host
100 E3	BamHI, EcoRI, PstI, KpnI	pDrive, pUC19, pbluescript SKII+, pCC1Fos	<i>E. coli</i> Top10

Subcloning of these fragments in either pDrive, pUC19, pBluescript SKII+ or pCC1Fos vectors did not work. Neither transposon mutagenesis using the EZ-Tn5™ Transposase (Epicentre, Madison, USA), nor long range PCR of putative regions had been successful. So the idea of subcloning each located gene separately into an entry and expression vector for over expression of the protein and further analysis has been achieved.

An operon encoding for 2 Glycosyltransferases (GT2 & GT3) and 1 methyltransferase (GT1) could be detected in bioinformatic analysis (III.4). GT3 has been detected via mass spectrometry (III.3.3) and was the most promising candidate so far. Furthermore one UDP-3-O-[3-hydroxymyristol]-glucosamine-N-Acyltransferase (N-Ace), Amidohydrolase (AH), Dehydrogenase (DH) and Polysaccharide export transporter (PET) have been determined as putative candidates responsible for the disruption of mature biofilms. All of these genes have been subcloned in different vectors and used for over expression experiments. Table III-3 shows a list of all subcloning strategies including *E.coli*, *Pichia pastoris*, *P.antarctica* and in vitro expression. It is visible that the over expression has only been possible for AH and DH but with no effect on the biofilm. In the cases of putative sugar affecting enzymes, which are known to interfere with the matrix component PIA in *S. epidermidis* 1457 biofilms over expression of proteins has not been successful.

Table III-3: Putative biofilm disrupting enzymes cloned into different vectors. All putative biofilm disrupting enzymes encoded on fosmid clone 100 E3 have been amplified via PCR and then subcloned into different plasmid, and expression vectors using variable host strains for over expression.

Gene	Vector	Tag	Host	Expression	Activity
GT1	pENTR	/	<i>E.coli</i> Oneshot Top10		
	pDEST15	N-Term GST	Entry host: <i>E.coli</i> Oneshot Top10 Expression hosts: <i>E. coli</i> BL21 AI, <i>E. coli</i> BL21 DE3, <i>E. coli</i> BL21 Star, <i>E. coli</i> Rosetta	No	
	pDEST17	N-Term HIS		No	
	pTZ19r	/	<i>E. coli</i> DH5α		

Gene	Vector	Tag	Host	Expression	Activity
GT1	pET19b	N-Term HIS	Entry host: <i>E. coli</i> DH5α Expression hosts: <i>E. coli</i> BL21 AI, <i>E. coli</i> BL21 DE3, <i>E. coli</i> BL21 Star, <i>E. coli</i> Rosetta	No	
	pET21a	C-term HIS		No	
	pDrive	/	<i>E. coli</i> Top10		
	pBad/Myc His A	C-term HIS	<i>E. coli</i> Rosetta, <i>E. coli</i> DH5α, <i>E. coli</i> Top10	No	
	pQE30	N-Term HIS	<i>E. coli</i> M15, <i>E. coli</i> XL-1 blue	No	
GT2	pENTR	/	<i>E. coli</i> Oneshot Top10		
	pDEST15	N-Term GST	<i>E. coli</i> BL21 AI, <i>E. coli</i> BL21 DE3, <i>E. coli</i> BL21 Star, <i>E. coli</i> Rosetta	Yes Inclusion Bodies	No
	pDEST17	N-Term HIS		No	
	pTZ19r	/	<i>E. coli</i> DH5α	No	
	pET19b	N-Term HIS	Entry host: <i>E. coli</i> DH5α Expression hosts: <i>E. coli</i> BL21 AI, <i>E. coli</i> BL21 DE3, <i>E. coli</i> BL21 Star, <i>E. coli</i> Rosetta	No	
	pET21a	C-term HIS		No	
	pDrive	/	<i>E. coli</i> Top10		
GT 2	pBad/Myc His A	C-term HIS	<i>E. coli</i> Rosetta, <i>E. coli</i> DH5α, <i>E. coli</i> Top10	No	
	pQE30	N-Term HIS	<i>E. coli</i> M15, <i>E. coli</i> XL-1 blue	No	
GT3 1278 bp	pDrive	/	<i>E. coli</i> Top10		
	pbluescript SKII+	/	<i>E. coli</i> Top10		
	pENTR	/	<i>E. coli</i> Oneshot Top10		

Gene	Vector	Tag	Host	Expression	Activity
GT3 1278 bp	pDEST15	N-Term GST	Entry host: <i>E.coli Oneshot Top10</i> Expression hosts: <i>E. coli</i> BL21 AI, <i>E. coli</i> BL21 DE3, <i>E. coli</i> BL21 Star, <i>E. coli</i> Rosetta	No	
	pDEST17	N-Term HIS	<i>E. coli</i> BL21 DE3, <i>E. coli</i> BL21 Star, <i>E. coli</i> Rosetta	Yes Inclusion Bodies	No
	pTZ19r	/	<i>E. coli</i> DH5α	No	
	pMALc2x	N-Term MBP	Entry host: <i>E. coli</i> DH5α Expression hosts: <i>E. coli</i> BL21 AI, <i>E. coli</i> BL21 DE3, <i>E. coli</i> BL21 Star, <i>E. coli</i> Rosetta	No, host lysis	
	pET19b	N-Term HIS	Entry host: <i>E. coli</i> DH5α	No	
	pET21a	C-term HIS	Expression hosts: <i>E. coli</i> BL21 AI, <i>E. coli</i> BL21 DE3, <i>E. coli</i> BL21 Star, <i>E. coli</i> Rosetta	No	
	pBBRMCS5	HIS Tag added through primer	Entry host: <i>E. coli</i> Top10 Expression host: <i>Pseudomonas antarctica</i>	No	
	pBad/Myc His A	C-term HIS	<i>E. coli</i> Rosetta, <i>E. coli</i> DH5α, <i>E. coli</i> Top10	No	
	pQE30	N-Term HIS	<i>E. coli</i> M15, <i>E.coli</i> XL-1 blue	No	
	pFLD1	C-Term HIS	Entry host: <i>E. coli</i> Stellar Expression host: <i>Pichia pastoris</i> X-33, <i>Pichia pastoris</i> SMD1168	No	
	in vitro	/	<i>E. coli</i>	No	

Gene	Vector	Tag	Host	Expression	Activity
GT3 2277 bp	pbluescript SKII+	/	<i>E. coli</i> Top10		
	pFLD1	C-Term HIS	Entry host: <i>E. coli</i> Stellar Expression host: <i>Pichia pastoris</i> X-33, <i>Pichia pastoris</i> SMD1168	No	
UDP-3-glucosamine-N-Acyltransferase	pDrive	/	<i>E. coli</i> Top10		
	pbluescript SKII+	/	<i>E. coli</i> Top10		
	pTZ19r	/	<i>E. coli</i> DH5α	No	
	pENTR	/	<i>E. coli</i> Oneshot Top10		
	pDEST15	N-Term GST	Entry host: <i>E. coli</i> Oneshot Top10 Expression hosts: <i>E. coli</i> BL21 AI, <i>E. coli</i> BL21 DE3, <i>E. coli</i> BL21 Star, <i>E. coli</i> Rosetta	Yes Inclusion Bodies	No
	pDEST17	N-Term HIS		No	
	pbluescript SKII+	/	<i>E. coli</i> DH5α		
	pET19b	N-Term HIS	Entry host: <i>E. coli</i> DH5α, <i>E. coli</i> Top 10 Expression hosts: <i>E. coli</i> BL21 AI, <i>E. coli</i> BL21 DE3, <i>E. coli</i> BL21 Star, <i>E. coli</i> Rosetta	No	
	pET21a	C-term HIS		No	
	pMALc2x	N-Term MBP	Entry host: <i>E. coli</i> DH5α, <i>E. coli</i> Top 10 Expression hosts: <i>E. coli</i> BL21 AI, <i>E. coli</i> BL21 DE3, <i>E. coli</i> BL21 Star, <i>E. coli</i> Rosetta	Yes only MBP	No

Gene	Vector	Tag	Host	Expression	Activity
UDP-3-glucosamine-N-Acyltransferase	pBBRMCS5	HIS Tag added through primer	Entry host: <i>E. coli</i> Top10 Expression host: <i>P. antarctica</i>	No	
	pBad/Myc His A	C-term HIS	<i>E. coli</i> Rosetta, <i>E. coli</i> DH5 α , <i>E. coli</i> Top10	No	
	pQE30	N-Term HIS	<i>E. coli</i> M15, <i>E. coli</i> XL-1 blue	No	
	pFLD1	C-Term HIS	Entry host: <i>E. coli</i> Stellar Expression host: <i>Pichia pastoris</i> X-33, <i>Pichia pastoris</i> SMD1168	No	
Polysaccharide Export Transporter	pBBRMCS5	HIS Tag added through primer	Entry host: <i>E. coli</i> Top10 Expression host: <i>Pseudomonas antarctica</i>	No	
	pFLD1	C-Term HIS	Entry host: <i>E. coli</i> Stellar Expression host: <i>Pichia pastoris</i> X-33, <i>Pichia pastoris</i> SMD1168	No	
Amidohydrolase	pbluescript SKII+	/	<i>E. coli</i> DH5 α , <i>E. coli</i> Top10		
	pET19b	N-Term HIS	<i>E. coli</i> BL21 DE3, <i>E. coli</i> Star	Yes	No
	pET21a	C-term HIS		Yes	No
	pTZ19r	/	<i>E. coli</i> Top10	No	
Dehydrogenase	pbluescript SKII+	/	<i>E. coli</i> DH5 α , <i>E. coli</i> Top10		
	pET19b	N-Term HIS	<i>E. coli</i> BL21 DE3, <i>E. coli</i> Star, <i>E. coli</i> BL21 AI	Yes	No
	pET21a	C-term HIS		Yes	No
	pTZ19r	/	<i>E. coli</i> Top10	No	

In vitro expression has been performed using the Expressway™ Cell-Free *E. coli* Expression system (Life technologies, Carlsbad, USA). The system is based on using the purified PCR product and the *E. coli slyD* Extract which is optimized to stabilise the DNA constructs during translation and to increase the amount of soluble protein. A feed buffer contains salts and substrates to enhance the yield of recombinant protein. Added Amino acids constructs the desired protein (see manual for further information). The in vitro expression reaction has been performed several times without obtaining recombinant protein.

Some proteins such as GT2, GT3 and N-Ace have been expressed in Inclusion bodies during classic over expression experiments. To avoid Inclusion bodies the expression has been performed at different temperatures (4 °C, 16 °C, 37 °C) and with different amounts of induction solution (0,01-1 M IPTG) for 3 to 24 h. The proteins have still been expressed in Inclusion bodies. Fig. III-37 shows an example SDS gel containing the soluble protein fraction, as well as the cell pellet, respectively Inclusion bodies of GT3. The protein is ligated in pMALc2x vector expressing the Maltose binding protein (MBP) as a tag induced with 0,3 mM IPTG after 3 h of growth at an OD of 0,5. The expression ran for 1 h at 37 °C and 19 h at 16 °C. The desired protein GT3 is 47,8 kDa in size plus 42,5 kDa MBP. It is visible that a protein product of about 90 kDa is expressed in the insoluble fraction. The single MBP has also been expressed without the desired protein.

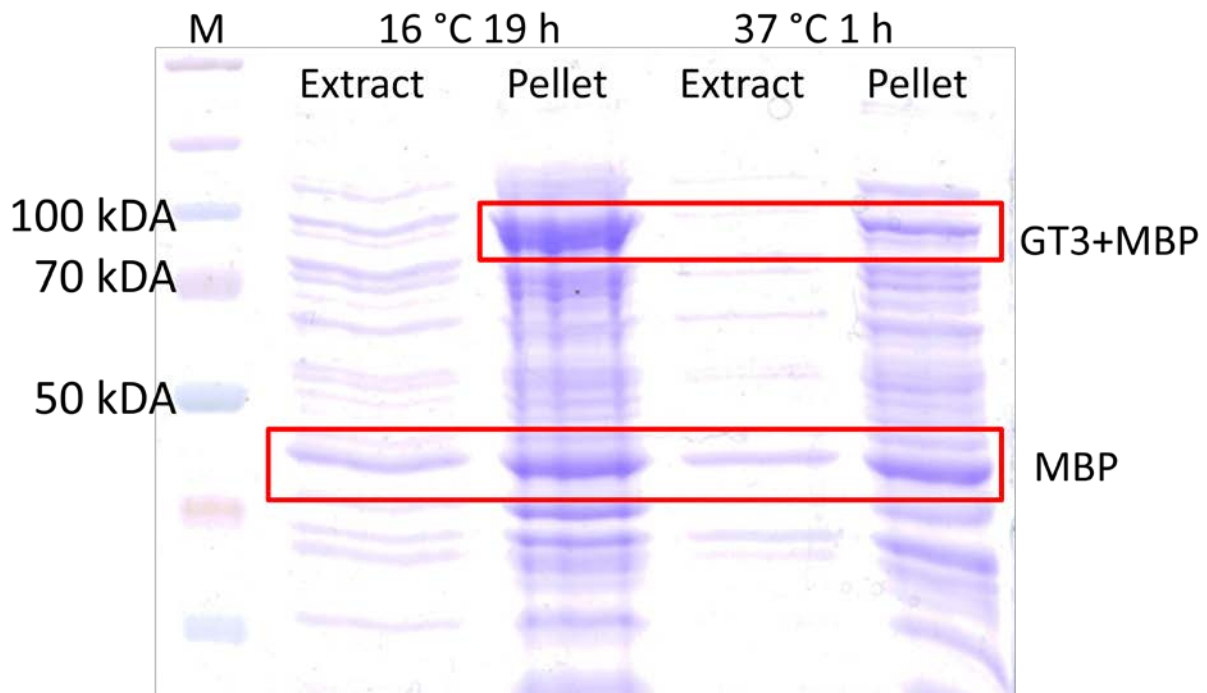


Fig. III-37: SDS gel of an over expression experiment of GT3 with MBP tag. The gel shows that the desired protein has only been expressed in the insoluble fraction. GT3 had neither been expressed in the soluble fraction at 37 °C nor if the expression temperature had been decreased down to 16 °C.

The Inclusion bodies have been purified for breaking and refolding the protein. Different protocols have been tried without success. The most promising protocol used was “Preparation and extraction of insoluble (Inclusion-Body) proteins from *Escherichia coli*” [51] that included the break up, washing steps, refolding and dialysis of the desired protein and tag. The *E. coli* cells have been pelleted via centrifugation at 5000 rpm for 15 min at 4 °C and then resuspended in lysis buffer containing Tris-HCl, EDTA, DTT and benzamidine HCl. The following wash steps have been performed with centrifugation steps in between. The pellet has been washed to extract the insoluble fractions using buffers containing 2 M Urea and Triton X-100. The extraction buffer contained 8 M guanidine HCl as the main agent. For further gel filtration and activity test of the protein it has been dialysed in MBP-binding buffer compatible with the Äkta system and 1xPBS for direct activity experiments. After gel filtration no protein could be detected and the fraction prior to gel filtration did not show any effect on the *S. epidermidis* 1457 biofilm in the biofilm disintegration assay. Fig. III-38 shows the SDS gel containing the wash fractions, as well as the refolding fractions and the product after dialysis.

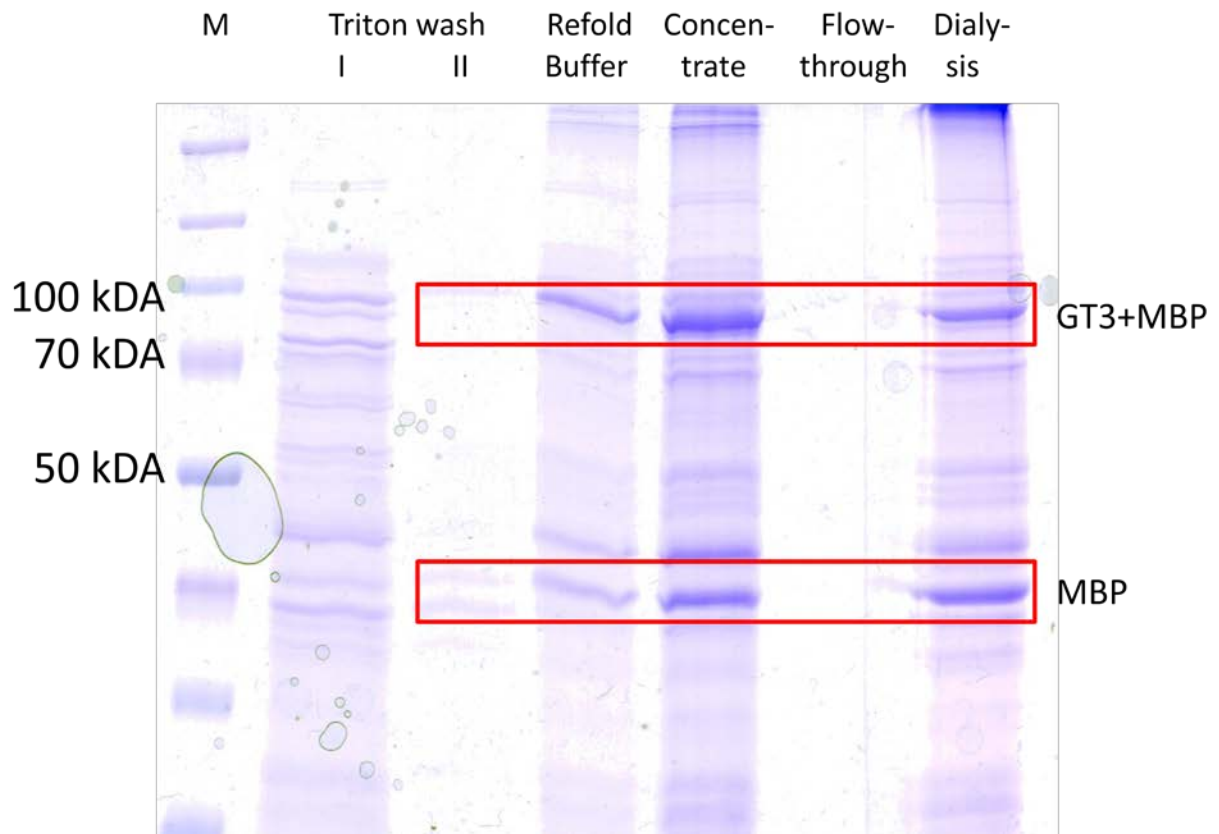


Fig. III-38: Steps of breaking inclusion bodies and refolding the protein. The wash steps I and II of the insoluble fractions showing that after the second wash almost no additional protein retained in the supernatant. After breaking the unfolded protein extracted from inclusion bodies it has been refolded. Lane 3 shows the proteins in **Refold Buffer** prior to concentration with 3 kDa Amicon filters, while lane 4 shows the **Concentrate** of the protein solution. Lane 5 showing the **Flow through** of the 3 kDa Amicon filter showing that no protein rushed through the filter. The concentrate has then been used for **Dialysis** on at 4 °C to exchange the refold buffer by 1 x PBS, or MBP-binding buffer. The protein solution in 1xPBS has been used for biofilm disintegration assays on *S. epidermidis* 1457 biofilms, but no activity could be achieved.

III.4. Bioinformatic analysis of fosmid clones, specifically 100 E3

The fosmid clones derived from the metagenomic library of the Elbe River that showed biofilm disrupting properties have been fully sequenced and analyzed using bioinformatics. Fosmid clone 100 E3 has been analyzed more precisely, because it showed the highest capability of destroying mature *S. epidermidis* 1457 biofilms. Therefore all chosen samples in this part rely on fosmid clone 100 E3. The ORFS detected via mass spectrometry (III.3.3) have been assumed to be putative biofilm disrupting proteins and used for subcloning into different plasmid vectors and hosts (III.3.4). These interesting enzymes have been further characterized in this chapter. All nucleotide and protein sequences in fasta format can be found in the appendix (VI.5).

III.4.1. Bioinformatic determination of putative biofilm disrupting enzymes

To determine the genes encoded on the fosmid clones and to lower the number of possible enzymes that were responsible for biofilm disruption all fosmid clones have been fully sequenced via Illumina sequencing. The table included in Fig. III-39 shows the length and the GC content of the fosmids. Since fosmid clone 100 E3 showed the highest disrupting properties the distinct analysis of this clone has been done. Fig. III-39 also shows the GC Plot of 100 E3. It was visible that the high GC content of 63,80 % of clone 100 E3 was mostly in the middle of the sequence around base 14.000-20.000. The GC Plot of fosmid clone 100 B3 and 64 F4 can be found in VI.3 of the Appendix.

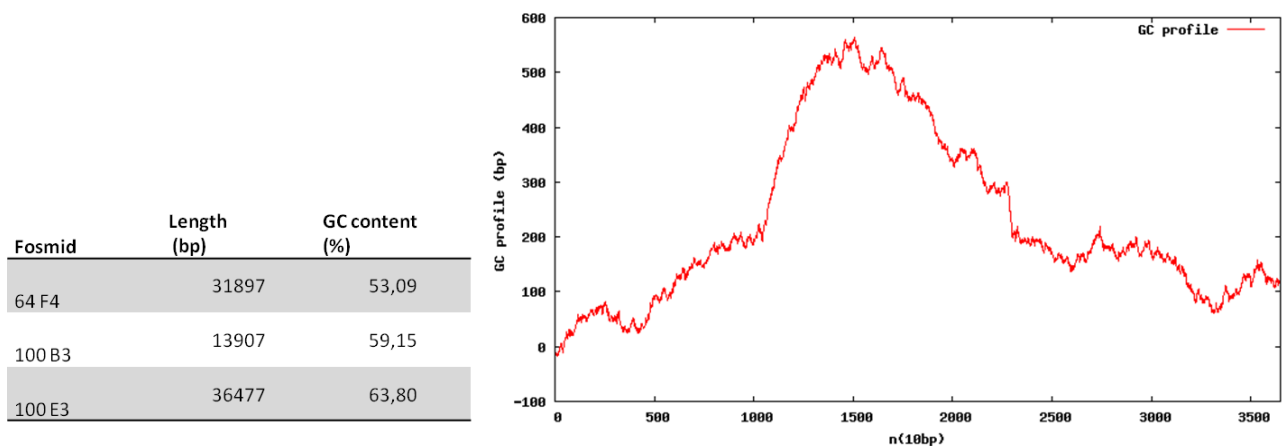


Fig. III-39: Length and GC content of fosmid clones 100 E3, 100 B3 and 64 F4 as well as the GC Plot of fosmid clone 100 E3. This illustration shows 100 E3 has a very high GC content of 63,80 %, while 100 B3 and 64 F4 have a GC content less than 60 %. The graph on the right shows the GC Plot of fosmid clone 100 E3 indicating the high GC content in the middle of the fosmid around base ~16.000.

The fosmid 100 E3 encodes 24 genes. Fig. III-40 shows a scheme of the encoded genes displaying the most promising candidates in green. The operon at the N-terminal side of the fosmid encoding an operon with 3 Glycosyltransferases (GT1-3) seemed most promising. But also a Polysaccharide export transporter (PET), as well as the UDP-3-O-[hydroxymyristol]-glucosamine-N-acyltransferase (N-ace) could be responsible for biofilm disruption and PIA degradation. The Dehydrogenase (DH) and Amidohydrolase (AH) that are encoded on the fosmid clone did not show any effect on the biofilm, nonetheless they have been checked for their GC content to determine the distribution of these nucleotide bases over fosmid clone 100 E3.

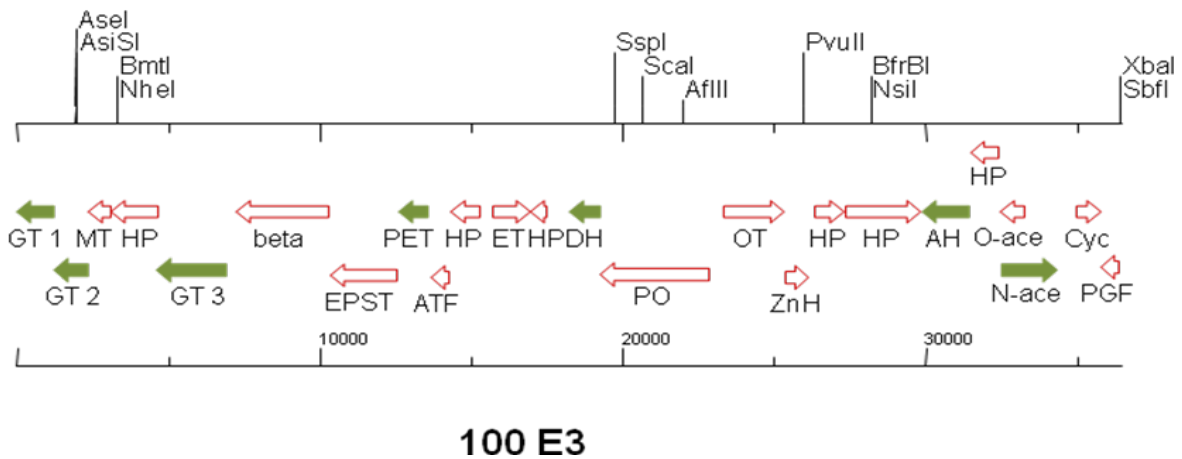


Fig. III-40: Scheme of fosmid clone 100 E3 showing all encoded genes and the annotated ORFs. Most promising enzyme candidates responsible for the biofilm disrupting effect are indicated in green. The operon at the N-terminal side of the fosmid encoding an operon with 3 Glycosyltransferases (GT1-3) and a Polysaccharide export transporter (PET). In the middle of the sequence a Dehydrogenase (DH) and Amidohydrolase (AH), as well as the UDP-3-O-[hydroxymyristol]-glucosamine-N-acyltransferase (N-ace) could also be responsible for biofilm disruption and PIA degradation.

Each of these ORFs has been analyzed for its GC content. Table III-4 shows the GC content of the putative biofilm disrupting enzymes. All Glycosyltransferases (GT1-3), as well as the sugar affecting proteins UDP-3-O-[hydroxymyristol]-glucosamine-N-acyltransferase (N-Ace) and Polysaccharide export transporter (PET) showed a very high GC content over 64 %, while the Amidohydrolase (AH) and Dehydrogenase (DH) showed a GC content of 61,79 %, respectively 59,35 %. Deriving from the filtration and mass spectrometry experiments GT3 has been the most promising candidate responsible for biofilm disruption. Fig. III-41 shows the GC Plot of GT3 pointing out, that the GC content is highest in between the bases 200 – 1000. The GC Plots of all other putative biofilm disrupting ORFs of fosmid clone 100 E3 can be found in VI.3 of the Appendix.

Table III-4: GC content in ORFs of fosmid clone 100 E3 indicating that the GC content is very high in all ORFs

ORF	Length (bp)	GC content (%)
GT1	1209	65,59
GT2	1137	64,47
GT3	1278	65,57
N-Ace	1803	64,00
PET	963	66,87
AH	1560	61,79
DH	1011	59,35

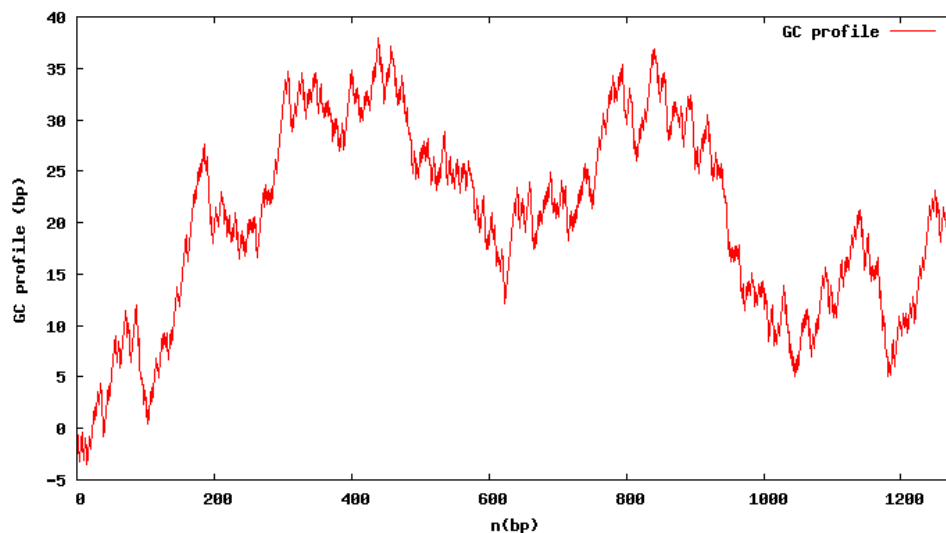


Fig. III-41: GC-Plot of Glycosyltransferase 3. This illustration of the GC content of Glycosyltransferase 3 (GT3) shows that the GC content is very high at almost 65 %. Especially around base pairs 450 and 850 the GC-Plot showed the highest GC peaks.

Analysing the fosmid sequence with NCBI Blast tools no significant similarity on nucleotide base could be detected, so no known organism could be assigned. The annotation of the ORFs has been done using NCBI Orf finder as well as Clone Manager Suite 7 (II.11). The translation of each ORF in its protein sequence has been done using Clone Manager Suite 7. This protein sequence has then been blasted using tblastx comparing the translated protein query to known protein sequences. By blasting either the whole fosmid sequence or the single ORF's nucleotide sequences with blastx the same results occurred. The similarity to known organisms has still been very low and for the whole fosmid sequence *Candidatus solibacter usitatus* had the highest score.

The annotated Amidohydrolase (AH), as well as the Dehydrogenase (DH) did not show any effect on the biofilm of *S. epidermidis* 1457 (III.3.4, table III-3), so these ORFs have not been further analyzed for their protein motifs and phylogenetic classification. The Glycosyltransferase 1-3, the Polysaccharide export transporter (PET) and the UDP-3-O-[hydroxymyristol]-glucosamine-N-acyltransferase (N-Ace) have been classified in a phylogenetic tree. Similarities to different organisms such as *Chloroflexus sp.* (GT1 & GT3), *Rhizobium sp.* (GT2), *Bryobacter aggregatus* (PET) and *Candidatus solibacter usitatus* (N-Ace) could be detected. The Glycosyltransferase-like proteins all belong to Glycosyltransferase group 1. Fig. III-42 shows the phylogenetic tree of the most promising enzyme candidates GT1-3, N-Ace and PET with its closest relative. The alignment file of the proteins can be found in the Appendix on (VI. 4).

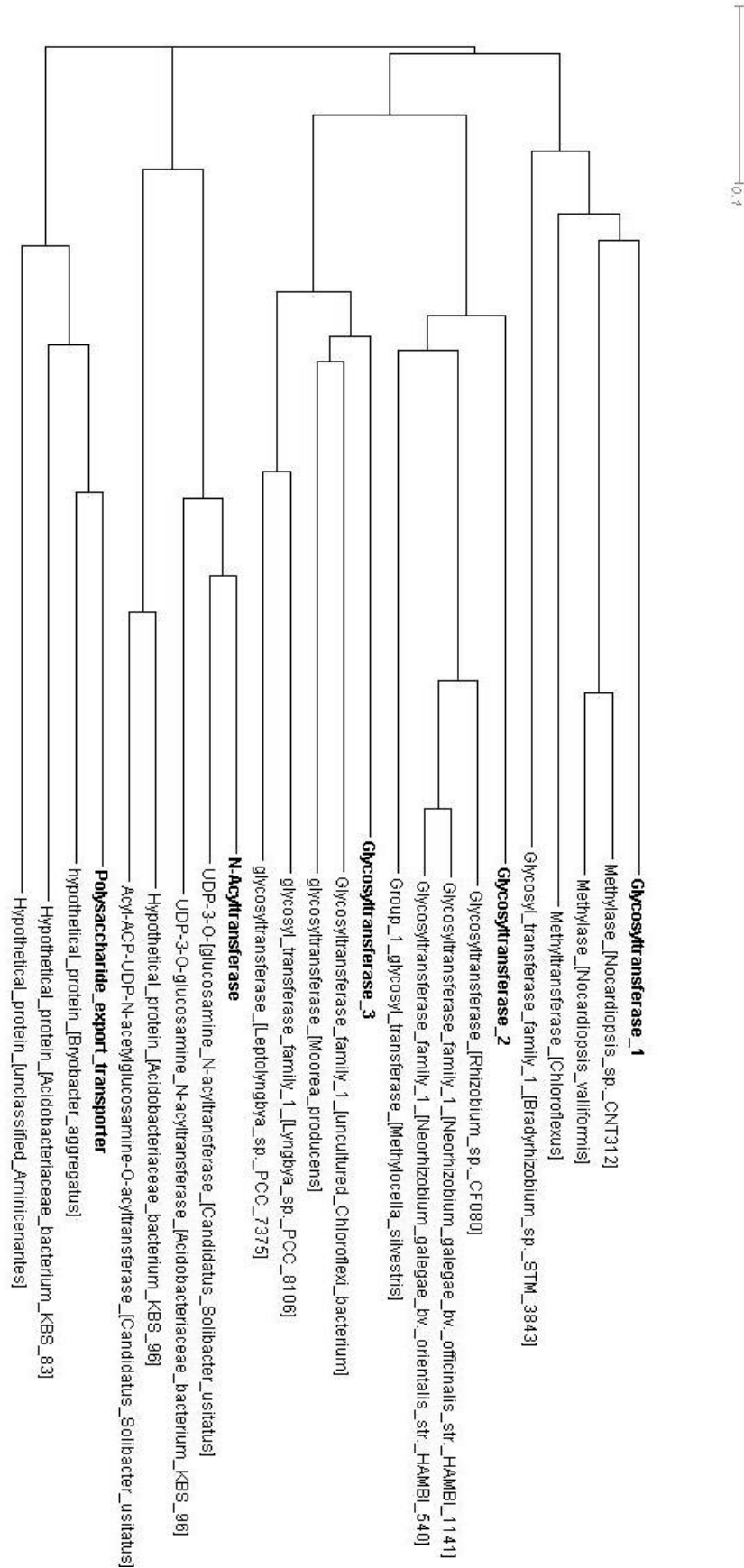


Fig. III-42: Phylogenetic tree of the most promising enzyme candidates encoded on fosmid clone 100 E3. The Glycosyltransferases 1 & 3 show similarities to *Chloroflexus sp.* and *Lyngbya sp.*, while Glycosyltransferase 2, as well as the N-Acyltransferase and Polysaccharide export transporter show similarities to *Rhizobium sp.* and *Candidatus solibacter usitatus*, or *Acidobacteria sp.* These bacterial species are common in soil, as well as marine habitats.

Based on the protein sequences of the enzymes a motif search for conserved domains has been done with each ORF. The search has been done online using Interpro (II.11) and all results are displayed in table III-5. For Glycosyltransferase 1 (GT 1) two conserved domains indicating a methyltransferase, as well as a Glycosyltransferase could be detected. The methyltransferase belongs to the group of S-adenosyl dependent methyltransferases (SAM) mainly responsible for the methylation of DNA. The detected Glycosyltransferase could be responsible for the transfer of glycosyl groups and belongs to transferases that invert the anomeric configuration of the target protein. Glycosyltransferase 2 and 3 (GT 2 & 3) showed conserved domains belonging to UDP-Glycosyltransferases in family 1 which also lead to inversion of the anomeric configuration of target structures after transferring the glycosyl group. Furthermore for GT 2 also the protein motif of Glycosyltransferase family 4 could be detected that leads to retention of the anomeric configuration.

Table III-5: Assembly of the protein motifs encoded in the most promising biofilm disrupting ORFs, showing the length of the protein, the integrated protein motif and its position as well as the function

Gene	Length (Amino acids, AA)	Protein motifs /Conserved domains	From AA ...to AA...	Function
GT 1	382	Methyltransferase	39-174	catalytic activity, transfer of methyl groups to DNA
		S-adenosyl-L-methionine-dependent methyltransferase (SAM)	38-195	
		UDP-Glycosyltransferase/ glycogen phosphorylase	292-359	
GT 2	378	Glycosyltransferase family 4	47-168	catalytic activity, transfer of glycosyl groups
		Glycosyltransferase family 1	186-345	
		UDP-Glycosyltransferase/ glycogen phosphorylase	3-371	
GT3	425	Glycosyltransferase family 1	221-378	catalytic activity, transfer of glycosyl groups
		UDP-Glycosyltransferase/ glycogen phosphorylase	29-400	
PET	320	Polysaccharide export protein	37-113	polysaccharide biosynthesis and/or export

Gene	Length (Amino acids, AA)	Protein motifs /Conserved domains	From AA ...to AA...	Molecular function
PET	320	Soluble ligand binding protein (SLBB)	208-247	Part of bacterial polysaccharide export proteins
N-Ace	601	Bacterial transferase hexapeptide repeat	376-405	Part of bacterial acyltransferases
			400-433	
			477-508	
			512-545	
		UDP-3-O-[3- hydroxymyristol] glucosamine N- acyltransferase	262-583	Lipid A biosynthetic process
		Trimeric LpxA-like (repeat region)	288-570	Lipid A biosynthetic process
		LpxD protein (non-repeat region)	279-343	

For the Polysaccharide export protein (PET) the conserved domain for bacterial export proteins has been detected as well as the soluble ligand binding protein motif (SLBB) that is typical for bacterial polysaccharide export proteins. The UDP-3-O-[hydroxymyristol]-glucosamine-N-acyltransferase (N-Ace) showed different conserved domains of which some overlap. First of all the typical conserved domain for UDP-3-O-[3-hydroxymyristol]-N-acyltransferases in bacteria could be detected that included four hexapeptide structures (HX) that are a necessary part of bacterial N-acyltransferases. This acyltransferases are supposed to be active in lipid A biosynthesis, as well as the LpxA motif that can be found in the repeat region also encoding the hexapeptide structures. The LpxD motif could be found in the non-repeat region, but is also a part of lipid A biosynthesis in bacteria. Fig. III-43 shows the schematic illustration of the ORFs with the conserved protein motifs.

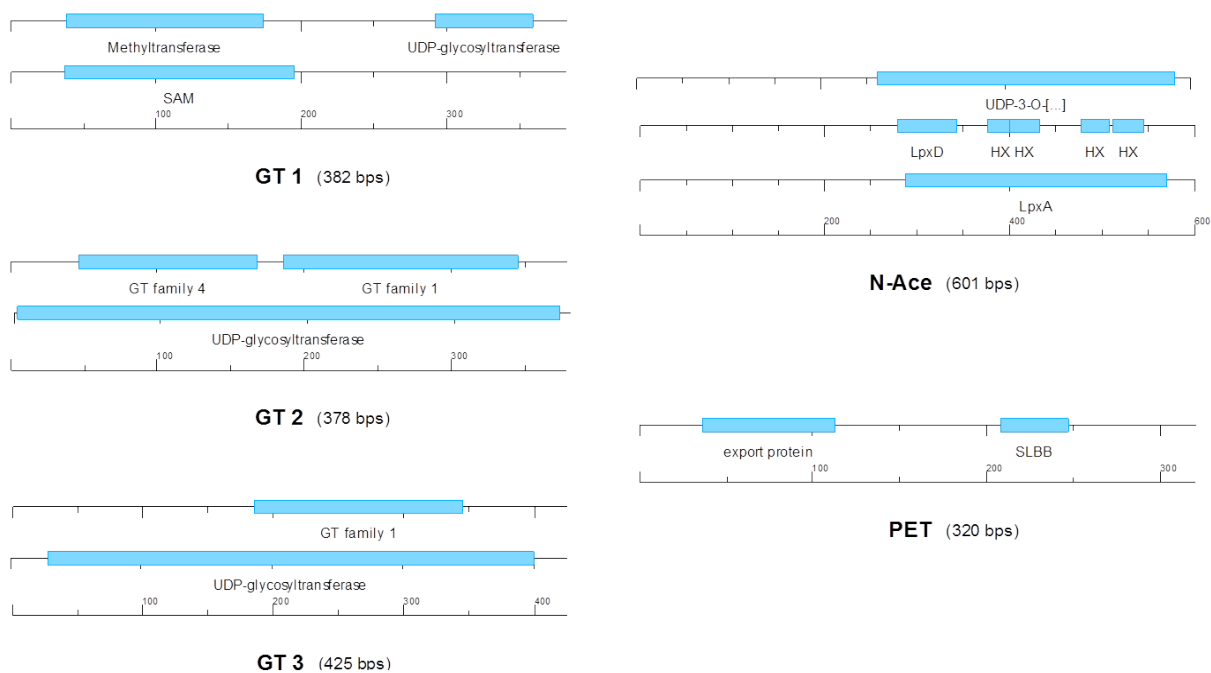


Fig. III-43: Protein motifs encoded by fosmid clone 100 E3. Glycosyltransferase 1 (GT 1) encodes an S-adenosyl dependent Methyltransferase (SAM) and a UDP-Glycosyltransferase. GT 2 & 3 show similar motifs belonging to Glycosyltransferase family 1 while for GT 2 also Glycosyltransferase family 4 could be annotated. The UDP-3-O-[hydroxymyristol]-glucosamine-N-acyltransferase (N-Ace, UDP-3-O-[...]) shows four hexapeptide repeats (HX) typical for bacterial transferases, as well as a LpxA and LpxD protein motif indicating lipid A biosynthesis. The Polysaccharide export protein (PET) shows the conserved domain for export proteins as well as a soluble ligand binding protein motif (SLBB).

IV. Discussion

IV.1. Proteins and Polysaccharides involved in biofilm formation

In this work the spatial organization and co-localization of biofilm associated proteins and polysaccharide PIA has been investigated in prototypic *S. epidermidis* strains 1457, 1457-M10 and 1585. Wild type strains as well as deletion clones lacking defined biofilm building proteins and deletion clones complemented with domains of the lacking biofilm building proteins on inducible vectors have been used. The main proteins of interest were the giant extracellular matrix binding protein (Embp), the accumulation associated protein (Aap) and the small basic protein (Sbp). Their positions inside the biofilm and for Aap the domain responsible for biofilm formation have been closer defined. For Embp the heterogeneity of its structure inside the biofilm and co-localization to well known polysaccharide intercellular adhesin (PIA) has been investigated. The main strategy to examine the proteins was fluorescent microscopy.

IV.1.1. Spatial PIA organization

As described in III.1.1 the formation of PIA depending biofilms has been investigated using static and flow live cell imaging. Wheat germ agglutinin conjugated to a red fluorescent protein gave the possibility to track PIA from the inoculation of the culture during the whole growth phase. In static cultures PIA expression started at the moment when the bacterial cells settled down to the surface for attachment. PIA seemed to form a core leading to small cell aggregates that grew in height before they started spreading over the whole surface to colonize the ground (video 1 in the appendix (VI.6.1 Video *S. epidermidis* 1457 PIA formation)). This led to the typical mushroom-like structure of PIA dependent biofilms. Since the starting structures grew faster in height than the later colonized parts, a thick cell carpet, as well as tower-like structures developed, and these are thought to maintain the availability of nutrients for cells organized within the biofilm [43]. Channels inside the mushroom-like structures and in the cell carpet transported amino acids, minerals and other nutrients [6]. The movement of medium through the channels could still be seen by single planktonic cells floating through the biofilm. This showed that PIA formed a scaffold around the cells but did not necessarily restrict their general movement abilities. In flow live cell experiments using *S. epidermidis* 1457, a biofilm positive, PIA expressing strain, attachment to the surface of the flow chamber and biofilm structures could be obtained (see appendix VI.6.3 Video *S. epidermidis* 1457 flow conditions). The biofilm was not as thick and evenly spread over the whole surface as in static cultures. It showed huge biofilm aggregates expressing PIA and planktonic cells floating in between these cell clusters. In the biofilm negative, PIA lacking strain *S. epidermidis* 1457-M10 no biofilm formation could be seen and no PIA has been produced (see appendix VI.6.2 Video *S. epidermidis* 1457-M10). This strain lacks the *icaADBC* operon that encodes PIA [9, 10, 110]. In neither static live cell

experiments, nor flow experiments a biofilm has been formed since no cells attached to the surface. All cells were moving and floating through the channel (see appendix VI.6.4 Video *S. epidermidis* 1457-M10 flow conditions).

IV.1.2. Spatial PIA and Sbp distribution

When it comes to the question of how the cells adhere to the surface the protein Sbp is most likely responsible for this step of biofilm formation. In part III.1.2 it can be seen that Sbp was always located on the bottom of the biofilm, showing a distinct layer on the colonized surface that faded out in the upper cell layers. Experiments with over head growing biofilms showed that this was not a phenomenon of gravity. The Sbp layer could be detected at the lower bacterial cells layers and the colonized surface. There must be regulation processes that led to Sbp expression from the moment of cell sedimentation to the surface until the first layers of cells were attached to each other. Regarding PIA it could be seen that it is spread through the whole biofilm structure, but not directly at the surface. PIA expression could be visualized at the microscope right from the moment when the bacterial culture was introduced into the microscope chamber. Sbp and PIA seemed to have a touching area, but this hypothesis could not be proved by co-localization analysis. Sbp could not be visualized during its early expression phase, since the production of a clone expressing *gfp* combined with the *sbp* promoter failed. The addition of pre-conjugated α -FLAG tag Cy5 antibody that should visualize the FLAG tag of *S. epidermidis* 1457 Δ *sbp*::pRB*sbp*FLAG₃xpCM29 (expresses Sbp with 3 FLAG tags) did not show any Sbp from the beginning of the growing culture. Only when Sbp has been immunostained in mature cultures it could be visualized. It could be shown that natural Sbp as well as recombinant expressed and pre-labelled Sbp both are located at the ground of the colonized surface only. These findings support the hypothesis of Sbp being the major surface attachment protein.

IV.1.3. Influence of sub-domains of Aap on *S. epidermidis* biofilm formation

One major biofilm forming protein is the Accumulation associated protein Aap [109, 111, 112]. This protein is composed of 3 domains, A, 212 and B, as well as an export signal (Fig. III-7) [95]. Determining the function of each single domain of Aap is essential for understanding the accumulation step in biofilm formation. Deletion mutants lacking the *aap* gene have been complemented with plasmid vector pCN::tetM (a tetracycline inducible vector) encoding either domain A including the export signal, domain B and the export signal, or domain B+ 212 and the export signal. *S. epidermidis* 1457 Δ *aap* deletion mutants had the natural ability to produce PIA and Sbp next to each domain of Aap, while the deletion mutants of *S. epidermidis* 1457-M10 Δ *aap* did not produce PIA, but Sbp. Furthermore *S. epidermidis* 1457-M10 Δ *aap* Δ *sbp* deletion mutants lacking the *aap* and *sbp* gene have been complemented with each domain of Aap. Strains expressing only one domain of Aap, but no PIA, or Sbp have been produced. Comparing all of these strains it could be seen, that the expression of domain A of Aap did not lead to the typical mushroom-like biofilm structure,

but to readily attached cell layers. The strains lacking PIA like *S. epidermidis* 1457-M10 Δ aap and *S. epidermidis* 1457-M10 Δ aap Δ sbp showed a cell lawn that could be easily removed from the surface. Analyzing microscopic images it could be seen that domain A was expressed throughout all cell layers, but all cells slightly moved in these layers. No strong attachment in between the cells could be visualized. This indicated that domain A of Aap is mainly a cell-surface attachment and a slight cell-cell attachment protein than responsible for biofilm structure [95]. In strains lacking Aap, PIA and Sbp domain A of Aap led to stronger attachment to the colonized surface than in strains where Sbp was expressed simultaneously. This led to the hypothesis that proteins can take over the function of other proteins to ensure biofilm formation and by this mechanism, cell survival. When PIA was expressed in combination with domain A of Aap in *S. epidermidis* 1457 Δ aap the biofilm structure did not differ from the *S. epidermidis* 1457-M10 strains that lack PIA. Also cell layers without the typical mushroom-like structure could be obtained. Additionally PIA was visible in between all cell layers leading to cell-cell attachment. So the cell lawn was higher than in strains lacking PIA, but the structure was the same. Investigating *S. epidermidis* 1457 Δ aap strains complemented with domain B of Aap showed a distinct biofilm structure with mushroom-like aggregates, channels that transport planktonic cells and medium as well as very strong cell-cell attachment. The visual appearance of the biofilm did not differ from the wild type *S. epidermidis* 1457 biofilm. Domain B, as well as PIA could be found throughout the whole biofilm. The height of domain B biofilms was lower than the height of the cell layers of deletion mutants complemented with domain A. This phenomenon occurred due to the strong, compact structure derived from domain B of Aap. Domain A only led to cell layers that were packed almost up to medium limit. Regarding *S. epidermidis* 1457-M10 Δ aap a clone expressing only domain B could not be obtained. But for *S. epidermidis* 1457-M10 Δ aap Δ sbp a clone expressing domain B could be produced. The structure of a biofilm could be monitored in this usually biofilm negative strain. Domain B was expressed through all layers of the biofilm leading to the typical mushroom-like structure. The biofilm height increased up to twice the height when domain A was present while the total amount of protein was less than when only domain A was expressed. This indicated that a higher amount of domain A might be necessary to keep the cell layers attached. A lower amount of domain B seemed to be sufficient for a strong cell-cell attachment and the typical biofilm structure. Regarding domain B+212 a slightly different picture could be monitored. For all strains, either PIA producing *S. epidermidis* 1457 Δ aap, *S. epidermidis* 1457-M10 Δ aap, or *S. epidermidis* 1457-M10 Δ aap Δ sbp the same biofilm morphology could be observed. Some small mushroom-like structures could be seen, while a thick cell layer was still present. The microscopic images seemed like a mixture of domain A and domain B expressing strains. This was also supported by the biofilm height of *S. epidermidis* 1457-M10 Δ aap and *S. epidermidis* 1457-M10 Δ aap Δ sbp expressing domain B+212 showing a height in the range between domain A and domain B expressing strains. The domain B+212 specific fluorescence signal volume inside the biofilm of *S. epidermidis* 1457-M10 Δ aapxpCN::DomB+212 was not as high as the domain A specific fluorescence

signal volume in *S. epidermidis* 1457-M10 Δ aapxpCN::DomA. For *S. epidermidis* 1457-M10 Δ aap Δ sbpxpCN::DomB+212 the amount of detected domain B+212 was in the middle range of domain A and domain B, that meant more domain B+212 than domain B was present, but less than domain A. Regarding *S. epidermidis* 1457 Δ aap complemented with domain B+212 the same results occurred and the biofilm showed a structure in between the structures of domain A, or domain B based biofilms. The distribution of PIA was still all over whole biofilm; its scaffold was not affected by the expression of single Aap sub-domains. In summary all these findings showed that every sub-domain of Aap led to a slightly different biofilm structure. As indicated in the introduction (1.4.2) Aap has to be processed prior to forming the typical mushroom-like structure. It is hypothesized that domain A and domain 212 have to be cleaved proteolytic after surface attachment to enable domain B to form the typical biofilm structure [28, 95]. This hypothesis is supported by the results of this work showing that a typical mushroom-like biofilm structure could only be achieved when domain B is present without domain A, or the 212 amino acid region.

IV.1.4.Co-localization of Embp and PIA and spatial distribution of Embp

Another very important protein involved in biofilm formation of PIA lacking strains is the extracellular matrix binding protein Embp [35, 36, 113]. It is hypothesized to have a similar function like PIA, but without the extreme strong attachment properties. Embp based biofilms are weaker and can be removed more easily [35, 36, 37]. The effect of this biofilm building protein together with the polysaccharide PIA has been investigated in this work showing that both matrix components together strengthen the biofilm and show co-localization. These findings have been checked with *S. epidermidis* 1585, a usually biofilm negative strain, that has the genetic ability to express Embp. This strain has been complemented with the tetracycline inducible $P_{xyl/tet}::embp$ promoter to increase Embp production and a second plasmid with the *icaADBC* operon to produce PIA (pTXica). Strains expressing each matrix component separately and both components together have been checked for their biofilm formation mainly via fluorescent microscopy, but also with electron- and dSTORM microscopy. First of all it could be proved by raster electron microscopy (REM) that *S. epidermidis* 1585 $P_{xyl/tet}::embp$ was able to form large cell aggregates and weak biofilms, while the wild type did not form aggregates but only tetrads. These findings have been supported by transmission electron microscopy (TEM) showing that a mesh-like matrix composed of Embp was exported in the extracellular space of the biofilm leading to cell-cell attachment. This matrix mesh was crinkled in the extracellular space due to extreme drying processes prior to TEM. This procedure can break the matrix structure into little fragments and changes the real appearance of the matrix [70]. To represent the matrix structure under conservative conditions dSTORM microscopy has been performed and showed very precisely the arrangement of Embp and PIA. Simultaneous expression of Embp and PIA in *S. epidermidis* 1585 $P_{xyl/tet}::embpxpTXicaxpCM29$ led to strong biofilms. The typical biofilm structure with mushroom-like towers and channels emerged from the clone expressing both matrix components. Embp lied elongated

connecting the cells to each other, while PIA filled the parts in between where Embp was not present. Embp showed heterogeneous structures that were not only horizontally stretched from one cell to another, but also vertical forming connections between cell layers and PIA structures. PIA formed a honey-comb-like scaffold, imbedding one bacterial cell in each comb. Embp and PIA had distinct co-localization sections mostly along the Embp strings that connected the cells. A co-localization analysis could show that 41,38 % of PIA co-localized to Embp, while 42,38 % of Embp were directly co-localized to PIA. Embp was supposed to be more closely attached to the bacterial cells than PIA, which could also be shown by co-localization analysis. 10,36 % of Embp were directly co-localized to the bacterial cells while ~ 25 % of the bacterial cells were attached to Embp. Regarding PIA only 7,74 % were co-localized to the bacterial cells. These findings indicated that Embp led to biofilm formation due to cell-cell connection while PIA formed the scaffold in which the bacterial cells were imbedded. The Embp-specific fluorescence signal in the microscope images from clones including *P_{xyl/tet}::embp*, a very high Embp expression of 4.000-7.000 μM^3 could be obtained. In comparison the wild type expressed only 100 μM^3 Embp naturally. Interestingly in the clone containing pTXica the amount of Embp decreased to approx. 800 μM^3 while the resulting biofilm was more compact and showed the distinct biofilm structure. The biofilm height increased to twice the height of a biofilm expressing only Embp. This indicated that PIA production suppressed Embp production, or the other way around when both matrix components were present. But still simultaneous expression led to stronger and higher biofilms. To prove this hypothesis the strain *S. epidermidis* 1457, a biofilm positive, PIA expressing strain has been complemented with *P_{xyl/tet}::embp*. Usually this wild type strain does not express Embp, but PIA and forms very strong high biofilms. The Embp-specific fluorescence signal in this clone was quite low around 75 μM^3 which was even less than the Embp-specific fluorescence signal in the wild type *S. epidermidis* 1585. Nonetheless when *S. epidermidis* 1457 *P_{xyl/tet}::embp* was induced for Embp expression the biofilm height was half as much as without Embp. The spatial distribution of Embp as well as the heterogeneity of Embp structure showed horizontal and vertical elongated fibers that have been the same as for *S. epidermidis* 1585 *P_{xyl/tet}::embp* x pTXica x pCM29. Co-localization analysis showed also for strain *S. epidermidis* 1457 *P_{xyl/tet}::embp* 40,81 % of co-localized Embp to PIA, while 32,08 % of PIA directly co-localized to Embp. This provided the idea that both matrix components had an impact on each other. In this case the expression of Embp did lead to downgraded biofilms, but they were still as strong as usual. A possible explanation could be that PIA was responsible for the strength of a biofilm. It supported cell-cell attachment and formed the biofilm scaffold. Its strong electrochemical properties strengthen the biofilm even more [27]. Embp could take the place of PIA in strains lacking PIA, but did not lead to biofilms as high and strong, as when PIA was involved. The difference in the consistency of bacterial biofilms depending on the exopolysaccharide involved could already been shown for *Pseudomonas aeruginosa* biofilms in which Psl leads to elastic and highly cross-linked biofilms, while Pel favors weaker, viscoelastic biofilms [71].

Concluding the findings indicate that in PIA lacking strains other proteins can take over the function of PIA to enable biofilm formation. In *S. epidermidis* 1457-M10 Aap substitutes PIA and domain B of Aap leads to the typical mushroom-like biofilm structure. In *S. epidermidis* 1585 Embp takes over the function of PIA. Table IV-1 shows the functions of each biofilm building protein and its substitution possibilities. This assumption has already been proposed for different bacterial species such as *Yersinia pestis* that performs auto-aggregation and biofilm formation without PIA [69]. Also for *icaADBC* negative *S. epidermidis* strains #12228, #14990 and #49134 the phenomenon of auto-aggregation without PIA could be observed [21, 70].

Table IV-1: Biofilm building matrix components and their functions

Steps of biofilm formation	Surface attachment	Accumulation	Final biofilm mushroom-like structure
Main factor	Sbp Sub-domain A of Aap	PIA Embp Sub-domain A and B+212 of Aap	PIA Embp Sub-domain B of Aap
Co-localization		Embp & PIA	Embp & PIA

IV.2. Antibiotic influence on *S. epidermidis* 1585 biofilm formation

S. epidermidis strains that do not form biofilms naturally sometimes show the ability of biofilm formation under stress conditions such as osmotic stress [37]. A common therapy in clinical daily routine is antibiotic treatment of patients and with this antibiotic stress for bacterial cells that can cause an infection [1]. This stressor has been tested for its influence on biofilm formation. *S. epidermidis* 1585 wild type has been used for these experiments showing that some classic antibiotics such as oxacillin, chloramphenicol, linezolid and tigecycline used for the treatment of staphylococcal infections lead to biofilm formation in this usually biofilm negative strain. The main biofilm supporting protein that was up regulated in this case was Embp. It could be shown by Embp Dot Blots and microscopic analysis that more Embp than in the wild type has been produced after antibiotic treatment. Biofilms occurred that adhered to glass and polystyrene surfaces. The amount of Embp increased up to 20 times compared to the constant background wild type Embp expression. Chloramphenicol and linezolid, both protein biosynthesis affecting antibiotics, led to the biofilm formation. Interestingly chloramphenicol treated biofilms showed an increase in height and Embp production; while linezolid treated *S. epidermidis* 1585 biofilms increased

in height, but did not show increased Embp production. Linezolid is supposed to be a novel effective antibiotic that has bacteriostatic properties on gram-positive bacteria, but some strains already show resistance against linezolid by different mechanisms [96]. Oxacillin belongs to the antibiotics that are used specifically for the treatment of staphylococci, but in experiments performed during this work oxacillin led to increased biofilm formation in *S. epidermidis* 1585. The Embp-specific fluorescence signal increased up to 10 times compared to the wild type background expression of Embp. The only antibiotic tested that did not lead to biofilm formation, or increased Embp production was erythromycin. The Embp production has been even lower than the background Embp expression in the wild type strain. The height of cell layers after erythromycin treatment was around half the height of biofilms induced with other antibiotics. Erythromycin is used for the treatment of gram positive microorganisms. It blocks the protein biosynthesis by binding to the 50S subunit so that tRNA molecules cannot bind anymore [65].

IV.2.1. Influence of Tigecycline and phagocytosis after Tigecycline induced biofilm formation on *S. epidermidis* 1585

A major focus has been laid on tigecycline, a novel anti biofilm agent that binds to ribosomes and disables protection proteins. It cannot be exported from the cell by classical tetracycline efflux pumps and is therefore supposed to be effective against resistant gram-positive microorganisms [64, 96]. A reason for microorganisms to form biofilms is the protection against external stress, such as nutrient stringency, osmotic stress, shearing forces and chemical stress such as antibiotics, antimicrobials, or disinfectants [56, 57]. One major advantage of biofilm formation is the protection against phagocytosis during host defense mechanisms that occur during infections [66, 67]. It is said, that neutrophils unable to move due to a mature biofilm take up less bacterial cells and do not effectively combat the infection [67, 95]. It could be detected that tigecycline concentrations between 0,3-0,6 µg/mL led to biofilm formation. The Embp-specific fluorescence signal volume was about 15 times higher in tigecycline treated biofilms than in the wild type strain. In the case of tigecycline treated *S. epidermidis* 1585 it has been tested if an antibiotic induced biofilm also persists against phagocytotic killing by mouse macrophages J774A.1 in vitro. Reckoning the number of internalized bacterial cells after 6 h post macrophage dissemination on tigecycline treated and control biofilms showed that significantly more bacterial cells could be internalized in the control biofilms than in tigecycline treated biofilms. The macrophages were stuck in the biofilm and led to holes in the biofilm structure without internalizing more than 7 bacterial cells while the macrophages on the control biofilm could internalize up to 20 bacterial cells. These findings supported the idea of biofilms as a survival strategy and an effective way to bypass host defense mechanisms. Interestingly for *S. epidermidis* 1585 the protective mechanism of protein based biofilm formation was induced by antibiotic stress, so there must be compensatory mechanisms on protein base to secure bacterial survival [97, 100].

IV.3. Influence of fosmid clone extracts 100 E3, 100 B3 and 64 F4 on *S. epidermidis* 1457 biofilms

The disruption of staphylococcal biofilms is essential for the treatment of implant infections. The matrix around the bacterial cells protects them from outer influences, such as phagocytosis, or antibiotics and is mainly responsible for strong cell-surface and cell-cell attachment [56]. Possible ways to disrupt a *S. epidermidis* biofilm could be the weakening of the matrix, or direct cell lysis. To find new ways of disrupting biofilms a metagenomic screening method has been developed in a previous thesis ("Disruption of *Staphylococcus epidermidis* biofilms through novel metagenomic enzymes" [Henke H A, 2011, master thesis]). The outcome of this screening have been three fosmid clones deriving from a metagenomic library based on Elbe River sediment that showed the capability of disrupting mature *S. epidermidis* 1457 biofilms. Each fosmid clone has been investigated more closely in this work, describing the effect on the biofilm by microscopic methods. Fosmid clones 100 B3 and 64 F4 showed a slight ability to disrupt the biofilm and decreased the biofilm volume up to 40 %. In comparison fosmid clone 100 E3 disrupted biofilms up to 80 %. Regarding the amount of dead cells inside the biofilm an increase after the addition of fosmid clone cell raw extracts to mature *S. epidermidis* 1457 biofilms could be obtained. It could be seen that after the treatment with fosmid clone extract of 64 F4 dead cells lay on top of the biofilm fragments. The affected cells after the treatment with fosmid clone extract 100 B3 lay in the middle and upper layers of the biofilm. In comparison the treatment with fosmid clone cell raw extract of 100 E3 led to dead cells and eDNA in the layers of the biofilm closest to the surface. Mixtures of all three extracts in all possible combinations decreased the effect on the biofilm compared to the single effect of 100 E3. The mixtures of extracts containing 100 B3 showed lower activity on the biofilm and a disruption of only 25, respectively 40 % and were with this lower than each extract itself. This indicated an inhibiting effect among the fosmid clone extracts. Even when fosmid clone extract 100 E3, that usually disrupted the biofilm up to 80 %, was present only 60 % disruption could be achieved when fosmid clone extract mixtures were used. The dead cells and eDNA after the treatment with extract mixtures of 100 B3 + 64 F4 could mainly be found on top of the biofilm fragments. Interestingly when the fosmid clone mixtures contained the extract of 100 E3 (e.g. 100 E3+64 F4, or 100 E3+100 B3, or all three together) also the lower biofilm levels showed an increased amount of dead cells, respectively eDNA than without fosmid clone extract 100 E3. This led to the hypothesis that the extract diffused through the biofilm and attacked matrix components, or bacterial cells in the lower levels. Regarding the proteinaceous structure of a *S. epidermidis* 1457 biofilm, the protein Sbp (small basic protein) is mainly located at the ground of the biofilm. A possible point of attacking the biofilm could be this surface attachment protein. Also PIA (polysaccharide intercellular adhesin) is located in a *S. epidermidis* 1457 biofilm and can be found in all cell layers. This polysaccharide could be another point of attack for components in the extract of fosmid clone 100 E3.

IV.3.1. Heat-inactivation of fosmid clone extracts and identification of gel-filtered proteins encoded on fosmid clone 100 E3

Concerning the heat stability of all extracts heat inactivation at ~ 65 °C has been performed and these extracts have been added to mature *S. epidermidis* 1457 biofilms. All extracts showed some biofilm disrupting activity but for the extract of 100 B3 and 64 F4 it decreased down to ~10 %. Surprisingly the heat inactivated extract of fosmid clone 100 E3 still showed a disruption of almost 60 %. This finding indicated heat stable enzymes, or non enzymatic components in the extract that were responsible for biofilm disruption. Table IV-2 sums up the characteristics of the fosmid clones closer defined in IV.3 and IV.3.1.

Table IV-2: Biofilm disruption characteristics of fosmid clones 64 F4, 100 B3 and 100 E3

Fosmid clone	Affected biofilm layer	Assumed point of attack	Disruption capability	Disruption capability after heat inactivation
64 F4	Upper layer	PIA, upper cells	~40%	~10%
100 B3	Middle and upper layers	PIA	~40%	~10%
100 E3	Ground layer	Sbp, PIA	~80 %	~60%

Further experiments have only been done with the highly active fosmid clone 100 E3. To break down the extract of fosmid clone 100 E3 that showed the highest activity in all experiments it has been filtered by gel filtration. Fractions containing proteins of different molecular weight groups could be collected and then tested in the biofilm disintegration assay, as well as in a PIA degradation assay. The experiments resulted in fraction B2 showing biofilm disrupting properties up to 78 % as well as PIA degradation. This fraction has then been prepared for mass spectrometry to identify the proteins collected in fraction B2 that had sizes between 17 – 70 KDa. Five samples showed distinct proteins located on the sequence and were annotated as sugar modifying enzymes. These have been defined as the most promising candidates of disrupting the biofilm and degrading PIA. A dehydrogenase (DH), amidohydrolase (AH), peroxidase (PO), oligo peptide transporter (OPT) and glycosyltransferase (GT3) have been identified during mass spectrometry. Since the whole fosmid sequence has been available also other enzymes such as two more glycosyltransferases (GT1 and GT2), as well as a UDP-3-O-[3-hydroxymyristol]-glucosamine-N-acyltransferase (N-Ace) and a polysaccharide export transporter (PET) have been determined to be possibly responsible for biofilm disruption. All these enzymes have been used for PCR and cloning experiments to receive over expression clones. Different expression vectors and *E. coli* hosts have been used in the over expression experiments, but no recombinant protein could be yielded. Mostly the expression hosts lysed during expression or expressed the protein only in the insoluble fraction, indicating the very strong activity of the compounds. Trials of varying the expression temperature, induction

concentration and time point of induction had no effect on the production of inclusion bodies. The effort of breaking these inclusion bodies and refolding the protein has not been successful. Glycosyltransferases are known to be difficult in high-level expression as well as purification [88]. AH and DH could be recombinantly expressed but had no effect on *S. epidermidis* 1457 biofilms. Furthermore *Pichia pastoris* and *Pseudomonas aeruginosa* have been used as expression host for the other enzymes. Sub cloning of the enzymes into host specific vectors worked well, but no recombinant protein could be obtained. Also the foreign hosts such as yeast and *P. antarctica* seemed to be affected by the proteins. The difficulties in expressing these enzymes showed their high potential of being an antimicrobial and anti-biofilm agent. Avoiding cell lysis during expression should be achieved by a cell free expression system with *E. coli* SlyD extract, but no protein could be detected. Simultaneous top down experiments have been performed during the master thesis “Molekularbiologische Untersuchung des Fosmidklons 100 E3 zur Desintegration von staphylokokkalen Biofilmen” (Aylin Bertram, 2012, data not published). The idea was to digest the whole fosmid and subclone smaller fragments in low expression vectors to narrow down the active region and with this the enzymes located in this region that are responsible for biofilm disruption. This approach was not successful and so long range PCR of defined regions has been done. Unfortunately no PCR products could be achieved, probably due to the extremely high GC content of over 60 % in the sequence of fosmid clone 100 E3. PCR methods to amplify regions with various high GC contents are widely discussed and multiplex approaches are recommended but difficult to achieve [72]. Chemicals like formamide, or DMSO as well as very large amounts of DNA polymerase are said to improve the specificity and outcome of such a PCR [72, 73]. These ideas have not been implemented during the master thesis.

Concluding one can find that the difficulties in expressing the glycosyltransferases, polysaccharide export protein and UDP-3-O-[3-hydroxymyristol]-glucosamine-N-acyltransferase indicated the high activity of these enzymes. Furthermore the results narrowed down the enzymes encoded on fosmid clone 100 E3 to these special candidates and make it even more likely that at least one of these enzymes is a new way to disrupt staphylococcal biofilms.

IV.4. Bioinformatic analysis of fosmid clones, specifically 100 E3

The fosmid clones that showed biofilm disrupting properties have been fully sequenced to analyze their genetic potential. The full sequences of the clones have been checked for their GC content and resulted in ~53 % and ~59% for fosmid clone 64 F4 and 100 B3. Fosmid clone 100 E3 has a GC content of over 63 % which is defined as a high GC content. This indicates strong DNA binding due to the triple hydrogen bonds and leads to a higher temperature stability [74, 75]. This known fact is supported by the finding that the extract of fosmid clone 100 E3 was still active on biofilms after heat treatment at 60-70 °C oN (III.3.2). With this high GC content it is also supposed that cells undergo autolysis and have a shorter live time [74]. Host lysis might be a possible explanation for the failure of expression of the high GC content enzymes encoded on fosmid clone 100 E3 (III.3.4). Regarding the full nucleotide sequence of

each fosmid clone to determine the origin of the DNA no similarity on nucleotide basis could be detected. This implicates that all fosmid clones comprise DNA of so far unknown organisms. When the full protein sequences of the fosmid clones were analyzed similarities of 3 %, or less could be found. For fosmid clone 100 B3 *Pirulella planctomyces*, for 64 F4 unknown organism and for 100 E3 *Candidatus solibacter usitatus* could be found. These findings supported the novelty of the DNA and encoded enzymes. Following sequence analysis has mainly been performed with fosmid clone 100 E3. Regarding the genetic structure of fosmid clone 100 E3 in total 24 genes could be annotated. Six hypothetical proteins, two hydrolases and four transport proteins could be detected. Proteins annotated as sugar modifying have been chosen to be the most promising candidates of disrupting a mature *S. epidermidis* 1457 biofilm, especially the polysaccharide based matrix. In addition mass spectrometry of a filtered fraction showed three proteins in fosmid clone 100 E3 that were indicated as promising candidates. Table IV-3 shows an overview of the most promising enzyme candidates encoded on fosmid clone 100 E3.

Table IV-3: Overview of putative biofilm disrupting enzyme candidates from fosmid clone 100 E3

Enzyme	GC content	Recombinant protein	Disruptive effect of recombinant protein	Closest relatives
Glycosyltransferase 1-3	All: >64 %	No	?	Rhizobia, Chloroflexi, Lyngbya
N-acyltransferase	64,00 %	No	?	Acidobacteriaceae
Polysaccharide export protein	66,87 %	No	?	Acidobacteriaceae, Aminicenantes
Amidohydrolase	61,79 %	Yes	No	Cytophagacea
Dehydrogenase	59,35 %	Yes	No	Acidobacteriaceae

These candidates include the glycosyltransferase 3 (GT3), as well as the amidohydrolase (AH) and dehydrogenase (DH). AH and DH have been successfully subcloned and over expressed but did not show any effect on *S. epidermidis* 1457 biofilms. Some enzymes encoded on fosmid clone 100 E3 that did not show during mass spectrometry have been further analyzed due to their annotation as possibly sugar modifying enzymes, such as glycosyltransferases 1 and 2 (GT1 & GT2). The UDP-3-O-[hydroxymyristol]-glucosamine-N-acyltransferase (N-Ace) and polysaccharide export transporter (PET) have also been identified as promising candidates. Together with GT3 they all show a high GC content of over 64 %. This explains the difficulties in PCR, ligation and over expression experiments. Considering the protein sequences of the enzymes similarities to known organisms could be detected for each protein. The results are summed up in the phylogenetic tree (Fig. III-42). GT1 showed relations to different S-adenosyl dependent methyltransferases from halophilic *Nocardiopsis sp.* and glycosyltransferase family 1 from *Bradyrhizobium sp.* [78]. GT2 and GT3

both showed similarities to glycosyltransferase family 1 of Rhizobia (GT2) and marine associated bacteria such as Chloroflexi and Lyngbya (GT3). These findings fitted to the DNA source of the metagenomic library that has been built out of Elbe River sediment. The Elbe River contains brackish water that is a habitat for marine, as well as sweet water microorganisms. The sediment itself can contain soil bacteria [76, 77]. The N-acyltransferase (N-Ace) showed relatives of the phyla Acidobacteriaceae and *Candidatus solibacter usitatus*, both known bacterial species common in soil, as well as in river sediments [76, 79]. The polysaccharide export protein (PET) showed similarities to hypothetical proteins of different Acidobacteriaceae and Aminicenantes, an uncultured not closer classified organism [80].

IV.4.1. Protein motifs and possible functions of the most promising enzymes encoded on fosmid clone 100 E3

On fosmid clone 100 E3 each promising enzyme candidate that might be responsible for biofilm disruption has been investigated more closely. PET has been annotated to be a polysaccharide export protein due to its conserved protein domain that is mainly responsible for the biosynthesis and export of polysaccharides in bacteria [81]. Additionally to the polysaccharide export protein motif a soluble ligand binding protein motif could be identified that is typical for bacterial export proteins, has a β -grasp fold and is capable of binding different ligands [82]. The idea why PET might be capable of disrupting the bacterial biofilm is that its biosynthesis and export properties interfere with the polysaccharide PIA and change the structure so that the biofilm loses its strength and the bacterial cells cannot hold on to each other and might be swapped off the surface. The N-acyltransferase showed protein motifs of a hexapeptide repeat protein typical for bacterial acyltransferases including in a trimeric LpxA-like region that is known to be involved in the first step of Lipid A synthesis [84]. Lipid A is a part of lipopolysaccharide (LPS) in the outer membrane of most Gram-negative bacteria. The non repeat region of the protein contained the LpxD motif that is also involved in Lipid A synthesis. The enzyme is known to produce UDP-2,3-diacyl-N-acetylglucosamine (GlcNAc). This constitutes the third step in the lipid A biosynthetic pathway and is known to be involved in cell envelope, biosynthesis and degradation of surface polysaccharides and lipopolysaccharides [83, 85]. This degradation of surface polysaccharides might be the important feature and the reason for the biofilm disrupting property of N-Ace. Regarding the glycosyltransferases GT2 and GT3 both showed the same protein motifs, a conserved domain of UDP-Glycosyltransferase/glycogen phosphorylase. They were classified as glycosyltransferase family 1 enzymes that lead to inversion of the anomeric configuration of the substrate [89]. The single displacement mechanism is somewhat analogous to the mechanism of inverting glycosidases [90]. This mechanism is proposed to be SN₂-like [88]. Glycosyltransferases catalyze the transfer of sugar moieties from activated donor molecules to specific acceptor molecules, such as proteins, forming glycosidic bonds [88]. Glycosyltransferase family 1 members may transfer UDP, ADP, GDP, or CMP linked sugars [88]. Many different enzymatic activities can be found in this family and reflect a wide range of biological functions [91]. The protein structure available for this

family has the GT-B topology and a distinct N- and C- terminal domain each containing a typical Rossmann fold [86, 88]. The two domains have high structural homology but minimal sequence homology supporting the low similarities during sequence alignments and nucleotide based origin search in this work. The large cleft that separates the two domains includes the catalytic center and permits a high degree of flexibility. The members of this family are found mainly in bacteria and archaea [86, 87, 88]. The idea why these glycosyltransferases may disrupt a *S. epidermidis* 1457 biofilm, respectively the PIA matrix lays in the capability of transferring sugar moieties and with this change the electrochemical, or the whole composition of PIA. This would lead to a loss of attachment ability in the matrix and may lead to the detachment of large cell lumps. Interestingly protein motif search for GT2 not only led to glycosyltransferase family 1, but also to glycosyltransferase family 4. This family does not show similarities for the whole catalytic domain, but only for a part of the domain. Therefore glycosyltransferases can be classified in this polyspecific glycosyltransferase family due to small protein sequence pieces, which makes a single sequence based classification of glycosyltransferases difficult [88]. Glycosyltransferases are known to have more functions than the one predicted and therefore might not only be capable of transferring a sugar molecule, but also cut off sugar molecules from bound structures [88]. This might be a way PIA is disrupted by these enzymes. The last promising candidate GT1 showed protein sequence-based similarities to an S-adenosyl-L-methionine dependent methyltransferase (SAM) as well as a UDP-glycosyltransferase. An S-adenosyl-methionine binding site has been detected as conserved feature. SAMs of class I are enzymes that use S-adenosyl-L-methionine as a substrate for methyl transfer [92]. There are at least five structurally distinct families of SAM, but class I is the largest and most diverse [92]. Some SAMs show the conserved binding site, but no methyltransferase activity [93]. Usually they methylate DNA, but also protein methylation can be performed and may result in a change of the protein function [94]. This could lead to weakening of the biofilm, but it is not clarified if GT1 has the methyltransferase activity, or the glycosyltransferase activity and it is not yet clarified which target could be attacked by GT1.

IV.5. Final conclusion

Concluding the findings of this work showed that the proteins Sbp, Aap and Embp have a distinct order inside the biofilm structure. Sbp could be shown to be an exclusive surface attachment protein, while Embp was evenly spread through the whole biofilm. The sub-domains A, B and B+212 of Aap showed to be involved in each step of biofilm formation. The surface attachment and slight cell-cell attachment was executed by domain A, while domain B+212 led to semi-structured accumulation in biofilms. And the final mushroom-like biofilm structure could be obtained by domain B. In summary Aap has to undergo proteolytic processing to gain its full function. PIA was the polysaccharide matrix compound that formed reliable biofilms with honey-comb structures. Embp and PIA simultaneously expressed led to remarkably strong biofilms and went into close co-localization. Antibiotic influence showed to be Embp stimulating and led to biofilms as intense as natural biofilms, even with protective mechanisms against phagocytosis.

In finding novel anti-biofilm compounds the highly active fosmid clone 100 E3 encodes for several enzymes capable of disrupting a mature *S. epidermidis* 1457 biofilm. The effectiveness of the fosmid clone extract could be proved and showed yet heat stability. New ways to disintegrate the matrix components PIA, or Sbp by enzymes could be achieved and holds the potential for the development of a novel agent in the combat against staphylococcal infections.

V. List of references

1. Rohde H, Mack D, Christner M, Burdelski C, Franke GC et al. (2006) Pathogenesis of staphylococcal device-related infections: from basic science to new diagnostic, therapeutic and prophylactic approaches. *Rev Med Microbiol* 17: 45-54.
2. Mack D, Rohde H, Harris LG, Davies AP, Horstkotte MA et al. (2006) Biofilm formation in medical device-related infection. *Int J Artif Organs* 29: 343-359.
3. Moretro T, Hermansen L, Holck AL, Sidhu MS, Rudi K et al. (2003) Biofilm formation and the presence of the intercellular adhesion locus *ica* among staphylococci from food and food processing environments. *Appl Environ Microbiol* 69: 5648-5655.
4. Rupp ME, Archer GL (1994) Coagulase-negative staphylococci: pathogens associated with medical progress. *Clin Infect Dis* 19: 231-243.
5. Mettler E, Carpentier B (1998) Variations over time of microbial load and physicochemical properties of floor materials after cleaning in food industry premises. *J Food Prot* 61: 57-65.
6. Götz F (2002) *Staphylococcus* and biofilms. *Mol Microbiol* 43: 1387-1378.
7. Ganeshnarayan K, Shah SM, Libera MR, Santostefano A, Kaplan JB (2008) Poly-N-Acetylglucosamine Matrix Polysaccharide Impedes Fluid Convection and Transport of the Cationic Surfactant Cetylpyridinium Chloride through Bacterial Biofilms. *Appl Environ Microbiol*
8. Götz F (2004) Staphylococci in colonization and disease: prospective targets for drugs and vaccines. *Curr Opin Microbiol* 7: 477-487.
9. Mack D, Siemssen N, Laufs R (1992) Parallel Induction by Glucose of adherence and a polysaccharide Antigen specific for plastic-adherent *Staphylococcus epidermidis*: Evidence for functional relation to intercellular adhesion. *Infection and Immunity*. Vol. 60, No. 5: 2048-2057.
10. Heilmann C, Schweitzer O, Gerke C, Vanittanakom N, Mack D et al. (1996) Molecular basis of intercellular adhesion in the biofilm-forming *Staphylococcus epidermidis*. *Mol Microbiol* 20: 1083-1091.
11. Rohde H, Kalitzky M, Kroger N, Scherpe S, Horstkotte MA et al. (2004) Detection of virulence-associated genes not useful for discriminating between invasive and commensal *Staphylococcus epidermidis* strains from a bone marrow transplant unit. *J Clin Microbiol* 42: 5614-5619.

12. Frebourg NB, Lefebvre S, Baert S, Lemeland JF (2000) PCR-Based assay for discrimination between invasive and contaminating *Staphylococcus epidermidis* strains. *J Clin Microbiol* 38: 877-880.
13. Wang X, Preston JF, III, Romeo T (2004) The *pgaABCD* locus of *Escherichia coli* promotes the synthesis of a polysaccharide adhesin required for biofilm formation. *J Bacteriol* 186: 2724-2734.
14. Kaplan JB, Velliyagounder K, Rangunath C, Rohde H, Mack D et al. (2004) Genes involved in the synthesis and degradation of matrix polysaccharide in *Actinobacillus actinomycetemcomitans* and *Actinobacillus pleuropneumoniae* biofilms. *J Bacteriol* 186: 8213-8220.
15. Foster TJ (2005) Immune evasion by staphylococci. *Nat Rev Microbiol* 3: 948-958.
16. Vuong C, Voyich JM, Fischer ER, Braughton KR, Whitney AR et al. (2004) Polysaccharide intercellular adhesin (PIA) protects *Staphylococcus epidermidis* against major components of the human innate immune system. *Cell Microbiol* 6: 269-275.
17. Knobloch JK, Von Osten H, Horstkotte MA, Rohde H, Mack D (2002) Minimal attachment killing (MAK): a versatile method for susceptibility testing of attached biofilm-positive and -negative *Staphylococcus epidermidis*. *Med Microbiol Immunol (Berl)* 191: 107-114.
18. Rice SA, McDougald D, Kumar N, Kjelleberg S (2005) The use of quorum-sensing blockers as therapeutic agents for the control of biofilm-associated infections. *Curr Opin Investig Drugs* 6: 178-184.
19. Ramasubbu N, Thomas LM, Rangunath C, Kaplan JB (2005) Structural analysis of dispersin B, a biofilm-releasing glycoside hydrolase from the periodontopathogen *Actinobacillus actinomycetemcomitans*. *J Mol Biol* 349: 475-486.
20. Richardson TH, Tan X, Frey G, Callen W, Cabell M et al. (2002) A novel, high performance enzyme for starch liquefaction. Discovery and optimization of a low pH, thermostable alpha-amylase. *J Biol Chem* 277: 26501-26507.
21. Rohde H, Burandt EC, Siemssen N, Frommelt L, Burdelski C et al. (2007) Polysaccharide intercellular adhesin or protein factors in biofilm accumulation of *Staphylococcus epidermidis* and *Staphylococcus aureus* isolated from prosthetic hip and knee joint infections. *Biomaterials* 28: 1711-1720.

22. Lambiase A, Rossano F, Del Pezzo M, Raia V, Sepe A, de Gregorio F, Catania MR. (2009) *Sphingobacterium* respiratory tract infection in patients with cystic fibrosis. *BMC Research Notes*. Vol. 2:262.
23. Dubey JP. (2003) Review of *Neospora caninum* and neosporosis in animals. The Korean journal of parasitology. Vol. 14, Nr. 1, 1-16.
24. Saw JH, Mountain BW, Feng L, Omelchenko MV, Hou S, Saito JA, Stott MB, Li D, Zhao G, Wu J, Galperin MY, Koonin EV, Makarova KS, Wolf YI, Rigden DJ, Dunfield PF, Wang L, Alam M. (2008) Encapsulated in silica: genome, proteome and physiology of the thermophilic bacterium *Anoxybacillus flavithermus* WK I. *Genome Biology*. Vol. 9, Issue 1, Article R 161.
25. Zhang Y, Li Y, Wang B, Wu Z, Zhang C, Gung X, Qiu Z, Zhang Y. (2005) Characteristics and living patterns of marine myxobacterial isolates. *Applied and environmental microbiology*. Vol. 71, No. 6, 3331-3336.
26. Jiyoung K, hoi JN, Kim P, Sok DE, Nam SW, Lee CH. (2009) LC-MS/MS profiling-based secondary metabolites screening of *Myxococcus xanthus*. *J. Microbiol. Biotechnol.* Vol. 19(1), 51-54.
27. Rohde H, Frankenberger S, Zähringer U, Mack D. (2010) Structure, function and contribution of polysaccharide intercellular adhesin (PIA) to *Staphylococcus epidermidis* biofilm formation and pathogenesis of biomaterial-associated infections. *European journal of Cell Biology*. Vol. 89, 103-111.
28. Conrady DG, Brescia CC, Horii K, Weiss AA, Hassett DJ, Herr AB. 2008. A Zinc-dependent adhesion module is responsible for intercellular adhesion in staphylococcal biofilms. *PNAS* (2008), vol. 108, no. 48: 19456-19461
29. Reiter KC, et al. 2013. Upregulation of *icaA*, *atlE* and *aap* genes by linezolid but not vancomycin in *Staphylococcus epidermidis* RP62A biofilms. *Int J of antimicrobial agents* (2013), <http://dx.doi.org/10.1016/j.ijantimicag.2013.12.003>
30. Macintosh RL, Brittan JL, Bhattacharya R, Jenkinson HF, derrick J, Upton M, Handley PS. 2009. The terminal A domain of fibrillar accumulation-associated protein (Aap) of *Staphylococcus epidermidis* mediates adhesion to human corneocytes. *J of bacteriology* (2009), vol. 191, no. 22:7007-7016

31. Patel JD, Colton E, Ebert M, Anderson JM. 2012. Gene expression during *S. epidermidis* biofilm formation on biomaterials, J Biomed Mater Res Part A 2012:100A:2863-2869
32. Liduma I, Tracevska T, bers U, Zilevica A. 2012. Phenotypic and genetic analysis of biofilm formation by *Staphylococcus epidermidis*. Medicina (Kaunas) (2012), 48(6).305-309
33. Juda M, Paprota K, Jaloza D, Malm A, Rybojad P, Gozdzik K. 2008. EDTA as a potential agent preventing formation of *Staphylococcus epidermidis* biofilm on polichloride vinyl biomaterials. Ann Agric Environ Med (2008), 15. 237-241
34. Cerca F, Franca A, Guimaraes R, Hinzmann M, Cerca N, Lobo da Cunha A, Azeredo J, Vilanova M. 2011. Modulation of poly-N-Acetylglucosamine accumulation within mature *Staphylococcus epidermidis* biofilms grown in excess glucose. Microbiol Immunol (2011), 55, 673-682
35. Christner M, Franke GC, Schommer NN, Wendt U, Wegert K, Pehle P, Kroll G, Schulze C, Buck F, Mack D, Aepfelbacher M. Rohde H. 2010. The giant extracellular matrix-binding protein of *Staphylococcus epidermidis* mediates biofilm accumulation and attachment to fibronectin. Molecular Microbiology (2010), 75 (1), 187-207
36. Christner M, Heinze C, Busch M, Franke GC, Hentschke M, Bayard Dühning S, Büttner H, Kotasinska M, Wischnewski V, Kroll G, Buck F, Molin S, Otto M, Rohde H. 2012. sarA negatively regulates *Staphylococcus epidermidis* biofilm formation by modulating expression of a 1 MDa extracellular matrix binding protein and autolysis-dependent release of eDNA. Molecular Microbiology (2012), 86(2), 394-410
37. Linnes JC, Ma H, Bryers JD. 2013. Giant extracellular matrix binding protein expression in *Staphylococcus epidermidis* is regulated by biofilm formation and osmotic pressure. Curr Microbiol (2013), 66:627-633
38. Manganelli R, van de Rijn I. 1999. Characterization of emb, a gene encoding the major adhesion of *Streptococcus defectives*. Infection and Immunity (1999), vol. 67, no.1:50-56

39. Clarke SR, Harris LG, Geoff Richards R, Foster SJ. 2002. Analysis of Ehb, a 1.1-Megadalton cell wall-associated fibronectin-binding protein of *Staphylococcus aureus*. *Infection and Immunity* (2002), vol. 70, no. 12:6680-6687
40. Juda M, Paprota K, Jaloza D, Malm A, Rybojad P, Goździuk. 2008. EDTA as a potential agent preventing formation of *Staphylococcus epidermidis* biofilm on polychloride vinyl biomaterials. *Ann Agric Environ Med* (2008), 15, 237-241
41. Hall-Stoodley L, Costerton J W, Stoodley P. 2004. Bacterial biofilms: from the natural environment to infectious diseases. *Nat. Rev. Microbiol* (2004), 2:95-108
42. Haenle M, Skripitz C, Mittelmeier W, Skripitz R. 2012. Economic impact of infected total knee arthroplasty. *Scientific world Journal* (2012), 2012:196515. doi:10.1100/2012/196515
43. Fey P D, Olson M E. 2010. Current concept sin biofilm formation of *Staphylococcus epidermidis*. *Future Microbiol* (2010) 5:197-33. doi:10.2217/fmb.10.56
44. McCann M T, Gilmore B F, Gorman S P. 2008. *Staphylococcus epidermidis* devide related infections: pathogenesis and clinical management. *J Pharm Pharmacol* (2008), 60:1551-71. doi:10.1211/jpp/60.12.0001
45. Scherr T D, Heim C E, Morrison J M, Kielian T. 2014. Hiding in plain sight: interplay between staphylococcal biofilms and host immunity. *Frontiers in Immunology* (2014), Vol. 5, Art. 37. doi:10.3389/fimmu.2014.00037
46. Mosser D M. 2003. The many faces of macrophage activation. *J Leukoc Biol* (2003), 73:209-12. doi:10.1189/jlb.0602325
47. Flemming H C, Wingender J. 2010. The biofilm matrix. *Nat. Rev. Microbiol* (2010), 8:623-633
48. Streit W R, Schmitz R A. 2004. Metagenomics-the key to the uncultured microbes. *Curr Opinion in microbiol* (2004), 7:492-498

49. Schmeisser C, Steele H, Streit W R. 2007. Metagenomics, biotechnology with non-culturable microbes. *Appl Microbiol Biotechnol* (2007), 75:955-962
50. Charlop-Powers Z, Milshteyn A, Brady S F. 2014. Metagenomic small molecule discovery methods. *Curr opinion in Microbiol* (2014), 19:70-75
51. Palmer I, Wingfield P T. 2004. Preparation and extraction of insoluble (Inclusion body) proteins from *Escherichia coli*. *Curr Protoc Protein Sci* (2004), CHAPTER: Unit-6.3. doi: 10.1002/0471140864.ps0603s38
52. Vuong C, Kocianova S, Voyich J M, Yao Y, Fischer E R, DeLeo F R, Otto M. 2004. A crucial role for exopolysaccharide modification in bacterial biofilm formation, immune evasion and virulence. *The journal of biological chemistry* (2004), Vol. 279 No 52, 54881-54886
53. Mullis S N, Falkinham III J O. 2013. Adherence and biofilm formation of *Mycobacterium avium*, *Mycobacterium intracellulare* and *Mycobacterium abscessus* to household plumbing materials. *Journal of appl microbiol* (2013), 115, 908-914
54. Rozej A, Cydzik-Kwiatkowska A, Kowalska B, Kowalski D. 2014. Structure and microbial diversity of biofilms on different pipe materials of a model drinking water distribution systems. *World J Microbiol Biotechnol* (2014). DOI 10.1007/s11274-014-1761-6
55. Xu F-F, Morohoshi T, Wang W-Z, Yamaguchi Y, Liang Y, Ikeda T. 2014. Evaluation of intraspecies interactions in biofilm formation by *Methylobacterium* species isolated from pink-pigmented household biofilms. *Microbes Environ* (2014). doi:10.1264/jsme2.ME14038
56. Taylor P, Yeung A T Y, Hancock R E W. 2014. Antibiotic resistance in *Pseudomonas aeruginosa* biofilms: Towards the development of novel anti-biofilm therapies (2014). *Journal of biotechnology*, doi: 10.1016/j.jbiotec.2014.09.003
57. Banat I M, Diaz de Rienzo M A, Quinn G A. 2014. Microbial biofilms: biosurfactants as antibiofilm agents. *Appl Microbiol biotechnol* (2014). doi: 10.1007/s00253-014-6169-6

58. Darouiche R O, Mansouri M D, Gawande P, Madhyastha S. 2009. Antimicrobial and antibiofilm efficacy of triclosan and DispersinB® combination. *Journal of antimicrobial chemotherapy* (2009), 64, 88-93
59. Bester E, Kroukamp O, Hausner M, Edwards E A, Wolfaardt G M. 2010. Biofilm form and function: carbon availability affects biofilm architecture, metabolic activity and planktonic cell yield. *Journal of appl microbiol* (2010), 110, 387-398
60. López D, Vlamakis H, Kolter R. 2010. Biofilms. *Cold Spring Harb Perspect Biol* (2010), 2010;2;a000398
61. Alandejani T, Marsan J, Ferris W, Slinger R, Chan F. 2009. Effectiveness of honees on *Staphylococcus aureus* and *Pseudomonas aeruginosa* biofilms. *Otolaryngology-Head and Neck surgery* (2009), 141, 114-118
62. Seper, A, Pressler K, Kariisa A, Haid A G, Roier S, Leitner D R, Reidl J, Tamayo R, Schild, S. 2014. Identification of genes induced in *Vibrio cholerae* in a dynamic biofilm system. *International Journal of Medical Microbiology* (2014), 304(5-6), 749–763. doi:10.1016/j.ijmm.2014.05.011
63. Reichhardt C, Fong J C N, Yildiz F, Cegelski L. 2014. Characterization of the *Vibrio cholerae* extracellular matrix: A top-down solid-state NMR approach (2014), doi: 10.1016/j.bbamem.2014.05.030
64. <http://www.drugbank.ca/drugs/DB00560>; 05.12.2014
65. <http://www.drugbank.ca/drugs/DB00199>; 05.12.2014
66. Arciola C R. 2010. Host defense against implant infection: the ambivalent role of phagocytosis. *Int J Artif Organs* (2010), 33(9):565-7
67. Guenther F, Stroh P, Wagner C, Obst U, Hänsch G M. 2009. Phagocytosis of staphylococci biofilms by polymorphonuclear neutrophils: *S. aureus* and *S. epidermidis* differ with regard to their susceptibility towards host defense. *Int L Artif Organs* (2009), 32(9):565-73

68. <http://www.drugbank.ca/drugs/db00601>; 07.12.2014
69. Rickard A H, Gilbert P, High N J, Kolenbrander P J, Handley P S. 2003. Bacterial coaggregation: an integral process of multi-species biofilms. *Trends in microbiology* (2003), 11:94-100
70. Schaudinn C, Stoodley P, Hall-Stoodley L, Gorur A, Remis J, et al. 2014. Death and transfiguration in static *Staphylococcus epidermidis* cultures. *PLoS ONE* (2014), 9(6):e100002. doi:10.1371/journal.pone.0100002
71. Chew S C, Kundukad B, Seviour T, van der Maarel J R C, Yang L, Rice S A, Doyle P, Kjelleberg S. 2014. Dynamic remodelling of microbial biofilms by functionally distinct exopolysaccharides. *mBio* (2014), 5(4):e01536-14. doi:10.1128/mBio.01536-14
72. Liu Q, Sommer S S. 1998. Subcycling-PCR for multiplex long-distance amplification of regions with high and low GC content: Application to the inversion hotspot in the factor VIII gene. *BioTechniques* (1998), 25:1022-1028
73. Sarkar G, Kapelner S, Sommer S S. 1990. Formamide can dramatically improve the specificity of PCR. *Nucleic Acids Research* (1990), Vol. 18, No 24, 7465
74. Levin R E, Van Sickle C. 1976. Autolysis of high-GC isolates of *Pseudomonas putrefaciens*. *Antonie Van Leeuwenhoek* (1976) **42** (1–2): 145–55. doi:10.1007/BF00399459. PMID 7999.
75. Yakovchuk P, Protozanova E, Frank-Kamenetskii M D. 2006. Base-stacking and base-pairing contributions into thermal stability of the DNA double helix. *Nucleic Acids Res*(2006). **34** (2): 564–74. doi:10.1093/nar/gkj454. PMC 1380284. PMID 16449200.
76. Kloep F, Manz W, Röske I. 2006. Multivariate analysis of microbial communities in the River Elbe (Germany) on different phylogenetic and spatial levels of resolution. *FEMS Microbiology Ecology* (2006), doi:10.1111/j.1574-6941.2006.00049.x
77. Kittelmann S, Friedrich M W. 2008. Identification of novel perchloroethene-respiring microorganisms in anoxic river sediment by RNA-based stable isotope probing. *Environmental microbiology* (2008), 10(1), 31-46

78. Chun J, Bae K S, Moon E Y, Jung S O, Lee H K, Kim S J. 2000. *Nocardiosis kunanensis* sp. nov., a moderately halophilic actinomycete isolated from a saltern. *Int J of systematic and evolutionary microbiology* (2000), 50 Pt 5: 1909-13
79. J. Dunbar, S. M. Barns, L. O. Ticknor, and C. R. Kuske. 2002. Empirical and theoretical bacterial diversity in four Arizona soils. *Appl. Environ. Microbiol.* (2002), 68:3035–3045
80. Farag I F, Davis J P, Youssef N H, Elshahed M S. 2014 Global Patterns of Abundance, Diversity and Community Structure of the *Aminicenantes* (Candidate Phylum OP8). *PLoS ONE* (2014), 9(3): e92139. doi:10.1371/journal.pone.0092139
81. Stevenson G, Andrianopoulos K, Hobbs M, Reeves P R. 1996. Organization of the *Escherichia coli* K-12 gene cluster responsible for production of the extracellular polysaccharide colanic acid. *Journal of Bacteriology* (1996);178(16):4885-4893
82. Burroughs A M, Balaji S, Iyer L M, Aravind L. 2007. A novel superfamily containing the β -grasp fold involved in binding diverse soluble ligands. *Biology Direct* (2007);2:4. doi:10.1186/1745-6150-2-4
83. Buetow L, Smith T K, Dawson A, Fyffe S, Hunter W N. 2007. Structure and reactivity of LpxD, the *N*-acyltransferase of lipid A biosynthesis. *Proceedings of the National Academy of Sciences of the United States of America* (2007);104(11):4321-4326. doi:10.1073/pnas.0606356104
84. Ulaganathan V, Buetow L, Hunter W N. 2007. Nucleotide substrate recognition by UDP-N-acetylglucosamine acyltransferase (LpxA) in the first step of lipid A biosynthesis. *J Mol Biol* (2007), 1;369(2):305-12
85. Vuorio, Piitta et al. 1994. The novel hexapeptide motif found in the acyltransferases LpxA and LpxD of lipid A biosynthesis is conserved in various bacteria. *FEBS letters* (1994), 337:3, 289-292
86. Coutinho P M, Deleury E, Davies G J, Henrissat B. 2003. An evolving hierarchical family classification for glycosyltransferases. *J Mol Biol* (2003), 328(2):307-17
87. Kikuchi N, Narimatsu H. 2006. Bioinformatics for comprehensive finding and analysis of glycosyltransferases. *Biochim Biophys Acta* (2006), 1760(4):578-83
88. Breton C, Snajdrová L, Jeanneau C, Koca J, Imberty A. 2006. Structures and mechanisms of glycosyltransferases (2006), 16(2):29R-37R
89. <http://www.cazy.org/GT1.html>; 12.12.2014

90. Lairson L L, Henrissat B, Davies G J, Withers S G. 2008. Glycosyltransferases: structures, functions, and mechanisms. *Annu Rev Biochem* (2008), 77:521-555[PMID: 18518825]
91. Kapitonov D, Yu R K. 1999. Conserved domains of glycosyltransferases. *Glycobiology* (1999), vol. 9 no. 10, 961-978
92. Schubert H L, Blumenthal R M, Cheng X. 2003. Many paths to methyltransfer: a chronicle of convergence. *Trends in biochemical sciences* (2003); 28(6):329-335. doi:10.1016/S0968-0004(03)00090-2.
93. Martin J L, McMillan F M. 2002. SAM (dependent) I AM: the S-adenosylmethionine-dependent methyltransferase fold. *Curr Opin Struct Biol* (2002), 12(6):783-93
94. Hanz G M, Jung B, Giesbertz A, Juhasz M, Weinhold E. 2014. Sequence-specific labeling of nucleic acids and proteins with methyltransferases and cofactor analogues. *J Vis Exp* (2014), (93) doi:10.3791/52014
95. Schaeffer C R, Woods K M, Longo G M, Kiedrowski M R, Paharik A E, Büttner H, Christner M, Boissy R J, Horswill A, Rohde H, Fey P D. 2014. Accumulation-associated protein (Aap) enhances *Staphylococcus epidermidis* biofilm formation under dynamic conditions and is required for infection in a rat catheter model. *Infect Immun* (2014), doi:10.1128/IAI.02177-14
96. Becker K, Heilmann C, Peters G. 2014. Coagulase-negative Staphylococci. *Clinical microbiology reviews* (2014), Vol. 27, no. 4, 870-926
97. Langklotz S, Bandow J E. 2014. Antibakterielle Strategien und bakterielle Abwehrmechanismen. *Biospektrum* (2014), doi:10.1007/s12268-014-0512-4
98. Malone C L, Boles B R, Lauderdale K J, Thoendel M, Kavanaugh J S, Horswill A R. 2009. Fluorescent reporters for *Staphylococcus aureus*. *J Microbiol Methods* (2009), 77(3):251-60
99. Vuong C, Gerke C, Somerville G A, Fischer E R, Otto M. 2003. Quorum-Sensing Control of biofilm factors in *Staphylococcus epidermidis*. *JID* (2003), 188:706-18
100. Schommer N, Christner M, Hentschke M, Ruckdeschel K, Aepfelbacher M, Rohde H. 2011. *Staphylococcus epidermidis* uses distinct mechanisms of biofilm formation to interfere with phagocytosis and activation of mouse macrophage-like cells 774A.1. *Infect Immun* (2011), Vol.79, No. 6, 2267-2276
101. Vuong C, Kocianova S, Yao Y, Carmody A B, Otto M. 2004. Increased colonization on indwelling medical devices by Quorum-sensing mutants of *Staphylococcus epidermidis* in vivo. *JID* (2004), 190, 1498-1505

102. Kaplan J B, Rangunath C, Velliyagounder K, Fine D H, Ramasubbu N. 2004. Enzymatic detachment of *Staphylococcus epidermidis* biofilms. Antimicrobial agent and chemotherapy (2004). Vol. 48, No. 7, 2633-2636
103. Büttner H, Mack D, Rohde H. 2015. Structural basis of *Staphylococcus epidermidis* biofilm formation: mechanisms and molecular interactions. *frontiers in cellular and infection microbiology* (2015); publishing in progress
104. Lewis K. 2005. Persister cells and the riddle of biofilm survival. *Biochemistry (Mosk)* (2005),70:267-274
105. Keren I, Kaldalu N, Spoering A, Wang Y, Lewis K. 2004. Persister cells and tolerance to antimicrobials. *FEMS Microbiol Lett* (2004), 230:13-18
106. Herrmann M. 2003. Salicylic acid: an old dog, new tricks and staphylococcal disease. *J Clin Invest* (2003), 112:149-151
107. Fitzpatrick F, Humphrey's H, O'Gara J P. 2005. The genetics of staphylococcal biofilm formation – will a greater understanding of pathogenesis lead to better management of device-related infection?. *Clin Microbiol Infect* (2005), 11:967-973
108. Gao F, Zhang C-T. 2006. GC-Profile: a web-based tool for visualizing and analyzing the variation of GC content in genomic sequences. *Nucleic Acids research* (2006), Vol. 34 web server issue, doi:10.1093/nar/gkl1040
109. Rohde H, Burdelski C, Bartscht K, Hussain M, Buck F, Horstkotte M A, Knobloch J K, Heilmann C, Herrmann M, Mack D. 2005. Induction of *Staphylococcus epidermidis* biofilm formation via proteolytic processing of the accumulation-associated protein by staphylococcal and host proteases. *Mol Microbiol* (2005), 55(6):1883-95
110. Mack D, Haeder M, Siemssen N, Laufs R. 1996. Association of biofilm production of coagulase-negative staphylococci with expression of a specific polysaccharide intercellular adhesin. *J Infect Dis* (1996), 174(4):881-4
111. Hussain M, Herrmann M, von Eiff C, Perdreau-Remington F, Peters G. 1997. A 140-kilodalton extracellular protein is essential for the accumulation of *Staphylococcus epidermidis* strains on surfaces. *Infect Immun* (1997), 65(2):519-24
112. Bateman A, Holden M T, Yeats C. 2005. The G5 domain: a potential N-acetylglucosamine recognition domain involved in biofilm formation. *Bioinformatics* (2005), 21(8):1301-3

113. Williams R J, Henderson B, Sharp L J, Nair S P. 2002. Identification of a fibronecton-binding protein from *Staphylococcus epidermidis*. *Infect Immun* (2002), 70(12):6805-10

VI. Appendix

VI.1. Used Sizemarker

VI.1.1.λ DNA *Hind* III/*ΦX-Hae* III

The size standard λ DNA *Hind* III/*ΦX-Hae* III (Finnzymes, Pittsburgh, USA) used for agarose gel electrophoresis.


	Fragment	Base pairs	DNA amount ng/10 µl
	1	23 130	238
	2	9 416	97
	3	6 557	68
	4	4 361	45
	5	2 322	24
	6	2 027	21
	7	1 353	126
	8	1 078	100
	9	872	81
	10	603	56
	11	*564	6
	12	310	29
	13a	281	26
	13b	271	25
	14	234	22
	15	194	18
	16a	125	1
	16b	118	11
	17	72	7

Figure VI-1: DNA Ladder λ DNA *Hind* III/*ΦX-Hae* III (Finnzymes, Pittsburgh, USA), each fragment shows 1 band in the gel.

VI.1.2.SDS gel protein marker

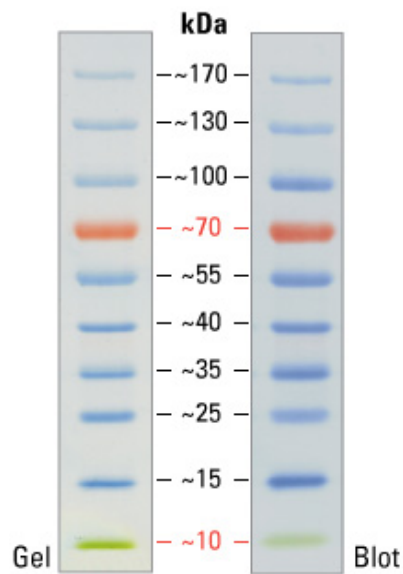


Figure VI-2: Images are from a 4-20% Tris-glycine gel (SDS-PAGE) and subsequent transfer to membrane. <http://www.thermoscientificbio.com/protein-electrophoresis/pageruler-prestained-protein-ladder/> (Thermo Scientific, Waltham, USA).

VI.2. Vector maps

VI.2.1.Plasmid vector pBluescript II SK +

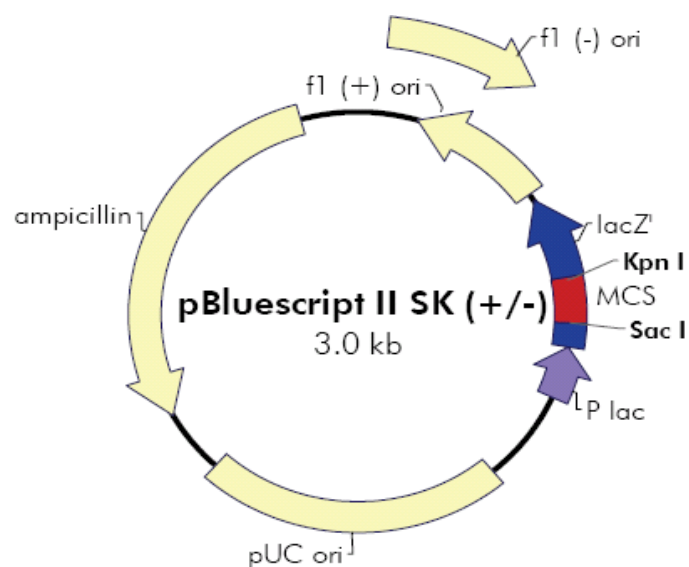


Figure VI-3: The vectorcard of plasmid vector pBluescript II SK + (Manual of pBluescript II SK + from Agilent Technologies, La Jolla, USA)

VI.2.2.Fosmid vector pCC1FOS

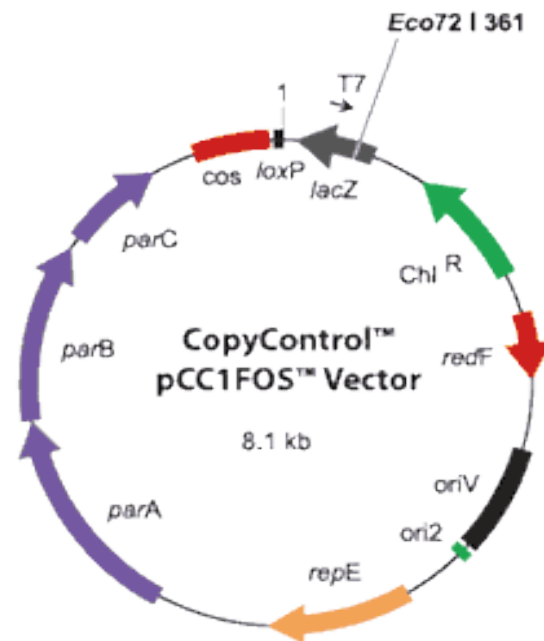


Figure VI-4: The vectorcard of fosmid vector pCC1FOS (http://www.epibio.com/images/catalog/i_CopyControl_VectorMap.gif; Access: 07.06.2009)

VI.2.3.Plasmid vector pUC19

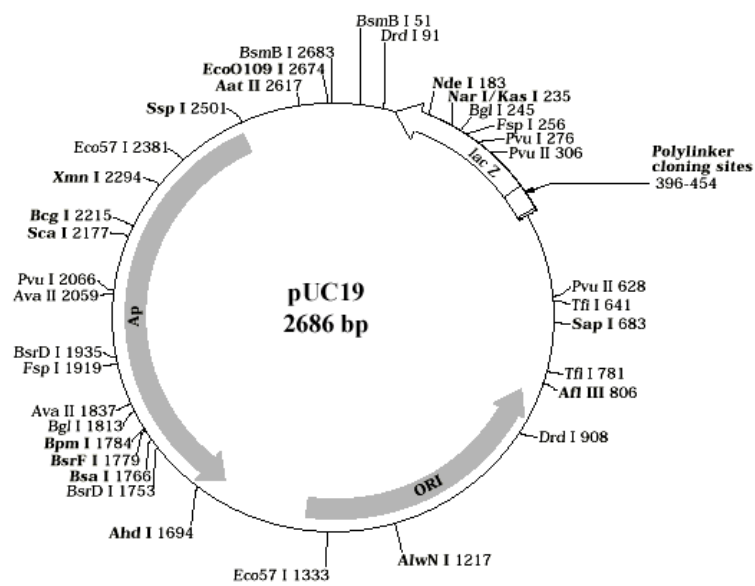


Figure VI-5: The vectorcard of plasmid vector pUC19 (http://www1.qiagen.com/literature/vectors_pcr.aspx; Access: 23.06.2011)

VI.2.4.Plasmid vector pET21 a

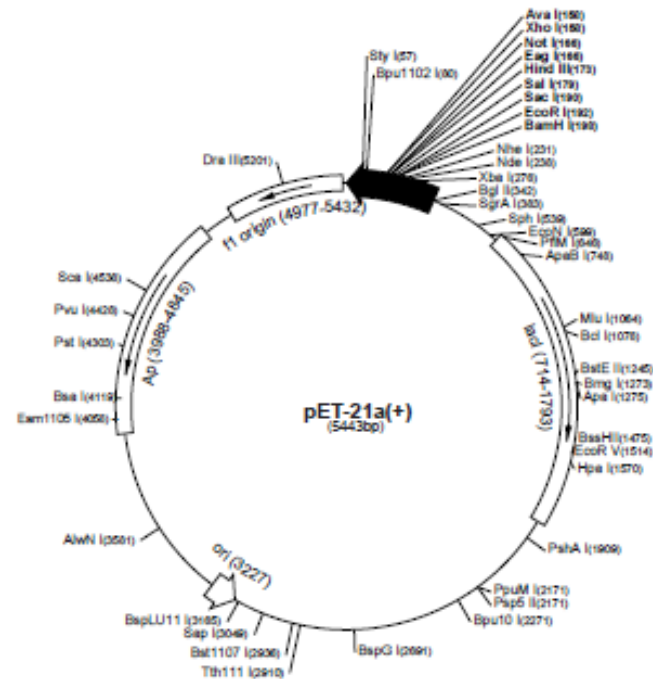


Figure VI-6: Expression vector pET21a, C-terminal HIS taq (Novagen, Merck Millipore, Darmstadt, Germany).

VI.2.5.Plasmid vector pET19b

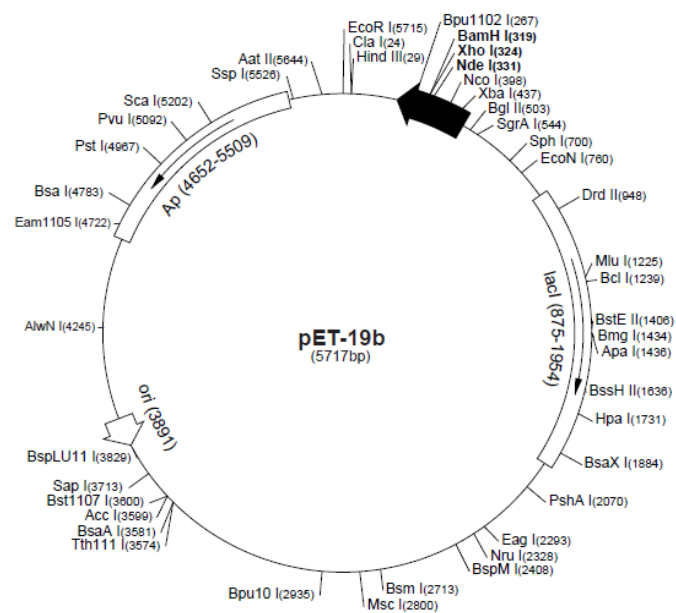


Figure VI-7: Expression vector pET19b, N-terminal HIS Taq (Novagen, Merck Millipore, Darmstadt, Germany).

VI.2.6.Entry vector, plasmid pENTR/D-TOPO

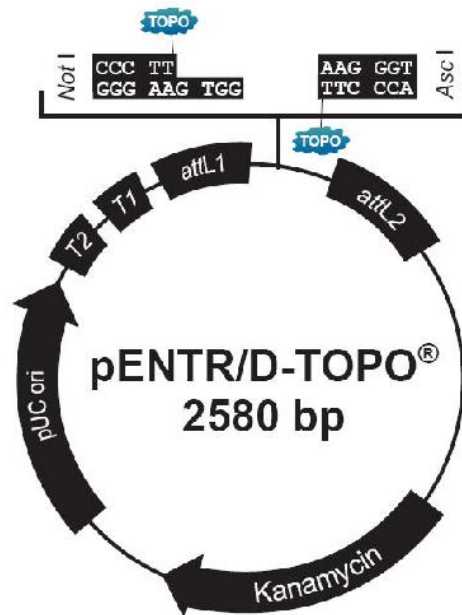


Figure VI-8: Plasmid vector pENTR/D-TOPO, entry vector for pDEST15 and pDEST17 (Invitrogen Life technologies, Carlsbad, USA).

VI.2.7.Expression vector pDEST15

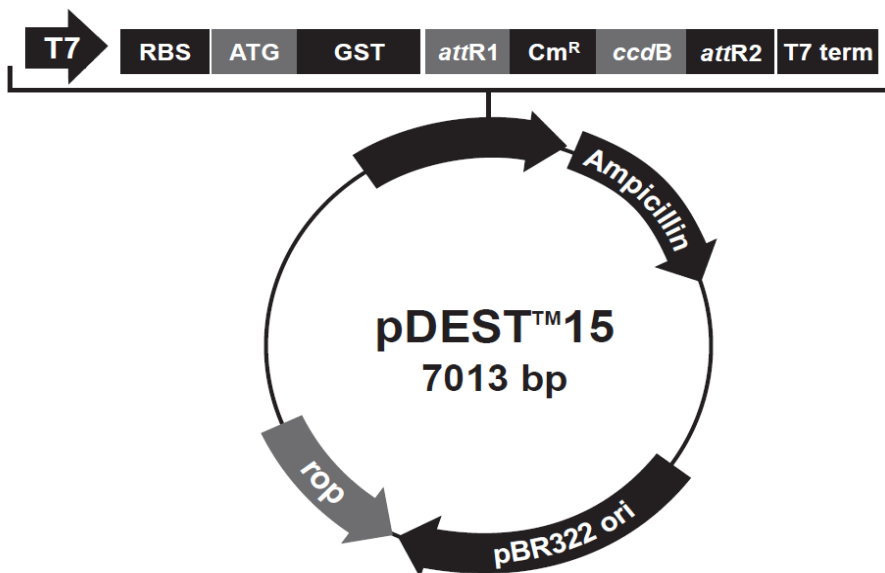


Figure VI-9: Expression vector pDEST15, N-terminal GST Taq (Invitrogen Life technologies, Carlsbad, USA).

VI.2.8.Expression vector pDEST17

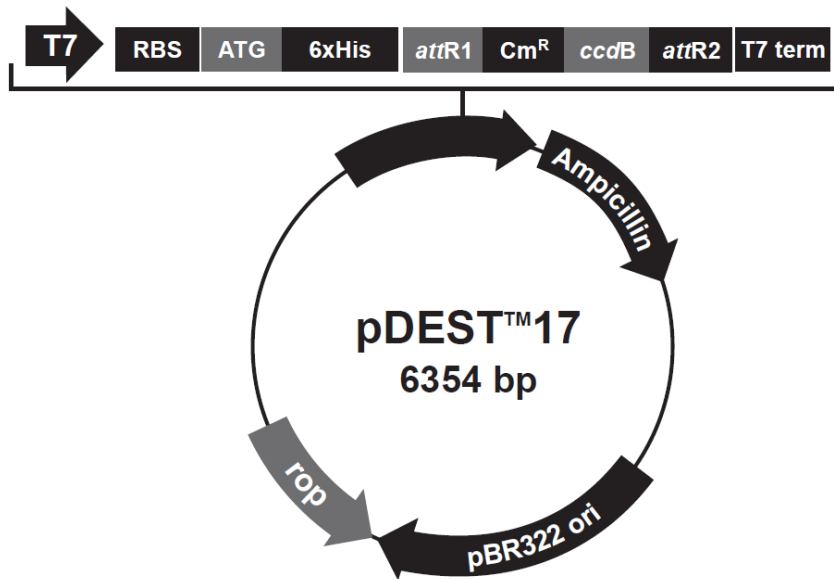


Figure VI-10: Expression vector pDEST17, N-terminal HIS Taq (Invitrogen Life technologies, Carlsbad, USA).

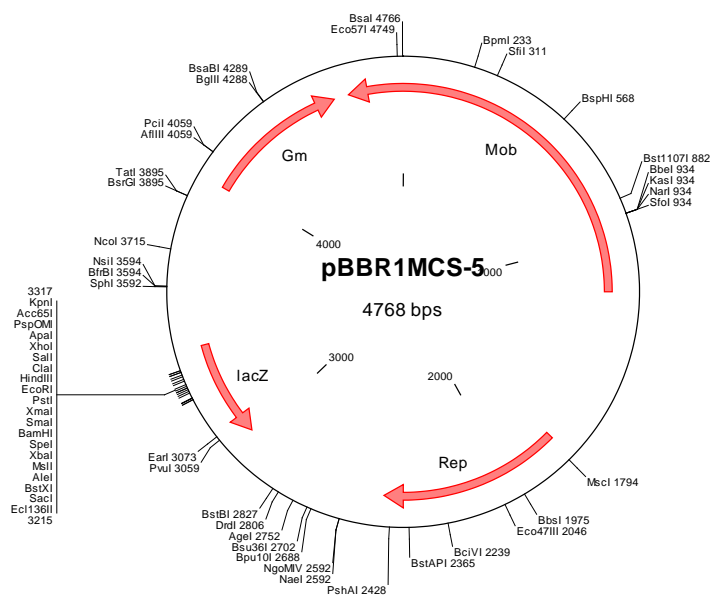
VI.2.9.Plasmid vector pBBR-MCS5 for *Pseudomonas antarctica*

Figure VI-11: Plasmid vector pBBR-MCS5 for *Pseudomonas antarctica*.

VI.2.10. Expression vector pFLD1 for *Pichia pastoris*

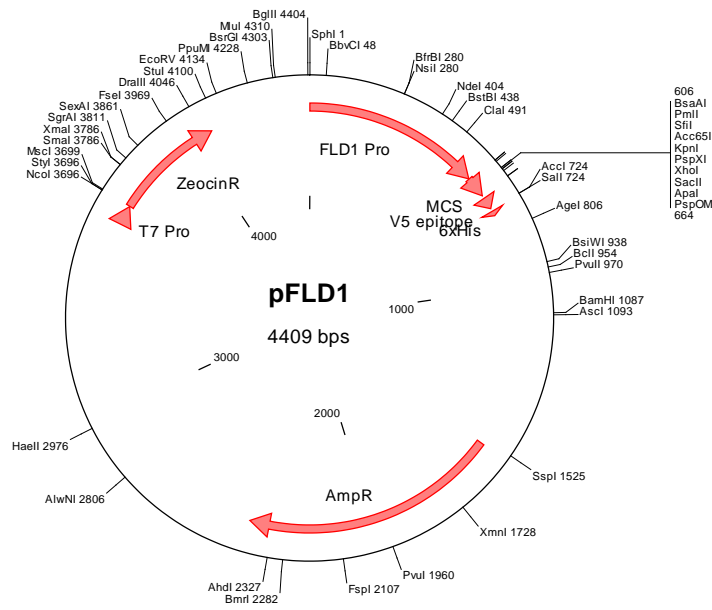


Figure VI-12: Expression vector pFLD1 for yeast expression in *Pichia pastoris* (Invitrogen Life technologies, Carlsbad, USA).

VI.2.11. Expression vector pMALc2x

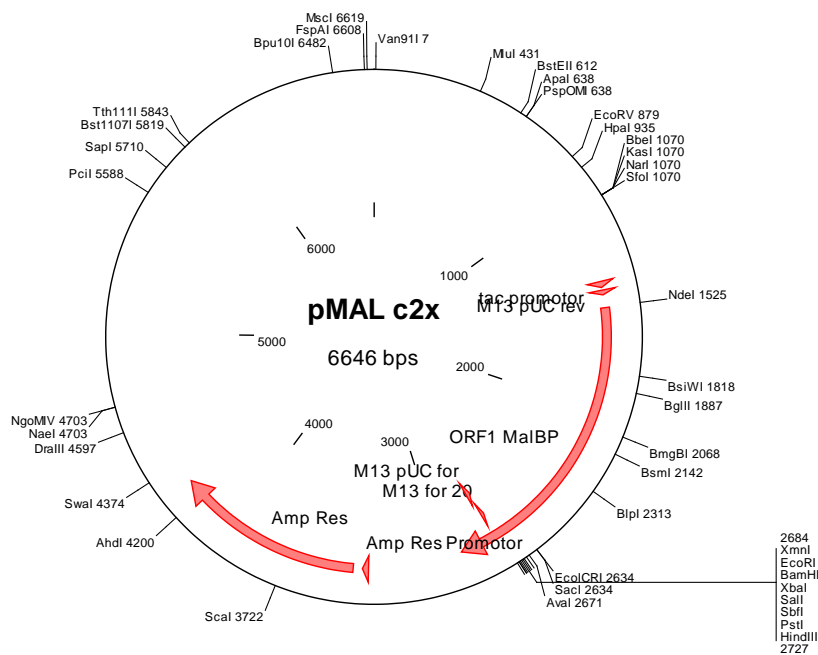


Figure VI-13: Expression vector pMALc2x, N-terminal Maltose binding protein (New England Biolabs, Frankfurt am Main, Germany).

VI.2.12. Plasmid vector pTZ19R

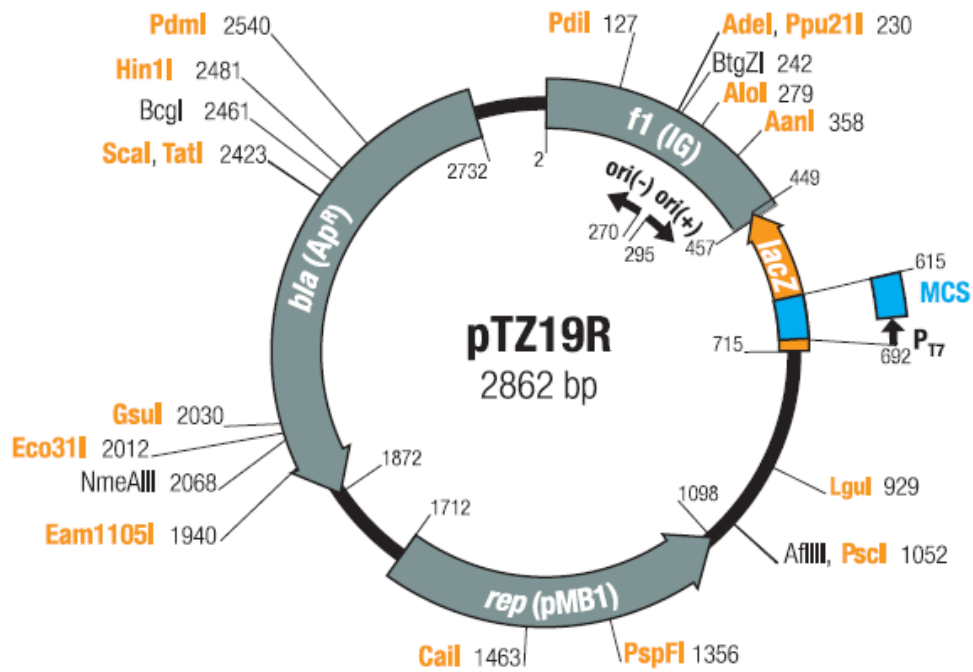


Figure VI-14: Phagemid vector pTZ19r (Thermos Scientific, Waltham, USA).

VI.2.13. Plasmid vector pDrive

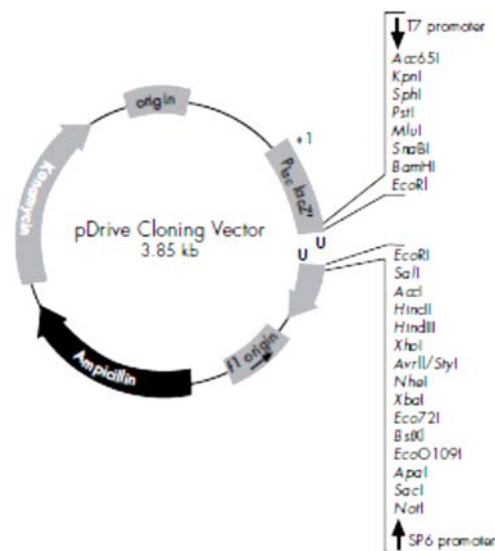


Figure VI-15: pDrive Cloning vector for PCR products (Qiagen, Hilden, Germany).

VI.2.14. Expression vector pBAD/Myc-His

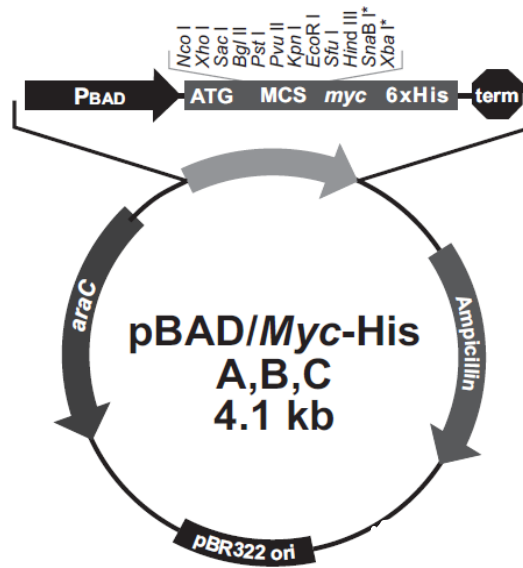


Figure VI-16: Expression vector pBAD/Myc-His, C-terminal His Taq (Invitrogen Life technologies, Carlsbad, USA).

VI.2.15. Plasmid vector pCN57

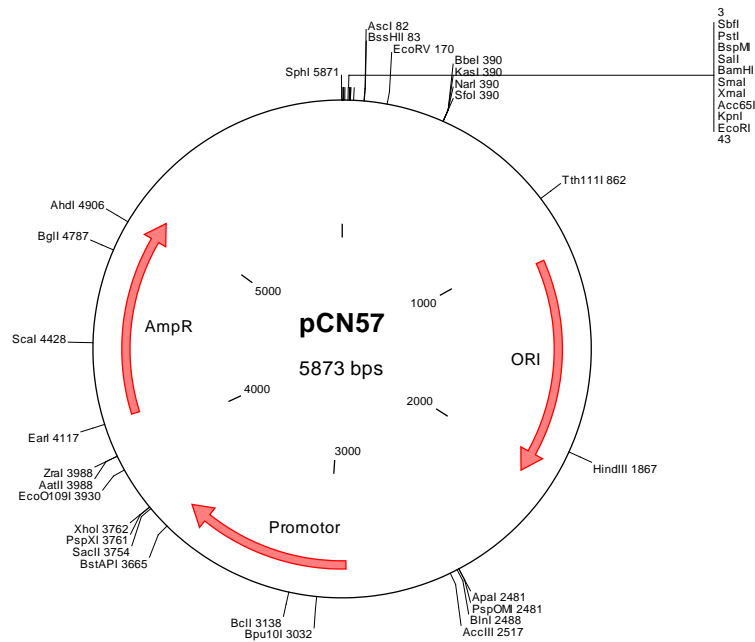


Figure VI-17: Tetracycline inducible vector pCN57 (modified at AG Rohde, UKE, Hamburg, Germany).

VI.3. GC Plots of fosmid clones 100 B3 & 64 F4 and putative biofilm disrupting ORFs of fosmid clone 100 E3

VI.3.1.GC Plot of fosmid clone 100 B3

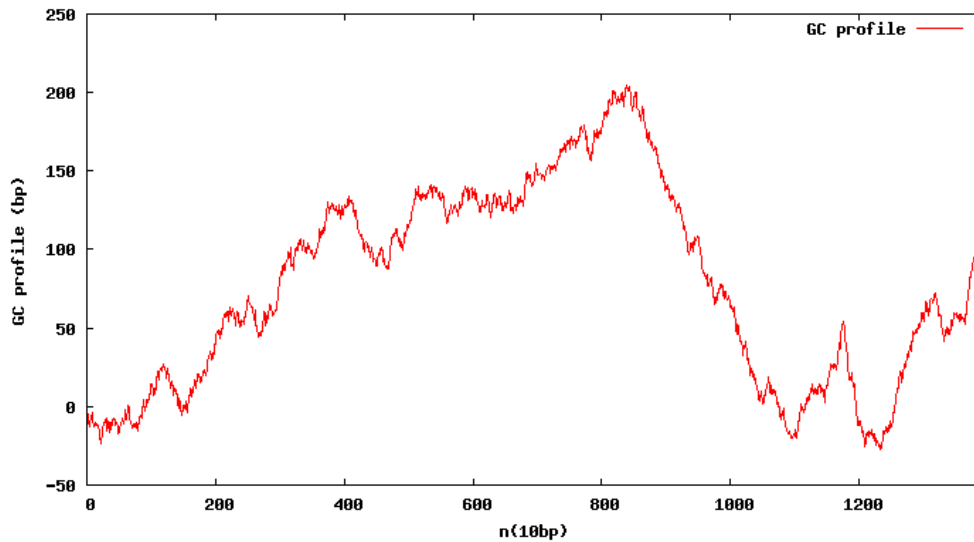


Figure VI-18: The GC content of fosmid clone 100 B3 shows the highest GC amount around base 8500 and has a total GC content of 59,15 %.

VI.3.2.GC Plot of fosmid clone 64 F4

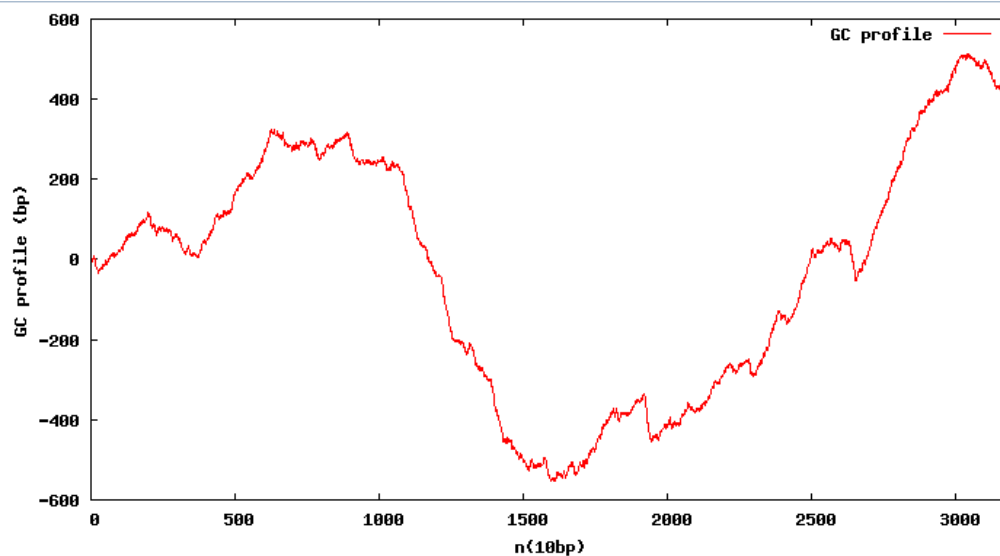


Figure VI-19: The GC content of fosmid clone 64 F4 shows the highest GC amount around base 30.000 and has a total GC content of 53,09 %.

VI.3.3.GC Plot of Glycosyltransferase 1 of fosmid clone 100 E3

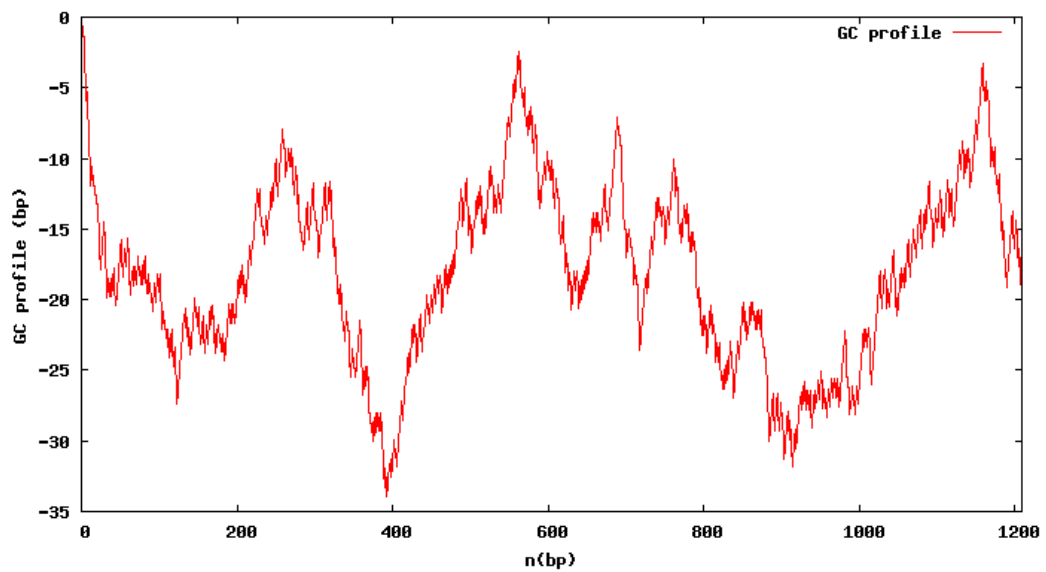


Figure VI-20: GC content of glycosyltransferase 1 of fosmid clone 100 E3 showing the highest peaks around base 10, 580 and 1150. The total amount of GC is 65,59 %.

VI.3.4.GC Plot of Glycosyltransferase 2 of fosmid clone 100 E3

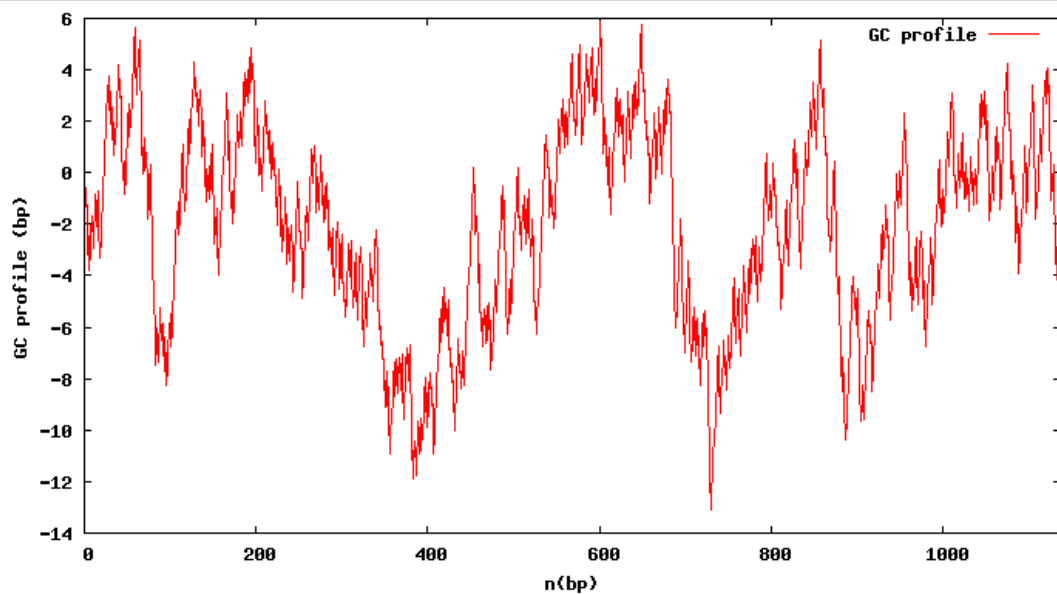


Figure VI-21: GC content of glycosyltransferase 2 of fosmid clone 100 E3 showing the highest peaks around base 50, 200, 600 and 850. The total amount of GC is 64,47 %.

VI.3.5.GC Plot of UDP-3-O-[3-hydroxymyristol]-N-acyltransferase of fosmid clone 100 E3

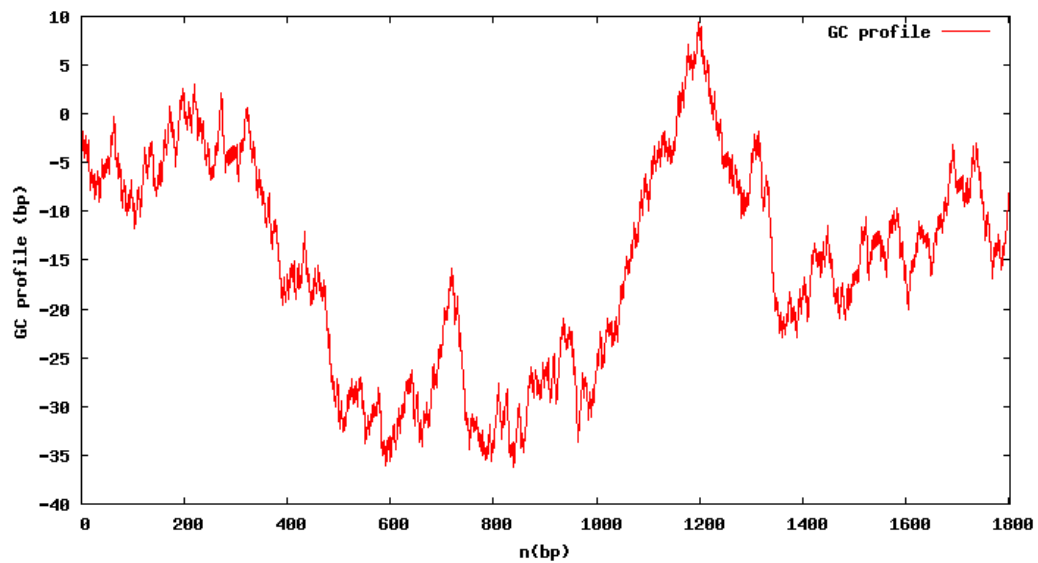


Figure VI-22: GC content of UDP-3-O-[3-hydroxymyristol]-N-acyltransferase of fosmid clone 100 E3 showing the highest peak around base 1200. The total amount of GC is 64,00 %.

VI.3.6.GC Plot of Polysaccharide export protein of fosmid clone 100 E3

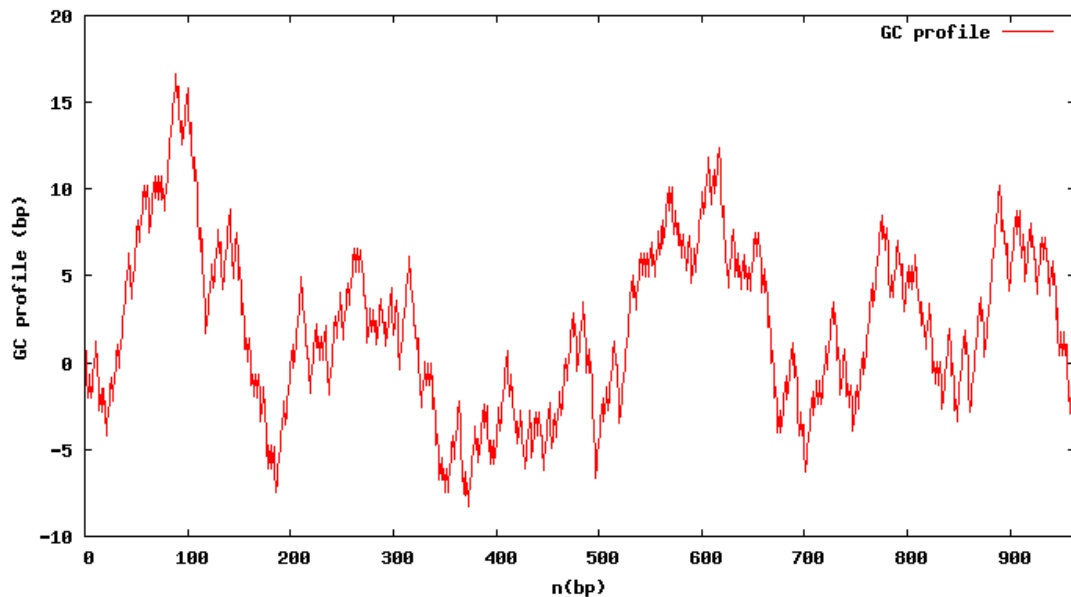


Figure VI-23: GC content of Polysaccharide export protein of fosmid clone 100 E3 showing the highest peaks around base 100 and 600. The total amount of GC is 66,87 %.

VI.4. Alignment file of putative biofilm disrupting enzymes and the closest relatives

Methylase [Nocardioopsis sp. CNT212]		
Methylase [Nocardioopsis walliformis]		
Glycoyltransferase family 1 [Neorhizobium galagae bv. officinalis str. DAMSI 1141]		
Glycoyltransferase family 1 [Neorhizobium galagae bv. orientalis str. DAMSI 543]		
Glycoyltransferase [Rhizobium sp. CF086]		
Group 1 glycoyl transferase [Methyloccella silvestris]		
Glycoyltransferase 2		
Glycoyltransferase family 1 [uncultured Chloroflexi bacterium]		
Glycoyltransferase [Moorosia producona]		
Glycoyltransferase 3		
glycoyl transferase family 1 [Lysinibacillus sp. PCC 8104]		
Glycoyltransferase [Leptolyngbya sp. PCC 7175]		
Polysaccharide export transporter		
hypothetical protein [Ryobacter aggregatus]		
Hypothetical protein [Acidobacteriaceae bacterium K85 83]		
N-Acyltransferase	MLTPEPTLALKEKDFRAGAYKELRQLTAAHLPAKALCPQIFPGLIHLITLPTAFYKRRERRNAVRRNAQDRCLELAKGHEVKAIFDCHLQLVLDLVYDGLAAKDRVYAKLAVYDGLRDCGLVYAVVAFDCRDRFKAASRRVYL	150
UDP-3-O-galucosamine N-acyltransferase [Candidatus Solibacter usitatus]		
UDP-3-O-galucosamine N-acyltransferase [Acidobacteriaceae bacterium K85 96]		
Hypothetical protein [Acidobacteriaceae bacterium K85 96]		
Acyl-ACP-UDP-N-acylglucosamine-O-acyltransferase [Candidatus Solibacter usitatus]		
Glycoyltransferase 3		
Hypothetical protein [unclassified Aminicantales]		
Methyltransferase [Chloroflexus]		
Glycoyl transferase family 1 [Bradyrhizobium sp. STM 3843]		
	i.....10.....20.....30.....40.....50.....60.....70.....80.....90.....100.....110.....120.....130.....140.....150	
<hr/>		
Methylase [Nocardioopsis sp. CNT212]		KRERERERLFPKRRDQDWTGVV 25
Methylase [Nocardioopsis walliformis]		KATRERERLFPKRRDQDWTGVV 25
Glycoyltransferase family 1 [Neorhizobium galagae bv. officinalis str. DAMSI 1141]		RSFAAFC 51
Glycoyltransferase family 1 [Neorhizobium galagae bv. orientalis str. DAMSI 543]		RSFAAFC 51
Glycoyltransferase [Rhizobium sp. CF086]		RSFAAFC 51
Group 1 glycoyl transferase [Methyloccella silvestris]		RSFAAFC 51
Glycoyltransferase 2		RSFAAFC 51
Glycoyltransferase family 1 [uncultured Chloroflexi bacterium]		RSFAAFC 51
Glycoyltransferase [Moorosia producona]		RSFAAFC 51
Glycoyltransferase 3		RSFAAFC 51
glycoyl transferase family 1 [Lysinibacillus sp. PCC 8104]		RSFAAFC 51
Glycoyltransferase [Leptolyngbya sp. PCC 7175]		RSFAAFC 51
Polysaccharide export transporter		RSFAAFC 51
hypothetical protein [Ryobacter aggregatus]		RSFAAFC 51
Hypothetical protein [Acidobacteriaceae bacterium K85 83]		RSFAAFC 51
N-Acyltransferase		RSFAAFC 51
UDP-3-O-galucosamine N-acyltransferase [Candidatus Solibacter usitatus]		RSFAAFC 51
UDP-3-O-galucosamine N-acyltransferase [Acidobacteriaceae bacterium K85 96]		RSFAAFC 51
Hypothetical protein [Acidobacteriaceae bacterium K85 96]		RSFAAFC 51
Acyl-ACP-UDP-N-acylglucosamine-O-acyltransferase [Candidatus Solibacter usitatus]		RSFAAFC 51
Glycoyltransferase 1		RSFAAFC 51
Hypothetical protein [unclassified Aminicantales]		RSFAAFC 51
Methyltransferase [Chloroflexus]		RSFAAFC 51
Glycoyl transferase family 1 [Bradyrhizobium sp. STM 3843]		RSFAAFC 51
150.....170.....180.....190.....200.....210.....220.....230.....240.....250.....260.....270.....280.....290.....300	

Methylase [Nocardopsis sp. CNT212] 127
Methylase [Nocardopsis vallsiformis] 127
Glycoyltransferase family 1 [Nocardobium galegae bv. officinalis str. EANG1 1141] 132
Glycoyltransferase family 1 [Nocardobium galegae bv. orientalis str. EANG1 540] 132
Glycoyltransferase [Rhizobium sp. CF088] 133
Group 1 glycoyl transferase [Methylocella silvestris] 133
Glycoyltransferase 2 133
Glycoyltransferase family 1 (uncultured Chloroflexi bacterium) 133
glycoyltransferase [Moorosia producens] 133
Glycoyltransferase 3 133
glycoyl transferase family 1 (Lynchya sp. POC 8166) 133
Glycoyltransferase [Leptolyngbya sp. POC 7175] 133
Polysaccharide export transporter 133
hypothetical protein [Bryobacter aggregatus] 133
Hypothetical protein [Acidobacteriaceae bacterium K85 83] 133
N-Acyltransferase 133
UDP-3-O-(glucosamine N-acyltransferase (Candidatus Solibacter usitatus) 133
UDP-2-O-glucosamine N-acyltransferase [Acidobacteriaceae bacterium K85 96] 133
Hypothetical protein [Acidobacteriaceae bacterium K85 96] 133
Acyl-ACP-UDP-N-acetylglucosamine-O-acyltransferase (Candidatus Solibacter usitatus) 133
Glycoyltransferase 1 133
Hypothetical protein [unclassified Aminicoanates] 133
Methyltransferase [Chloroflexus] 133
Glycoyl transferase family 1 [Bradyrhizobium sp. STM 2843] 133



Methylase [Nocardopsis sp. CNT212] 234
Methylase [Nocardopsis vallsiformis] 234
Glycoyltransferase family 1 [Nocardobium galegae bv. officinalis str. EANG1 1141] 234
Glycoyltransferase family 1 [Nocardobium galegae bv. orientalis str. EANG1 540] 234
Glycoyltransferase [Rhizobium sp. CF088] 234
Group 1 glycoyl transferase [Methylocella silvestris] 234
Glycoyltransferase 2 234
Glycoyltransferase family 1 (uncultured Chloroflexi bacterium) 234
glycoyltransferase [Moorosia producens] 234
Glycoyltransferase 3 234
glycoyl transferase family 1 (Lynchya sp. POC 8166) 234
Glycoyltransferase [Leptolyngbya sp. POC 7175] 234
Polysaccharide export transporter 234
hypothetical protein [Bryobacter aggregatus] 234
Hypothetical protein [Acidobacteriaceae bacterium K85 83] 234
N-Acyltransferase 234
UDP-3-O-(glucosamine N-acyltransferase (Candidatus Solibacter usitatus) 234
UDP-2-O-glucosamine N-acyltransferase [Acidobacteriaceae bacterium K85 96] 234
Hypothetical protein [Acidobacteriaceae bacterium K85 96] 234
Acyl-ACP-UDP-N-acetylglucosamine-O-acyltransferase (Candidatus Solibacter usitatus) 234
Glycoyltransferase 1 234
Hypothetical protein [unclassified Aminicoanates] 234
Methyltransferase [Chloroflexus] 234
Glycoyl transferase family 1 [Bradyrhizobium sp. STM 2843] 234



Methylase [Neocardicola sp. CNT312]	I T F R R P M Y R R R R S P T L V Y F R G E I	361
Methylase [Neocardicola villiformis]	I T F V E R L P R R R S P T L V Y L F R E R E E I	363
Glycosyltransferase family 1 [Neorhizobium galegae bv. officinalis str. BANGI_1141]	A M L L P D P M A A R M E A G Y E V E S P L I M F R E D N L E I S A L I S	368
Glycosyltransferase family 1 [Neorhizobium galegae bv. orientalis str. BANGI_540]	A M L L P D P M A A R M E A G Y E V E S P L I M F R E D N L E I S A L I S	368
Glycosyltransferase [Rhizobium sp. CF080]	A M L L A N G E T A A R M E A G A G V E S P L I M F R E D N L E I S A L I S	370
Group 1 glycosyl transferase [Methylocella silvestris]	I D L L K E D P A G E R R R R R R R T V E A D Y L A S F R F D S P I I S D L D F S E E R Y A S E S Q I E F	403
Glycoyltransferase 2	Y T V I D E R M A S R N L A G S T V Y L Q Y S R F R E R L A G I I S E I R E P L A N T	379
Glycosyltransferase family 1 [uncultured Chloroflexi bacterium]	W Q I T P F E R A Q M E N A R S A L E T N W G I M S R L L A G S E	399
glycosyltransferase [Nocera producens]	I Q A T N G E R E R I R R L K R Y V E S N W N G I D D Q L A L Q V I N G	400
Glycosyltransferase 3	E A T E I D S R R R R I A A R P A A S P M C M E I G E D W L L S A A K S L A K I S G D I G S I L S G S I I G S	429
glycosyl transferase family 1 [Lysobya sp. PCC 8106]	Y T A E M S R R R M A G A S D E P V C K R P M C I R C H A C L A S E I I S	409
Glycosyltransferase [Leptolyngbya sp. PCC 7375]	I E L A C D P L R E T M E A S R E L V S R P M C A R A S L R C L P Q D A V P E R	412
Polysaccharide export transporter	Y P L A N T I S Y I T M S R E L I S T A S E P A S P A A S P L V M E R	320
hypothetical protein [Bryobacter aggregatus]	Y T I M E N I V L Y I S M E R E R M E M W M H E V T R P M A Q S L V M E R	314
Hypothetical protein [Acidobacteriaceae bacterium K85_83]	Y E L A N T I S Y I T M S R E L I S T A S E P A S P A A S P L V M E R	322
N-Acyltransferase	R P F L R E L L A P A L L S P L R E R L R G R E F Y A L R S S R K	601
UDP-3-O-(glucosamine N-acyltransferase [Candidatus Solibacter usitatus])	R P F L R E L L A P A L L S P L R E R L R G R E F Y A L R S S R K	342
UDP-3-O-glucosamine N-acyltransferase [Acidobacteriaceae bacterium K85_96]	R P F L R E L L A P A L L S P L R E R L R G R E F Y A L R S S R K	336
Hypothetical protein [Acidobacteriaceae bacterium K85_96]	S L K L I A L P R R R R I P R S P Q S I T P P V G R E R R C S R	362
Acyl-ACP-UDP-N-acetylglucosamine-0-acyltransferase [Candidatus Solibacter usitatus]	S L K L I A L P R R R I P R S P Q S I T P P V G R E R R C S R	362
Glycosyltransferase 1	F R D N Y T K Q M L A T L R R R R R R L P M L R L P R I A L M A L A S I M C R V Y S S S I F S T I N G	403
Hypothetical protein [unclassified Aminicomantae]	S Q L L D I V V Y S T I D	302
Methyltransferase [Chloroflexus]	I E R E R R P C P T P C T P T R R R T I P A T I C	370
Glycosyl transferase family 1 [Bradyrhizobium sp. STM 3843]	Y R P Q S P I V G A P Q Y V Y F V I V A S M C Y P P I D I R E W R S P P A R K L K P S P L V L P P P C P S P A P V Y E M A N Y S A P A L L S L S A Y L T H L Q Q M A P L Y L Y P P Y L A N E Y E R A G L A P C L A P R L G L G Y	566

.....610.....620.....630.....640.....650.....660.....670.....680.....690.....700.....710.....720.....730.....

Figure VI-24: The Alignment file of the glycosyltransferases, the N-acyltransferase and polysaccharide export protein and their closest relatives. The scheme shows that conserved regions for glycosyltransferase family 1 are similar in the glycosyltransferases 1-3. In the case of the N-acyltransferase of fosmid clone 100 E3 distinct regions show that all UDP-3-O-glucosamine-N-acyltransferases of the closest relatives share the same protein motifs. The polysaccharide export transporter shows conserved domains indicating the export transporter function but only shows close relatives that are have been annotated as hypothetical proteins.

VI.5. Nucleotide and protein sequences of putative biofilm disrupting enzymes on fosmid clone 100 E3

>Amidohydrolase (Nucleotide sequence, 1560 bp)

CTACTTGACGGTCGGGTACTGAATCCCAACTGCTCCAGGTATGTTTTGACTTTGATGG
 GTCGTAGCGCAACTTCTTGAGCTCCGGCCGAATCTCTCATTGTTTGTCCCGGTTTCAGCTC
 GACCGGCGCGGTGGTGCCTTCGGGAATCAGCGGCTTCATTTTATGTCCTTCGTCTGTTC
 CGCGAAGTACGCCTGGGCGTCCTGAGGATCTGGGGATTACAGCAGCAGGTTCGAGAGCCGT
 CATCGCATGGGCCTTCGCGCCCGCGCTGGCTCCCTTGTGCGCGATGGGCGTCGCGACCGC
 GATTCCGCTGGACCAAGTATGCCCCGATCATGCCCGGTATGTTTCGCGGGATAGGAGAGATT
 CACCGTCGGCAGGTTCCAGGCCACCTCCGCGATGTCATCGGAACCGGCGCCCCGCGCTCC
 TTCGGCAGGGGGCTTCAGCTCGGAGACCTCCTTCTTGAGTCCTCCACCTTGACTTCAA
 CTCCGTTTGCGCCGCGCGCGAGTTTCTCGTCATCCTCCGTCCATTTCCGGCATGCCGAC
 GCGTTTGATGTTGGCGTACAAAGCCTCGGCCAGAGGTTTGTGAAGTGTCGCGCCAGGT
 GGCCGCGAGCACGCGCTCCGTATGGTCGTATCGGTCATCATGGCCGCGCCGTTGGCGAC
 CTTTCGTGCCGATGTCGTGGAGTTCCTTGATCCGGTCATAATCGAACTCCCGGAAGAAATA
 CCAGACCGTGGCCAGGGGCGGGACAACGTTCCGGCTGGTCTCCGCCCTTGACGATCACGTA
 ATGGGAGCGCTGATCCGGCCGGATGTGCTCGCGGCGGAAGTTCCATCCAATGTCCATCAA
 CTC AACGGCGTCCAGGGCGCTGCGGCCATCCACGGAGACCCGGCGCTGTGCGCGCTGCG
 TCCGTGAAAGGTGTA CTGCGTCGAGACGAGCCCCGAGCCGCTCGCGCCGTAACGCGTTCC
 AAATTCGCTGCTGACATGGCTGCTCAGCATCACGTGACGTCGCGAAACATTCCCGCCAC
 TACCATGTATGTGCGGCTCCCGAGCAATTCCTCGGCGATCCCGGGATAGACGCGGATCGT
 GCCCGGAATCTTGTACCGCTGCATGAGGTTCTTACCACAAGGGCCGCGGTGATATTGAC
 GCCCTGCCCGGTATTGTGTCCCTCGCCGTGCCCGGACCGTTTGCATCAACGGAGCCTG
 ATAGGCGACCCCCGGCTTTTGGAGAGGTTTCCGGCAGCCCGTCGATGTCCGTCATGAATCC
 GATCACGGGTTTGCCGGAGCCCCAACTGGCGATGAACGCGGTGGGCATGCCGGCCGCCCC
 GCGCTGGACCGTGAACCCTTCCTTTTCGAGGATATTGACCAGATAAGCGGACGACTCGAA
 TTCCTGGTATCCCAGTTCGCGAAGCTGAACAGCGAATCGACGATCTGCTGGGTATTGT
 GCGCGGGCATCCACCATCTCGCCGGCCGCTGTTTCAACTGGTCGATCGGGGGAGCCTG
 CGAGAACGCGAGCGCGGCGCAGACCGGTAGGCACACGATGATTCGTTTCAAATCCGCAT

>Amidohydrolase (Protein sequence, 519 AA)

MRILKRIIVCLPVCAALAFSQAPPIDQLKQAAGEMVDARATMTQQIVDSL
 FSFAELGYQEFESSAYLVNILEKEGFTVQRGAAGMPTAFIASWGSQKPIV
 GFMTDIDGLPETSQKPGVAYQAPLIANGPGHGEGHNTGQGVNITAALVVK
 NLMQRYKIPGTIRVYPGIAEELLGSRTYMMVAGMFRDVDVMLSSHVSSEF
 GTRYGASGSGLVSTQYTFHGRSAHSAGSPWMGRSALDAVELMDIGWNFRR
 EHIRPDQRSHYVIVKGGDQPNVVPPLATVWYFFREFDYDRIKELHDIGTK
 VANGAAMMTDTTMTERVLAATWPGHFNKPLAEALYANIKRVGMPKWTEDD
 EKLARAAQTELKSKVEGLKKEVSELKPPAEGARGAGSDDIAEVAWNLPTV
 NLSYPANIPGMIGHHWSSGIAVATPIAHKGASAGAKAHAMTALDLLLNPK
 ILKDAQAYFAEQTKDIKWKPLIPEGTTAPVELNRDKMERFGPELKKLRYD
 PSKYKTYLEQLGIQYPTVK

>Dehydrogenase (nucleotide sequence, 1020 bp)

CTAATGCGTGGCGCTCTTCAACGAGTAAGAGCTTAGGACCTTCATGTAATTGGCGCGGCT
 GAAAGCCGACGGGTCGGCGACCGAACGGCGGCTCATGCTGCCCTGCATCTGCCGGATCGA
 TTCGTACTIONGCTCTTCCATCCATGCCTTCAGATCCGCAAGCACCGTCTCGACATGGTC
 GATCCCATGCTTCAGCAGGGCCGAGGTCATCATGGCGACCCGCGCGCCGGCCATCATCGA
 CTTCAAGACGTCTGCGCCGTATGGACACCGCCGGTGATCGCCATGTCCGCCTTGATGTT
 CCCATGAAGCGTGGCCACCCAGTGCAGCCTCAGCAGCAGTTCGTGAGGCGCGCTCAGATG
 CAGATTCGGCGTCACTTCCAGGGCTTCAAGATCGAAGTCCGGCTGATAGAAGCGGTTGAA
 CACCACGAGAGCGTCGGCGCCCGCCTTGCCAGCTTAGTCGCCATGTGAGCCGTGCGGCT
 GAAGTACGGCCCCAGCTTCACGGCGACCGGAATTCCAATGCTCGCCTTGACGTGCGACAC
 CAGGCTCGTGTACATCTCTTCAATCTGCTCGCCGAAACCTCCGGATCGTTGGCCAGGTA
 GAAGATGTTCAATTCCAGCGCGTCGGCACCGGCCTGCTCCATCTCCTTCGCGTACCGGAT
 CCAGCCGCCGTTTCGAGACACCGTTCAAACCTGGCGATGATCGGGATGTTACCGCCTGCTT
 CGCTTTACGAATATGCTCCAGGTACCCCTCGGGTCCGAGATTGTACCGGGTCATGTCCGG
 AAAGTAGGATACGGACTCGGCAAACTCTCGGTGCCGTAAGAAAGAACTCGTGGAGTTC
 CTCGCTTTCAAGCGTGATCTGCTCCTCGAACAGAGAATGCAGCACCCACCGCTCCGATCCC
 GCGTCTCCATCCGTAAGATGTTCCCGACGTGCTCGCACACGGAGACGGCGAAGCCAC
 CACCGGGTCTTCCAGGGTCAGACCCATGTAGGAAGTGGAAAGGTCAAGCAT

>Dehydrogenase (Protein sequence, 336 AA)

MLDLSTSYMGLTLKNPVVASPSPLCEHVGNI LR MEDAGIGAVVLHSLFEE
 QITLESEELHEFLSYGTESFAESVSYFPDMTRYNLGPEGYLEHIRKAKQA
 VNIPIIASLNGVSNNGWIRYAKEMEQAGADALELNIFYLANDPEVSGEQI
 EEMYTSLVSHVKASIGIPVAVKLGOPYFSATAHMATKLDKAGADALVVFNR
 FYQPDFLEALEVTPNLHLSAPHELLRLHWVATLHGNIKADMAITGGVH
 TAQDVLKSMAGARVAMMTSALLKHGIDHVETVLADLKAWMEEHEYESIR
 QMQGSMRRSVADPSAFSRANYMKVLSSYSLSKATH

>Glycosyltransferase 1 (nucleotide sequence, 1147 bp)

TGAATTGTAATACGACTACTATAGGGCGAATTCGAGCTCGGTACCCGGG
 GATCCCACCGAATGCGAGCAGCGAGACCTGCCATCGAGAGAGCCAGCCTC
 CAAAGCAGAGACAGCCATCCAAGGCGCCGCGCAGAGTGTGCCGCGAGAG
 GATGGCAAGGCTCGCTGGATCTCCGTCTCGACACCCGCCTCCTCCAGGC
 GGTCCCTCAGAGGGCCGTCCCGCGGCAGGATCACTCGCACGGCGTGGCCG
 TAGCCCGCCAGATGCGAGGACAAGCGAAGAAGTGAGCGGCTTGCGCCGTA
 CAGATCGGCGCCGTTGGCGACAAACAGAATCCTCATCAGCGTGTAAACGGT
 CTCGCCGCAATTCGCTCGAAAGAGAGCGAGCTCGAGATTCACTCCCGTCCG
 CGAGACCCGCCCTCCGGCCCAGCGCGTCCAAGGGCCATGCGCCCAGAGCC
 AGCGTCCGCTCCAACGGCGTCTCGGAGCCACGGGGGGGGTTCCGGCAATGG
 TTCCCGCGAGGCACTTCCAGGCGCCGAGAAGCAGGGAGTCCGCGCCGCGA
 GCGGGCTCGCGCACAAACAGGATCTCCAGTACGAAAAGACCGGCTCCCT
 GTCCACAAGCGACATTCGCTTTCCAAGGATGCGCTCGTAGGCTGCGAGGG
 AGCGGCGCTGGACGTGTGGGGCGATCTGCCGGCCGGCGGTACAAATACA
 TCCGAGACAAGCAGATATCCGGCGCCAGCCCGCACGCGGGAGGAGAGCTT
 CCGGAGCGCGGCTTCGAAACTCCGGTCGTCTACGAGGTGATAGAGAACGT
 CGATCGCCGTCACAAGGTCGAACTCCTCGGTTCGCGATAGCCGGGTGCGCC
 CAGTCTCGCGTCGTCAGGTCGTGATCAGAAATTGGCCGTTCCGGGTACGC
 TTTCCGGCACTGTTCCGCTGCCGCTCGCAGAGGTGGAAGCCGAGCCAGC
 GTTCCACACCGAGCCTGCTCCAGACCGGCCCGTAACTTCCGACTCCGACG
 GCGGCCTCGAGGATACGCCGGGGCCGGAAGCCGTTCTGCGCCGAAACAG
 CCGCAGGACGGCGTTCCGCCTGAGCCGGTAGGCCTGGCGGTTGAAGCCGT

CCCCAAGACCCGCGTAGCCAACCGCCGCGAGCGAACCCCTGGTTGCCGGCG
 TGGCGGCGGATCCAGTAATCGTGGTTCTCGTAAGTGAAACCGGCCGGATC
 GGATGTCAT

>Glycosyltransferase 1 (protein sequence, 382 AA)

MTSDPAGFTYENHDYWIRRHAGNQGSLAAVGYAGLGDGFNRQAYRLRNA
 VLRLFRRRNGFRPRRILEAAVGVGSYGPVWSRLGVERWLGFDLCEAAAEQ
 CRKAYPNGQFLIDDLTTRDWAHPAIAATEEFDLVTAIDVLYHLVDDRSFEA
 ALRKLSSRVRAGAGYLLVSDVFVTAGRQIAPHVQRRSLAAYERILGKRMS
 LVDREPVFVSLGDPVVREPARGADSLLLGAWKCLAGTIAGTPPVAPRRRW
 SDAGSGRMALGRAGPEGGRDGSERARSLSSELRRDRYTLMRILFVANG
 ADLYGASRLLRLSSHLAGYGHAVRVILPRDGPLRDRLEEAGVETEIQAS
 LAILSRHTLRGAFGWLSLLWRLALSMAGLAAR

>Glycosyltransferase 2 (nucleotide sequence, 1137 bp)

TCATGTCGCAGCCTCGATCGGCCGCCGGAGACTCGCGGAGAATCTCCG
 CCAGGCGCCTTCGGAAATGCTCATGCGTATATTGGAGGGTCACTGTGCGG
 TGGCCGGCCAGCCCCATCCGGGTGGCGGTCTCAGGATCCTTGACGAGCGT
 TTCGATGGCGCCGGCGATCTTCTCCGGCGACCTCGGGTCCACGCAGATTC
 CGTTGACCCCGTGAGTGACCACTTCGGAACCTCGCATCCACGTTCCCCGCT
 ACAACGGGCAGCCGGTGCTTCCAGGCTTCGAGGAACACGATGCCGAACCC
 TTCTCCCGTCGATGGCAACGCGAAAGCGTGCGCACTCCGGTATGTCTGTT
 CGAGTTGCCGGTCGTCGAGGTAGCCGAGGAAATGCACGCTGGAGGCGACT
 CCCAGTTCCGCCGCCAGCCTCTCGAACTGTTCCCGGAGAGGTCCGCCGCC
 GGCGATGTAGTAGTGACCTCCTTGCGGCTCCGCCGAGAATTGCCAGCG
 CCCGGATCACGCTGTGCATCCTTTGTGCCGGGCGCCGTCATCGAGTCGG
 GCCACCGACAGCAGGCGGAACTCGCCGTTACGGGGAGTGGCTTCGAGCGG
 GATTTCCAAGGAACCGCGGGACACGTCAACCGCGTTCGGCAGGACCCGGA
 ACAAGTCTTCCGGCAACCCGTAGGCGACCGTCATTTTTTTCGCGCCGTAAAG
 CGGCTTACCGAGACGATCCGGTCCATTAATCGCGCCCCCAACCGCTCACG
 GACCGGGATGCGATCGCGGAAGGGCTCCCTCCATGCCTCGCGCCCATGGA
 CGCACAACACATGGCGCGAACGCGGGCTGAGAAACCGCGCCACGGCAGCC
 AACGGCGCAACAAGAATGTGCCCGTAAAGAATGACATCGGGCCGGGAGAG

GAAAACCTCCCGGCAGAACGCCGCCACCGCACGCACTTTGCCGCGGCTGC
 AGCCGGAAAATCTCAGCCGTTCCGGGAAGTTGGCCGGAAGGCGGCCGATCG
 TCCCGCAGCGCAATGACGCTCGCATCGAGTCGGAGAGGACGCCCCAGCTC
 AGATAGGCAGCGGAGAACGCGCCGGTTGAACTGTTCCATCCCGCCCATCG
 CCCCCTAAACGCCAGCGCGACGAAAACCAATCTCAT

>Glycosyltransferase 2 (protein sequence, 378 AA)

MRLVFVALGVYGAMGGMEQFNRRVLRCLSELGRPLRLDASVIALRDDRPP
 SGQLPERLRFSGCSRKVRVAFAFCREVFLSRPDVILYGHILVAPLAAVA
 RFLSPRSRHVLCVHGREAWAREPFRDRIPVRERL GARLMDRIVSVSRFTAQ
 KMTVAYGLPEDLFRVLPNAVDSVRSLSLEIPLEATPRNGEFRLLSVARLDD
 GARHKGCD SVIRALAILRRSRKEVHYIAGGGPLREQFERLAAELGVASS
 VHFLGYLDDRQLEQTYRSAHAFALPSTGEGFGIVFLEAWKHRLPVVAGNV
 DASSEVVTHGVNGICVDPRSPEKIAGAIETLVKDPETATRMGLAGHRTVT
 LQYTHEHFRRRLAEILRECLRRPIEAAT

> Glycosyltransferase 3 (nucleotide sequence, 1278 bp)

TCATCGGGTTGGGATCCCCTCCGCGGACCGGAGGGTAATGCCCCCTCGC
 CGCCGGAACCGATGCCGCGGAACGTTTCGCGGCGCTTCATACAGTTGG
 TTGAGGCGGTCGCCGGTCTCCCGCCAGCACCATCGGCTCGCGGCCACTG
 GCGGGCGGCTTCGCCGCGGCGTCGCCGTCCCTCCGGATCCATAATCATGG
 CCCTCAGCGCTCATGGATGCGTTGCACGGCTTGATCGGGTGTGTCCGGG
 TCCAGCACGATACCGCCCCGGTCGGAGACCACGTGCCGCGTGCCGGCGGC
 CCGGAGGCAAATCACCGGACGGCCAGCCATCATCGCCTCGAGCGGTGCAT
 AGCCGAACTGCTCGTGCAACTTGGGTGCAAGAGCGCATCGGCGGCGGGC
 AGTTCCTCGAAGACCTCGGGACGTGTCCGCGCTCCGGCGAACTGAATCGC
 GGTCGCGCACTGATGTTCCCTCCGCAAGTTGCTTGAGAAAGCCTAGCTCCG
 GACCGTCTCCGATGATCCGGTACTCCGAGGCCGGGAATTCGCGATGGAGA
 CGGGTGAAGGCGAGGATGCCAGACTGATTCCCTTCAGCCCCTTTAGCTG
 CCCGATGGAAACCACTCGGAATACGCCGGCGCGCCGCTGCGGAATCCGCA
 GTAGCCGGGCAATTTCCCTCCGGCTCCAGGCCTCCGAGGGGAAAGGTCACC
 ACCGGCAACCCTTTACGCCAGACGGACCGGTGCTGCCCGACAGGATCAG
 ACGGGCGCGGACCCCGTGACGGCGGTGGCGATGCAGCCGAGCCAATTGA

CGGCGAGATTTCTGACCGCCTCGGTGCGCACGCGCCCGCCACGACATGTTC
 CGGAGGAATAACCAGGGCGTCGTCTGACGGATTCCGGCGCTCCAGATAAA
 CGGAACGCCGAGCCAGCCCATGAAACTCGGCATCCAGGAGTTCACAAAAG
 TCACGTGCTGGACGATATCGAACCGGACCTCGCTGTTCCAGCGTCGAGCT
 TCCAGAAAGGCGGTAACCTGCCAGGCGGCGTAGTACAAGTGAGTCACCGA
 GCGCCGCAGCCACGATGAACCGAGCGGTCCGGGGGGACGCAGAAACCGGA
 ACTCGACGGCCGGCATGGGCTCCTCGCGCAGCCTGGCCTCGATGAATGGC
 CGATTGTGCTCGTCGGTTAGAATGGATACATCGTGGCGCAAGCCGGCCTG
 ACGGACCACACCCACCCCTACGCCGGGCTCCGAGCCGGCGCCTGGCAGGC
 AAGCAAACGCCGAGAGTAGAATCTTCAT

>Glycosyltransferase 3 (protein sequence, 425 AA)

MKILLSAFACLPGAGSEPGVGVVVRQAGLRHDVSILTDEHNRPFIEARL
 REEPMPAVEFRFLRPPGPLGSSWLRRSVTHLYAAWQVTAFLARRWNSE
 VRFDIVQHVTFNWSMPSFMGWLGVVFIWSAGIRQTPWFLRNMSWRAR
 ATEAVRNLAVNWLGCIAVAVTGSRRARLILSGSDRSVWRKGLPVVTFPLGG
 LEPEEIARLLRIPQRRAGVFRVVSIGQLKGLKGISLILAFTRLHREFPA
 SEYRIIGDGPFLGFLKQLAEHQCATAIQFAGARTRPEVFEELAAADALL
 HPSLHEQFGYAPLEAMMAGRPVICLRAAGTRHVVS DRGGIVLDPDTPDQA
 VQRIHEALRAMIMDPEGRRRRGEAARQWAASRWCWRETGDRLNQLYESAA
 KRSAGIGSGGEGGITLRS AEGIPTR

>N-acyltransferase (nucleotide sequence, 1803 bp)

ATGATCGGTTGGGATTTCCGTCTCGATGCGCTGAAGCGCGGTCTCGAGCCTGAGGCCGGA
 GCGGTAAAGGATCGTGTAAGCGGTCTTGAGCGAGCCGATCTCTTCGCGCGTGAAGCCGGC
 CCGCTTCAGCCCGACGAGATTCAGTCCGACGGGAACCGCCCGGAAGCCGGCGTACAGGAA
 GAACGGCGGCGCGTCTGCTGTTGAGTCCCGAGTTGCCGGCGATCATTGCCAGCTTGCCTAT
 GAGGGAGAACTGGTGCACGCCACCCCGCCGGATATGAATGCCTGGTCTCCACCTCGAC
 GTAACCGGCCAGCAGGGCGCAGCTACAGATCACGGTGTTATCGCCAACCTTGACAGTTGTG
 GCGGATATGTCCCGAGGTCATGATGTAGTTGCCGTTGCCGATCCGGGTGACCGATTCCGG
 CTTGGTGCCGCGCGAAATCGTGTAGTGCTCCCGATCCGGTTGTCGTCTCCGATATGAAG
 GTAACCTCGTTCACCCGTAAACGCCTTGTCGAGGGGGTCCGGTGCCAAGCACGGTTCGGGA
 CGAGATCTCATTCCGGTCTCCGAGCGTCGTCCAGCGCTTGATATGGACGTAGGCCTCCAA

CCGGCAGGATGCGCCGATGCGCACGTCCGGCTCGACCACGCAGTATTCGCCGATTACGGT
 ACCCGGACCGATCGTCGCGCCGGCATGCACCCGGGACGTCCGGCGGACGACGGCGGAGGG
 ATCAATCGGCATAACCTTGTATCATACTCAGTAGCCGGTGAGGAGGTGACTGTGAGGGTA
 CGTGAGCTGGCCGAATGGCTCGGCGCGCCGTTTGAAGGGGACGGCGAAAAAGACCTCGAT
 CGCGCCGGGACAATCGAGAGCGCCGGCGCGTCCGAACTGGCGTTCGTCTCGAGCCGCAAG
 GCAGCGAAACAGGCCGGGTTTTTCGGCGGGCGGGCTGCCTGATCGTGCCACTGGAACATGAA
 AATACCCCGCCGGAACGGTGATTGCGGTACCGGACCCCGGACGGCGTTTGCTCGCGCC
 GTCAGCAGGTTGCACCCCTTCGCGCCGGTTCGTCGCCGAGTCCACCCCTCGGCGATCGTC
 GCGCCGGATGCGCGGATCGAACCCGGCGTGGCGATCGGTCCCATGGCCGTGGTAGGAGAG
 GGATCGTGCGTCGGGGCCGGATCGGCCATCGGCGCGGGTTGCTCCATCGGGAGGCGCGTG
 ACGATTGGAGAACGCTGTATCGTTCACGCGAATGTGACGGTCTATGACGACGTGGACATC
 GGCAATGGCGTGATCCTGCATTCCGGATGCGTGCTCGGCGCCGACGGGTTTCGGGTTTCGTT
 TTACAGGGGGACTGTTATCAAAAGTTTTCCACAGATCGGAAGGGTGTCCGTCCGGCGACAAC
 GTGGAGATCGGGGCGAACGCCTGCGTAGATCGGGCGGGCTCGGAGTCACGTGGATCGGC
 GAAGGCGCCAAACTCGACAACATGGTCCATGTGGCGCACAACCTGCCGGATCGGACGCCAC
 GTCGTGGTGGCGGGCGAGACCGGTTTTTCGGGTGGCGTGGTGGTGGAGGACTACGCTGTC
 ATCGGGGGGCAGGTGGGAGTCGGAGACAAAGCTCGAATCGAATCACGGGCGGTGCTCGGG
 AGCGGCTGTGGTGTCTGACCTCCAAGATCGTGCGGGCAGGCCAGGTGGTCTGGGGGACT
 CCGGCCCGTCCGCTCAAAGAGCACCTCGAGCTACTGGCGAACCTCGGCCGGCTTCCGGAC
 ATGAGAAGAGAGTTAGCCGAGTTGAAGAAGCGCGTGCAGGCTCTTGAGGGCAGCCGGCGG
 GAA

>N-acyltransferase (protein sequence, 601 AA)

MIGWDFRLDALKRGGLEPEAGAVKDRVSGLERADLFAEAGPLQPDEIQSD
 GNRPEAGVQEERRRVAVESRVAGDHCQLAYEGELVHAHPAGYECLVLHLD
 VTGQQGAATDHGVIANLAVVGDMSRGHVAVADPGDRFRLGAARNRVVL
 PDPVVSDMKVTSFTRKRLVEGVGAKHGSGRDLIPVSERRPALDMDVGLQ
 PAGCADAHVRLDHAVFADYGTRTDRRAGMHPGRRRDDGGGINRHNLVSYS
 VAGEEVTVRVRELAEWLGAPFEGDGEKDLDRAGTIESAGASELAFVSSRK
 AAKQAGFSAAGCLIVPLEHENTPPRTVIRVPDPRTAFARAVSRLHPFAPV
 VPGVHPSAIVAPDARIEPGVAIGPMAVVGEGSCVAGSAIGAGCSIGRRV
 TIGERCIVHANVTYDDVDIGNGVILHSGCVLGADGFGFVLQGDYQKFP
 QIGRVSVDNVEIGANACVDRAALGVTWIGEGAKLDNMVHVAHNCRIGRH

VVVAQTGFSGGVVVEDYAVIGGQVGVGDKARIESRAVLGSGCGVLTSKI
VRAGQVWVGTPARPLKEHLELLANLGRLPDMRRELAELKRVQALEGSRRE

>Polysaccharide export protein (nucleotide sequence, 963 bp)

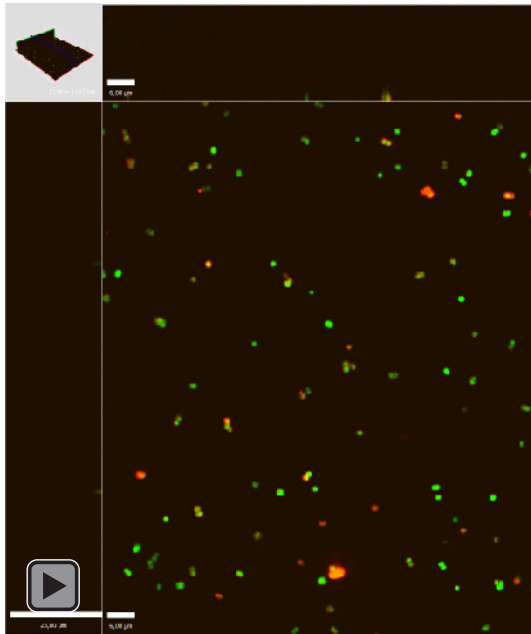
CTACCTGCGCCAAACGAGGATGCCGGACCCGTCGCCGCGCCGAAGCCGGCGACCCGCTC
GATGGCGGTGGAGGTGAGCCGGCGGCCGCTGTTGTCTGGGGATGTACAGAATGTCATTAGC
GGCCAGCGGCACATCCGGCGCTTTGCGCTTCATGATCTGCTTGAGCTCGATGGGAATCTC
GTGCTTGCCGCCGGTGGCCGCGTCGCGCCGGTAGATGAACGCCCGACTCGTCGCATAGGG
CGCGAGGCCTTCGGCCAGCGCCAGCACCTGAAGAACCGTGGTCTCGGCAGTGTCCGGCAT
CGGATAGGCGCCGGGCTTCTTGACATTCCCCACGACGAAGATCTTGCTGACCTCCGGCAC
GCGGATTTCTCTCCGCCCGTCAGCCGCAGGTTGAGCTCCGGGTCGGCCGCATCGATCAG
TCCCTTACCCGGGATCCGCTGCACAAGCGCCGTTGGCTCCGCTCCCGGACCGGCCTGAAC
CCGGCTAACCAGAATTTCCGGGCCAGCCTCCGCGCTCAATCCGCCCGCCCGGGTTCAGCGC
GTCGAGCAGCGTCACCGGTCCCACCGCCTGGAACGTGACTGGACTCCGAACCGAGCCGGC
GACGGCGATCGGACGGCTATGATACTCGGCGATCGTCACCGTGACCACCGGGTCCACAAG
CACTTCTTCTTCTTGAGCGCCTCGGCGAGAGAACTCAAGGGCGGCAGGGAGCAGCCC
CTCGGCCCTGATCTTCCGCTTGAGCATCGGGAGGCGGACCGCCCCGTCCGCGCCGACACG
AATGGTCCGGCTCAGTTCGGAGCTCCGTACACACTGACCGCAATCAGGTCGTTCCGGCCC
GATCTTCTGCGCGGGGAGATTGGCCCCGCCGAGATCGCCCGGCGCGGGCGGATCTCACTTG
CCCCGCTGCTTGAAGGCCACAGAACCGGCACCACTAGCCACAACCTTGCTGCTGAAACG
CAT

>Polysaccharide export protein (protein sequence, 320 AA)

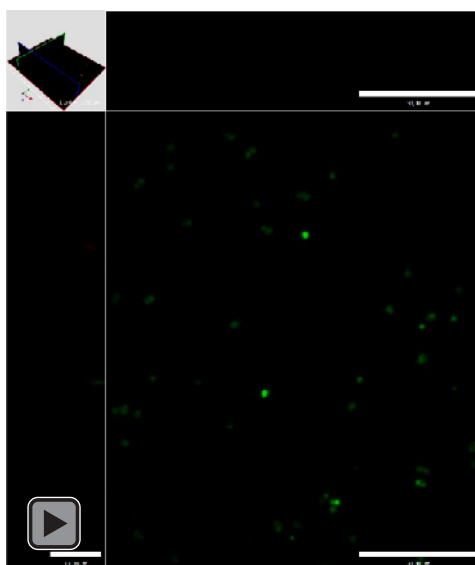
MRFSSKLWLVVPVLWAFQAAGQVRSAPGDLGGANLPAQKIGPNDLIAVS
VYGAPELSRTIRVGADGAVRLPMLKRKIRAEGLLPAALEVSLAEALQEEE
VLVDPVVTVTIAEYHSRPIAVAGSVRSPVTFQAVGPVTLLDALTRAGGLS
AEAGPEILVSRVQAGPGAEPALVQRIPVKGLIDAADPELNLRRTGGEEI
RVPEVSKIFVVGNVKPGAYPMPDTAETTVLQVLALAEGLAPYATSRAFI
YRRDAATGGKHEIPIELKQIMKRKAPDVPLAANDILYIPDNSGRRLTSTA
IERVAGFGAATASGILVWRR

VI.6. Videos

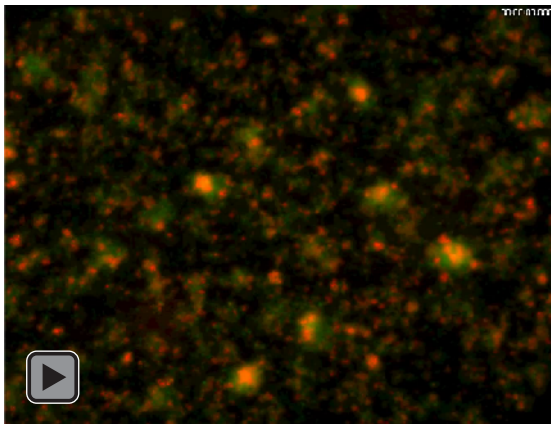
VI.6.1.Video *S. epidermidis* 1457 PIA formation



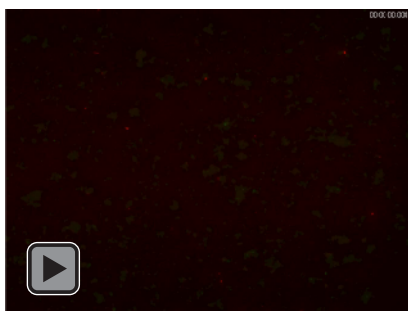
VI.6.2.Video *S. epidermidis* 1457-M10



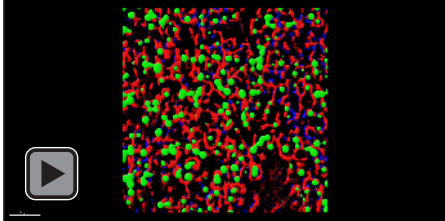
VI.6.3.Video *S. epidermidis* 1457 flow conditions



VI.6.4.Video *S. epidermidis* 1457-M10 flow conditions



VI.6.5.Video *S. epidermidis* 1457 3D dSTORM Embp+PIA



VII. Acknowledgment

First of all I want to thank all employees of the department of medical microbiology, virology and hygiene at the University hospital Hamburg-Eppendorf (UKE) and the department for common microbiology and biotechnology at the University of Hamburg. I want to thank especially Prof. Dr. Wolfgang Streit and Prof. Dr. Holger Rohde for their trust and the opportunity to work on such interesting topics. Special thanks go to Dr. Antonio Virgilio Failla and Dr. Bernd Zobiak from the UKE Microscopy Imaging Facility (umif) for their great support concerning all microscopes and image analysis. Furthermore special thanks to Dr. Dennis Eggert, Dr. Rudolph Reimer and Carola Schneider at the HPI in Hamburg for great dSTORM, REM and TEM images.

A very special acknowledgment goes to the Werner-Otto-Stiftung of the UKE that financed my work from 2011-2013 and the "Promotionsförderung der Universität Hamburg" for financing the final year of the doctoral thesis.

Then I would like to thank my family for the general support during all those years of study. I would also like to thank MSc Biology Anja Wiechmann for her great support via Skype. She gave me new ideas and possibilities on experiments. A very special gratitude goes to my loving boyfriend Rolf who always makes me smile.

VIII. Declaration on oath

I hereby declare, on oath, that I have written the present dissertation on my own and have not used other than the acknowledged resources and aids.

Hamburg, 27.03.15



Hanaë Agathe Henke